

**Studies on the structure & function of HAM1, an  
atypical nucleotide cleansing protein of the human  
malignant malaria parasite**

**Thesis submitted for the degree of  
Doctor of Philosophy (Science) at  
Jadavpur University**

**Debanjan Saha**

**Department of Infectious Diseases & Immunology  
CSIR-Indian Institute of Chemical Biology  
Kolkata, India**

**&**

**Jadavpur University  
Kolkata, India**



**2024**



# बसु विज्ञान मंदिर BOSE INSTITUTE



(विज्ञान एवं प्रौद्योगिकी विभाग, भारत सरकार के एक स्वायत्त संस्था)  
(An Autonomous institute of Department of Science & Technology, Govt. of India)

## मुख्य कैम्पस / Main Campus :

93/1, आचार्य प्रफुल्ल चंद्र रोड, कोलकाता - 700 009  
93/1 Acharya Prafulla Chandra Road, Kolkata - 700 009  
फोन / Phone : 2350-7073 (निदेशक / Director)  
इपीएबीएक्स / EPABX 2350-6619 / 6702 / 2402 / 2403, 2303-0000 / 1111  
फैक्स / Fax : 91-33-2350-6790

## शतवार्षिकी भवन / Centenary Building :

पी - 1 / 12, सी.आई.टी. स्कीम- VII एम, कोलकाता 700 054  
P - 1 / 12, C.I.T.Scheme VII - M, Kolkata - 700054  
फोन / Phone : 2355-7434 (निदेशक / Director), 2355-0595 (रजिस्ट्रार / Registrar)  
इपीएबीएक्स / EPABX 2355-9416 / 9219 / 9544, 2569-3271, फैक्स / Fax : 91-33-2355-3886

## समन्वित शैक्षिक परिसर / Unified Academic Campus :

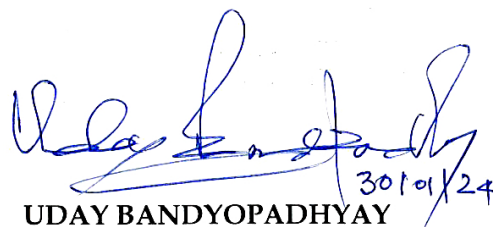
ब्लॉक - ईएन, प्लॉट नं - 80, सेक्टर- V, सॉल्ट लेक सिटी, कोलकाता - 700 091  
Block - EN, Plot No. -80, Sector - V, Salt Lake City, Kolkata - 700 091  
फोन / Phone 2355-7434 (निदेशक / Director)  
इपीएबीएक्स / EPABX 2569-3123 / 28, फैक्स / Fax : 91-33-2569-3127.

संदर्भ सं. / Ref. No. \_\_\_\_\_

दिनांक / Date :

## CERTIFICATE FROM THE SUPERVISOR

This is to certify that the thesis entitled “Studies on the structure & function of HAM1, an atypical nucleotide cleansing protein of the human malignant malaria parasite”, submitted by Sri Debanjan Saha, who got his name registered on 18.09.2018, for the award of Ph.D. (Science) degree of Jadavpur University, is absolutely based upon his own work under the supervision of Prof. Uday Bandyopadhyay and that neither this thesis nor any part of it has been submitted for either any degree/diploma or any other academic award anywhere before.

  
UDAY BANDYOPADHYAY

उदय बंदोपाध्याय / Uday Bandyopadhyay  
निदेशक / Director  
बसु विज्ञान मंदिर  
BOSE INSTITUTE  
कोलकाता / Kolkata

*To my mom & dad:*

*Couldn't have come this far without your unconditional  
love and out-and-out support.*

*To saving humankind:*

*I'm still working on it!!*

# Acknowledgements

"It was the best of times, it was the worst of times, it was the age of wisdom, it was the age of foolishness, it was the epoch of belief, it was the epoch of incredulity, it was the season of Light, it was the season of Darkness, it was the spring of hope, it was the winter of despair." — *Charles Dickens, A Tale of Two Cities*

The stage is set for the thesis by introducing the duality of human experience, suggesting that the protagonist's experience was one of growth and a steep learning curve. The **Doctor of Philosophy (PhD)** pursuit was an enduring, daring adventure of non-linear kinetics. Nevertheless, the PhD left me impoverished, without money, but richer in thoughts. Committing several years of my life to such an endeavour meant relying on the goodwill, patience, and support of others, especially during trying times that invariably arose when least expected. In black and white, I express my gratitude towards them.

**Prof. Uday Bandyopadhyay**, my PhD supervisor, deserves the pinnacle of credit for guiding me throughout my doctoral tenure with his remarkable academic counsel, unwavering optimism and unparalleled observational competency in science. From infrastructural to research consumables support, he sponsored me in affluence. He provided me with an Everest of freedom in scientific research, allowing me to become a free-spirited, unrestrained thinker and troubleshooter in science, above and beyond. His teachings taught me the invaluable lesson of patience, especially when faced with disarrayed experimental outcomes. The vibrant discussions with him throughout my term, whether in the confines of a highly academic laboratory setting or by the sidewalk chai shop, will remain an indelible and enigmatic remembrance for a lifetime. Under his guidance, my time in the lab has been nothing short of transformative, laying the foundation for my scholastic success and shaping me into the adept individual I am today.

I am deeply grateful to my research advisory members (RAC), namely, **Prof. Parimal Karmakar** from the Department of Life Science & Biotechnology at Jadavpur University and **Dr Indu Bhusan Deb** from the Department of Organic & Medicinal Chemistry at CSIR-Indian Institute of Chemical Biology (IICB) for their critical

research advice and external oversight throughout my PhD work. Dr Deb's exceptional support and leadership as the lab in charge during my supervisor's transition to the director at Bose Institute, Kolkata, has been a true inspiration. I am incredibly thankful for Dr Deb's invaluable contribution to our laboratory.

I extend special thanks to the former directors of CSIR-IICB, namely, **Prof. Samit Chattopadhyay** and **Prof. Arun Bandyopadhyay**, for allowing me to conduct my research at this institute with all access to the central instrumental facilities. I am obliged for the generous access to laboratory instrumentation provided by the faculties, **Dr Subrata Adak**, **Dr Saumen Datta**, **Dr Nahid Ali**, and **Dr Nakul Chandra Maiti**, on the Jadavpur campus.

I gratefully acknowledge the financial support from the **CSIR**, which enabled me to pursue my PhD studies.

The enduring value of a seven-year tenure in a laboratory lies not in the confines of its walls or the precision of its instruments but in the camaraderie, support, and friendship forged among its members. This fabric of shared experiences and unwavering bonds transforms a mere workplace into a sanctuary, a second home where we live, breathe, and thrive. I vividly recall the countless hours spent within those hallowed rooms, where the lines between colleague and companion blurred, replaced by a profound sense of belonging. I cherish the fond memories of those shared meals, hushed conversations, and spontaneous laughter that enriched my days. Indeed, the human connection, the unspoken language of companionship, renders a laboratory more than just a place of work; it is a crucible where friendships are forged, resilience is nurtured, and the pursuit of knowledge becomes a shared adventure.

As a wide-eyed Master's student embarking on my scientific journey, I stepped into the lab, eager to learn and explore the intricacies of experimental biology. However, the initial days were a whirlwind of information and challenges, leaving me overwhelmed and uncertain. With unwavering patience and infectious enthusiasm, **Dr Asim Azhar Siddiqui**, my esteemed senior, took me under his wing, nurturing my curiosity and instilling a profound appreciation for the intricate world of malaria research. He was not merely a mentor but a companion and source of unwavering support. His approachability, helpfulness, and genuine warmth created an

environment where I felt empowered to ask questions, make mistakes, and grow as a young scientist. He taught me that science is not merely about facts and figures; it's about the pursuit of knowledge, the thrill of discovery, and the profound impact we can make on the world through research. I am forever grateful for his unwavering support and inspiration during those formative years. I carry his lessons with me as I continue to navigate the world of scientific exploration.

**Dr Somnath Mazumder**, a cherished lab senior, stood as a pillar of unwavering support beyond academic pursuits. Whenever motivation waned, or challenges loomed, his words of encouragement rekindled my spirit. He guided me through the intricacies of scientific writing, ensuring that my ideas were conveyed with clarity and impact. When deadlines loomed large, Somnath da would motivate the team for increased productivity interspersed with delectable culinary delights, showing his genuine care for his colleagues' well-being. He embraced my challenges as if they were his own, always ready with a solution or a listening ear. Such unwavering dedication is a rare gem in today's world, and I am incredibly fortunate to have encountered such a senior during my doctoral journey.

Another senior, **Dr Chinmoy Banerjee**, stood as a beacon of inspiration, unyielding passion, composure, and dedication to science. His profound verbal advice extended far beyond the realm of critical scientific queries, encompassing world politics and the finest cinematic masterpieces. Chinmoy da's presence fostered an environment where intellectual curiosity and a thirst for knowledge were encouraged and celebrated.

Teaming up with **Dr Subhashis Debsharma** has been an invaluable experience. His continuous assistance throughout my doctoral journey has been a source of immense gratitude. From his brilliant ideas that enriched my research to his calm demeanour during a minor lab fire (set by me!) incident, Subhashis has consistently demonstrated his unwavering friendship. His presence in the lab, especially during the pandemic, made the lab experience far less stressful and more enjoyable. I am genuinely grateful to have had him as a companion on this journey.

With **Dr Shiladitya Nag's** unhesitating support, I navigated the complexities of protein biology, developing a firm foundation for my research journey, and I am thankful for that. The journey through the lab was not just a pursuit of scientific

knowledge but a web of friendships, laughter, and shared unforgettable experiences. My fellow lab member, **Saikat Pramanik**, epitomised this spirit. His infectious laughter echoed through the lab spaces, creating an atmosphere of lightheartedness and camaraderie. And when hunger pangs struck, Saikat's culinary skills transformed the lab into a haven of delectable Indian cuisine, and his culinary creations were a symphony of flavours.

I extend my heartfelt gratitude to my esteemed lab seniors, **Dr Shameel Iqbal**, **Dr Rudranil De**, **Dr Shubhra Jyoti Saha**, and **Dr Samik Bindu**, for their scientific contributions to my doctoral journey. Their sociability, laughter-filled moments, and shared culinary adventures have enriched my tenure beyond measure. I am particularly grateful for Shameel da's sage advice, encapsulated in his wisdom phrase '*Suno sabki, par karo aapni!*', resonating deeply with me and guiding my life's pursuits.

Also, I am indebted to **Mr Surjendu Debnath**, my lab's technical assistant, for his support and guidance, which helped me to get the hang of animal handling.

**“Making friends in a new environment is like starting a new chapter in a book. It can be exciting and daunting at the same time, but it's worth it in the end.”—  
*Anonymous***

Such was my PhD camaraderie, all forged in the fire of shared experiences and mutual respect. My jovial bubble, a vibrant tapestry of friends from diverse Indian states, was woven during the coursework of 2017 and sealed with an unforgettable trip to Tajpur. From then on, our bonds deepened through innumerable journeys, near and far; endless chats and culinary adventures; shared stories of triumph and sorrow; and the nuanced spectrum of friendship, with some bonds resonating deeper than others. **Varsha**, **Priya**, **Aleepta**, **Debajyoti**, **Dipayan**, **Sukanya**, **Priyanka**, and **Moumita** became my bosom companions, their presence enriching my PhD journey beyond measure. Though distance now separates us, their voices remain a dial tone away, and I cherish the hope of a reunion soon! **Priti** and **Shrabastee**, two other remarkable confidantes, shared my positive proclivity for banters, both useless and helpful, making the final stretch of my PhD less daunting. Academically, too, I had the privilege of collaborating with these talented and dedicated individuals.

I am thankful to **Atanu**, who took the time to accommodate my special request for help with protein crystallography, a subject I was a novice at the time. Despite the tight deadline, I also extend my deepest gratitude to **Dr Uttam Pal**, who promptly assisted me with a critical phase of my research project. His professionalism and willingness to help are exemplary.

I am profoundly grateful to my friendly colleagues, **Sumit, Vivek, Sujay, Dwipanjana, Gourab, Krishnendu, Saroj da, Milon da, Ayan da, Sambit da, Anirban da, Rajeev da, Yuthika, Puja**, and **Aneek**, for making my CSIR-IICB journey complete, both scientifically and non-scientifically.

**Mr Suresh Kumar** and **Mr Sandip Chakraborty** from Central Instrumentation are the most proficient and helpful research technicians I have ever worked with. I am genuinely grateful for their assistance.

I offer my most sincere gratitude to the **house-cleaning staff** and the dexterous **gardeners** of the institute. Their dedication and meticulous work have transformed our campus into a sparkling oasis, teeming with vibrant blooms during the flowering season. They are the unsung heroes of CSIR-IICB, and their selfless service truly humbles me.

**“Life is like a box of chocolates. You never know what you're gonna get.” —  
*Forrest Gump (1994)***

This quote perfectly captures the unpredictability of life. It reminds us that life is full of surprises, both good and bad. One of my life's most exciting and rewarding experiences occurred during my PhD tenure. In the summer of 2022, through the **Newton-Bhabha PhD scholarship**, I had the privilege of working at the London School of Hygiene & Tropical Medicine (LSHTM) and exploring England to the fullest for five unforgettable months. My time in London was a kaleidoscope of experiences, connections, friendships, emotions, and cultural immersions. To all the amazing people I met and befriended in London, thank you for making my experience so special. I want to express my gratitude to the **British Council** and **DBT-India** for providing me with the financial support to pursue this incredible opportunity. I am also grateful to my mentors and colleagues at the LSHTM for their guidance, support, and encouragement. I am truly blessed to have had this once-in-



a-lifetime opportunity. It has shaped me into a more confident, resilient, and globally-minded individual.

**Asst. Prof. Christiaan van Ooij** deserves my deepest gratitude for hosting me in his lab for the placement despite the two-year delay caused by the COVID-19 pandemic. His helpfulness, humility, approachability, and encouragement, combined with his deep knowledge of the subject, are truly exemplary.

**Aline** was the linchpin of my fantastic endeavours in London. From birthdays to bakings to quick getaways, she made it all happen. She was my food venture ally, my research hand, and a respected senior friend. **Julian** is a friendship I will cherish forever. From food ventures to sending me a basket of Christmas gifts from Oxford to India, he has always gone above and beyond. **Elena** deserves a prized place in my heart for all the travels we shared across London and for being such a wonderful person. I am so grateful for her friendship. I would also like to thank **Tansy, Giulia, Penny, Alfonso, Matt, Linfeng, Cesc, Pepi, Richard, Dan, Becky, Zeeshan, Pej, Archie,** and **Gisela (one of the finest lab managers I have come across!)** for being a part of my superb memories in London. My old and new friends, **Sanmoy, Souradeep, Abhijeet,** and **Pradosh**, transformed the British landscape into a vibrant *desi* place. They kept the spirit of India alive, whether through steaming plates of dal-chawal and refreshing ThumsUps or their uniquely *desi* approach to gossip! I am so fortunate to have had the opportunity to meet and befriend such amazing people from different parts of the sphere.

I also extend my heartfelt gratitude to my university friend, **Somesh**, who has been a steadfast companion through thick and thin. His unwavering support and encouragement have made my PhD journey immeasurably smoother. Having a loyal and dependable friend is something that I am truly grateful for.

I extend my deepest gratitude to my school buddies, **Tanmoy, Shouvick, Shubrangshu, Atish, Budhaditya,** and **Souvik**, for keeping me sane with their engaging conversations, witty banter, and stimulating discussions on topics ranging far beyond the realm of PhD research. They helped me take breaks, laugh, and remember that life is more than just academics.



**"Life is a journey from innocence to experience." — Oscar Wilde**

Through the vicissitudes of life, we learn and grow, one step at a time. I am thankful to my **parents** and **former educators** at every level, from St. Augustine's Day School to Maulana Azad College to Ballygunge Science College, who have served as the supporting rungs on the ladder of my personal and academic growth.

The education at the **BioNetVision** coaching centre was instrumental in my mastery of previously unfamiliar subjects, fostering knowledge and self-assurance.

I am eternally grateful to my mom, **Mrs Smritikana Saha** and dad, **Mr Dulal Chandra Saha**, for their undying love and unwavering support. They have always been my most zealous advocates, believing in me even when I doubted myself. Despite my late hours in the lab, missed social functions and numerous ups and downs, they remained patient and compassionate, providing me with extraordinary financial support and unending encouragement. Their unwavering faith in me has been my pillar of strength and has enabled me to follow my dreams. I owe everything to them and am the person I am today because of their constant guidance. My affection for you all surpasses what I can express through words. This thesis is a testament to the power of unconditional love and its impact on someone's life.

I also want to thank my **close relatives** for their steadfast support throughout my PhD years. Your love and encouragement have been invaluable. And to my late **grandparents**, I thank you for your enduring blessings. I know you are watching over me, and I am so grateful for your love.

**"You have to trust yourself that you're going to make it through this, no matter how hard it is." — Oprah Winfrey**

Finally, having completed my PhD journey, I am proud of **myself** for persevering through the inevitable highs and lows. Throughout the journey, I have exercised great patience, tackled obstacles, managed people, knit projects, and conquered my imposter syndrome. Even during the times when my mental health was in tatters, I somehow remained resilient. So, I acknowledge my resilience with deep gratitude.

*Debanjan Saha*

# Preface

One of the worst infectious diseases, malaria still threatens nearly half of the world's population and kills hundreds of thousands of people in 2022, predominantly African children. The five species of single-celled eukaryotic *Plasmodium* parasites that cause malaria in people—most notably *Plasmodium vivax* and *Plasmodium falciparum*—are spread via the bite of *Anopheles spp.* mosquitoes. By combining vector control techniques (such as pesticide spraying and the use of bed nets sprayed with insecticide) with medications for both treatment and prevention, malaria is managed. Using artemisinin-based combination therapy has helped to reduce the number of deaths caused by malaria significantly, but the evolution of drug resistance threatens to undo this gain. New diagnostic tools, medications, and insecticides have been developed due to improvements in our understanding of the disease's underlying molecular foundation. Several brand-new combination medicines with efficacy against drug-resistant parasites are being tested in clinical settings to increase compliance. This ambitious effort to end malaria includes fresh ideas that might result in vaccinations or inventive vector control methods. Nevertheless, notwithstanding these successes, malaria must be entirely eradicated by a concerted international effort on several fronts.

**Chapter 1**, under the '**Review of Literature**' section in the thesis, is a time travel from 400 BCE to the present day describing the aetiology of malaria with a historical perspective linked to it. The miscreant family of *Plasmodium spp.* and their phylogenetic lineages linked to demographic spread are also discussed. The basic lifecycle of *Plasmodium spp.* including the sporozoite, asexual and sexual stages, is detailed along with its vector, *Anopheles spp.*, which is spread across the globe. Malaria pathogenesis and its severe manifestations are incorporated in this review. Various diagnostic techniques (clinical to molecular approach) and subsequent available forms of treatment (past, present and futuristic goals) are discussed here. Prevention of the disease through vector mitigation is studied, too.

**Chapter 2**, under the '**Review of Literature**' section in the thesis, encompasses the genetic makeup and the intricacies associated with the *Plasmodium* group of parasites. The metabolic pathways of nucleotides, including the purine and the pyrimidine pathways, are batted around. Accordingly, the aberrations associated

with such pathways are discussed next, and how different molecular players in the parasite resolve the faulty metabolic chores is explored in depth.

**Chapter 1**, under the '**Experimental Insights**' section in the thesis, demonstrates various experimental details, including the detailed biophysical, bioinformatic, biochemical and genetic analysis of *Pf*HAM1. This study examines cloning, over-expression, purification and identification strategies of *Pf*HAM1, its oligomeric information, enzyme kinetics, binding affinity, CRISPR-Cas9 knockouts, and confocal/live-cell fluorescent imaging.

**Chapter 2**, under the '**Experimental Insights**' section in the thesis, further analyses the X-ray crystal structure of the novel *Plasmodium falciparum* HAM1 protein and its interactions with cognate substrates.

This scientific study delves into the involvement of the *Pf*HAM1 protein in the malaria parasite's daily nucleotidic metabolic functions. It is discovered that this protein plays a crucial role in avoiding the integration of harmful nucleotides into the nucleic acids, which promotes genomic stability. By utilising biophysical, biochemical, genetic, and structural analysis techniques on *Pf*HAM1, this research seeks to enhance our comprehension of *Plasmodium falciparum* biology and aid in developing future therapeutic interventions.

# Abbreviations

**°C:** Celsius

**3D:** 3-dimensional

**6-TITP:** 6-thio-inosine-5'-triphosphate

**ACT:** Artemisinin-based Combination Therapy

**ADA:** Adenosine deaminase

**AdSS:** Adenylosuccinate synthetase

**AMP:** Adenosine-5'-monophosphate

**AMPDA:** Adenosine-5'-monophosphate deaminase

**ATC:** Aspartate transcarbamoylase

**ATP:** Adenosine-5'-triphosphate

**ATSB:** Attractive toxic sugar bait

**BCE:** Before the Common Era

**BLI:** Biolayer interferometry

**Bp:** Base pair

**C-terminal:** Carboxy terminal

**cAMP:** Adenosine 3',5'-cyclic monophosphate

**Cas9:** CRISPR-associated protein 9

**CD:** Circular dichroism

**CDC:** Centre for Disease Control and Prevention

**cDNA:** Complementary DNA

**CE:** Common Era

**cKO:** Conditional knockout

**CM:** Cerebral malaria

**CMP:** Cytidine-5'-monophosphate

**CO<sub>2</sub>:** Carbon dioxide

**CPS:** Carbamoyl phosphate synthetase

**CQ:** Chloroquine

**Cq:** Quantification cycle

**CR1:** Complement receptor 1

**CRISPR:** Clustered Regularly Interspaced Short Palindromic Repeats

**CRP:** C-reactive protein

**CSA:** Chondroitin sulphate

**CTP:** Cytidine-5'-triphosphate

**DAPI:** 4',6-diamidino-2-phenyl indol

**DARC:** Duffy Antigen Receptor for Chemokines

**DBP:** Duffy-binding proteins

**DDT:** Dichlorodiphenyltrichloroethane

**DHFR:** Dihydrofolate reductase

**DHOase:** Dihydroorotase

**DHODH:** Dihydroorotate hydrogenase

**DIC:** Differential interference contrast

**DIG:** Digoxigenin

**DLS:** Dynamic light scattering

**DMSO:** Dimethyl sulfoxide

**DNA:** Deoxyribonucleic acid

**ECL:** Enhanced chemiluminescence

**EDTA:** Ethylenediaminetetraacetic acid

**EGS:** Ethylene glycol bis(succinimidyl succinate)

**ELISA:** Enzyme-linked immunosorbent assay

**EM:** Electron microscopy

**EMP1:** Erythrocyte Membrane Protein 1

**ENT:** Equilibrative nucleoside transporters

**FACS:** Fluorescence-activated cell sorting

**FAD:** Flavin adenine dinucleotide

**FAM:** Fluorescein

**FDA:** Food and Drug Administration

<b>FMN:</b> Flavin mononucleotide	<b>K<sub>cat</sub>:</b> Catalytic activity
<b>FNT:</b> Facilitated nucleobase transporter	<b>K<sub>d</sub>:</b> Dissociation constant
<b>FPLC:</b> Fast protein liquid chromatography	<b>kDa:</b> Kilodaltons
<b>G6PD:</b> Glucose-6-phosphate dehydrogenase	<b>kJ:</b> Kilojoules
<b>gDNA:</b> Genomic DNA	<b>K<sub>m</sub>:</b> Michaelis Menten value
<b>GM:</b> Genetically modified	<b>LAMP:</b> Loop-mediated isothermal amplification
<b>GMP:</b> Guanosine-5'-monophosphate	<b>LDH:</b> Lactate dehydrogenase
<b>GMPS:</b> Guanosine-5'-monophosphate synthase	<b>LLIN:</b> Long-lasting insecticidal nets
<b>GTP:</b> Guanosine-5'-triphosphate	<b>LSM:</b> Larval source management
<b>GTS:</b> Global Technological Strategy	<b>M:</b> Molar
<b>HAP:</b> 6-N-hydroxylaminopurine	<b>MAD:</b> Multiple-wavelength anomalous dispersion
<b>HGXPT:</b> Hypoxanthine-guanine-xanthine-phosphoribosyl transferase	<b>MALDI-TOF-MS:</b> Matrix-assisted laser desorption ionization / Time-of-flight / Mass spectrometry
<b>HI:</b> House improvement	<b>Mb:</b> Megabytes
<b>HPLC:</b> High-performance liquid chromatography	<b>MD:</b> Molecular dynamics
<b>HRP-2:</b> Histidine-Rich Protein-2	<b>MDA:</b> Mass drug administration
<b>HTS:</b> High-throughput screens	<b>MEF:</b> Mouse embryonic fibroblast
<b>IDP:</b> Inosine-5'-diphosphate	<b>MIR:</b> Multiple isomorphous replacement
<b>IFA:</b> Immunofluorescence antibody	<b>mM:</b> Millimolar
<b>IMP:</b> Inosine-5'-monophosphate	<b>MMV:</b> Medications for Malaria Venture
<b>IMPDH:</b> Inosine-5'-monophosphate dehydrogenase	<b>mNG:</b> mNeon Green
<b>IPTG:</b> Isopropyl $\beta$ -D-1-thiogalactopyranoside	<b>Mol:</b> Moles
<b>IPTp:</b> Intermittent preventive therapy in pregnancy	<b>MR:</b> Molecular replacement
<b>IRS:</b> Indoor residual spraying	<b>MSA:</b> Multiple sequence alignment
<b>ITC:</b> Isothermal calorimetry	<b>NAD:</b> Nicotinamide adenine dinucleotide
<b>ITN:</b> Insecticide-treated mosquito nets	<b>NDP:</b> Nucleotide diphosphate
<b>ITP:</b> Inosine-5'-triphosphate	<b>NGS:</b> Next-generation sequencing
<b>K<sub>av</sub>:</b> Distribution coefficient	<b>NHS:</b> National Health Service
<b>Kb:</b> Kilobases	<b>NMR:</b> Nuclear magnetic resonance
	<b>nPCR:</b> Nested PCR
	<b>NPP:</b> New permeability pathways

<b>NTP:</b> Nucleotide triphosphate	<b>SDS-PAGE:</b> Sodium dodecyl-sulfate
<b>O.D.:</b> Optical density	polyacrylamide gel electrophoresis
<b>OPRT:</b> Orotate	<b>SEC-MALS:</b> Size exclusion
phosphoribosyltransferase	chromatography / Multi-angle light
<b>ORF:</b> Open reading frame	scattering
<b>PAM:</b> Protospacer adjacent motif	<b>SEM:</b> Standard error of the mean
<b>PBS:</b> Peripheral blood sample	<b>Seq:</b> Sequencing
<b>PBS:</b> Phosphate-buffered saline	<b>sgRNA:</b> Single guide RNA
<b>PBS-T:</b> Phosphate buffered saline-	<b>SLI:</b> Selection-linked integration
Tween 20	<b>SPZ:</b> Sporozoite
<b>PCR:</b> Polymerase Chain Reaction	<b>SSR:</b> Simple Sequence Repeats
<b>PDB:</b> Protein data bank	<b>SSUrRNA:</b> Small subunit ribosomal
<b>PEG:</b> Polyethylene glycol	RNA
<b>Pf:</b> <i>Plasmodium falciparum</i>	<b>TB:</b> Tuberculosis
<b>PI3K:</b> Phosphatidylinositol-3-kinase	<b>tHDA:</b> Thermophilic helicase-
<b>PIR:</b> Plasmodium Interspersed Repeats	dependent amplification
<b>Pk:</b> <i>Plasmodium knowlesi</i>	<b>TNF-<math>\alpha</math>:</b> Tumour Necrosis Factor
<b>Pm:</b> <i>Plasmodium malariae</i>	<b>TTP:</b> Thymidine-5'-triphosphate
<b>PNP:</b> Purine nucleoside phosphorylase	<b>UDP:</b> Uridine-5'-diphosphate
<b>Po:</b> <i>Plasmodium ovale</i>	<b>UMP:</b> Uridine-5'-monophosphate
<b>PP<sub>i</sub>:</b> Pyrophosphate	<b>UMT:</b> Urine malaria test
<b>PRT:</b> Purine phosphoribosyl transferase	<b>UPR:</b> Unfolded protein response
<b>Pv:</b> <i>Plasmodium vivax</i>	<b>UTP:</b> Uridine-5'-triphosphate
<b>QBC:</b> Quantitative Buffy Coat	<b>UTR:</b> Untranslated region
<b>qRT:</b> Quantitative real-time	<b>v/v:</b> Volume / Volume
<b>RBC:</b> Red blood cell	<b>V<sub>c</sub>:</b> Column volume
<b>RDT:</b> Rapid diagnostic test	<b>V<sub>e</sub>:</b> Elution volume
<b>Rh4:</b> Reticulocyte-binding-homologue 4	<b>Vir:</b> Virulence
<b>RNA:</b> Ribonucleic acid	<b>V<sub>max</sub>:</b> Maximum velocity
<b>ROS:</b> Reactive oxygen species	<b>V<sub>o</sub>:</b> Void volume
<b>RPM:</b> Rotations per minute	<b>w/v:</b> Weight / volume
<b>RPMI:</b> Roswell Park Memorial Institute	<b>WGA:</b> Wheat germ agglutinin
<b>rRNA:</b> Ribosomal RNA	<b>WHO:</b> World Health Organization
<b>SAD:</b> Single-wavelength anomalous	<b>WT:</b> Wild type
dispersion	<b>XDP:</b> Xanthosine-5'-diphosphate
<b>SD:</b> Standard deviation	<b>XMP:</b> Xanthosine-5'-monophosphate

**XRC:** X-ray crystallography

**XTP:** Xanthosine-5'-triphosphate

**μM:** Micromolar

# Table of Contents

Acknowledgements	i
Preface	viii
Abbreviations	x

---

## Review of Literature

---

### 01 | A Comprehensive Review of Malaria

Introduction	1
Time travel: Aetiology of Malaria	2
The Genesis: <i>Plasmodium et. al.</i>	9
The family tree: Species of <i>Plasmodium</i>	12
From an epidemiological point of view	21
Life of a Malaria parasite	24
The malign transporter: <i>Anopheles et. al.</i>	27
Disease pathogenesis & phenotypic manifestations	
Pathogenesis	29
Manifestations	34
Disease management: Detection to Therapy	37
Clinical diagnosis	37
Laboratory diagnosis	37



Molecular diagnosis	39
Capsules of the Past	44
Capsules of the Present	46
Capsules of the Future	49
Malaria prevention is better than cure	51
Chemoprophylaxis	51
Vaccine development	51
Vector control	53
Conclusion	56
References	58

## 02 | House-cleaning Staff and their Metabolic Chores in the Malaria Parasite

Genome architecture in <i>Plasmodium</i> spp.	73
Nucleotide metabolism in the parasite	76
Purine metabolism	77
Pyrimidine metabolism	81
Aberrations & the house-cleaning staff in malaria parasite	83
NuDiX superfamily	85
dUTPases	86
All- $\alpha$ -helical NTPases	87
ITPases	87
Conclusion	95
References	97

## Experimental Insights

### 01 | Functional Characterisation of *PfHAM1*

Introduction	110
Experimental procedures	
Bioinformatics of <i>PfHAM1</i>	113
Culturing of parasites and transfections	113
Genomic DNA isolation, total RNA extraction and PCR amplification of the gene	114
Cloning, over-expression, purification and MALDI-TOF / TOF MS / MS analysis	114
Antibody generation from recombinant <i>PfHAM1</i> and western blotting	115
Circular dichroism	116
Dynamic light scattering studies	116
Chemical cross-linking studies	117
Gel filtration chromatography for oligomeric status determination	117
Size exclusion chromatography – multi-angle light scattering (SEC-MALS)	117
Enzymatic kinetics	118
Isothermal calorimetry (ITC)	119
Biolayer Interferometry (BLI)	119
Stage-specific expression of <i>pfham1</i> by qRT-PCR	119
Generation of plasmids (Fusion & CRISPR-Cas9 constructs) and Cas9 guide RNA sequences	120
Live cell imaging	121
Immunofluorescence studies	121
Growth assays	122
Statistical analysis	122
Ethics declarations	123
Results	
Bioinformatics of <i>PfHAM1</i>	124
Cloning, over-expression, purification and validation of <i>PfHAM1</i>	127
<i>PfHAM1</i> is a homodimer	130
Pyrophosphohydrolase activity of <i>PfHAM1</i>	132
ITC studies reveal strong binding of dITP as a substrate to <i>PfHAM1</i>	135
BLI studies show a 1:1 stoichiometric binding pattern	137

Transcriptional expression of <i>pfham1</i> is maximum in the trophozoite stage	139
Live cell imaging of <i>PfHAM1</i> shows its predominant localisation in the cytoplasm	140
Immunofluorescence studies confirm cytoplasmic localisation	143
<i>PfHAM1</i> is dispensable in the blood stages of the lifecycle as shown using conditional knock-outs (cKO)	144
Discussion	148
Conclusion	152
Additional information	153
References	155

## 02 | Structural Characterisation of *PfHAM1*

Introduction	163
Experimental procedures	
Protein purification	166
Protein crystallisation, data collection and refinement	166
Molecular docking and dynamic simulations	167
Results	
<i>PfHAM1</i> is a homodimer with monomers arrayed in a parallel pattern	169
Molecular dynamics identified critical residues involved in substrate binding	173
Discussion	180
Conclusion	186
References	187
Synopsis	190
Publications	192
Conferences & Fellowships	194

---

# Review of Literature | Chapter 1

---

## A Comprehensive Review of Malaria

## **A. Introduction**

Malaria is a parasitic disease caused by five different single-celled eukaryotic *Plasmodium* parasites (mainly *Plasmodium vivax* and *Plasmodium falciparum*) that are transferred to humans through mosquito bites by *Anopheles spp.* Malaria is one of the world's most severe infectious diseases, endangering more than half of the world's population and killing hundreds of thousands in 2020, especially children from Africa. As per recent WHO Reports 2022, an estimated 247 million malaria cases occurred in 2021 and 619,000 deaths globally. A combination of vector control strategies (such as insecticide-treated bed nets and pesticide spraying) and pharmaceuticals can be used to treat and prevent the disease. The widespread use of artemisinin-based combination therapy has significantly reduced malaria-related mortality; nevertheless, drug resistance threatens to undo this achievement. Advances in our comprehension of the underlying molecular basis of disease have fueled the development of new diagnostics, medicines, and insecticides. Several novel combination treatments are being investigated in clinical studies to examine if they work against drug-resistant parasites and may be used in single-dose regimens to improve compliance. This grandiose malaria-eradication plan by 2030 also includes novel approaches that could lead to new vector control strategies or malaria vaccines. Despite these accomplishments, malaria elimination will need a well-coordinated worldwide effort on numerous fronts.

## **B. Time travel: Aetiology of Malaria**

Many diseases have been veiled in enigma throughout history, with their roots accredited to supernatural and mystical powers. For example, an 'ovarian teratoma', called after a Greek monster, is a tumour of skin, hair, teeth, and adult tissues. The famous Aristotle connected 'teratomas' to the patient's hair consumed and deposited in various body tissues. According to specific ideas, 'teratomas' result from carnal experiences with the devil, evidence of witchcraft, expression of a nightmare or 'incubus', or a punishment for wrongdoings. Malaria has long been a part of this enigmatic cluster of illnesses.

For many decades, illnesses like cholera and malaria were considered to be produced by 'miasma (ancient Greek: pollution, defilement)', a lethal mist laden with particles from decaying materials or 'miasmata'. Anything afloat above ground was unnoticeable to the naked human eye before the development of the microscope, which was referred to as "air," including dust particles and germs; this early aetiological notion may have been near to the truth.

In the work *"On Airs, Waters, and Places,"* Hippocrates explored the aetiology of specific ailments in 400 BCE. The disease was formerly known as "marsh fevers," "agues" (derived from the Latin *febris acuta*), "tertian fevers," "quartan fevers," and "intermittent fevers" before the word "malaria" was established. The majority of the vocabulary is derived from Hippocrates' works, which detailed the unfitness of the air in specific places about deadly illnesses such as quartan fevers:

*"This disease is habitual to them both in summer and in winter, and in addition, they are very subject to dropsies of a most fatal character; and in summer dysenteries, diarrhoeas, and protracted quartan fevers frequently seize them, and these diseases, when prolonged, dispose such constitutions to dropsies, and thus prove fatal"* (Hippocrates; Adams, 1886).

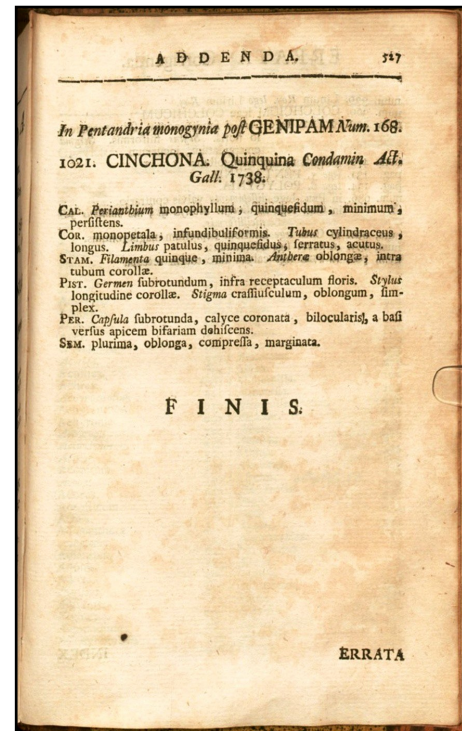
The "foul air" or miasma idea of malaria aetiology remained accepted after mosquitoes were established to be the disease's transmission factor in the 19<sup>th</sup> century CE. On the other hand, the link connecting sickness and insects dates back to antiquity. It took almost 1,500 years for the term "malaria" to be coined. According to historian and Florence chancellor Leonardo Bruni's *Historia Florentina*, malaria originates in the miasma theory (Leonardo Bruni, 2001-2007).

"There is a horrid thing called the malaria, that comes to Rome every summer, and kills one," Horace Walpole stated in a letter on 5 July 1740 (Bruce-Chwatt, 1977). In 1827, John MacCulloch was the first to use the term in English literature (scientific). In 1893, however, the first person to observe malarial parasites in the blood, Charles Laveran, detested the name malaria. He disliked the phrase and preferred the term 'paludisme' (Latin: 'palus' means 'swamp'), which is still used in the French regions today (Bruce-Chwatt, 1981). Malaria refers only to the disease and its symptoms (not the causative agent). The aetiological concept of "bad air" prevailed until the late nineteenth century, maybe due to the disease's name. To protect himself from 'miasma', African explorer cum journalist Henry Morton Stanley (1857–1922) installed a glass screen on his canoe, which he utilised for his travels on the Congo River (Cook and Webb, 2000).

Quinine is a medicinal substance obtained from the bark of the Cinchona tree (Lee, 2002). In the landmark treatise *Genera Plantarum*, Swedish botanist Carl Linnaeus named the genus of this tree in 1742. Francesco Torti established a new standard of care for Peruvian bark use in 1756. According to his gorgeously illustrated publication, only sporadic fevers responded to *cinchona* bark treatment (Torti, 1756).



**Figure 1:** A Torti Fever tree shaped like a stylised *cinchona* plant. (Courtesy: The John Carter Brown Library at Brown University)



**Figure 2:** The *Cinchona* genus is listed by Linnaeus. (Courtesy: Bayerische Staatsbibliothek, München)

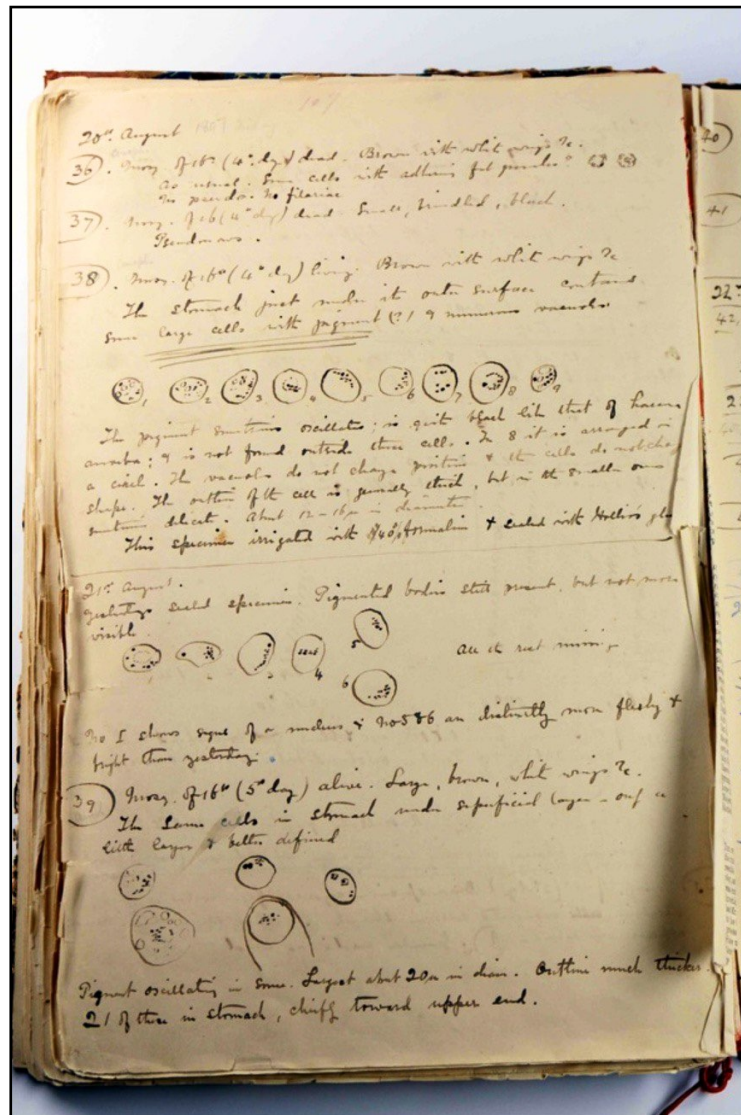
Albert Freeman Africanus King, an American physician, compiled 19 findings in support of the mosquito as the source of malarial sickness by 1883 (KING, 1883):

- 1) Malaria is most frequent in mosquito-infested environments (rainforests, swamps, fens, and marshes).
- 2) Malaria is most frequent when the weather is warm enough for mosquitoes to thrive.
- 3) Malaria does not thrive in cold weather.
- 4) Malaria is particularly prevalent in the tropical and coastal parts of the world.
- 5) Malaria is prevalent in densely forested areas.
- 6) Forests may hamper malaria transmission.
- 7) Malaria has the potential to spread to regions thousands of kilometres distant.
- 8) When dirt is dug, malaria can spread to previously unaffected areas.
- 9) A vast body of water may prevent malaria.



- 10) Previously, malaria-infected nations may be able to become malaria-free once the illness has been eradicated.
- 11) Malaria poses the most significant hazard near the earth's surface.
- 12) Malaria transmission is at its peak at night.
- 13) The risk of contracting malaria is higher after sleeping in the open night air.
- 14) Malaria is prevented by fire.
- 15) Malaria is prevented by breathing city air.
- 16) Malaria is most common in the late summer and early fall.
- 17) Canvas curtains, gauze veils, and mosquito nets all help to prevent malaria.
- 18) Malaria affects newborns at a considerably lower rate than it does adults.
- 19) The white race is the most vulnerable to marsh fevers, whereas the black race is the least sensitive.

Ronald Ross, a British army surgeon, was the first to present conclusive evidence that mosquitoes carried malaria. Ross conducted a two-year investigation in Secunderabad (India) under the guidance of Patrick Manson, microscopically studying hundreds of brindled grey and white mosquitoes fed malarial blood in search of a parasite within the mosquito. In 1897, he obtained a few spotted-winged mosquitoes. Ross blood-fed these mosquitoes from a patient, Husein Khan, whose blood included many crescent-shaped cells. Ross discovered characteristic pigmented structures in the stomach wall of these spotted-winged mosquitoes, now called the *Anopheles* species. Ross inferred that the pigment (haemozoin) was causally associated with malaria since mosquitoes cannot manufacture it (Ross, 1923).



**Figure 3:** Book I, page 107 of Ross' Diary and Notes of Malaria Researches. (Courtesy: Archives Service, London School of Hygiene & Tropical Medicine)

This dark pigment is now known to be created during haemoglobin digestion and produced by the malaria parasite via biocrystallisation (Hempelmann, 2007). In an autopsy, haemozoin (brown pigment) in organs is a significant sign of malarial illness.

In 1897, Robert Koch, whose primary aim was to control tuberculosis (TB), began malaria fieldwork. During his research in Africa, he observed that all children in some malaria-infested communities had splenomegaly and malaria. However, as

children aged, the disappearance of splenomegaly was seen, and their blood no longer harboured detectable parasites. The children eventually developed immunity to malaria. He supported the mosquito-borne notion he developed during a trip to India in 1883.

Between 1885 and 1892, Bartolomeo Camillo Golgi studied the malaria parasite's asexual cycle, comparing its phases to those seen in various types of malaria. Golgi observed that distinct *Plasmodium* species generated the two forms of intermittent malarial fevers ('tertian', which occurs every alternate day, and 'quartan', which occurs every 3<sup>rd</sup> day) and that the fever paroxysms concurred with the rupture and release of merozoites into the circulation (Golgi, 1891).

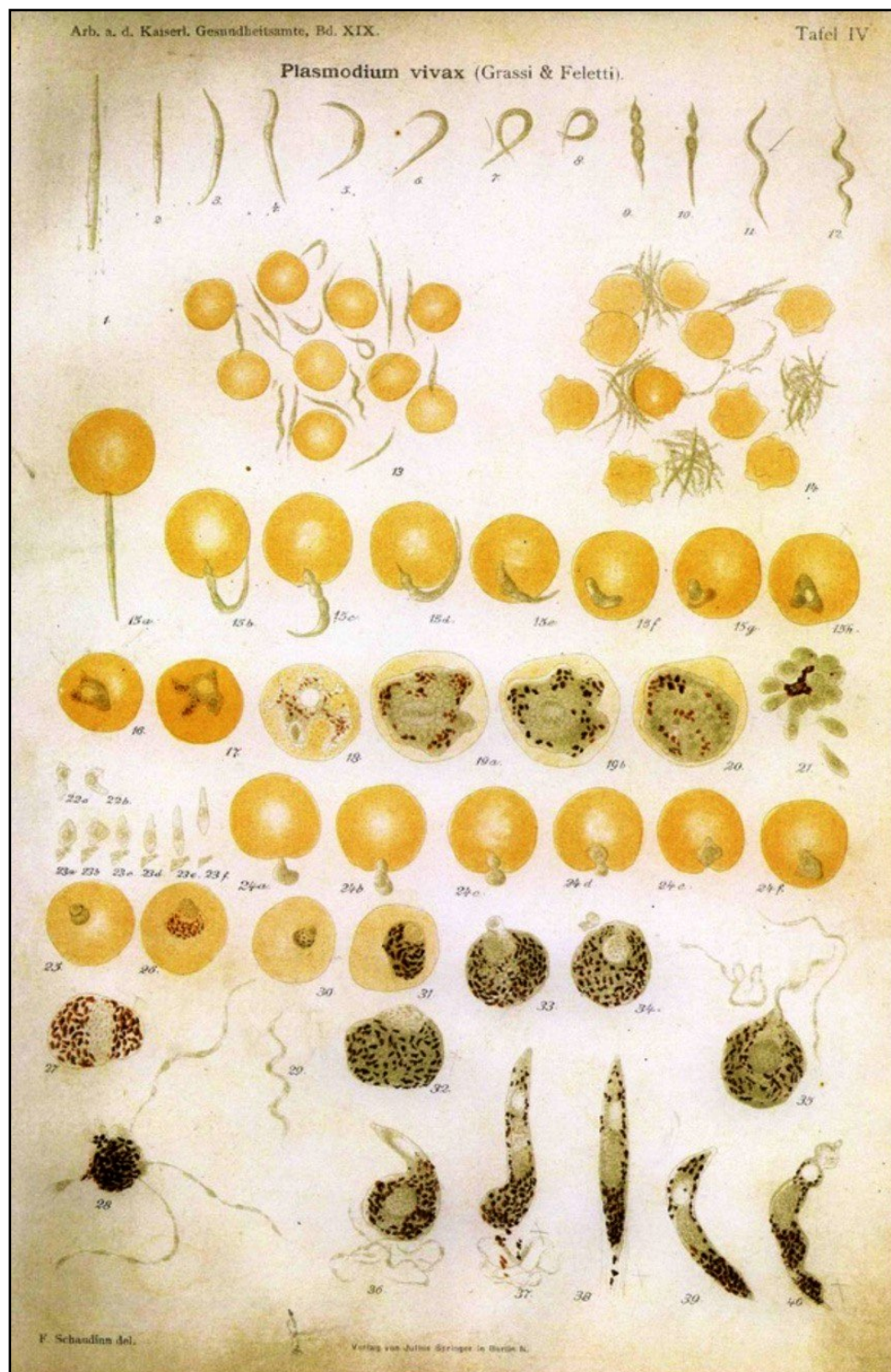


**Figure 4:** A daisy-like malaria blood preparation by Golgi. (Courtesy: Museum for the History of the University of Pavia)

Until 1947, when Cyril Garnham and Henry Shortt proclaimed that a period of division in the liver preceded the parasite development in blood, Schaudinn's



explanation of infective sporozoites of *P. vivax* directly penetrating erythrocytes dominated scholarly opinion.



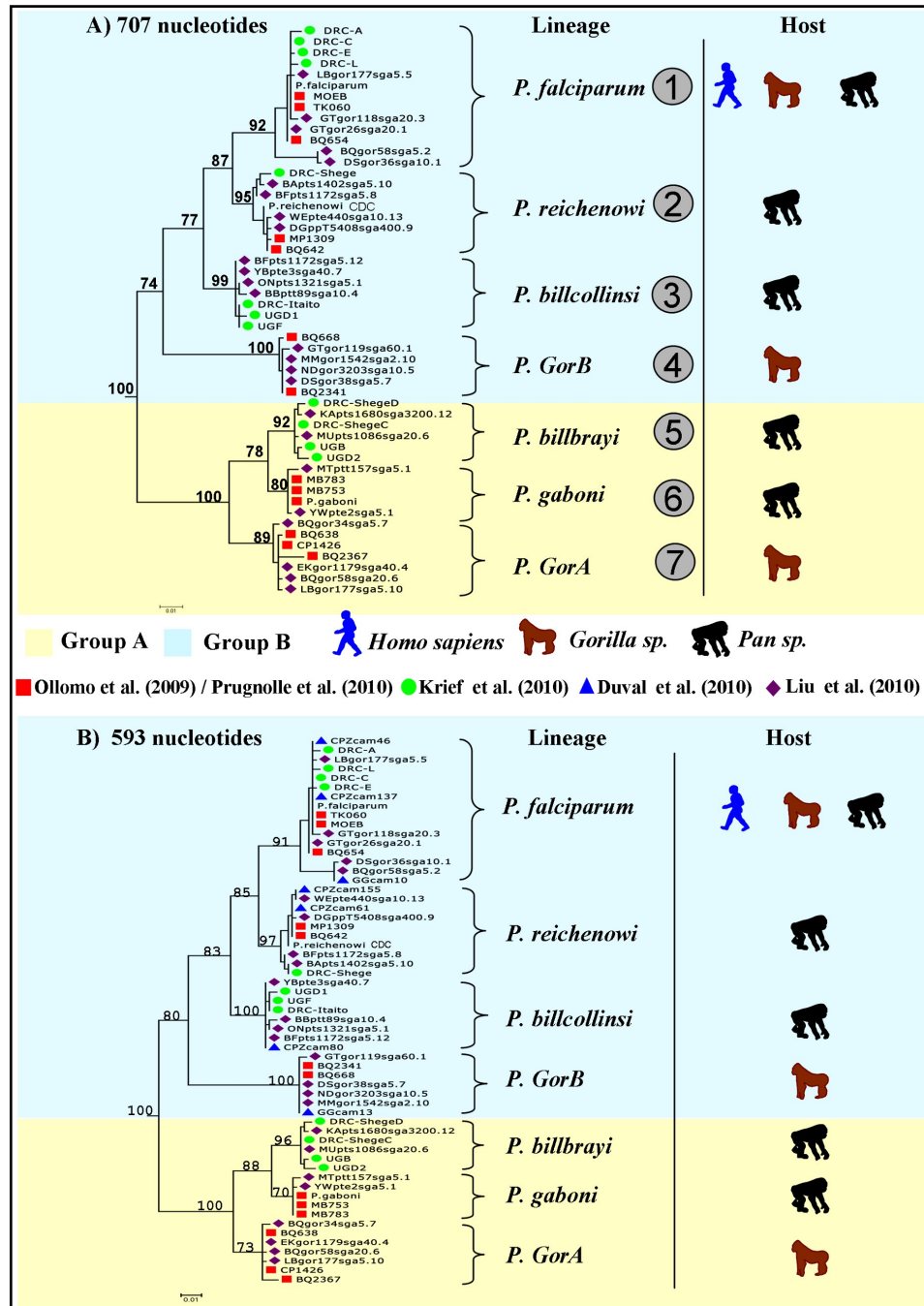
**Figure 5:** Infective sporozoites directly enter erythrocytes in cells numbered 15 a h; from Schaudinn's drawings. (Courtesy: Tropeninstitut Hamburg)

### **C. The Genesis: *Plasmodium et. al.***

*Plasmodium ovale*, *Plasmodium malaria*, *Plasmodium falciparum*, and *Plasmodium vivax* are the four types of *Plasmodium* that are typically considered human parasites. These species are only distantly related to one another, implying that adaptation to humans has occurred multiple times over the genus' existence. However, it is still being determined when and where these associations originated (Stephen Matthew Rich, 1970).

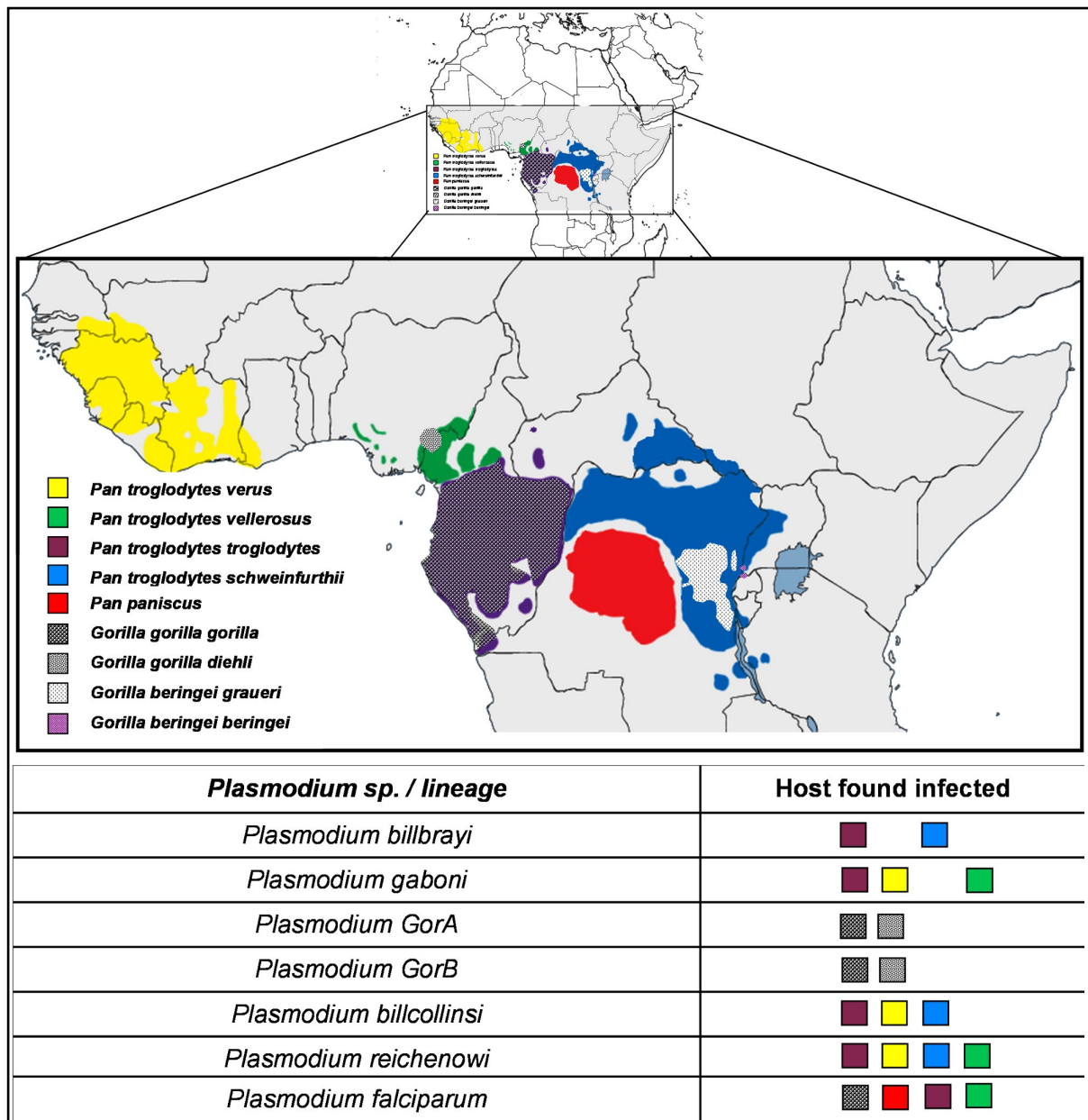
Initial molecular phylogenetic studies of the genus '*Plasmodium*' found *P. falciparum* to be grouped with two species of avian parasites rather than mammalian species, suggesting *P. falciparum* is the outcome of a shift from birds to humans (Waters et al. , 1991). However, the *Haemosporidia* phylogeny research has flaws due to the small number of in-group species included in the phylogenetic analysis and the use of 18S rDNA sequences (Martinsen et al. , 2008). In subsequent research, *Plasmodium reichenowi*, a parasite isolated from a chimpanzee, was found to be *P. falciparum*'s closest sister taxon. According to Escalante and Ayala, these two parasites may have diverged simultaneously as humans and chimps, and *P. falciparum* did not originate straight from the malarial parasite of avian origin. Despite this, the parasites *P. falciparum* and *P. reichenowi* were assumed to represent a sister lineage of parasites seen in birds and reptiles (Escalante and Ayala, 1994). Some concluded that the said clade should be in the mammalian group due to its closeness to primates/rodent *Plasmodium* (Ayala et al. , 1999, Leclerc et al. , 2004), while others drew similarity to parasites from birds (Kissinger et al. , 2002, McCutchan et al. , 1996, Rathore et al. , 2001). Due to biases in the portrayal of particular species, the few loci numbers studied, and poor rooting, there was so much disagreement over the origin of *P. falciparum*. Finally, it was only later that the origin of *P. falciparum* was proven by adding more taxa from primates (particularly great apes). In brief, Liu *et al.*, in September 2010, published research on species of *Plasmodium* diversity in African Great Apes built on a substantial stockpile of faecal samples from three subspecies of chimps (*P. t. schweinfurthii*, *P. troglodytes*, and *P. troglodytes ellioti* [also called *P. t. vellerosus*]), bonobos, and two subspecies of gorillas, *G. gorilla graueri* and *G. gorilla gorilla*. Their findings concluded that there are six *Plasmodium* species in the *Laverania* subgenus: three in chimps (designated C1–C3) and three in gorillas (designated G1–G3). These species have been described before; however, due to the enhanced collection depth, this research gives a more comprehensive picture of the variety of

*Laverania* species infecting the Great Apes. This study confirms explicitly the presence of a wide range of *P. falciparum*-related parasites in gorillas but finds none in natural populations of chimps or bonobos. This latter observation contradicts all previous ideas by pointing to a gorilla origin for human *P. falciparum* (Liu et al. , 2010).



**Figure 6:** The *Laverania* subgenus phylogeny based on partial *CytochromeB* sequences and strains isolated. (Prugnolle et al. , 2011b)





**Figure 7:** Distribution of various subspecies of bonobos, chimps, and gorillas in Africa, as well as depiction of *Plasmodium* species dispersion in these subspecies. (Prugnolle et al., 2011b)

## D. The family tree: Species of *Plasmodium*

Malaria is a parasitic ailment spread by mosquitoes and caused by the unicellular parasite *Plasmodium*. They are obligate intracellular parasites that infect and proliferate in RBCs after a clinically silent liver replication phase. *Plasmodia* belong to the phylum 'Apicomplexa', and their evolution from the 'Coccidian' stem includes the incremental addition of more complex life-cycle stages restricted to a single host. Finally, for these parasites to survive, they must complete their life cycle in two different, evolutionarily distinct hosts (namely, mosquito and human). Within the sub-order *Haemosporidiidea*, the genus *Plasmodium* is separated into the sub-genus *Plasmodium* and *Laverania*.

<b>Domain</b>	Eukaryota
<b>Kingdom</b>	Chromalveolata
<b>Superphylum</b>	Alveolata
<b>Phylum</b>	Apicomplexa
<b>Class</b>	Aconoidasida
<b>Order</b>	Haemosporida
<b>Sub-order</b>	Haemosporidiidea
<b>Family</b>	<i>Plasmodiidae</i>
<b>Genus</b>	<i>Plasmodia</i>
<b>Sub-genus</b>	<i>Plasmodium; Laverania</i>
<b>Species</b>	<i>P. falciparum</i> <i>P. malariae</i> <i>P. ovale</i> <i>P. vivax</i> <i>P. knowlesi</i>

**Table 1:** Classification of human protozoa of the genus *Plasmodium*.



*Plasmodium falciparum*, *Plasmodium vivax*, *Plasmodium malariae*, and *Plasmodium ovale* are the four species of *Plasmodium* that are known to cause human malaria. Several simian species, including *P. cynomolgi bastianelli*, *P. cynomolgi cynomolgi*, *P. brasilianum*, *P. simiovale*, *P. schwetzi*, *P. knowlesi*, and *P. inui*, can infect humans either naturally or inadvertently (H. M. Gilles, 1993). Since 2004, the latter has emerged as a significant cause of human malaria in Southeast Asia, mainly Malaysian Borneo (Singh et al. , 2004). *Plasmodium* has been officially classified into ~200 species, each infecting a different set of hosts.

Characteristics	<i>P. falciparum</i>	<i>P. knowlesi</i>	<i>P. malariae</i>	<i>P. ovale</i>	<i>P. vivax</i>
<b>Pre-erythrocytic stage (days)</b>	5–7	8–9	14–16	9	6–8
<b>Pre-patent period (days)</b>	9–10	9–12	15–16	10–14	11–13
<b>Erythrocytic cycle (days)</b>	48	24	72	50	48
<b>Red cells affected</b>	All	All	Mature erythrocytes	Reticulocytes	Reticulocytes
<b>Parasitaemia (per µL)</b>					
• <b>Average</b>	20,000–500,000	600–10,000	6000	9000	20,000
• <b>Maximum</b>	20,00,000	2,36,000	20,000	30,000	1,00,000
<b>Febrile paroxysm (hours)</b>	16–36 or longer	8–12	8–10	8–12	8–12
<b>Severe malaria</b>	Yes	Yes	No	No	Yes
<b>Relapses from liver forms</b>	No	No	No	Yes	Yes
<b>Recurrences</b>	Yes (treatment failure)	Yes	Yes (as long as 30–50 years after primary attack)	No	Yes (poor care)

**Table 2:** Infection characteristics of five species of *Plasmodium* infecting humans.

*Plasmodium* contains three genomes: a nuclear genome with 14 linear chromosomes, a circular plastid genome of 35 kb housed in the apicoplast obtained from red algae, and a linear mitochondrial genome, one of the smallest known.

- *Plasmodium falciparum*

*Plasmodium (Laverania) falciparum* (Welch, 1896) is the parasite that causes malaria in humans. It is very virulent and lethal. It was first found in 1880 by Charles Alphonse Laveran, an Army Surgeon of French origin stationed in Constantine (Algeria), and termed *Oscillaria malariae* by him (Cook, 2007). *P. falciparum* malaria is endemic in 85 countries, with 2.57 billion people living in areas where the virus can spread (Guerra et al. , 2008). 1.44 billion people live in areas with reliable transmission, primarily in Africa (which accounts for 52% of the total worldwide) and South, Central, and East Asia (about 46%) (Gething et al. , 2011). Estimating the clinical malaria burden caused by *P. falciparum* is a complex task made more difficult by various factors, including insufficient and incomplete national reporting systems and erroneous diagnoses that could lead to overestimating disease rates.

*P. falciparum*'s whole genome was sequenced and made public in 2002, marking a considerable advancement in the fight against this deadly parasite (Gardner et al. , 2002). The nuclear genome, organised into 14 linear chromosomes, contains around 5,365 genes, of which 1,817 are known to have functions. Only 334 (18.5%) of the 1,817 functional genes of *P. falciparum* were unique to the former species, with 81.6% conserved with those of *P. vivax* (Sharma et al. , 2010). *P. falciparum* genome includes more A+T than *P. vivax* and *P. knowlesi*. Although it has the smallest genome size, it has the most simple sequence repeats or SSRs, which are assumed to be accountable for genomic complexity and fast evolutionary flexibility (Tyagi et al. , 2011). The proteome analysis of the four phases of the parasite life cycle (sporozoite, merozoite, trophozoite, and gametocyte) revealed that nearly 50% of the sporozoite proteins are unique to this stage. In contrast, merozoite, trophozoite, and gametocytes had between 20% to 30% unique proteins. Furthermore, just 152 proteins (6%) were detected in all four major stages, and the significant proteome diversity of each step of the *Plasmodium* life cycle revealed that genes involved in the standard processes were expressed in a highly coordinated manner (Florens et al. , 2002).

The exoerythrocytic schizogony in *P. falciparum* is a quick process that usually takes 5.5 days and results in the formation of a schizont with weird shapes and many merozoites. Each liberated merozoite invades an erythrocyte following the rupture of liver schizonts, a complex process that necessitates the identification of receptors (on the erythrocyte) and ligands (on the merozoite). Early research on *P. falciparum* revealed sialic acid, glycophorin A, B, and C as putative merozoite invasion receptors (Deas and Lee, 1981, Miller et al. , 1977, Pasvol et al. , 1982). In 2010, a sialic acid-independent erythrocyte receptor for *P. falciparum* adhesin PfRh4, called complement receptor 1 (CR1), was discovered. None of the parasite strains studied showed these receptor-ligand pairings to be critical (Tham et al. , 2010).

The presence of immature rings in the blood is a symptom of erythrocytic schizogony, although the maturation stages are seldom observed in the peripheral circulation. The infected erythrocytes do not increase throughout development, and the mature schizont comprises typically 8–32 merozoites. *P. falciparum* gametocytes multiply in the internal organs for eight to ten days after parasitaemia begins. Five morphologically different substages of *P. falciparum* gametocytogenesis have been identified (Hawking et al. , 1971). Only adult crescent-shaped *P. falciparum* gametocytes (Stage V) are released into the bloodstream, infecting mosquitoes. In contrast, immature *P. falciparum* gametocytes (Stages I–IV) are kept out of circulation (Bousema and Drakeley, 2011).

Human *P. falciparum* genome comprises a single lineage within the G1 clade of gorilla parasites, according to a 2010 research, showing that human *P. falciparum* is of gorilla rather than chimp origin (Hafalla et al. , 2011). Furthermore, multiple studies have shown that *P. falciparum*, which was previously thought to be solely human eccentric, may transmit to gorillas, chimps, and bonobos, suggesting that these African apes could serve as a viable tank for the malignant form of human malaria (Prugnolle et al. , 2011a, Prugnolle et al. , 2010, Rayner et al. , 2011).

- *Plasmodium vivax*

*Plasmodium vivax* (Grassi and Feletti, 1890) causes "benign tertian fever," yet some subsequent reports have cast doubt on the lack of life-threatening consequences associated with this infection (Baird, 2007). In 1886, Camillo Golgi categorised it as a separate malaria parasite from *P. malariae* after reporting the classic 'tertian' and

'quartan' fever paroxysms and refuting Laveran's assumption of the existence of one malaria species (Golgi, 1886).

The complete genome of the *P. vivax* Salvador I strain was sequenced and released in the year 2008; its nuclear genome is more significant than that of *P. falciparum*, at 26.8 megabytes (Mb), and it has chromosomes with an isochore structure that is unique among human *Plasmodium* species (Carlton et al. , 2008). It contains the most GC-rich *Plasmodium* genome sequenced (42.3%), with 5,433 predicted protein-coding genes. A recent proteome investigation of *P. vivax* identified seven proteins that were wholly unique to *P. vivax* and 16 proteins that had no similarity with *P. falciparum* (2 *Vir* and 8 *P-fam* proteins), all of which are likely involved in *P. vivax* virulence/ antigenicity (Acharya et al. , 2011).

*Plasmodium vivax* is a tropical parasite with a low infection rate in central and western Sub-Saharan Africa. According to current estimates, *P. vivax* transmission is hazardous to 40% of the world's population, resulting in 130–435 million vivax malaria clinical episodes per year (Guerra et al. , 2010). The number of simian malaria species present in Southeast Asia and biological and physical similarities between *P. vivax* and macaque parasites has been used to put the emergence of *P. vivax* in Southeast Asia (P. C. C. Garnham, 1967). The significant prevalence of 'Duffy negativity' (the lack of the Duffy blood type antigen) in human populations across Sub-Saharan Africa has been proposed as evidence for *P. vivax*'s African origin (Carter, 2003). *P. vivax* was incorporated into *Homo sapiens* in Asia by a *Plasmodium* parasite present in macaques, and the data from entire mitochondrial genomes, nuclear genes, and plastid genes proves the same (Escalante et al. , 2005, Jongwutiwes et al. , 2005).

*P. vivax* sporozoites in the liver develop into either early /primary tissue schizonts or hypnozoites, which cause late infection relapse (Krotoski, 1985, Krotoski et al. , 1980). All forms of *P. vivax* can be seen in the peripheral blood during erythrocytic development, and their appearance is more significant than that of other human *Plasmodia* species at most stages. It is also responsible for boosting the deformability of host cells by causing them to expand (H. M. Gilles, 1993). Because the parasite likes to infect young red blood cells (reticulocytes), its reproductive capability appears limited, as parasitemia levels seldom exceed 2% of circulating erythrocytes. Since *P. vivax* merozoites must interact with the "Duffy antigen receptor for

chemokines (DARC)" to infiltrate erythrocytes, Duffy-negative people are assumed to be naturally immune to the human *P. falciparum* (Miller et al. , 1976). Although the very high number of Duffy-negative persons in Central and West Africa has long been regarded as the most likely reason for *P. vivax* malaria scarcity in those regions, the parasite appears to have discovered a way around it (Mendes et al. , 2011). The immature trophozoite proliferates and produces the characteristic malaria pigment; after that, it takes on amoeboid characteristics, and a huge vacuole forms a "hole" within the ring until the nucleus divides. The adult schizont has 12 to 18 merozoites and fills the host cell (H. M. Gilles, 1993, P. C. C. Garnham, 1967). The production of gametocytes is assumed to begin with the formation of *P. vivax* merozoites and can be observed within three days of the discovery of the initial asexual parasites (Bousema and Drakeley, 2011). After fertilisation, the sexual cycle in the *Anopheles* mosquito requires 16 days at 20°C and 8–10 days at 28°C, although the sporogonic process is unlikely to be completed below 15°C (H. M. Gilles, 1993).

- *Plasmodium ovale*

*Plasmodium ovale* was discovered in an East African patient with malaria RBCs having an oval shape with fimbriated borders in 1922, and the malaria parasite was given the name *P. ovale* by Stephens (Stephens, 1922). Based on the sequences of the small subunit ribosomal RNA (SSUrRNA) gene, it has been revealed that *P. ovale* belongs to two distinct haplotypes: variant and classic (Win et al. , 2004). Sutherland and colleagues proposed the names *P. ovale wallikeri* (variant type) and *P. ovale curtisi* (classic type) after two malariologists, David Walliker (1940–2007) and Christofer Curtis (1939–2008) (Su, 2010, Sutherland et al. , 2010). *P. ovale* can be found in Sub-Saharan Africa, Southeast Asia (Vietnam, Philippines, Thailand, and Myanmar), the Indian subcontinent, the Middle East, Indonesia's East Timor, and Papua New Guinea (Mueller et al. , 2007). Between the injection of sporozoites and the initial detection of parasites in peripheral blood, *P. ovale* has a prepatent period of 12 to 20 days, with an average of 14.5 days. Due to the restricted growth of younger erythrocytes, parasitaemia is usually modest during *P. ovale* infection. It induces erythrocytic changes like those found in *P. vivax*, whereas schizonts and gametocytes may resemble those of *P. malariae*. At 28°C, the mosquito's sporogonic cycle takes 12–14 days to complete. *P. ovale* is thought to be the cause of a recurring infection that begins in the liver as latent ("hypnozoites") exoerythrocytic stages (Collins and Jeffery, 2005, H. M. Gilles, 1993).

- *Plasmodium malariae*

*Plasmodium malariae* (Laveran, 1880), the parasite that causes "quartan malaria," exists all over the world's major malaria-endemic areas, albeit in a scattered distribution (Collins and Jeffery, 2007, Mueller et al., 2007). *P. malariae* infections are significantly prevalent in Sub-Saharan Africa and the southwest Pacific and least common in the Middle East, Asia, and South and Central America. In 1886, Camillo Golgi explained the relationship between the development cycle (48 and 72 hours, respectively) and the frequency of fever paroxysm in *P. vivax* and *P. malariae* (Golgi, 1886).

The *Anopheles* mosquito (15 days) and humans (15 days in the liver, 72 hours in the blood) have a modest development rate for the parasite. *P. malariae* is assumed to be the progenitor of *P. brasilianum*, a parasite that infects and has naturally adapted to New World monkeys; both can infect monkeys and humans (H. M. Gilles, 1993). The prepatent period for *P. malariae* varies greatly, ranging from 16 to 59 days. *P. malariae* has no quiescent liver stage forms. Still, it can remain in the blood with low levels of parasitaemia for extraordinary lengths of period, possibly for the lifetime of the human host, producing recrudescence even after 30–40 years or longer. At 20°C, the *Anopheles* mosquito's sporogonic cycle takes 30–35 days, while at 28°C, it might take less than 14 days (Chadee et al. , 2000, Collins and Jeffery, 2007, Vinetz et al. , 1998).



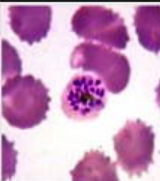
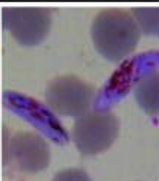
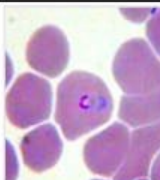
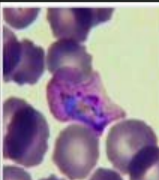
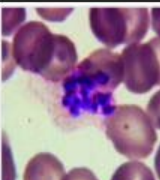
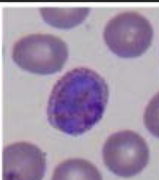
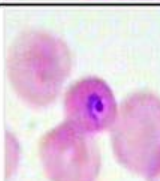
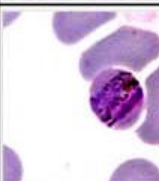

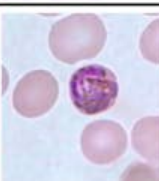

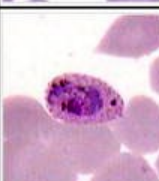
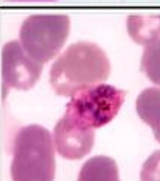
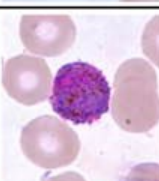

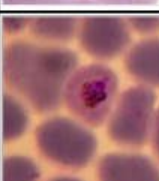
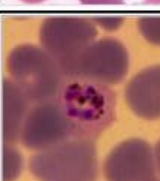
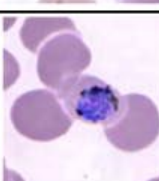
- *Plasmodium knowlesi*

*Plasmodium knowlesi* (Sinton and Mulligan 1932) is a simian *Plasmodium* that was possibly initially discovered in the blood of *Macaca fascicularis* by the Italian malariologist Giuseppe Franchini. It was then examined by Napier, Campbell, Das Gupta, and Knowles before being entirely defined by Sinton and Mulligan, who coined it *P. knowlesi* in tribute to Dr Knowles's pioneering work (Coatney GR, 1971, Knowles and Gupta, 1932) (Sinton and Muliigan, 1933). In terms of phylogeny, *P. knowlesi* is more closely linked to *P. vivax* than other human *Plasmodia*, and the process of merozoites entering erythrocytes requires the association of Duffy-binding proteins (DBP) with the 'Duffy antigen receptor for chemokines (DARC)' (Chitnis and Miller, 1994, Singh et al. , 2003). However, there are significant phenotypic differences between *P. vivax* and other parasites, like host blood cell



preference, the absence of a latent liver stage, and asexual cycle length. *P. knowlesi*'s genome has been sequenced (Pain et al. , 2008). *P. knowlesi* was the first malaria parasite with antigenic variation discovered (Brown and Brown, 1965). It causes human malaria in many parts of Southeast Asia and the Malaysian Borneo peninsula (Kantele and Jokiranta, 2011).

The principal natural hosts of *P. knowlesi* are pig-tailed macaques (*M. nemestrina*) and long-tailed (*Macaca fascicularis*). Following infection, all phases of *P. falciparum*'s life cycle are visible in the peripheral blood. It takes 24 hours for an intra-erythrocytic lifecycle to complete (unique for all malaria parasites of primates) (Chin et al. , 1965, Coatney GR, 1971). The immature ring forms are similar to those observed in *P. falciparum* infection. In contrast, the intra-erythrocyte parasites are similar to the band forms seen in *P. malariae* infection at later stages of maturity (Singh et al., 2004). There are as many as 16 merozoites in a mature schizont, with a mean of ten. The sexual forms grow more slowly than the asexual forms, requiring around 48 hours to complete; the macrogametocyte is spherical with blue-stained cytoplasm and fills the host cell after maturation, whereas the microgametocyte is smaller and has pink-stained cytoplasm (Brown and Brown, 1965). *P. knowlesi* has been linked to a high degree of parasitaemia and severe symptoms similar to *P. falciparum* malaria, with a potentially fatal outcome (Cox-Singh et al. , 2008).

Human Malaria					
Stages Species	Ring	Trophozoite	Schizont	Gametocyte	
<i>P. falciparum</i>					<ul style="list-style-type: none"> <li>Parasitised red cells (pRBCs) not enlarged.</li> <li>RBCs containing mature trophozoites sequestered in deep vessels.</li> <li>Total parasite biomass = circulating parasites + sequestered parasites.</li> </ul>
<i>P. vivax</i>					<ul style="list-style-type: none"> <li>Parasites prefer young red cells</li> <li>pRBCs enlarged.</li> <li>Trophozoites are amoeboid in shape.</li> <li>All stages present in peripheral blood.</li> </ul>
<i>P. malariae</i>					<ul style="list-style-type: none"> <li>Parasites prefer old red cells.</li> <li>pRBCs not enlarged.</li> <li>Trophozoites tend to have a band shape.</li> <li>All stages present in peripheral blood</li> </ul>
<i>P. ovale</i>					<ul style="list-style-type: none"> <li>pRBCs slightly enlarged and have an oval shape, with tufted ends.</li> <li>All stages present in peripheral blood.</li> </ul>
<i>P. knowlesi</i>					<ul style="list-style-type: none"> <li>pRBCs not enlarged.</li> <li>Trophozoites, pigment spreads inside cytoplasm, like <i>P. malariae</i>, band form may be seen</li> <li>Multiple invasion &amp; high parasitaemia can be seen like <i>P. falciparum</i></li> <li>All stages present in peripheral blood.</li> </ul>

**Figure 8:** In a thin blood film, five different human malaria *Plasmodium* species and their life phases. (Poostchi et al. , 2018)



## **E. From an epidemiological point of view**

Malaria remains the most common parasite disease worldwide despite comprehensive control and elimination methods conducted through international and national malaria control programmes. Hundreds of millions were infected with malaria, tens of millions perished (mainly in Sub-Saharan Africa), many thousands of pregnant women died during delivery owing to malaria-related problems, and millions of infants were born with low birth weight, resulting in premature death or disability. On the other hand, the first two decades of the new century have been dubbed the "Golden Age of Malaria Control." According to the World Health Organization's (WHO) most current annual global malaria report in 2022, an approximated 247 million malaria cases were reported in 84 malaria-endemic countries (including French Guiana), up from 245 million in 2020, with the majority of the rise coming from the WHO African Region. Two hundred thirty million malaria cases were estimated at the Global Technological Strategy for Malaria 2016–2030 (GTS) baseline 2015. Malaria incidence (cases per 1000 people at risk) decreased from 82 in 2000 to 57 in 2019 before rising to 59 in 2020. The rise in 2020 was linked to service disruptions during the COVID-19 epidemic.

Twenty-nine countries accounted for 96% of worldwide malaria cases, with Mozambique (4%), Uganda (5%), the Democratic Republic of the Congo (12%), and Nigeria (27%) accounting for nearly 50% of all cases. The WHO South-East Asia Region was responsible for around 2% of all malaria cases worldwide. Malaria cases have decreased by 76%, from 23 million in 2000 to about 5 million in 2021. Malaria cases have reduced by 82% in this region, from around 18 cases per 1000 people at risk in 2000 to roughly 3 cases in 2021. Malaria cases decreased by 38% in the WHO Eastern Mediterranean Region, from over 7 million in 2000 to around 4 million in 2015. Cases increased by 44% between 2016 and 2021. In 2021 the WHO Western Pacific Region was expected to have 1.4 million cases, down 49% from the 3 million cases in 2000. In 2021, China was declared malaria-free, and Malaysia had no instances of non-zoonotic malaria for four years. Malaria infections fell by 60%, and case incidence fell by 70% in the WHO Americas Region between 2000 and 2021. In recent years, the region's development has been hampered by a significant spike in malaria in the Bolivarian Republic of Venezuela. In 2016, Sri Lanka was declared malaria-free, and it remains so. Malaria-free status has been maintained in the WHO European Region since 2015. India was responsible for 79% of the cases (World

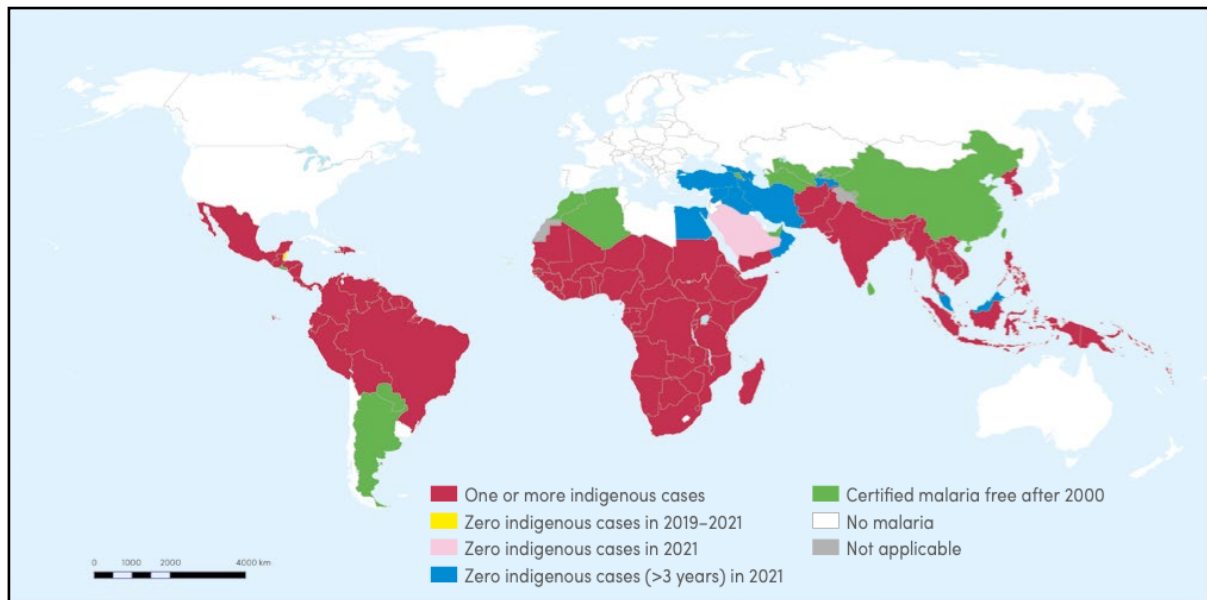
Health Organization. *World Malaria Report*; WHO: Geneva, Switzerland, 2021). The frequency of malaria infections and deaths in India increases during the summer and fall monsoon seasons (Baghbanzadeh et al. , 2020, Singh et al. , 2009). Around 95% of India's population live in malaria-endemic areas, with malaria cases of about 80% occurring in about 20% of people living in rural, hilly, and difficult-to-access regions (World Health Organization. *World Malaria Report*; WHO: Geneva, Switzerland, 2019).

Malaria mortality decreased steadily worldwide from 2000 to 2019. Malaria mortality increased by 12% in 2020 compared to 2019 owing to service interruptions during the COVID-19 epidemic, reaching an estimated 619,000 deaths. In all, 29 nations accounted for 96% of malaria fatalities worldwide. In 2021, four countries accounted for slightly over half of all malaria fatalities worldwide: the United Republic of Tanzania (4%), Niger (4%), the Democratic Republic of the Congo (13%), and Nigeria (31%). In the WHO South-East Asia Region, India accounted for nearly 83% of all malaria fatalities. In 2020, the percentage of overall malaria mortality in children under five was around 76%.

The newest global malaria study also revealed two more critical areas of concern. In 11 countries (United Kingdom (imported cases), Equatorial Guinea, China, Ethiopia, Myanmar, Ghana, Sudan, Zambia, Nigeria, Uganda and Tanzania), deletions in the *P. falciparum* histidine-rich protein *pfhrp2* and *pfhrp3* genes have been established (World Health Organization. *World Malaria Report*; WHO: Geneva, Switzerland, 2021). As a result, quick diagnostic procedures relying on *HRP2* detection cannot detect the parasites. *PfKelch13* mutations that provide fragmented resistance to artemisinin, the first-line therapy for *P. falciparum* infections, have also been discovered. Another drug resistance has arisen in malarial parasites (antifolates, naphthoquinones, antibiotics such as clindamycin and doxycycline, and 4-aminoquinolines), and a few new targets for the development of new antimalarial medications have recently been found (Shibeshi et al. , 2020).

Imported malaria cases into malaria-free and non-endemic countries are quickly becoming recognised as a substantial public health concern for both developed and developing countries. The danger of vector-borne diseases like malaria has grown as the ecology and climate have changed due to global warming (Rossati et al. , 2016). In many malaria-free and non-endemic nations, the epidemiological characteristics

of imported malaria have evolved as a result of increased travel for business and pleasure, as well as migratory movements for jobs or owing to geopolitical conflicts (Loutan, 2003, Mischlinger et al. , 2020, Norman et al. , 2020).



**Figure 9:** In 2000, countries with indigenous instances were identified, and their status by 2021 was determined. (WHO Reports, 2022)

## **F. Life of a Malaria parasite**

Malaria is spread mainly through bites from infected *Anopheles* mosquitoes that have taken a blood meal from a parasitaemia patient. Contaminated blood transfusions, infected needles, transplantation, and transmission from a woman to her foetus during pregnancy are all less common ways to get infected.

All five species that infect people have a nearly identical life cycle, which is divided into three stages:

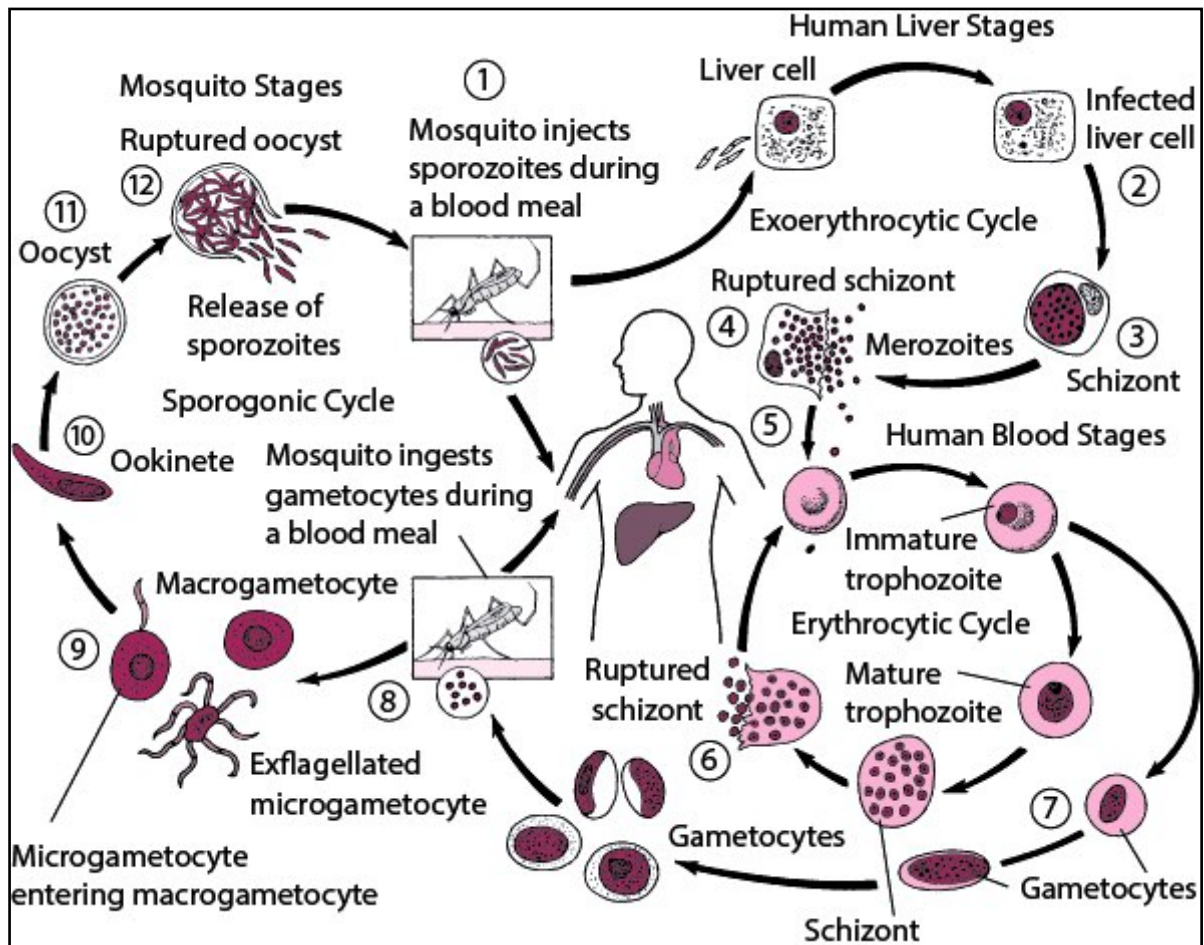
1. Sporozoite infection of a human
2. Asexual reproduction
3. Sexual reproduction

The first two stages occur solely in the body of a human, but the third stage begins in the human and ends in the mosquito.

- ❖ When a female *Anopheles* mosquito bites a person, sporozoites-infected saliva is injected into the circulation, resulting in human disease. This is the first **stage of infection**.
- ❖ The following step in the malaria life cycle is **asexual reproduction**, which is grouped into two phases: pre-erythrocytic/exoerythrocytic and erythrocytic. Sporozoites pass through blood circulation to the liver (first target) within 30-60 minutes of parasite inoculation. In 6-7 days, the sporozoites enter the liver cells and begin dividing, forming schizonts. Each schizont produces thousands of merozoites (exoerythrocytic schizogony), which are discharged into the bloodstream, signalling the termination of the asexual reproductive stage's exoerythrocytic phase. However, sporozoites from *P. ovale* and *P. vivax* may not complete the reproductive process and stay latent in the liver (hypnozoites); they may then be awakened after a lengthy period, resulting in relapses entering the bloodstream (as merozoites) for weeks, months, or even years later. The liver phase is not pathogenic and has no signs or indicators of sickness. Based on the parasite species, the period varies. Merozoites discharged into the bloodstream are directed to the red blood cells, their second target (RBCs). They signal the start of the erythrocytic phase by invading the cells. The ring stage, which

transforms into a trophozoite, is the first stage after the invasion. Because trophozoites cannot digest heme, they convert it to haemozoin and digest globin, a source of amino acids for reproduction. The erythrocytic schizont is the next cellular stage (at first, immature and then mature schizont). Each adult schizont undergoes erythrocytic schizogony, and new generation merozoites are formed, which are released into the circulation when RBCs rupture to infect additional RBCs. When parasitaemia and clinical symptoms arise, this is the time to act. The liver phase only happens once, whereas the erythrocytic phase occurs several times; the release of merozoites after each cycle causes the febrile waves.

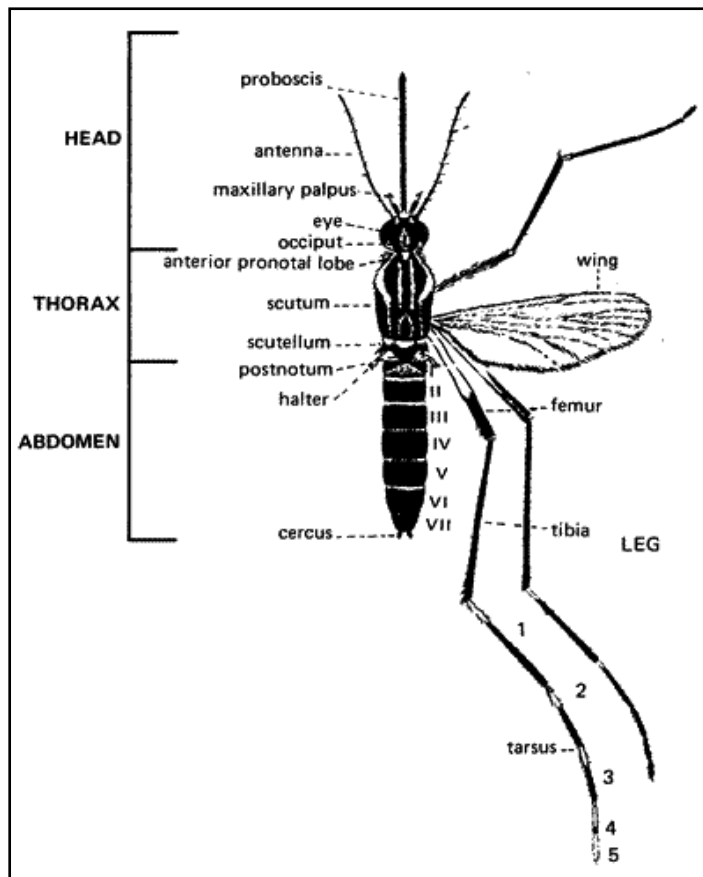
- ❖ The **sexual reproductive stage** in RBCs is the second scenario; the parasite differentiates into male and female gametocytes, a non-pathogenic version of the parasite. The gametocytes are taken up with the blood meal when a female *Anopheles* mosquito bites an infected individual (mosquitoes can only be infected if they feed when gametocytes are in circulation in human blood). During a process known as gametogenesis, the gametocytes mature and form microgametes (male) and macrogametes (female). For each *Plasmodium* species, the gametocyte maturation time varies from 8-10 days for *P. falciparum*, 6-8 days for *P. malariae*, and 3-4 days for *P. ovale* and *P. vivax*. The microgamete nucleus divides thrice in the mosquito gut, yielding eight nuclei; each nucleus fertilises a macrogamete, making a zygote. The zygote becomes the so-called ookinete after the nuclei fuse. The ookinete then penetrates the mosquito's midgut wall, which encysts into an oocyst development. The ookinete nucleus divides inside the oocyst, producing thousands of sporozoites (sporogony). The third stage (sexual reproduction/sporogony) has ended. Sporogony can persist anywhere from 8 to 15 days. Only a few hundred sporozoites make it to the salivary glands of the mosquito when the oocyst ruptures. As a result, when the infected mosquito eats blood, it injects its contaminated saliva into the next target, starting a new cycle.



**Figure 10:** Lifecycle of *Plasmodium*. (Courtesy: *Malaria* chapter by Richard D. Pearson)



## G. The malign transporter: *Anopheles et. al.*



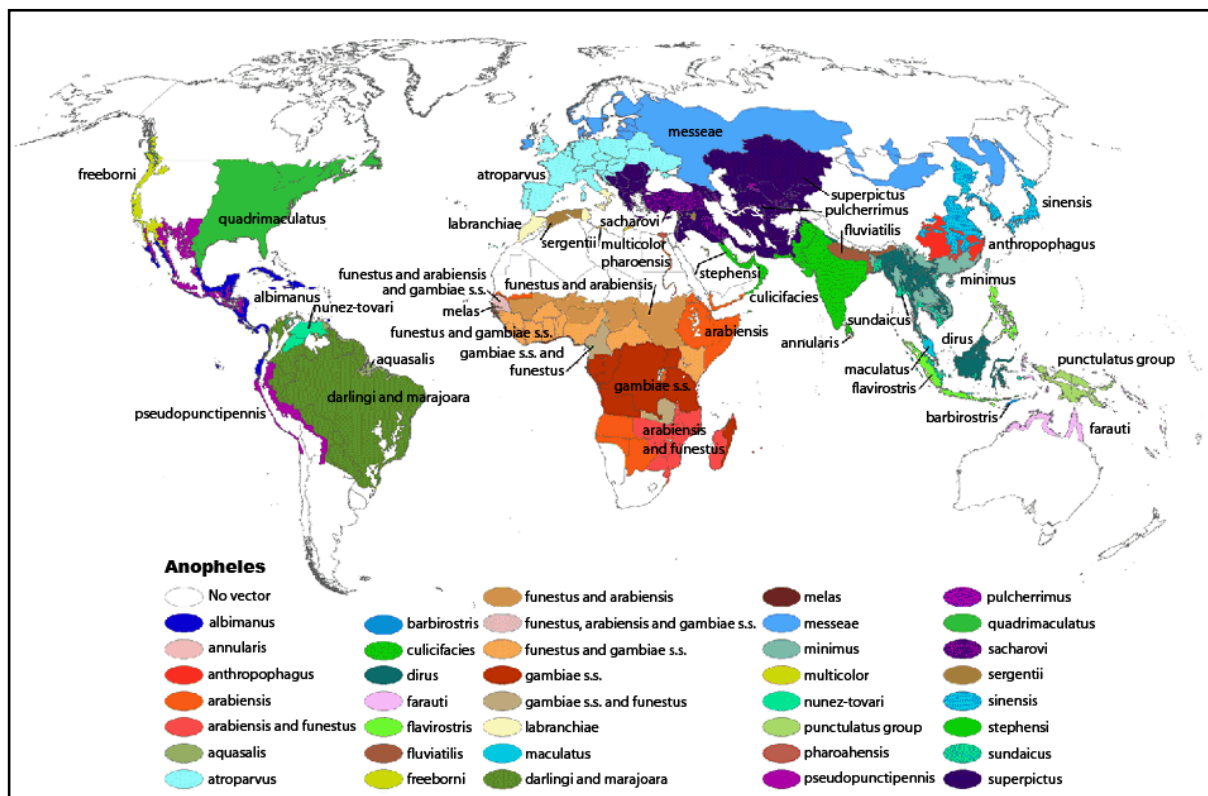
**Figure 11:** Female adult mosquito. (Courtesy: Global Health, Division of Parasitic Diseases and Malaria, CDC)

Little study on *Anopheles* taxonomy was done until the discovery that mosquitoes transmit microfilariiae and malarial protozoa in the last two decades of the nineteenth century, which sparked a rush to collect, name, and categorise these insects. Johann Wilhelm Meigen, a German entomologist known for his groundbreaking Diptera investigations, first described *Anopheles* as a mosquito genus in 1818. Between 1901 and 1910, Frederick V. Theobald wrote a book on the world's mosquitoes, published in five volumes.

The *Plasmodium* species, the causative agents of malaria, are transmitted by mosquitoes of the *Anopheles* genus. More than

400 species of *Anopheles* mosquito have been identified, with roughly 70 of these being prospective malaria vectors (Sinka et al. , 2012). *Anopheles* (cosmopolitan, 182 species), *Cellia* (Old World, 220 species), *Baimaia* (Oriental, one species), *Lophopodomyia* (Neotropical, six species), *Kerteszia* (Neotropical, 12 species), *Stethomyia* (Neotropical, five species) and *Nyssorhynchus* (Neotropical, 39 species) are the seven sub-genera of genus *Anopheles*. *Anopheles*, *Nyssorhynchus*, *Kerteszia*, and *Cellia* are four sub-genera that transmit human malaria parasites. It has been shown that the bulk of *Anopheles* vector species are complexes of sister species. A natural vector's life cycle begins when a female *Anopheles* mosquito feeds a gametocytic parasite forms found in the blood of an infected vertebrate host.

Classifying a mosquito as a vector must demonstrate anthropophilicity and have the same *Plasmodium* species/strain as in patients from the exact geographic location. *Plasmodium* oocysts in the midgut of a mosquito indicate parasite foundation in a field susceptible vector. Sporozoites in the dissected mosquito salivary gland suggest that the *Plasmodium* parasite has completed its life cycle and may be transferred to humans by a bite. Furthermore, the infection rate (*i.e.*, the percentage of *Plasmodium*-infected individuals in a mosquito population) is critical in interpreting malaria dynamics and transmission biology in a specific geographic location. On the other hand, the presence of an apparent plenitude of a species in the ingested blood meal is inadequate to incriminate a mosquito as a vector (Smith et al. , 2014).



**Figure 12:** Dominant or Potentially Important Malaria Vectors: Global Distribution (Robinson Projection). (Kiszewski et al. , 2004)



## H. Disease pathogenesis & phenotypic manifestations

### ❖ Pathogenesis

Pathogenesis, or the process by which the disease develops for a human malaria clinical sickness, is a complicated narrative with numerous characters, settings, and possible outcomes. The observed effect of evolution in malaria, as with any truly effective parasite, is an undisturbed passage from mosquito to human to mosquito with very little influence on the host and vector. Though malaria impacts individuals, communities, countries, and the world, from the parasite's angle, a healthy host serving two blood meals with a touch of fever in between is the standard. Many factors outside the parasite influence how, where, and why various disease states originate (or dissipate), most of which are under human control.

The six malaria parasites that infect humans (*P. vivax*, *P. falciparum*, *P. ovale wallickeri*, *P. ovale curtisi*, *P. knowlesi*, and *P. malariae*) go through ten or more morphological states, replicate from single to 10,000+ cells, and have a population ranging from one to  $>10^6$  cells during the mosquito–human life-cycle (Cator et al. , 2012, Josling and Llinas, 2015, Liu et al. , 2011, Mohandas and An, 2012, Stone et al. , 2015). A tiny number of these morphological stages induce clinical illness in humans, and the vast majority of malaria patients across the globe have fewer symptoms (WHO. 2015. World malaria report 2015. World Health Organization, Geneva.). Fever, anaemia, and coma are examples of human clinical diseases caused by the parasite's pre-programmed biology working with the human pathophysiological reaction (Hafalla et al., 2011, Oakley et al. , 2011). Parasite genetic diversity of crucial proteins, co-infections, co-morbidities, treatment delays, human polymorphisms, and environmental variables are all caveats and corollaries that contribute variance to this host-parasite interaction (Goncalves et al. , 2014).

#### • Uncomplicated Malaria

According to the WHO, uncomplicated malaria is characterised as having symptoms (fever), but no clinical or test evidence indicates the severity of vital organ dysfunction. The first hepatic schizont rupture and discharge of merozoites into the peripheral circulation can only start the symptoms of malaria infection in any sick patient. This event will go unnoticed by most persons who will become clinically ill.

As the parasites strive through their asexual life cycle of merozoite invasion, trophozoite growth, and schizont rupture over 24 - 48 hours, the degree of parasitaemia reflects the amount of human reaction (fever, tumour necrosis factor [TNF- $\alpha$ ] and C-reactive protein [CRP]) until the patient exceeds a threshold of awareness and "feels unwell." (Oakley et al., 2011). Uncomplicated malaria is easily treated with antimalarials specific to the parasite during each symptomatic episode, and most of the patients resolve the infection with adequate treatment and adherence.

*P. falciparum* (Pf) causes malaria by altering the surface of infected red blood cells and developing a sticky phenotype, which keeps the parasite out of circulation for about half of its asexual life cycle, which is rare for malaria parasites (Grau and Craig, 2012). Infected erythrocytes can attach to the platelets, endothelium, or uninfected red blood cells (Fairhurst and Wellem, 2006). The parasite's cytoadherent ("sticky cell") state is caused by Pf erythrocyte membrane protein 1 (PfEMP1), which is generated via *var* gene transcription (Smith et al. , 2013). The gene(s) above are among the most varied in the parasite's genome and population. Immune selection pressure and epigenetics are two methods that control their expression. *Var* gene expression is a feature of the parasite's biology that occurs in all infections, even in asymptomatic and uncomplicated malaria. Regardless of disease variation, Pf sequestration (temporary removal of the parasite from circulation by red cell surface attachment) occurs with every human infection for half of the asexual life cycle. In a low-level infection, when a single mosquito bite has transmitted a single brood of synchronous parasites, patients may have negative peripheral blood smears. This may be true for travellers or those living in low-endemicity areas. On the other hand, patients in highly endemic areas may be bitten frequently and appear with persistent fever and a persistently positive blood smear.

Unlike *P. falciparum*, but like all other human malaria parasites, *Plasmodium vivax* (Pv) does not suffer lengthened sequestration post-infection (Costa et al. , 2011). As a result, the parasite is more likely to be cleared by the spleen and seen on a peripheral blood smear during an infection. The attraction for reticulocytes is one of Pv's distinctive traits, as is the use of the Duffy antigen for invasion, but not solely (Moreno-Perez et al. , 2013, Zimmerman et al. , 2013). The amoeboid form of Pv is the diagnostic form, having finger-like extensions in the cytoplasm that are specific to Pv and lack the standard round-to-oval structure. Patients come with fever and

several other symptoms identical to those seen in other malaria infections. Unlike Pf and *P. malariae*, Po (*P. ovale*) and Pv may "re-emerge" when hypnozoites (dormant forms that survive months to years in the liver after a single sporozoite exposure) discharge merozoites (which have a single hepatic schizont rupture shortly after sporozoite invasion). As a result, the clinical onset of an illness (months to years after exposure) may be a pointer to one of these species.

Po's two sympatric species are impossible to distinguish, share clinical signs, and respond to treatment similarly. Despite their similar behaviour to Pv, Po does not need the Duffy blood group antigen for penetration into the RBCs. Po is diagnosed on a peripheral blood smear by the oval appearance of infected RBCs, the comet form of the trophozoite, and the presence of finger-like extensions of the red cell membrane. Po's ring, schizont, and gametocyte stages are strikingly identical to Pv's.

***P. malariae* (Pm)** is the mildest malaria infection, with multiple well-defined clinical attributes. Due to the prolonged parasite life cycle, sufferers have a fever every 72 hours during an infection. The quantity of merozoites produced with each schizont rupture is lower in these patients than in other types of malaria, and consequently, the parasitaemia is overall lower (Collins and Jeffery, 2005, Mueller et al., 2007). The immune response is more potent because of the long life cycle and low degree of infection. As a result, Pm is frequently thought to be the source of chronic malaria, which can linger for decades. The accumulation of immunological complexes in the kidneys, which can lead to nephritis, is a specific complication of Pm (Das, 2008). Individuals with malaria symptoms and forms suggestive of Pm should be tested for *P. knowlesi* and Pf in the clinic since the chances of finding symptoms and co-infection are more significant than in asymptomatic Pm patients (Singh and Daneshvar, 2013).

***P. knowlesi* (Pk)** is found in Indonesian/Malaysian Borneo, with cases reported in other Southeast Asian countries. Contact with mosquitoes that nourish on long-tailed and pig-tailed macaques is required for transmission because no human-to-human (through mosquito) transference has been documented. The disease is characterised by fever, chills, headache, and atypical symptoms such as upper respiratory symptoms, nausea/vomiting, jaundice, and myalgia/arthritis. Because of Pk's recent emergence in humans (zoonosis) and the lack of time for human adaptation, lethal repercussions have happened and continue to occur at a higher

rate than Pv and Pf proportionately (Muller and Schlagenhauf, 2014, Singh and Daneshvar, 2013).

- **Severe Malaria**

*P. vivax*: Death from the disease is extremely rare during infection, with only Pv and no other co-morbidities. Severe illness and catastrophic results have been documented in the presence of co-morbidities. Chronic illness can induce severe anaemia and malnutrition, which predispose to co-infections and a weak immune response due to the relapsing pattern of the liver. The ultimate common pathway, like severe Pf and Pk (and any severe infection), might entail respiratory distress, hepato-renal failure, and shock. Coma has been documented with Pv infection on rare occasions. However, the reason is dissimilar in Pf infection, where the parasite sequestration to elevated measures in the brain is observed in terminal cases (Anstey et al. , 2012, Costa et al. , 2012).

*P. knowlesi*: Pk has a higher rate of severe disease (8%), proportionally, than Pf or Pv, and a higher mortality rate (3%). Pk-severe disease begins with the same symptoms as a mild disease, such as fever, and develops to include respiratory distress, hypotension, hyperbilirubinemia, acute renal failure, and shock (Antinori et al. , 2013). Coma is not usually present in Pk fatal cases, which is required for a Pf cerebral malaria diagnosis. The "common pathway" of any severe infection (e.g., bacterial sepsis, Pf, etc.) is caused by a heightened human immune reaction in the context of an untreated or delayed-in-treatment infection. It is unlikely to be attributable to organism-specific processes. Pk has been linked to other morbid illnesses, such as Gram-negative sepsis (Menezes et al. , 2012).

- **Cerebral Malaria**

The clinicopathological syndrome of cerebral malaria (CM) is caused by *P. falciparum*'s unique capacity to attach to endothelium in adults and children. Children under five are at maximum danger for the disease in highly endemic regions, with fatality rates ranging from 10% to 20%. In contrast, persons of all ages are at risk in low-endemic areas, with higher adult mortality rates. A modest amount of infection (1% parasitaemia) in the non-immune population (travellers) can cause clinical indications of CM, which can be fatal. CM symptoms may begin as

a standard malaria presentation and quickly develop into a comatose state (within minutes to hours). A clinical diagnosis of CM can be made by looking for indications of malaria retinopathy in the retina (Seydel et al. , 2015). At autopsy, *P. falciparum* parasites in more than 20% of brain capillaries, as assessed by histological sections or tissue smear, is the disease's diagnostic pathological characteristic (Taylor et al. , 2004). Ring haemorrhages, fibrin thrombi, axonal damage, darkening of the brain, and capillary leakage are other pathological signs that can be seen (Dorovini-Zis et al. , 2011). Adult patients, particularly those with a lengthy course of the disease, are more likely to develop multi-organ failure and acute respiratory distress syndrome with diffuse alveolar destruction (Hanson et al. , 2010, Maude et al. , 2014, Medana et al. , 2011). Even though the pathobiology of CM is unknown, detailed information derived from clinical and pathological studies has outlined a string of events and pathways in the disease panorama.

- **Placental Malaria**

The Pf parasite can produce a range of pathogenic changes in the pregnancy setting due to its proclivity to sequester and the massive sink of new placental chemicals like chondroitin sulphate (CSA). PfEMP1 proteins produced by the *var2CSA* genes bind to CSA and remove parasites from circulation when they pass through the placenta, whereas non-CSA binding parasites remain in circulation. The non-CSA binding parasites appear destroyed by maternal antibodies produced in earlier infections, while the placenta acts as a protected zone for parasite proliferation. In addition to the direct implications of placental binding, substantial mononuclear cell infiltrates may be present. Pv has also been linked to pregnancy issues such as anaemia, miscarriage, low birth weight, congenital malaria, and Pf (Anstey et al., 2012, Costa et al., 2012).

- **Acidosis**

Acidosis is a complex metabolic condition caused by a variety of factors. Acidosis is a complication of malaria induced by several reasons. *Plasmodium* lactate dehydrogenase (pLDH) is produced by the malaria parasite, which produces lactic acid and lowers pH. Direct central inhibition of the respiratory centres leads to abnormal breathing patterns in acidosis, which may add to the imbalance in pH via

sequestration, sleepiness, and brain edema (Planche and Krishna, 2006, Taylor et al. , 2012).

## ❖ Manifestations

*P. vivax* takes 12-17 days to mature. For *P. falciparum*, the incubation period is 9-14 days. *P. ovale* incubation is 16-18 days or longer, and *P. malariae* takes around a month (about 18-40 days) or longer (maybe years). However, in temperate climates, certain strains of *P. vivax* may not cause clinical disease for months or even years after infection.

Malaria has several symptoms that are universal to all types of the disease.

- The malarial paroxysm is characterised by fever and rigours.
- Splenomegaly
- Anemia
- Hepatomegaly
- Jaundice

Malarial paroxysm is caused by the haemolysis of infected RBCs, discharged merozoites, other malaria antigens and the inflammatory response they evoke. Sudden chills, malaise, a fever of 39-41°C, polyuria, fast and thready pulse, myalgia, headache, and nausea are all symptoms of a classic paroxysm. The fever goes down after 2 - 6 hours, and there is heavy sweating for 2 - 3 hours, followed by severe weariness. During the early stages of an illness, fever is typical. In accepted infections, malarial paroxysms occur every 2 - 3 days, depending on the species. The first week of clinical illness generally ends with splenomegaly, but it is not always seen in *P. falciparum* infections. The spleen has grown in size and is delicate and vulnerable to severe rupture. As functional immunity develops, splenomegaly may decrease with recurring malaria infections. The spleen may become fibrotic and solid after several attacks or grow substantially enlarged in some people (tropical splenomegaly). Splenomegaly is frequently accompanied by hepatomegaly.

***P. falciparum* manifestations:** For its microvascular effects, *P. falciparum* causes the most severe illness. It's the only species that can lead to death if left untreated; non-immune people can die within days of developing symptoms. Temperature spikes

and symptoms are usually random, but they can become synchronous, with temperature spikes happening at 48-hour intervals, especially in partly immune inhabitants of endemic regions. Patients with cerebral malaria may have various symptoms, including agitation, seizures, and coma. Diarrhoea, icterus, epigastric discomfort, ocular haemorrhages, algid malaria (a shock-like syndrome), and severe thrombocytopenia are all possible complications. Volume depletion, vascular occlusion due to parasitic erythrocytes, or deposition of immune complexes can all cause renal failure. Hemoglobinemia and hemoglobinuria caused by intravascular hemolysis can lead to blackwater fever (called for the dark colour of urine), which can develop spontaneously or after quinine medicament. Hypoglycemia is prevalent; however, quinine therapy and concomitant hyperinsulinemia can increase it. Low birth weight, spontaneous abortion, stillbirth, or congenital infection are all possible outcomes of placental involvement.

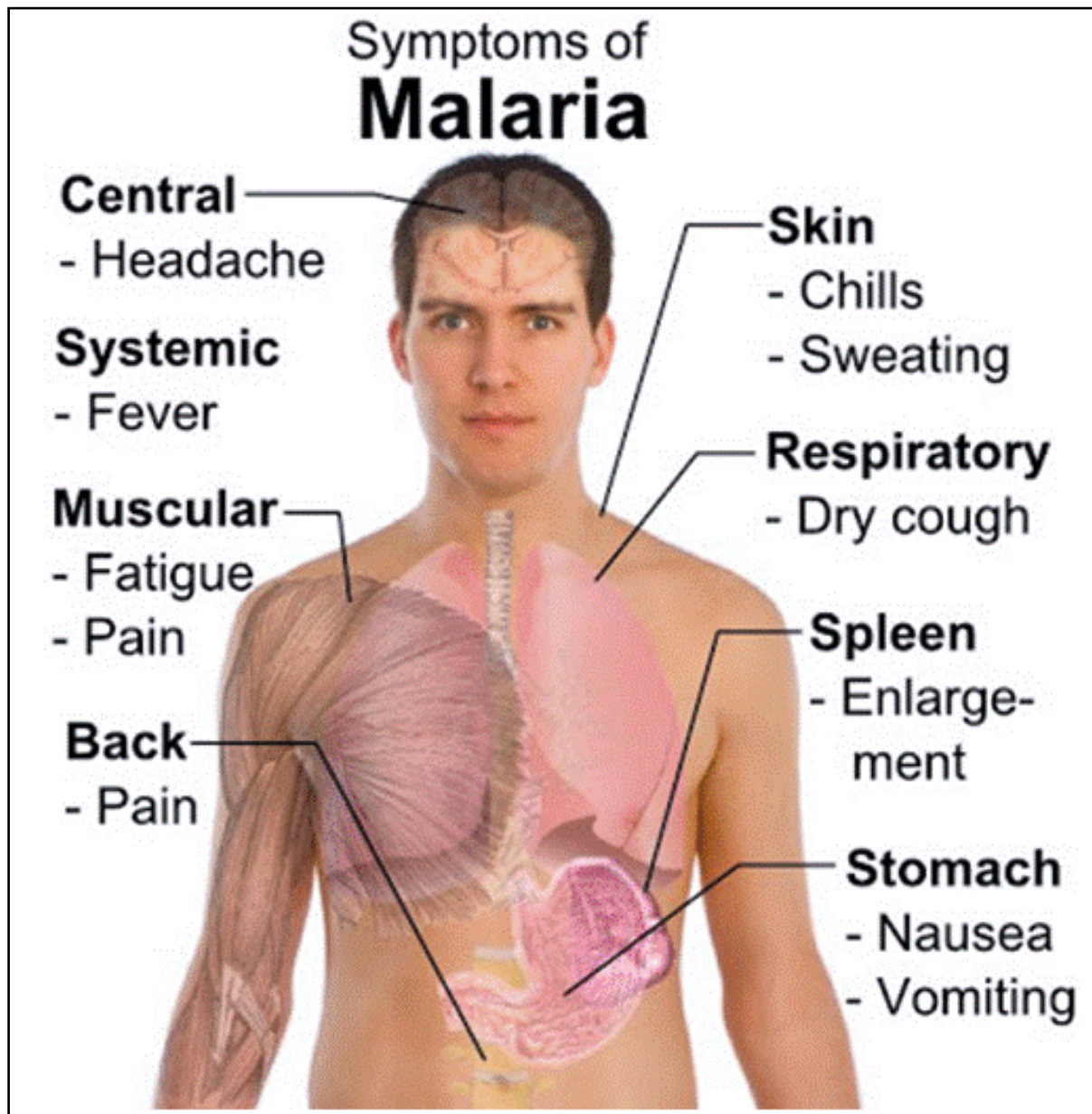
***P. vivax*, *P. ovale*, *P. malariae*, and *P. knowlesi* manifestations:** Vital organs are rarely harmed by *P. vivax*, *P. ovale*, or *P. malariae*. Splenic rupture or uncontrolled hyperparasitemia in asplenic patients are the most common causes of death.

*P. ovale* has a clinical course that is similar to *P. vivax*. Temperature spikes occur at 48-hour intervals in established illnesses, forming a tertian pattern.

*P. malariae* infections can go unnoticed for years. Still, low-level parasitaemia can lead to immune complex-mediated nephritis, tropical splenomegaly or nephrosis as soon as symptomatic fever follows a quartan pattern.

*P. knowlesi* is linked with the full range of malaria symptoms. Unlike *P. falciparum*, the infection is more common in men above 15 years of age who live near the forest areas. Temperatures tend to rise and fall daily. The severity of the condition worsens as the sufferer gets older. The 24-hour asexual replication cycle can result in high parasitaemia rates and, if left untreated, mortality. Although thrombocytopenia is frequent, it is rarely related to bleeding.





**Figure 13:** Pictorial representation of Malaria symptoms. (Courtesy: Malaria Parasite Metabolic Pathways (MPMP))



## **I. Disease management: Detection to Therapy**

Malaria must be **diagnosed** quickly and accurately if it is to be treated effectively. The worldwide aftermath of malaria has generated attentiveness to growing reliable diagnostic processes for resource-strapped regions where malaria is a substantial societal burden and wealthier countries where malaria diagnostic expertise is dearth (Bell et al. , 2005). Malaria is a potentially life-threatening illness that should be treated as such. According to the CDC website, delays in diagnosis and treatment are the primary causes of mortality in various countries. Malaria diagnosis involves finding malaria parasites or their antigens in a patient's blood. Though this task is straightforward, diagnosis accuracy depends on several factors. The five malaria species: endemicity of different species, various stages of erythrocytic schizogony, population movement, inter-relationship between levels of transmission, immunity, parasitaemia, drug resistance, signs/symptoms; recurrent malaria problems, parasite sequestration in deeper tissues, persisting viable/non-viable parasitaemia, and the use of chemoprophylaxis; such all can impact the interpretation of malaria diagnostic result(s).

- **Clinical diagnosis**

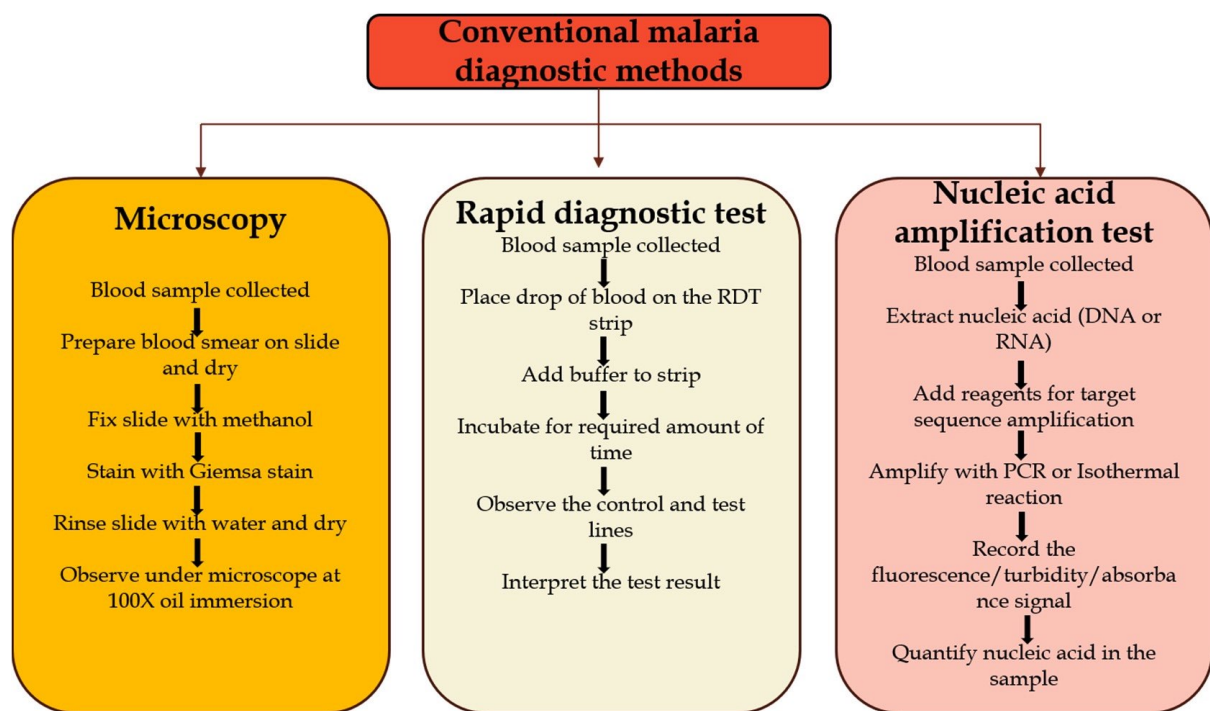
Malaria is traditionally diagnosed clinically by medical experts. This approach is the cheapest and most extensively used. Clinical diagnosis is based on the patient's signs, symptoms, and physical findings during the examination. Fever, weakness, headache, chills, myalgia, abdominal discomfort, dizziness, diarrhoea, vomiting, nausea, itching, and anorexia are some of the first signs of malaria. A clinical diagnosis of malaria is challenging due to the random nature of the signs and symptoms, which overlay considerably with other common, potentially fatal viral or bacterial infections and other feverish disorders. Malaria symptoms are similar to those of other tropical illnesses, which makes diagnosis more difficult.

- **Laboratory diagnosis**

Malaria diagnosis that is quick and accurate not only relieves pain but also reduces community transmission.

- ❖ **Staining thin and thick peripheral blood samples (PBS) for microscopic diagnosis:** Malaria is generally identified by examining stained slides containing blood films with Giemsa, Field's or Wright's stains under a microscope (Warhurst and Williams, 1996). This approach has mostly stayed the same since Laveran discovered the malaria parasite and Romanowsky's breakthroughs in staining techniques in the late 1800s. More than a century later, microscopic observation cum pinpointing of *Plasmodium* species in Giemsa-stained thick blood films (presence/absence screening) and thin blood films remain the benchmark for laboratory diagnosis (confirming the species) (Bharti et al. , 2007). The most significant flaw in microscopic inspection is its limited sensitivity, relatively at low parasite concentrations.
- ❖ **Quantitative buffy coat (QBC) method:** The QBC method was created to improve parasite identification under the microscope and make malaria diagnosis easier (Clendennen et al. , 1995). This approach involves colouring parasite DNA with fluorescent dyes like acridine orange and observing the results with epifluorescence microscopy. The parasite nuclei glow bright green, while the cytoplasm glows yellow-orange (Chotivanich et al. , 2007).
- ❖ **Rapid diagnostic tests (RDTs):** Since the WHO recognised the dire need for novel, simple, accurate, fast, and cost-effective diagnostic procedures for identifying the presence of *Plasmodium spp.* to get the better of the limits of light microscopy, several new malaria-diagnostic tools have been created (WHO, 1996). RDTs are used to identify antigens and employ an immuno-chromatographic method in which blood is injected into one end of the strip, and the findings are shown as lines on the strip surface (Wilson, 2012). *Plasmodium* histidine-rich protein (pHRP-2), *Plasmodium* aldolase and *Plasmodium* lactate dehydrogenase (pLDH) are the antigens used in this approach. *P. falciparum* has pHRP-2, although pLDH and *Plasmodium* aldolase are present in all species (Amir et al. , 2018, Mouatcho and Goldring, 2013). As the clarity and solidness of RDTs for use in rustic endemic regions have improved, RDT diagnosis in non-endemic areas is becoming more feasible, potentially decreasing the time to treatment for instances of imported (foreign) malaria. RDTs are quick and easy to use and don't require any extra equipment or electricity (Erdman and Kain, 2008).

- ❖ **Serological tests:** Identifying antibodies against asexual blood-stage malaria parasites are commonly used to diagnose malaria using serological techniques. In recent decades, the immunofluorescence antibody test (IFA) has proven to be a dependable serologic test for malaria (She et al. , 2007). IFA takes time and is subjective yet extremely sensitive and specific (Sulzer et al. , 1969).



**Figure 14:** A flowchart depicting the various malaria diagnostic procedures currently in use. (Ragavan et al., 2018)

### • Molecular diagnosis

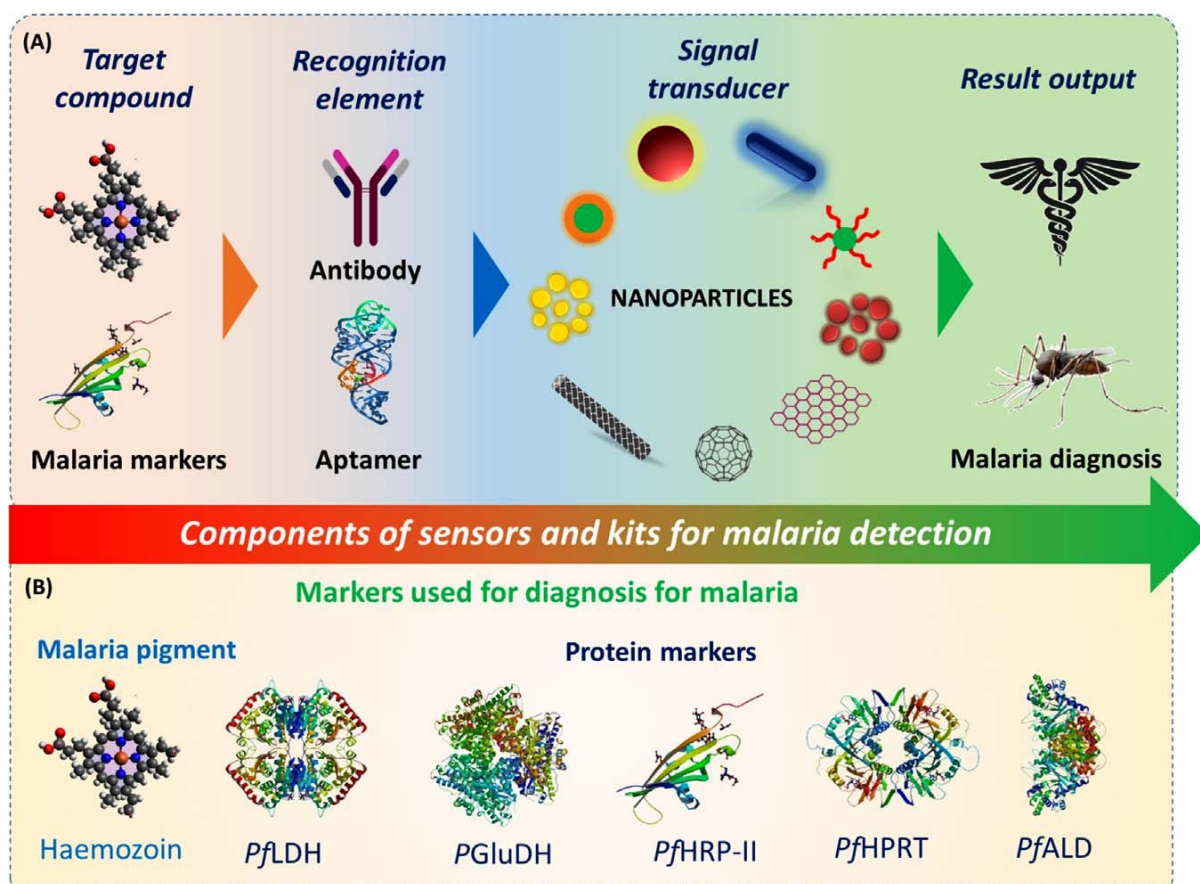
As previously said, traditional malaria diagnostic methods still need improvement. Many laboratories urgently require new diagnostic procedures with high sensitivity, specificity, and slight subjective variation.

- ❖ **Polymerase chain reaction (PCR):** In a blood sample, PCR-based approaches detect the presence of malaria target genes. Multiplex real-time PCR, nested conventional PCR and reverse transcriptase PCR are some of the variations of this test (Vasoo and Pritt, 2013). Most of these approaches focus on genes in the malaria parasite's 18S rRNA (Cordray and Richards-Kortum, 2012). PCR-based

tests are particularly beneficial for identifying asymptomatic and submicroscopic individuals missed by microscopy and RDTs.

- ❖ **Loop-mediated Isothermal Amplification (LAMP) technique:** LAMP is a modern technique for nucleic-acid amplification that was initially published in 2000 and has since been updated to allow for easier viewing of amplified products using a fluorescent/colourimetric dye like calcein or hydroxy naphthol blue (HNB) (Abdul-Ghani et al. , 2012, Notomi et al. , 2000).
- ❖ **Isothermal Thermophilic Helicase-Dependent Amplification (tHDA):** In using tHDA for malaria diagnosis, the 18S rRNA gene is directly amplified from whole blood without heat denaturation or PCR amplification. Digoxigenin (DIG) or fluorescein (FAM) labelled probes hybridise to the amplicon, and the amplification product is identified using an anti-FAM or anti-DIG antibody-labeled lateral-flow strip (Li et al. , 2013).
- ❖ **Saliva-Based Test with Nucleic-Acid Amplification:** The identification of a *Plasmodium* gene, *P. falciparum* dihydrofolate reductase or 18S rRNA gene in saliva using a nested-polymerase chain reaction is used in this saliva-based malaria diagnostic (nPCR) (Mfuh et al. , 2017).
- ❖ **Transdermal Haemozoin Detection:** This method uses An ultrasonic sensor to detect haemozoin-generated vapour nano-bubbles. A brief laser pulse sent via the skin to blood vessels localises heat and evaporates the liquid surrounding the haemozoin crystals. Within the malaria parasite, evaporation of liquid causes the expansion and collapsing of small vapour nano-bubbles. After the laser is turned on, the probe detects an auditory pulse and generates an electrical signal as an acoustic trace. The prototype was used to test a patient with proven malaria, and haemozoin-generated vapour nano-bubbles were found (Lukianova-Hleb et al. , 2014).
- ❖ **Urine-Based Malaria Test:** The *Plasmodium* protein pHRP-2 is detected in urine malaria testing. The urine malaria test (UMT) is a commercially accessible test that includes soaking the test strip into a urine sample for a couple of minutes and then incubating for twenty minutes. Like the frequently used RDT, a positive

(+) result is shown by dark-coloured line(s) on the test strip (Oguonu et al. , 2014).



**Figure 15:** (A) Malaria diagnosis sensors. (B) Malaria diagnosis markers. (Ragavan et al., 2018)

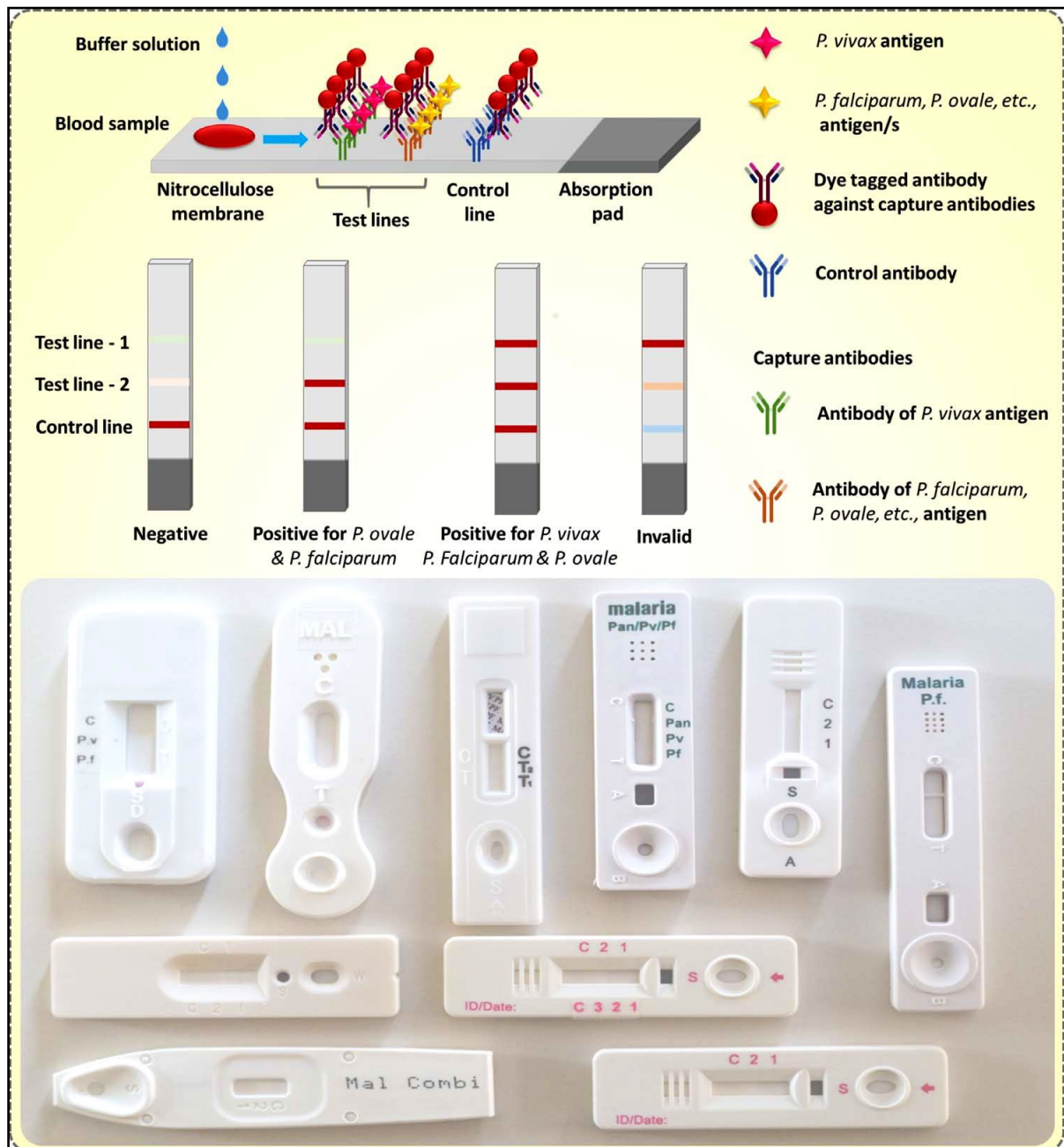
Other sophisticated techniques like mass spectrometry, flow cytometry, and microarrays are utilised in identification strategies in malaria research laboratories. However, utilisation of such resources in regular diagnostic practises requires expert technicians, ample funds, and a lot of resources.

Without a viable vaccine, the **therapeutic** use of antimalarial medicines remains the sole option for preventing and managing malarial disease. The emergence of drug-resistant *Plasmodium* species has been shown in several investigations to limit the efficacy of most antimalarial medicines (Patel et al. , 2017). Resistance was documented for all known antimalarial drugs, emphasising the urgent need to develop new ones that target validated and novel targets (Menard and Dondorp,

2017). It is critical to create a novel antimalarial agent effective against transmissible gametocyte stages and intraerythrocytic proliferative asexual parasites, particularly resistant parasite species (Mishra et al. , 2017). Several enzymes, transporters, ion channels, interacting molecules in RBC invasion, molecules involved in parasite oxidative stress, haemoglobin degradation and lipid metabolism are intriguing new targets for developing new antimalarial medicines against quickly evolving malarial parasites (Sahu et al. , 2008).

Since the 1940s, antimalarial treatments based on natural, semi-synthetic, and synthetic chemicals have been developed (Burrows et al. , 2014). Existing antimalarial drugs are divided into quinoline, antifolate, and artemisinin derivatives. A single treatment that can eliminate all *Plasmodium* species has yet to be created or manufactured. As a result, to effectively combat malarial infection, a combination of medications is typically given simultaneously.

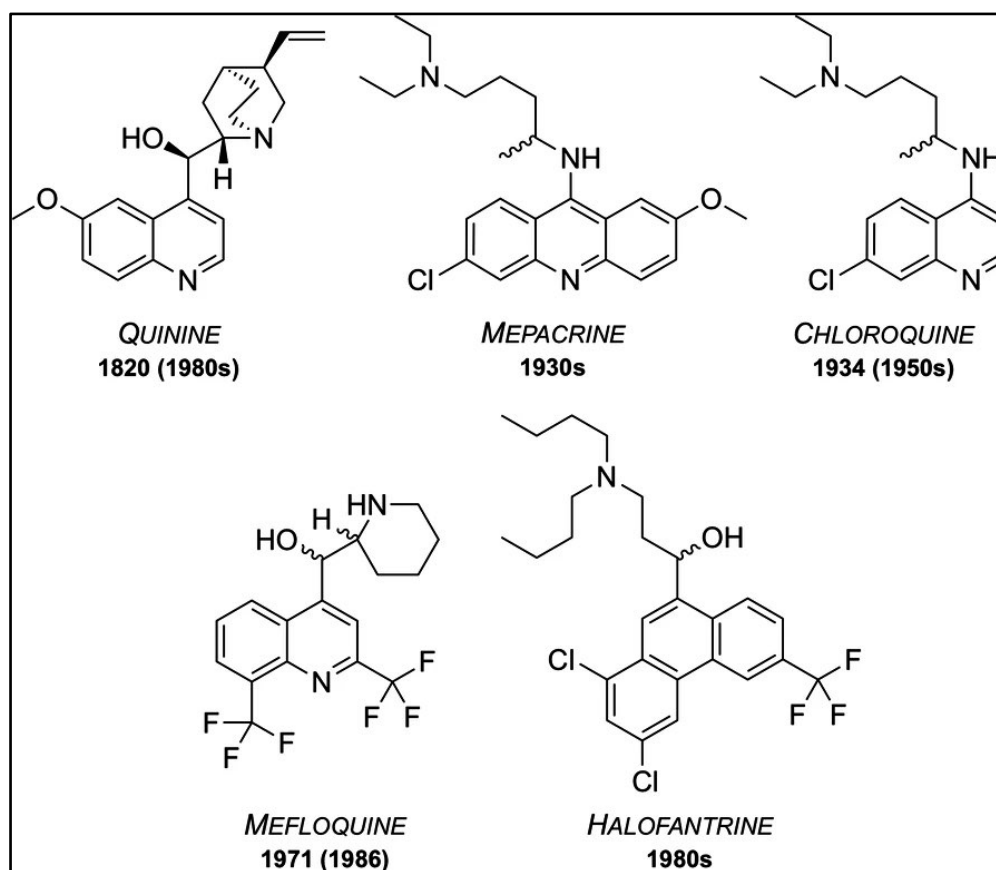




**Figure 16:** The idea behind the lateral flow immunoassay for diagnosing *Plasmodium* species. (Ragavan et al. , 2018)

## Capsules of the Past:

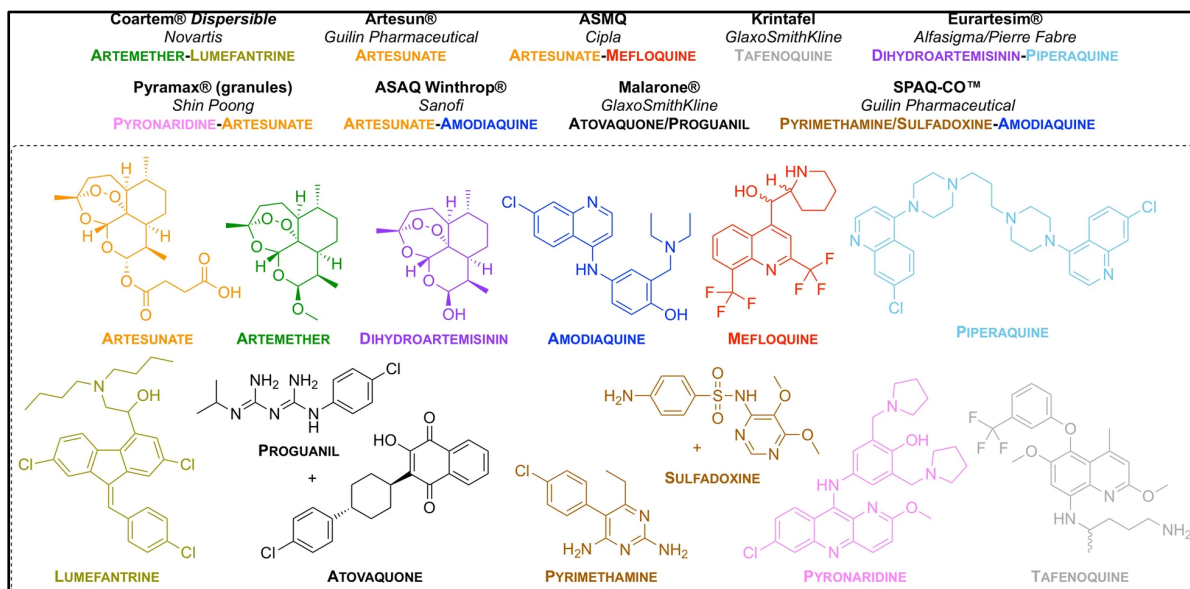
- **Quinine:** Several different natural and synthetic chemicals have been created since the discovery of quinine, the first chemically purified effective therapy for malaria, in 1820. However, parasite strains developed resistance as time passed, making them less effective. As a result, its use has ceased or been limited to specific circumstances.
- **Chloroquine:** In the 1940s, chloroquine (CQ) was used to cure all types of malaria with little side-effects (Assoc, 1946). CQ resistance was first observed in the 1950s, and subsequently, resistant malaria parasite strains (K1, 7GB, W2, Dd2, and others) are now employed in potency evaluation assays to demonstrate efficacy (Mushtaque and Shahjahan, 2015).
- **Mefloquine:** It was first used to treat chloroquine-resistant malaria and has since been used as curative and preventative medicine. The first mention of resistance was in 1986 (Brasseur et al. , 1986). This structurally related quinoline drug is thought to interfere with haemoglobin digestion in the parasite's blood stage (Foley and Tilley, 1997).
- **Mepacrine/Quinacrine:** This antimalarial derivative of methylene blue was discovered in 1891 and helped treat malaria (Schirmer et al. , 2003). It is no longer utilised because of the high risk of adverse effects like toxic psychosis, although it is still used in combination (Weina, 1998).
- **Halofantrine:** Initially, it was used to treat all kinds of the *Plasmodium* parasite. Due to the significant toxicity risks and inconsistent pharmacological qualities, it is only used as curative medicine and not for prophylactic (Croft, 2007).



**Figure 17:** Antimalarial drugs discovered between 1820-1980s. Resistance recorded (in bracket). (Tse et al., 2019)

## Capsules of the Present:

There are now 14 drugs for curative treatment of malaria and four medications for preventative treatment on the WHO Model List of Essential Medicines, with the treatments prepared as single compounds or combinations.



**Figure 18:** Approved new drug formulations for malaria treatment. Adapted from (Tse et al. , 2019)

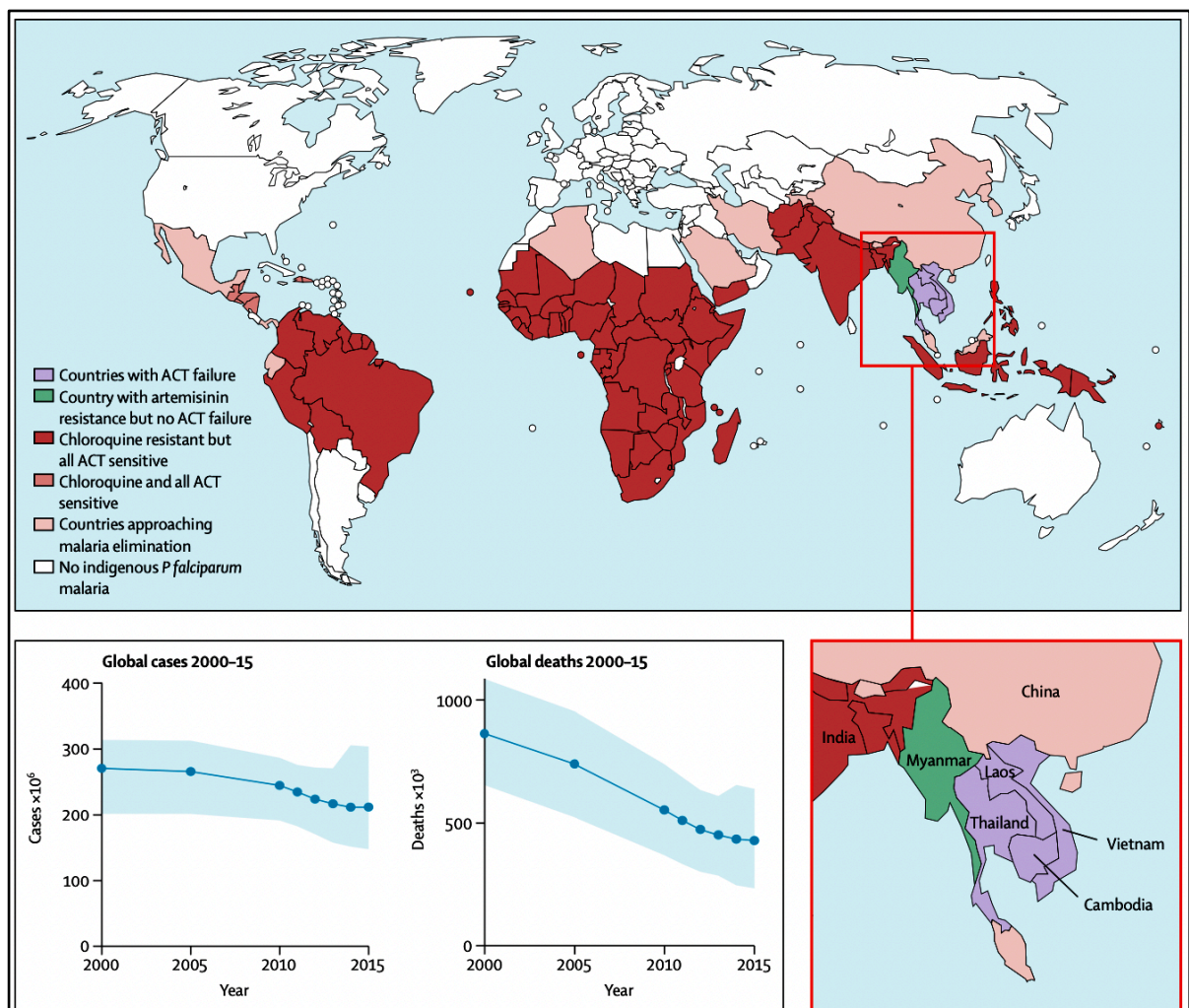
- Artemisinin and its derivatives:** Tu Youyou was the first to isolate artemisinin from the *Artemisia annua* plant, which has long been utilised in Chinese traditional medicine (J, 1979). Youyou received the joint Nobel Prize in Physiology or Medicine in 2015 for "her discoveries concerning a novel therapy against malaria". All multi-drug-resistant variants of *P. falciparum* have been demonstrated to be susceptible to artemisinin. Artemisinin derivatives such as artemether, artesunate, and arteether are the most common. These semi-synthetic compounds are pro-drugs converted to dihydroartemisinin (active metabolite). Artemisinins have played a critical role in the fight against malaria, with Artemisinin-based combination therapy (ACT) accounting for most contemporary medicines (Eastman and Fidock, 2009). Artemisinin resistance was reported in western Cambodia in 2008 (Noedl et al. , 2008), albeit slowly. A paper published in February 2018 identified 30 cases of artemisinin resistance in Southeast Asia, including resistance to the dihydroartemisinin–piperaquine pairing treatment (Amato et al. , 2018). Its mechanistic action is still debatable

with multiple modes of action. The most widely recognised idea is that heme activates the molecule, causing it to produce free radicals, which harm the parasite survival proteins (Wang et al. , 2015). In 2013, the mechanism of action was determined using a computational approach based on prior investigations that indicated heme and *Pf*ATP6 (Ca<sup>2+</sup> transporter) as probable entities (Shandilya et al. , 2013). Artemisinin has recently been related to the upregulation of the unfolded protein response (UPR) pathways, which may be associated with parasite development inhibition (Mok et al. , 2015). According to another study, *P. falciparum* phosphatidylinositol-3-kinase (*Pf*PI3K) is strongly inhibited by artemisinin (Mbengue et al. , 2015).

- **Amodiaquine:** It was created for the first time in 1948 (Berliner et al. , 1948). When used with artesunate, it is primarily used to treat uncomplicated *P. falciparum* malaria. It is thought to inhibit hemozoin formation in the parasite. It is used in combination with artesunate.
- **Piperaquine:** It was created as part of China's National Malaria Elimination Program in the 1960s (Chen et al. , 1982). It accumulates in the digestive vacuole and interferes with heme detoxification (Vennerstrom et al. , 1992). It is partnered with dihydroartemisinin.
- **Lumefantrine/Benflumetol:** It was initially synthesised in 1976 as part of "Project 523," a Chinese antimalarial research endeavour that also yielded the discovery of artemisinin (Cui and Su, 2009). According to research, it inhibits protein and nucleic acid(s) synthesis by preventing the production of  $\beta$ -haematin by complexation with hemin (Combrinck et al. , 2013). It is paired with artemether.
- **Pyronaridine:** The Institute of Chinese Parasitic Disease was the first to synthesise pyronaridine in the 1970s (Zheng et al. , 1979). Combined with artesunate, it inhibits  $\beta$ -haematin formation (Croft et al. , 2012).
- **Tafenoquine:** It was discovered in 1978 at the Walter Reed Army Institute of Research and was later approved by the US FDA as the first novel one-dose therapy for *P. vivax* malaria in almost sixty years. It is hypothesised to be a pro-drug converted to quinone-tafenoquine (active) during metabolism (Ebstie et al. , 2016).



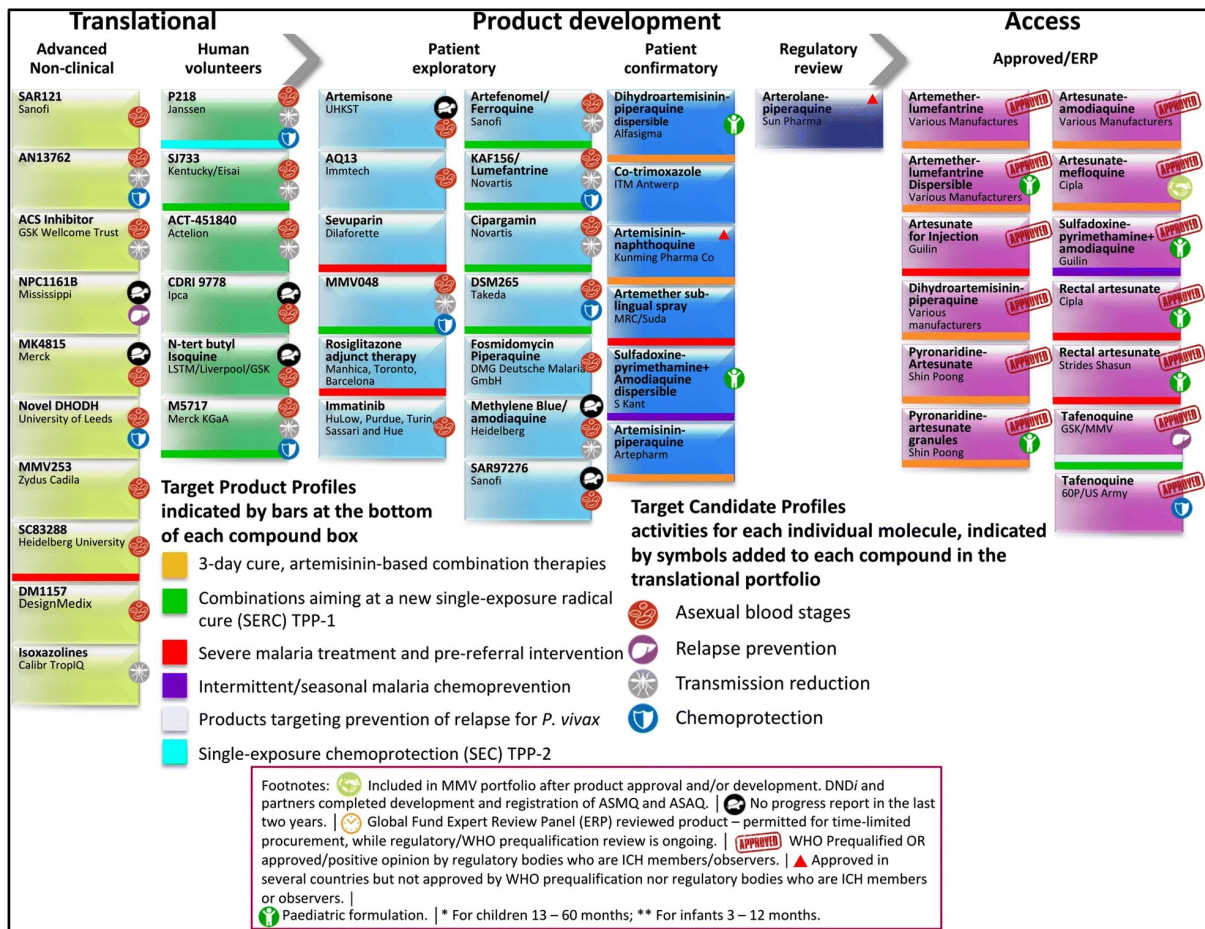
- **Proguanil & Atovaquone:** Proguanil was one of the earliest antifolate antimalarial medications, while atovaquone was initially used to treat protozoan infections in 1991 (Curd et al. , 1945). Atovaquone inhibits mitochondrial electron transport by inhibiting the cytochrome bc1 complex (Fry and Pudney, 1992). When taken alone, proguanil inhibits dihydrofolate reductase (DHFR) by disrupting deoxythymidylate production through its metabolite, cycloguanil.
- **Pyrimethamine & Sulfadoxine:** Pyrimethamine was developed as part of the research that earned Elion, Hitchings, and Black the Nobel Prize in Physiology or Medicine in 1988 for "*their discoveries of important principles for drug treatment*". In the initial 1960s, sulfadoxine was developed. However, resistance has developed (Laing, 1965). Dihydrofolate reductase is inhibited by pyrimethamine, while dihydropteroate synthetase is inhibited by sulfadoxine.



**Figure 19:** Worldwide distribution of drug-resistant *Plasmodium falciparum*. (Ashley et al. , 2018)



## Capsules of the Future:

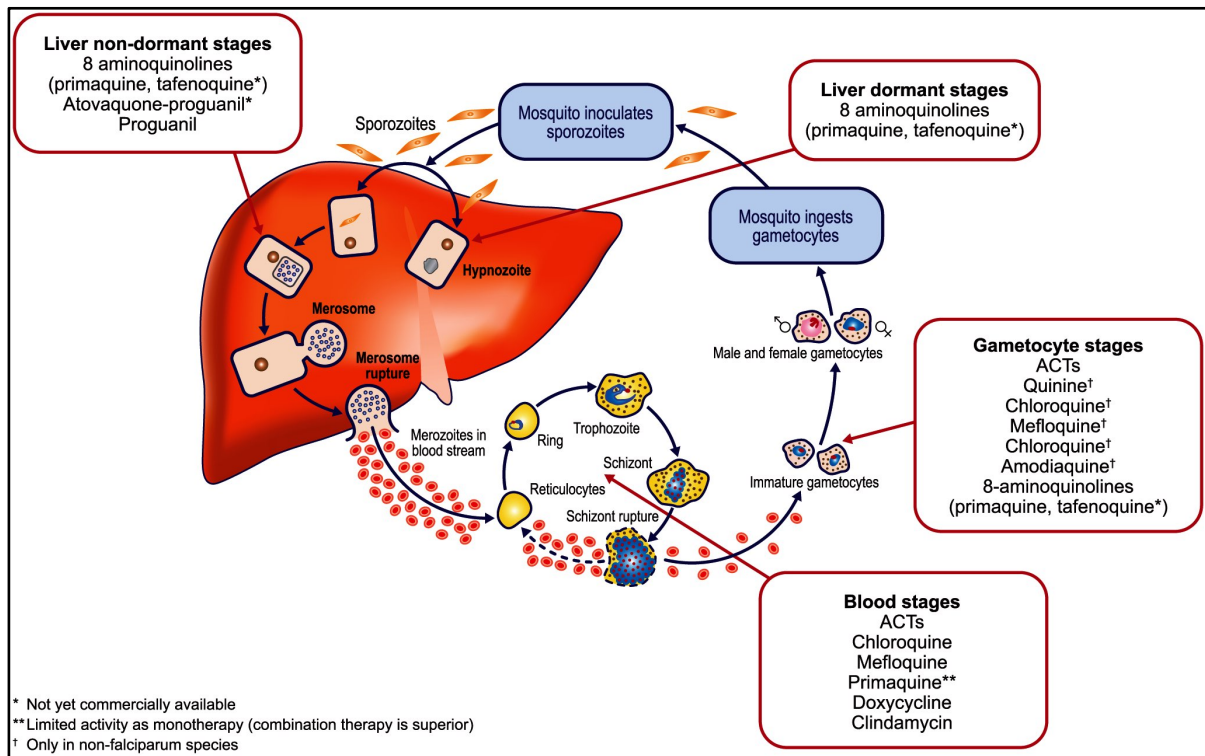


**Figure 20:** A snapshot of MMV-funded initiatives at various phases of the drug research and development pipeline. (Courtesy: MMV supported projects webpage)

The Medications for Malaria Venture (MMV) has been at the forefront of discovering and evolving novel medications for treating malaria since its inception in 1999. MMV has been partnering with pharmaceutical companies and institutions globally to develop novel antimalarials to aid in the fight against malaria.

The recent increase in malaria parasite resistance to current treatments is alarming because it limits our ability to control this devastating disease. In recent years, high-throughput screens (HTS) have discovered numerous new chemotypes emerging as promising antimalarial candidates. Aside from efficacy, pharmacokinetic compatibility, toxic side effects, and resistance potential would all be essential considerations in the progress of a successful drug. Comprehending the pathways

that lead to antimalarial drug resistance might help us prevent resistance to new antimalarial drug generations from forming in the future.



**Figure 21:** Sites of action for various antimalarials [shown in *P. vivax* model].  
 (Bassat, 2011)

## **J. Malaria prevention is better than cure**

Chemoprophylaxis, vaccination, vector control, and bite avoidance are all effective ways to prevent malaria.

### **❖ Chemoprophylaxis**

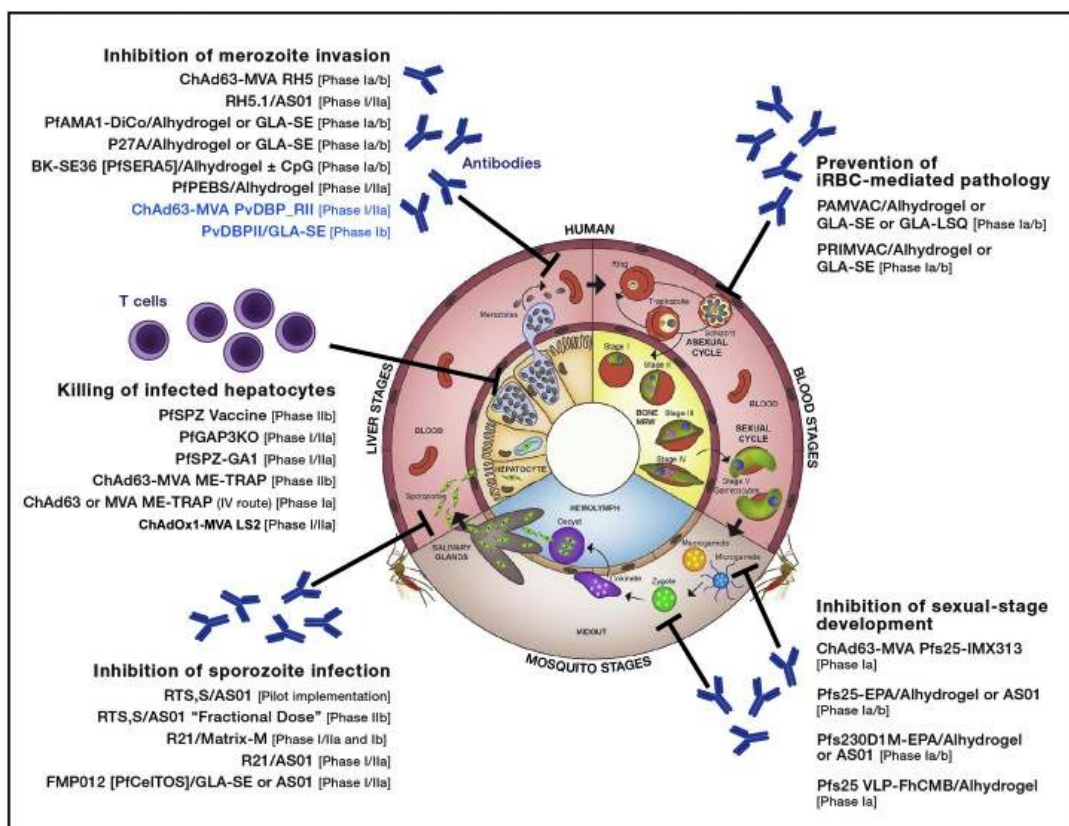
Malaria chemoprophylaxis entails giving medication to healthy people to prevent them from contracting an infection that they have a low likelihood of contracting. The risk of infection and death, as well as the risk of side effects, must be balanced while using malaria chemoprophylaxis (Petersen, 2004). Chemoprophylaxis is intended for young children, travellers, and pregnant women. Intermittent preventive therapy in pregnancy (IPTp) and newborns has been sluggish to catch on in various locations, and sulfadoxine-pyrimethamine resistance threatens their effectiveness (Desai et al. , 2015, Radeva-Petrova et al. , 2014). Alternative antimalarials, such as dihydroartemisinin–piperaquine, are being studied. Seasonal malaria chemoprevention in children with sulfadoxine–pyrimethamine and amodiaquine has been extensively embraced. It has aided in the reduction of malaria in Sahel areas of Africa with substantial seasonal transmission (Cisse et al. , 2016). Malaria and drug resistance hazards should be evaluated with the perils of drug toxicity when choosing chemoprophylaxis to prevent malaria in travellers. Prophylaxis with atovaquone-proguanil and doxycycline is routinely administered. Weekly preventive doses of mefloquine are a practical alternative, although they are controversial because of worries about neurotoxicity. Drug primaquine is an effective causative prophylactic medication that provides better protection against *P. vivax* malaria (hypnozoite stages). However, it must be used when G6PD deficiency has been ruled out (Kolifarhood et al. , 2017).

### **❖ Vaccine development**

Malaria subunit vaccines defend against proteins exposed at key stages of the parasite's life cycle. The objective is to reduce infection rates by attacking sporozoite stages with one of the surface proteins involved in homing to the liver and host cell traversal/invasion. Based on the *P. falciparum* circumsporozoite protein, the RTS,S/AS01 vaccine, underwent the maximum research. RTS,S/AS01 gave considerable protection against *P. falciparum* malaria infections in African kids over 3 to 4 years in

landmark research; in children, vaccination efficacy was 36.3% with a 20-month booster and 28.3% without (Rts, 2015). WHO is sponsoring the pilot deployment of the four-dose regimen in children aged 5–17 months in three countries, allowing for studying long-term effects and their practicality.

An intravenous injection of irradiation-attenuated sporozoites, the *P. falciparum* sporozoite (*PfSPZ*) vaccine, takes a different strategy for developing sporozoite-based protection. *PfSPZ* is presently in clinical trials in Africa (Sissoko et al. , 2017); the problems will most likely revolve around achieving long-term protection against all other strains. Using merozoite-stage proteins as vaccine targets aims to decrease asexual reproduction and guard against disease rather than inducing sterile immunity, thus enabling immunity to form naturally. At the same time, the vaccinated individual is shielded against acute sickness. Another asexual stage vaccination aims to prevent parasitised cells from attaching to CSA1 and protect against placental malaria by targeting the product of the *PfEMP1* VAR2CSA type (Fried and Duffy, 2015). Antibodies created by transmission-blocking vaccinations against sexual-stage antigens are ingested in the mosquito blood meal, potentially giving population-level protection.



**Figure 22:** Candidate Malaria Vaccines in Clinical Development. (Draper et al. , 2018)



## ❖ Vector control

Vector control refers to actions against a disease vector to restrict the vector's capacity to transmit the disease by safeguarding disease-prone areas. Malaria susceptibility is determined by local vector populations' vectorial capability, which includes not only the existence of the vector but also its human-biting habits, population size, and lifespan in connection to the sporogony cycle. Climate, local environment, and human and vector activity significantly impact each characteristic. To ensure maximum effectiveness, vector control strategies must be tailored to the local environment (Smith Gueye et al. , 2016).

- **Insecticide-treated mosquito nets (ITNs):** The insecticide in long-lasting insecticidal nets (LLINs) lasts up to three years, whereas the insecticide in conventionally treated nets lasts up to 12 months. The WHO suggested that all health agencies should increase ITN circulation, focusing on young children and pregnant women, as these are the most vulnerable populations (WHO. Insecticide-treated mosquito net: a WHO position statement. Geneva: World Health Organization; 2007). The only insecticide class permitted for use on ITNs is pyrethroids. There is considerable concern that the emergence of pyrethroid resistance would jeopardise malaria reduction and eradication efforts (N'Guessan et al. , 2007).
- **Indoor residual spraying (IRS):** The Global Malaria Eradication Campaign's primary approach was indoor residual spraying, eradicating malaria in many countries and dramatically decreasing its burden on others. It has primarily targeted low/seasonal transmission areas. Still, its latest expansion into high transmission areas has been criticised owing to long-term maintainable issues (WHO. Global technical strategy for malaria 2016–2030. Geneva: World Health Organization; 2015). If utilised broadly in high transmission areas, IRS can be much more expensive because it requires many spray rounds to protect the population. Even though some insecticides, such as dichlorodiphenyltrichloroethane (DDT), are effective at controlling mosquitoes, some governments have banned them due to environmental concerns. It is only recommended for usage under specified circumstances by WHO.

- **Larval source management (LSM):** LSM manages water areas that could serve as mosquito breeding grounds to avoid immature development. This can be classified into habitat modification, habitat manipulation, biological control, and larviciding; larvicides are most commonly used (Fillinger and Lindsay, 2011).

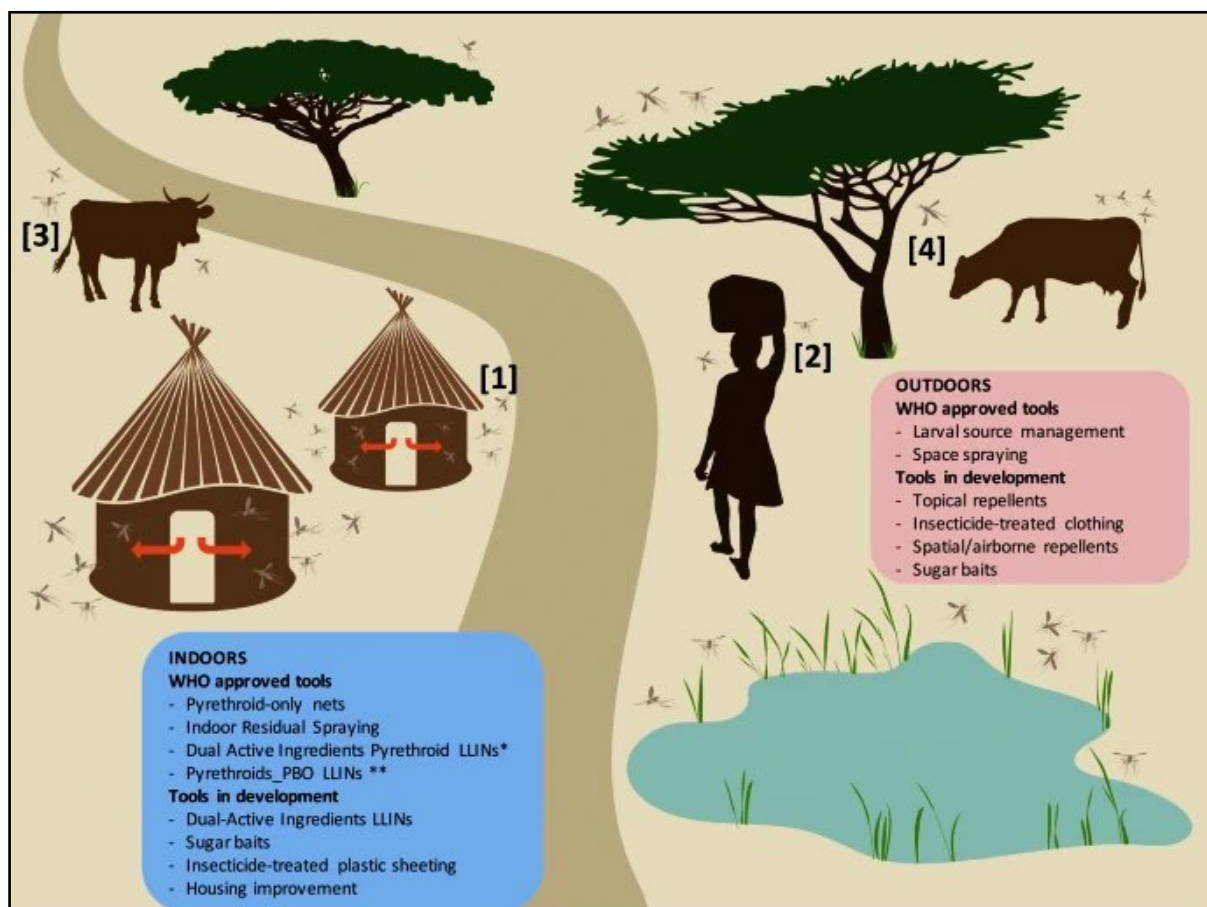
The following techniques are still under development:

- **House improvement (HI):** Modern buildings are more malaria-resistant than older houses built of natural materials, which have various openings, thereby allowing mosquito entry routes, and HI can provide protection equivalent to ITNs in some situations (Tusting et al. , 2015).
- **Mass drug administration (MDA):** It occurs when a curative dose of a treatment (drug) is given to the whole population of a geographic region without first testing for infection and regardless of whether or not symptoms are present. In recent years, mass ivermectin therapy has proven to be a triumph story in malaria reduction, particularly for residual malaria. However, the method is expensive and requires a lot of logical persuasion from the community involved.
- **Livestock targeting:** Most malaria vector species have a more varied feeding pattern, surviving on animals and people. Mosquitoes that feed on livestock could be targeted by treating livestock facilities (for example, cattle barns with IRS) (Barreaux et al. , 2017). Insecticides applied directly to cattle via sponging, dipping, or spraying have been shown to kill mosquitoes and retard malaria in humans (Hewitt and Rowland, 1999, Rowland et al. , 2001).
- **Attractive toxic sugar bait (ATSB):** ATSB approaches are a novel type of vector control that kills male and female mosquitoes outdoors while they seek essential sugar supplies. The ATSB method employs a fruit or flower aroma to attract mosquitoes, a sugar solution to stimulate feeding, and an oral toxin to kill them (Beier et al. , 2012, Muller et al. , 2010).
- **Genetically modified (GM) mosquitoes:** *Anopheles* mosquitoes have been genetically modified to make them unable to reproduce or resistant to malaria and then released into the wild. For example, the advancement of gene-editing technologies like CRISPR/Cas9 can make this fantasy a reality. Although there



are several safety and ethical concerns to be addressed, this technique of malaria control is becoming a realistic option (Greenwood, 2017).

The protozoan that causes malaria was found more than 130 years ago. During this time, several scientific breakthroughs have happened, some of which have led to treatments that help minimise sickness and mortality, such as the discovery and evolution of antimalarial drugs and insecticides. Advancement toward eradication in certain countries shows that available technology can be adequate to obliterate malaria if the required circumstances are met, such as access to health care, political commitment, and substantial human and financial resources.



**Figure 23:** Mosquito dispersion in a typical rural area, depicted schematically. (Sougoufara et al. , 2020)

## K. Conclusion

Malaria, a disease produced by *Plasmodium* parasites, has been a problem for humans for a long time. Malaria has become a chemotherapy-curable disease with the help of natural and chemically synthesised antimalarials. Malaria patients are treated with synthetic antimalarials like artemisinin and chloroquine, and mosquito vector-controlling agents like insecticides are also used significantly, leading to a significant decline in malaria load today. Despite this, the disease remains a significant problem, killing hundreds of thousands yearly.

The growth and dissemination of chemotherapy-resistant parasites are some of the issues that make malaria treatment difficult. To address this issue, researchers are looking for new antimalarial compounds with targets distinct from those of existing antimalarials. When such inhibitors are used with existing antimalarials, the likelihood of parasites developing resistance to each medication is significantly reduced. In the modern world, *Plasmodium* parasites can readily spread from endemic to non-endemic locations because of increased human migration. Although malaria-free countries and places steadily increase, imported malaria remains a prevalent health issue in many areas and countries. *Plasmodium* species may survive for long periods in humans with no symptoms. Carriers of asymptomatic *Plasmodium* parasites can develop malaria unprompted and disseminate it to zero-malaria countries and territories. When these individuals participate in blood transfusions and organ transplantation as donors, they may spread the parasite.

*P. falciparum* and other *Plasmodium* species that infect humans share a convergent evolutionary trait that allows them to infect humans. The number of *Plasmodium* species that naturally cause malaria in humans is currently restricted, although new zoonotic malaria might emerge at any instance. The corporal distance between primates and humans varies depending on the amount of community development, which might affect the chance of non-human *Plasmodium* species producing zoonotic malaria in *Homo sapiens*. *Plasmodium* species can also shift their insect hosts. Avian malaria parasites develop and generate infectious sporozoites in non-anopheline mosquitoes, unlike malaria parasite species that infect mammals. This suggests that mammalian *Plasmodium* species evolve immunity to non-anopheline mosquitos like *Aedes* and *Culex* and use them as transmission vectors. Some non-anopheline mosquito species are found worldwide and may reproduce in harsh environments,

including seashores, tunnels, and metropolitan areas. If the *Plasmodium* species that causes malaria in people could complete its vector stage development in non-anopheline mosquitoes, the ramifications on human society may be tremendous.

Due to the apparent parasite's biology and human activity, humans and *Plasmodium* parasites interact regularly. Comprehension of the underlying biology of the malaria parasites that cause these transitions and leveraging that knowledge for malaria control must help establish a healthy global society.

## **L. References**

1. Abdul-Ghani R, Al-Mekhlafi AM, Karanis P. Loop-mediated isothermal amplification (LAMP) for malarial parasites of humans: would it come to clinical reality as a point-of-care test? *Acta Trop*. 2012;122:233-40.
2. Acharya P, Pallavi R, Chandran S, Dandavate V, Sayeed SK, Rochani A, et al. Clinical proteomics of the neglected human malarial parasite *Plasmodium vivax*. *PLoS One*. 2011;6:e26623.
3. Amato R, Pearson RD, Almagro-Garcia J, Amaratunga C, Lim P, Suon S, et al. Origins of the current outbreak of multidrug-resistant malaria in southeast Asia: a retrospective genetic study. *Lancet Infect Dis*. 2018;18:337-45.
4. Amir A, Cheong FW, De Silva JR, Lau YL. Diagnostic tools in childhood malaria. *Parasit Vectors*. 2018;11:53.
5. Anstey NM, Douglas NM, Poespoprodjo JR, Price RN. *Plasmodium vivax*: clinical spectrum, risk factors and pathogenesis. *Adv Parasitol*. 2012;80:151-201.
6. Antinori S, Galimberti L, Milazzo L, Corbellino M. *Plasmodium knowlesi*: the emerging zoonotic malaria parasite. *Acta Trop*. 2013;125:191-201.
7. Ashley EA, Pyae Phyo A, Woodrow CJ. Malaria. *Lancet*. 2018;391:1608-21.
8. Assoc JAM. ACTIVITY of a new antimalarial agent, chloroquine (SN 7618). *J Am Med Assoc*. 1946;130:1069.
9. Ayala FJ, Escalante AA, Rich SM. Evolution of *Plasmodium* and the recent origin of the world populations of *Plasmodium falciparum*. *Parassitologia*. 1999;41:55-68.
10. Baghbanzadeh M, Kumar D, Yavasoglu SI, Manning S, Hanafi-Bojd AA, Ghasemzadeh H, et al. Malaria epidemics in India: Role of climatic condition and control measures. *Sci Total Environ*. 2020;712:136368.
11. Baird JK. Neglect of *Plasmodium vivax* malaria. *Trends Parasitol*. 2007;23:533-9.
12. Barreaux P, Barreaux AMG, Sternberg ED, Suh E, Waite JL, Whitehead SA, et al. Priorities for Broadening the Malaria Vector Control Tool Kit. *Trends Parasitol*. 2017;33:763-74.
13. Bassat Q. The use of artemether-lumefantrine for the treatment of uncomplicated *Plasmodium vivax* malaria. *PLoS Negl Trop Dis*. 2011;5:e1325.
14. Beier JC, Muller GC, Gu W, Arheart KL, Schlein Y. Attractive toxic sugar bait (ATSB) methods decimate populations of *Anopheles* malaria vectors in arid environments regardless of the local availability of favoured sugar-source blossoms. *Malar J*. 2012;11:31.

15. Bell DR, Jorgensen P, Christophel EM, Palmer KL. Malaria risk: estimation of the malaria burden. *Nature*. 2005;437:E3-4; discussion E-5.
16. Berliner RW, Earle DP, Taggart JV, Zubrod CG, Welch WJ, Conan NJ, et al. Studies on the Chemotherapy of the Human Malaras. Vi. The Physiological Disposition, Antimalarial Activity, and Toxicity of Several Derivatives of 4-Aminoquinoline. *J Clin Invest*. 1948;27:98-107.
17. Bharti AR, Patra KP, Chuquiyauri R, Kosek M, Gilman RH, Llanos-Cuentas A, et al. Polymerase chain reaction detection of *Plasmodium vivax* and *Plasmodium falciparum* DNA from stored serum samples: implications for retrospective diagnosis of malaria. *Am J Trop Med Hyg*. 2007;77:444-6.
18. Bousema T, Drakeley C. Epidemiology and infectivity of *Plasmodium falciparum* and *Plasmodium vivax* gametocytes in relation to malaria control and elimination. *Clin Microbiol Rev*. 2011;24:377-410.
19. Brasseur P, Druilhe P, Kouamouo J, Brandicourt O, Danis M, Moyou SR. High level of sensitivity to chloroquine of 72 *Plasmodium falciparum* isolates from southern Cameroon in January 1985. *Am J Trop Med Hyg*. 1986;35:711-6.
20. Brown KN, Brown IN. Immunity to malaria: antigenic variation in chronic infections of *Plasmodium knowlesi*. *Nature*. 1965;208:1286-8.
21. Bruce-Chwatt LJ. John Macculloch, M.D., F.R.S. (1773-1835) (The precursor of the discipline of malariology). *Med Hist*. 1977;21:156-65.
22. Bruce-Chwatt LJ. Alphonse Laveran's discovery 100 years ago and today's global fight against malaria. *J R Soc Med*. 1981;74:531-6.
23. Burrows JN, Burlot E, Campo B, Cherbuin S, Jeanneret S, Leroy D, et al. Antimalarial drug discovery - the path towards eradication. *Parasitology*. 2014;141:128-39.
24. Carlton JM, Adams JH, Silva JC, Bidwell SL, Lorenzi H, Caler E, et al. Comparative genomics of the neglected human malaria parasite *Plasmodium vivax*. *Nature*. 2008;455:757-63.
25. Carter R. Speculations on the origins of *Plasmodium vivax* malaria. *Trends Parasitol*. 2003;19:214-9.
26. Cator LJ, Lynch PA, Read AF, Thomas MB. Do malaria parasites manipulate mosquitoes? *Trends Parasitol*. 2012;28:466-70.
27. Chadee DD, Tilluckdharry CC, Maharaj P, Sinanan C. Reactivation of *Plasmodium malariae* infection in a Trinidadian man after neurosurgery. *N Engl J Med*. 2000;342:1924.

28. Chen L, Qu FY, Zhou YC. Field observations on the antimalarial piperazine. *Chin Med J (Engl)*. 1982;95:281-6.
29. Chin W, Contacos PG, Coatney GR, Kimball HR. A Naturally Acquired Quotidian-Type Malaria in Man Transferable to Monkeys. *Science*. 1965;149:865.
30. Chitnis CE, Miller LH. Identification of the erythrocyte binding domains of *Plasmodium vivax* and *Plasmodium knowlesi* proteins involved in erythrocyte invasion. *J Exp Med*. 1994;180:497-506.
31. Chotivanich K, Silamut K, Day NPJNZJoMLS. Laboratory diagnosis of malaria infection--a short review of methods. 2007;61.
32. Cisse B, Ba EH, Sokhna C, JL ND, Gomis JF, Dial Y, et al. Effectiveness of Seasonal Malaria Chemoprevention in Children under Ten Years of Age in Senegal: A Stepped-Wedge Cluster-Randomised Trial. *PLoS Med*. 2016;13:e1002175.
33. Clendennen TE, 3rd, Long GW, Baird JK. QBC and Giemsa-stained thick blood films: diagnostic performance of laboratory technologists. *Trans R Soc Trop Med Hyg*. 1995;89:183-4.
34. Coatney GR CW, Warren M, Contacos PG. *Plasmodium knowlesi*. The Primate Malaria 1971.
35. Collins WE, Jeffery GM. *Plasmodium ovale*: parasite and disease. *Clin Microbiol Rev*. 2005;18:570-81.
36. Collins WE, Jeffery GM. *Plasmodium malariae*: parasite and disease. *Clin Microbiol Rev*. 2007;20:579-92.
37. Combrinck JM, Mabothe TE, Ncokazi KK, Ambele MA, Taylor D, Smith PJ, et al. Insights into the role of heme in the mechanism of action of antimalarials. *ACS Chem Biol*. 2013;8:133-7.
38. Cook G. Alphonse Laveran 1845–1922 discovery of the causative agent of malaria in 1880. *Tropical Medicine: An Illustrated History of The Pioneers* 2007.
39. Cook GC, Webb AJ. Perceptions of malaria transmission before Ross' discovery in 1897. *Postgrad Med J*. 2000;76:738-40.
40. Cordray MS, Richards-Kortum RR. Emerging nucleic acid-based tests for point-of-care detection of malaria. *Am J Trop Med Hyg*. 2012;87:223-30.
41. Costa FT, Lopes SC, Albrecht L, Ataíde R, Siqueira AM, Souza RM, et al. On the pathogenesis of *Plasmodium vivax* malaria: perspectives from the Brazilian field. *Int J Parasitol*. 2012;42:1099-105.



42. Costa FT, Lopes SC, Ferrer M, Leite JA, Martin-Jaular L, Bernabeu M, et al. On cytoadhesion of *Plasmodium vivax*: raison d'etre? *Mem Inst Oswaldo Cruz*. 2011;106 Suppl 1:79-84.
43. Cox-Singh J, Davis TM, Lee KS, Shamsul SS, Matusop A, Ratnam S, et al. *Plasmodium knowlesi* malaria in humans is widely distributed and potentially life threatening. *Clin Infect Dis*. 2008;46:165-71.
44. Croft AM. A lesson learnt: the rise and fall of Lariam and Halfan. *J R Soc Med*. 2007;100:170-4.
45. Croft SL, Duparc S, Arbe-Barnes SJ, Craft JC, Shin CS, Fleckenstein L, et al. Review of pyronaridine anti-malarial properties and product characteristics. *Malar J*. 2012;11:270.
46. Cui L, Su XZ. Discovery, mechanisms of action and combination therapy of artemisinin. *Expert Rev Anti Infect Ther*. 2009;7:999-1013.
47. Curd FH, Davey DG, Rose FL. Studies on synthetic antimalarial drugs; some biguanide derivatives as new types of antimalarial substances with both therapeutic and causal prophylactic activity. *Ann Trop Med Parasitol*. 1945;39:208-16.
48. Das BS. Renal failure in malaria. *J Vector Borne Dis*. 2008;45:83-97.
49. Deas JE, Lee LT. Competitive inhibition by soluble erythrocyte glycoproteins of penetration by *Plasmodium falciparum*. *Am J Trop Med Hyg*. 1981;30:1164-7.
50. Desai M, Gutman J, L'Lanziva A, Otieno K, Juma E, Kariuki S, et al. Intermittent screening and treatment or intermittent preventive treatment with dihydroartemisinin-piperaquine versus intermittent preventive treatment with sulfadoxine-pyrimethamine for the control of malaria during pregnancy in western Kenya: an open-label, three-group, randomised controlled superiority trial. *Lancet*. 2015;386:2507-19.
51. Dorovini-Zis K, Schmidt K, Huynh H, Fu W, Whitten RO, Milner D, et al. The neuropathology of fatal cerebral malaria in malawian children. *Am J Pathol*. 2011;178:2146-58.
52. Draper SJ, Sack BK, King CR, Nielsen CM, Rayner JC, Higgins MK, et al. Malaria Vaccines: Recent Advances and New Horizons. *Cell Host Microbe*. 2018;24:43-56.
53. Eastman RT, Fidock DA. Artemisinin-based combination therapies: a vital tool in efforts to eliminate malaria. *Nat Rev Microbiol*. 2009;7:864-74.

54. Ebstie YA, Abay SM, Tadesse WT, Ejigu DA. Tafenoquine and its potential in the treatment and relapse prevention of *Plasmodium vivax* malaria: the evidence to date. *Drug Des Devel Ther.* 2016;10:2387-99.
55. Erdman LK, Kain KC. Molecular diagnostic and surveillance tools for global malaria control. *Travel Med Infect Dis.* 2008;6:82-99.
56. Escalante AA, Ayala FJ. Phylogeny of the malarial genus *Plasmodium*, derived from rRNA gene sequences. *Proc Natl Acad Sci U S A.* 1994;91:11373-7.
57. Escalante AA, Cornejo OE, Freeland DE, Poe AC, Durrego E, Collins WE, et al. A monkey's tale: the origin of *Plasmodium vivax* as a human malaria parasite. *Proc Natl Acad Sci U S A.* 2005;102:1980-5.
58. Fairhurst RM, Wellems TE. Modulation of malaria virulence by determinants of *Plasmodium falciparum* erythrocyte membrane protein-1 display. *Curr Opin Hematol.* 2006;13:124-30.
59. Fillinger U, Lindsay SW. Larval source management for malaria control in Africa: myths and reality. *Malar J.* 2011;10:353.
60. Florens L, Washburn MP, Raine JD, Anthony RM, Grainger M, Haynes JD, et al. A proteomic view of the *Plasmodium falciparum* life cycle. *Nature.* 2002;419:520-6.
61. Foley M, Tilley L. Quinoline antimalarials: mechanisms of action and resistance. *Int J Parasitol.* 1997;27:231-40.
62. Fried M, Duffy PE. Designing a VAR2CSA-based vaccine to prevent placental malaria. *Vaccine.* 2015;33:7483-8.
63. Fry M, Pudney M. Site of action of the antimalarial hydroxynaphthoquinone, 2-[trans-4-(4'-chlorophenyl) cyclohexyl]-3-hydroxy-1,4-naphthoquinone (566C80). *Biochem Pharmacol.* 1992;43:1545-53.
64. Gardner MJ, Hall N, Fung E, White O, Berriman M, Hyman RW, et al. Genome sequence of the human malaria parasite *Plasmodium falciparum*. *Nature.* 2002;419:498-511.
65. Gething PW, Patil AP, Smith DL, Guerra CA, Elyazar IR, Johnston GL, et al. A new world malaria map: *Plasmodium falciparum* endemicity in 2010. *Malar J.* 2011;10:378.
66. Golgi C. Demonstration der Entwicklung der Malariaparasiten durch Photographien. *Zeitschrift für Hygiene.* 1891;10:136-44.
67. Golgi CJASM. Malarial infection. 1886;10:109-35.
68. Goncalves RM, Lima NF, Ferreira MU. Parasite virulence, co-infections and cytokine balance in malaria. *Pathog Glob Health.* 2014;108:173-8.

69. Grau GE, Craig AG. Cerebral malaria pathogenesis: revisiting parasite and host contributions. *Future Microbiol.* 2012;7:291-302.
70. Greenwood B. Elimination of malaria: halfway there. *Trans R Soc Trop Med Hyg.* 2017;111:1-2.
71. Guerra CA, Gikandi PW, Tatem AJ, Noor AM, Smith DL, Hay SI, et al. The limits and intensity of *Plasmodium falciparum* transmission: implications for malaria control and elimination worldwide. *PLoS Med.* 2008;5:e38.
72. Guerra CA, Howes RE, Patil AP, Gething PW, Van Boeckel TP, Temperley WH, et al. The international limits and population at risk of *Plasmodium vivax* transmission in 2009. *PLoS Negl Trop Dis.* 2010;4:e774.
73. H. M. Gilles DAW, Leonard Jan Bruce-Chwatt. Gilles HM. The malaria parasites. Bruce-Chwatt's essential malariology. 3 ed1993.
74. Hafalla JC, Silvie O, Matuschewski K. Cell biology and immunology of malaria. *Immunol Rev.* 2011;240:297-316.
75. Hanson J, Lee SJ, Mohanty S, Faiz MA, Anstey NM, Charunwattana P, et al. A simple score to predict the outcome of severe malaria in adults. *Clin Infect Dis.* 2010;50:679-85.
76. Hawking F, Wilson ME, Gammage K. Evidence for cyclic development and short-lived maturity in the gametocytes of *Plasmodium falciparum*. *Trans R Soc Trop Med Hyg.* 1971;65:549-59.
77. Hempelmann E. Hemozoin biocrystallization in *Plasmodium falciparum* and the antimalarial activity of crystallization inhibitors. *Parasitol Res.* 2007;100:671-6.
78. Hewitt S, Rowland M. Control of zoophilic malaria vectors by applying pyrethroid insecticides to cattle. *Trop Med Int Health.* 1999;4:481-6.
79. Hippocrates; Adams F. On Airs, Waters, and Places. The genuine works of Hippocrates ; translated from the Greek with a preliminary discourse and annotations1886.
80. J CM. Antimalaria studies on Qinghaosu. *Chin Med J (Engl).* 1979;92:811-6.
81. Jongwutiwes S, Putaporntip C, Iwasaki T, Ferreira MU, Kanbara H, Hughes AL. Mitochondrial genome sequences support ancient population expansion in *Plasmodium vivax*. *Mol Biol Evol.* 2005;22:1733-9.
82. Josling GA, Llinas M. Sexual development in *Plasmodium* parasites: knowing when it's time to commit. *Nat Rev Microbiol.* 2015;13:573-87.
83. Kantele A, Jokiranta TS. Review of cases with the emerging fifth human malaria parasite, *Plasmodium knowlesi*. *Clin Infect Dis.* 2011;52:1356-62.

84. KING PAFA. INSECTS AND DISEASE—MOSQUITOES AND MALARIA. Popular Science Monthly 1883.
85. Kissinger JC, Souza PC, Soarest CO, Paul R, Wahl AM, Rathore D, et al. Molecular phylogenetic analysis of the avian malarial parasite *Plasmodium* (Novyella) juxtanucleare. J Parasitol. 2002;88:769-73.
86. Kiszewski A, Mellinger A, Spielman A, Malaney P, Sachs SE, Sachs J. A global index representing the stability of malaria transmission. Am J Trop Med Hyg. 2004;70:486-98.
87. Knowles R, Gupta BMD. A Study of Monkey-Malaria, and Its Experimental Transmission to Man. Ind Med Gaz. 1932;67:301-20.
88. Kolifarhood G, Raeisi A, Ranjbar M, Haghdoust AA, Schapira A, Hashemi S, et al. Prophylactic efficacy of primaquine for preventing *Plasmodium falciparum* and *Plasmodium vivax* parasitaemia in travelers: A meta-analysis and systematic review. Travel Med Infect Dis. 2017;17:5-18.
89. Krotoski WA. Discovery of the hypnozoite and a new theory of malarial relapse. Trans R Soc Trop Med Hyg. 1985;79:1-11.
90. Krotoski WA, Krotoski DM, Garnham PC, Bray RS, Killick-Kendrick R, Draper CC, et al. Relapses in primate malaria: discovery of two populations of exoerythrocytic stages. Preliminary note. Br Med J. 1980;280:153-4.
91. Laing AB. Treatment of Acute *Falciparum* Malaria with Sulphorthodimethoxine (Fanasil). Br Med J. 1965;1:905-7.
92. Leclerc MC, Hugot JP, Durand P, Renaud F. Evolutionary relationships between 15 *Plasmodium* species from new and old world primates (including humans): an 18S rDNA cladistic analysis. Parasitology. 2004;129:677-84.
93. Lee MR. Plants against malaria. Part 1: Cinchona or the Peruvian bark. J R Coll Physicians Edinb. 2002;32:189-96.
94. Leonardo Bruni JH. History of the Florentine people. 2001-2007.
95. Li Y, Kumar N, Gopalakrishnan A, Ginocchio C, Manji R, Bythrow M, et al. Detection and species identification of malaria parasites by isothermal tHDA amplification directly from human blood without sample preparation. J Mol Diagn. 2013;15:634-41.
96. Liu W, Li Y, Learn GH, Rudicell RS, Robertson JD, Keele BF, et al. Origin of the human malaria parasite *Plasmodium falciparum* in gorillas. Nature. 2010;467:420-5.
97. Liu Z, Miao J, Cui L. Gametocytogenesis in malaria parasite: commitment, development and regulation. Future Microbiol. 2011;6:1351-69.

98. Loutan L. Malaria: still a threat to travellers. *Int J Antimicrob Agents*. 2003;21:158-63.
99. Lukianova-Hleb EY, Campbell KM, Constantinou PE, Braam J, Olson JS, Ware RE, et al. Hemozoin-generated vapor nanobubbles for transdermal reagent- and needle-free detection of malaria. *Proc Natl Acad Sci U S A*. 2014;111:900-5.
100. Martinsen ES, Perkins SL, Schall JJ. A three-genome phylogeny of malaria parasites (*Plasmodium* and closely related genera): evolution of life-history traits and host switches. *Mol Phylogenet Evol*. 2008;47:261-73.
101. Maude RJ, Barkhof F, Hassan MU, Ghose A, Hossain A, Abul Faiz M, et al. Magnetic resonance imaging of the brain in adults with severe falciparum malaria. *Malar J*. 2014;13:177.
102. Mbengue A, Bhattacharjee S, Pandharkar T, Liu H, Estiu G, Stahelin RV, et al. A molecular mechanism of artemisinin resistance in *Plasmodium falciparum* malaria. *Nature*. 2015;520:683-7.
103. McCutchan TF, Kissinger JC, Touray MG, Rogers MJ, Li J, Sullivan M, et al. Comparison of circumsporozoite proteins from avian and mammalian malarias: biological and phylogenetic implications. *Proc Natl Acad Sci U S A*. 1996;93:11889-94.
104. Medana IM, Day NP, Sachanonta N, Mai NT, Dondorp AM, Pongponratn E, et al. Coma in fatal adult human malaria is not caused by cerebral oedema. *Malar J*. 2011;10:267.
105. Menard D, Dondorp A. Antimalarial Drug Resistance: A Threat to Malaria Elimination. *Cold Spring Harb Perspect Med*. 2017;7.
106. Mendes C, Dias F, Figueiredo J, Mora VG, Cano J, de Sousa B, et al. Duffy negative antigen is no longer a barrier to *Plasmodium vivax*--molecular evidences from the African West Coast (Angola and Equatorial Guinea). *PLoS Negl Trop Dis*. 2011;5:e1192.
107. Menezes RG, Pant S, Kharoshah MA, Senthilkumaran S, Arun M, Nagesh KR, et al. Autopsy discoveries of death from malaria. *Leg Med (Tokyo)*. 2012;14:111-5.
108. Mfuh KO, Tassi Yunga S, Esemu LF, Bekindaka ON, Yonga J, Djontu JC, et al. Detection of *Plasmodium falciparum* DNA in saliva samples stored at room temperature: potential for a non-invasive saliva-based diagnostic test for malaria. *Malar J*. 2017;16:434.
109. Miller LH, Haynes JD, McAuliffe FM, Shiroishi T, Durocher JR, McGinniss MH. Evidence for differences in erythrocyte surface receptors for the malarial

- parasites, *Plasmodium falciparum* and *Plasmodium knowlesi*. *J Exp Med*. 1977;146:277-81.
110. Miller LH, Mason SJ, Clyde DF, McGinniss MH. The resistance factor to *Plasmodium vivax* in blacks. The Duffy-blood-group genotype, FyFy. *N Engl J Med*. 1976;295:302-4.
111. Mischlinger J, Ronnberg C, Alvarez-Martinez MJ, Buhler S, Paul M, Schlagenhauf P, et al. Imported Malaria in Countries where Malaria Is Not Endemic: a Comparison of Semi-immune and Nonimmune Travelers. *Clin Microbiol Rev*. 2020;33.
112. Mishra M, Mishra VK, Kashaw V, Iyer AK, Kashaw SK. Comprehensive review on various strategies for antimalarial drug discovery. *Eur J Med Chem*. 2017;125:1300-20.
113. Mohandas N, An X. Malaria and human red blood cells. *Med Microbiol Immunol*. 2012;201:593-8.
114. Mok S, Ashley EA, Ferreira PE, Zhu L, Lin Z, Yeo T, et al. Drug resistance. Population transcriptomics of human malaria parasites reveals the mechanism of artemisinin resistance. *Science*. 2015;347:431-5.
115. Moreno-Perez DA, Ruiz JA, Patarroyo MA. Reticulocytes: *Plasmodium vivax* target cells. *Biol Cell*. 2013;105:251-60.
116. Mouatcho JC, Goldring JPD. Malaria rapid diagnostic tests: challenges and prospects. *J Med Microbiol*. 2013;62:1491-505.
117. Mueller I, Zimmerman PA, Reeder JC. *Plasmodium malariae* and *Plasmodium ovale*--the "bashful" malaria parasites. *Trends Parasitol*. 2007;23:278-83.
118. Muller GC, Beier JC, Traore SF, Toure MB, Traore MM, Bah S, et al. Successful field trial of attractive toxic sugar bait (ATSB) plant-spraying methods against malaria vectors in the *Anopheles gambiae* complex in Mali, West Africa. *Malar J*. 2010;9:210.
119. Muller M, Schlagenhauf P. *Plasmodium knowlesi* in travellers, update 2014. *Int J Infect Dis*. 2014;22:55-64.
120. Mushtaque M, Shahjahan. Reemergence of chloroquine (CQ) analogs as multi-targeting antimalarial agents: a review. *Eur J Med Chem*. 2015;90:280-95.
121. N'Guessan R, Corbel V, Akogbeto M, Rowland M. Reduced efficacy of insecticide-treated nets and indoor residual spraying for malaria control in pyrethroid resistance area, Benin. *Emerg Infect Dis*. 2007;13:199-206.



122. Noedl H, Se Y, Schaefer K, Smith BL, Socheat D, Fukuda MM, et al. Evidence of artemisinin-resistant malaria in western Cambodia. *N Engl J Med*. 2008;359:2619-20.
123. Norman FF, Comeche B, Chamorro S, Perez-Molina JA, Lopez-Velez R. Update on the major imported protozoan infections in travelers and migrants. *Future Microbiol*. 2020;15:213-25.
124. Notomi T, Okayama H, Masubuchi H, Yonekawa T, Watanabe K, Amino N, et al. Loop-mediated isothermal amplification of DNA. *Nucleic Acids Res*. 2000;28:E63.
125. Oakley MS, Gerald N, McCutchan TF, Aravind L, Kumar S. Clinical and molecular aspects of malaria fever. *Trends Parasitol*. 2011;27:442-9.
126. Oguonu T, Shu E, Ezeonwu BU, Lige B, Derrick A, Umeh RE, et al. The performance evaluation of a urine malaria test (UMT) kit for the diagnosis of malaria in individuals with fever in south-east Nigeria: cross-sectional analytical study. *Malar J*. 2014;13:403.
127. P. C. C. Garnham KJO. *Malariology: Malaria Parasites and Other Haemosporidia*.
128. *SCIENCE*. 1967;157.
129. Pain A, Bohme U, Berry AE, Mungall K, Finn RD, Jackson AP, et al. The genome of the simian and human malaria parasite *Plasmodium knowlesi*. *Nature*. 2008;455:799-803.
130. Pasvol G, Jungery M, Weatherall DJ, Parsons SF, Anstee DJ, Tanner MJ. Glycophorin as a possible receptor for *Plasmodium falciparum*. *Lancet*. 1982;2:947-50.
131. Patel P, Bharti PK, Bansal D, Ali NA, Raman RK, Mohapatra PK, et al. Prevalence of mutations linked to antimalarial resistance in *Plasmodium falciparum* from Chhattisgarh, Central India: A malaria elimination point of view. *Sci Rep*. 2017;7:16690.
132. Petersen E. Malaria chemoprophylaxis: when should we use it and what are the options? *Expert Rev Anti Infect Ther*. 2004;2:119-32.
133. Planche T, Krishna S. Severe malaria: metabolic complications. *Curr Mol Med*. 2006;6:141-53.
134. Poostchi M, Silamut K, Maude RJ, Jaeger S, Thoma G. Image analysis and machine learning for detecting malaria. *Transl Res*. 2018;194:36-55.
135. Prugnolle F, Ayala F, Ollomo B, Arnathau C, Durand P, Renaud F. *Plasmodium falciparum* is not as lonely as previously considered. *Virulence*. 2011a;2:71-6.

136. Prugnolle F, Durand P, Neel C, Ollomo B, Ayala FJ, Arnathau C, et al. African great apes are natural hosts of multiple related malaria species, including *Plasmodium falciparum*. *Proc Natl Acad Sci U S A*. 2010;107:1458-63.
137. Prugnolle F, Durand P, Ollomo B, Duval L, Ariey F, Arnathau C, et al. A fresh look at the origin of *Plasmodium falciparum*, the most malignant malaria agent. *PLoS Pathog*. 2011b;7:e1001283.
138. Radeva-Petrova D, Kayentao K, ter Kuile FO, Sinclair D, Garner P. Drugs for preventing malaria in pregnant women in endemic areas: any drug regimen versus placebo or no treatment. *Cochrane Database Syst Rev*. 2014;2014:CD000169.
139. Ragavan KV, Kumar S, Swaraj S, Neethirajan S. Advances in biosensors and optical assays for diagnosis and detection of malaria. *Biosens Bioelectron*. 2018;105:188-210.
140. Rathore D, Wahl AM, Sullivan M, McCutchan TF. A phylogenetic comparison of gene trees constructed from plastid, mitochondrial and genomic DNA of *Plasmodium* species. *Mol Biochem Parasitol*. 2001;114:89-94.
141. Rayner JC, Liu W, Peeters M, Sharp PM, Hahn BH. A plethora of *Plasmodium* species in wild apes: a source of human infection? *Trends Parasitol*. 2011;27:222-9.
142. Ross R. *Memoirs with a Full Account of the Great Malaria Problem and Its Solution*. 1923.
143. Rossati A, Bargiacchi O, Kroumova V, Zaramella M, Caputo A, Garavelli PL. Climate, environment and transmission of malaria. *Infez Med*. 2016;24:93-104.
144. Rowland M, Durrani N, Kenward M, Mohammed N, Urahman H, Hewitt S. Control of malaria in Pakistan by applying deltamethrin insecticide to cattle: a community-randomised trial. *Lancet*. 2001;357:1837-41.
145. Rts SCTP. Efficacy and safety of RTS,S/ AS01 malaria vaccine with or without a booster dose in infants and children in Africa: final results of a phase 3, individually randomised, controlled trial. *Lancet*. 2015;386:31-45.
146. Sahu NK, Sahu S, Kohli DV. Novel molecular targets for antimalarial drug development. *Chem Biol Drug Des*. 2008;71:287-97.
147. Schirmer RH, Coulibaly B, Stich A, Scheiwein M, Merkle H, Eubel J, et al. Methylene blue as an antimalarial agent. *Redox Rep*. 2003;8:272-5.
148. Seydel KB, Kampondeni SD, Valim C, Potchen MJ, Milner DA, Muwalo FW, et al. Brain swelling and death in children with cerebral malaria. *N Engl J Med*. 2015;372:1126-37.

149. Shandilya A, Chacko S, Jayaram B, Ghosh I. A plausible mechanism for the antimalarial activity of artemisinin: A computational approach. *Sci Rep*. 2013;3:2513.
150. Sharma M, Dash AP, Das A. Evolutionary genetic insights into *Plasmodium falciparum* functional genes. *Parasitol Res*. 2010;106:349-55.
151. She RC, Rawlins ML, Mohl R, Perkins SL, Hill HR, Litwin CM. Comparison of immunofluorescence antibody testing and two enzyme immunoassays in the serologic diagnosis of malaria. *J Travel Med*. 2007;14:105-11.
152. Shibeshi MA, Kifle ZD, Atnafie SA. Antimalarial Drug Resistance and Novel Targets for Antimalarial Drug Discovery. *Infect Drug Resist*. 2020;13:4047-60.
153. Singh B, Daneshvar C. Human infections and detection of *Plasmodium knowlesi*. *Clin Microbiol Rev*. 2013;26:165-84.
154. Singh B, Kim Sung L, Matusop A, Radhakrishnan A, Shamsul SS, Cox-Singh J, et al. A large focus of naturally acquired *Plasmodium knowlesi* infections in human beings. *Lancet*. 2004;363:1017-24.
155. Singh SK, Singh AP, Pandey S, Yazdani SS, Chitnis CE, Sharma A. Definition of structural elements in *Plasmodium vivax* and *P. knowlesi* Duffy-binding domains necessary for erythrocyte invasion. *Biochem J*. 2003;374:193-8.
156. Singh V, Mishra N, Awasthi G, Dash AP, Das A. Why is it important to study malaria epidemiology in India? *Trends Parasitol*. 2009;25:452-7.
157. Sinka ME, Bangs MJ, Manguin S, Rubio-Palis Y, Chareonviriyaphap T, Coetzee M, et al. A global map of dominant malaria vectors. *Parasit Vectors*. 2012;5:69.
158. Sinton J, Muliigan HJ, RotMSol. A critical review of the literature relating to the identification of the malarial parasites recorded from monkeys of the families Cercopithecidae and Colobidae. 1933;3.
159. Sissoko MS, Healy SA, Katile A, Omaswa F, Zaidi I, Gabriel EE, et al. Safety and efficacy of PfSPZ Vaccine against *Plasmodium falciparum* via direct venous inoculation in healthy malaria-exposed adults in Mali: a randomised, double-blind phase 1 trial. *Lancet Infect Dis*. 2017;17:498-509.
160. Smith Gueye C, Newby G, Gosling RD, Whittaker MA, Chandramohan D, Slutsker L, et al. Strategies and approaches to vector control in nine malaria-eliminating countries: a cross-case study analysis. *Malar J*. 2016;15:2.
161. Smith JD, Rowe JA, Higgins MK, Lavstsen T. Malaria's deadly grip: cytoadhesion of *Plasmodium falciparum*-infected erythrocytes. *Cell Microbiol*. 2013;15:1976-83.

162. Smith RC, Vega-Rodriguez J, Jacobs-Lorena M. The Plasmodium bottleneck: malaria parasite losses in the mosquito vector. *Mem Inst Oswaldo Cruz*. 2014;109:644-61.
163. Sougoufara S, Ottih EC, Tripet F. The need for new vector control approaches targeting outdoor biting Anopheline malaria vector communities. *Parasit Vectors*. 2020;13:295.
164. Stephen Matthew Rich FJA, Krishna R. Dronamraju, Paolo Arese. Evolutionary Origins of Human Malaria Parasites. *Malaria: Genetic and Evolutionary Aspects* 1970.
165. Stephens JWW. A New Malaria Parasite of Man. *Annals of Tropical Medicine & Parasitology* 1922;16.
166. Stone W, Goncalves BP, Bousema T, Drakeley C. Assessing the infectious reservoir of falciparum malaria: past and future. *Trends Parasitol*. 2015;31:287-96.
167. Su XZ. Human malaria parasites: are we ready for a new species? *J Infect Dis*. 2010;201:1453-4.
168. Sulzer AJ, Wilson M, Hall EC. Indirect fluorescent-antibody tests for parasitic diseases. V. An evaluation of a thick-smear antigen in the IFA test for malaria antibodies. *Am J Trop Med Hyg*. 1969;18:199-205.
169. Sutherland CJ, Tanomsing N, Nolder D, Oguike M, Jennison C, Pukrittayakamee S, et al. Two nonrecombining sympatric forms of the human malaria parasite *Plasmodium ovale* occur globally. *J Infect Dis*. 2010;201:1544-50.
170. Taylor TE, Fu WJ, Carr RA, Whitten RO, Mueller JS, Fosiko NG, et al. Differentiating the pathologies of cerebral malaria by postmortem parasite counts. *Nat Med*. 2004;10:143-5.
171. Taylor WRJ, Hanson J, Turner GDH, White NJ, Dondorp AM. Respiratory manifestations of malaria. *Chest*. 2012;142:492-505.
172. Tham WH, Wilson DW, Lopaticki S, Schmidt CQ, Tetteh-Quarcoop PB, Barlow PN, et al. Complement receptor 1 is the host erythrocyte receptor for *Plasmodium falciparum* PfRh4 invasion ligand. *Proc Natl Acad Sci U S A*. 2010;107:17327-32.
173. Torti F. Therapeutice specialis ad febres periodicas perniciosas. Cui subnectuntur responsiones jatro-apologeticae ad clarissimum Ramazzinum: addita in hac quinta editione auctoris vita a Ludovico Antonio Muratorio conscripta, atque aliis ejusdem opusculis. 1756.

174. Tse EG, Korsik M, Todd MH. The past, present and future of anti-malarial medicines. *Malar J*. 2019;18:93.
175. Tusting LS, Ippolito MM, Willey BA, Kleinschmidt I, Dorsey G, Gosling RD, et al. The evidence for improving housing to reduce malaria: a systematic review and meta-analysis. *Malar J*. 2015;14:209.
176. Tyagi S, Sharma M, Das A. Comparative genomic analysis of simple sequence repeats in three *Plasmodium* species. *Parasitol Res*. 2011;108:451-8.
177. Vasoo S, Pritt BS. Molecular diagnostics and parasitic disease. *Clin Lab Med*. 2013;33:461-503.
178. Vennerstrom JL, Ellis WY, Ager AL, Jr., Andersen SL, Gerena L, Milhous WK. Bisquinolines. 1. N,N-bis(7-chloroquinolin-4-yl)alkanediamines with potential against chloroquine-resistant malaria. *J Med Chem*. 1992;35:2129-34.
179. Vinetz JM, Li J, McCutchan TF, Kaslow DC. *Plasmodium malariae* infection in an asymptomatic 74-year-old Greek woman with splenomegaly. *N Engl J Med*. 1998;338:367-71.
180. Wang J, Zhang CJ, Chia WN, Loh CC, Li Z, Lee YM, et al. Haem-activated promiscuous targeting of artemisinin in *Plasmodium falciparum*. *Nat Commun*. 2015;6:10111.
181. Warhurst DC, Williams JE. ACP Broadsheet no 148. July 1996. Laboratory diagnosis of malaria. *J Clin Pathol*. 1996;49:533-8.
182. Waters AP, Higgins DG, McCutchan TF. *Plasmodium falciparum* appears to have arisen as a result of lateral transfer between avian and human hosts. *Proc Natl Acad Sci U S A*. 1991;88:3140-4.
183. Weina PJ. From atabrine in World War II to mefloquine in Somalia: the role of education in preventive medicine. *Mil Med*. 1998;163:635-9.
184. WHO B. A rapid dipstick antigen capture assay for the diagnosis of *falciparum* malaria. WHO Informal Consultation on Recent Advances in Diagnostic Techniques and Vaccines for Malaria. *Bull World Health Organ*. 1996;74:47-54.
185. Wilson ML. Malaria rapid diagnostic tests. *Clin Infect Dis*. 2012;54:1637-41.
186. Win TT, Jalloh A, Tantular IS, Tsuboi T, Ferreira MU, Kimura M, et al. Molecular analysis of *Plasmodium ovale* variants. *Emerg Infect Dis*. 2004;10:1235-40.
187. Zheng XY, Xia Y, Gao FH, Chen C. [Synthesis of 7351, a new antimalarial drug (author's transl)]. *Yao Xue Xue Bao*. 1979;14:736-7.

188. Zimmerman PA, Ferreira MU, Howes RE, Mercereau-Puijalon O. Red blood cell polymorphism and susceptibility to *Plasmodium vivax*. *Adv Parasitol.* 2013;81:27-76.



---

## Review of Literature | Chapter 2

---

House-cleaning Staff and their Metabolic  
Chores in the Malaria Parasite

## **A. Genome architecture in *Plasmodium* spp.**

Since the first blueprint of the *P. falciparum* 3D7 genome was completed in 2002 (Gardner et al. , 2002), malaria parasite's genomic research has progressed quickly, thanks to advances in next-generation sequencing (NGS) technologies and lower prices (Le Roch et al. , 2012). Publicly available databases now contain the genetic information of avian, rodent, and primate parasites, including the disease models like *P. chabaudi*, *P. berghei*, *P. reichenowi*, *P. yoelii*, *P. cynomolgi*, *P. gallinaceum*, and *P. relictum* (Ansari et al. , 2016, Bohme et al. , 2018, Carlton et al. , 2002, Otto et al. , 2014a, Otto et al. , 2014b, Pasini et al. , 2017, Tachibana et al. , 2012), in addition to the genetic code of predominant species that infect humans (Carlton, 2003, Gardner et al., 2002, Pain et al. , 2008, Rutledge et al. , 2017). From studies of parasite evolution, genome diversity, drug resistance, and population genetics (Chan et al. , 2015, de Oliveira et al. , 2017, Hupalo et al. , 2016, Manske et al. , 2012, Miles et al. , 2016, Miotto et al. , 2013, Ocholla et al. , 2014, Talundzic et al. , 2018), data from an extensive number of laboratory lines and field isolates of *P. vivax* and *P. falciparum* have been uploaded in the database, resulting in the generation of an improved reference *P. falciparum* genome with massively polished annotation (Bohme et al. , 2019). Single-cell sequencing approaches have recently offered exciting results for mixed infections, genetic recombination, and parasite development (Nair et al. , 2014, Poran et al. , 2017, Trevino et al. , 2017).

*Plasmodium* parasites are haploid throughout their life cycle, except for a brief diploid phase after fertilisation in the mosquito midgut. Various *Plasmodium* species' genomes are generally twice to thrice larger than that of *Saccharomyces cerevisiae*, varying from 20 to 35 megabases (Mb) and including a circular plastid genome of 35 kb, 14 chromosomes, and numerous copies of 6 kb mitochondrial DNA. Approximately 5,300 protein-encoding genes were discovered, similar to the number in *S. pombe*. Antigenic variation genes are primarily found in the sub-telomeric regions of chromosomes. This intracellular parasite's genome encodes fewer transporters and enzymes than the genomes of free-living eukaryotic microorganisms. Still, many genes are devoted to host-parasite interactions and immune evasion. The apicoplast is the organelle involved in fatty-acid and isoprenoid metabolism, which receives many nuclear-encoded proteins. The genomic sequence of *P. falciparum* clone 3D7 was determined using the whole chromosome shotgun sequencing technique. *Plasmodium* spp. has a wide range of

adenine-thymine (AT) concentrations, for example, 80% AT in *P. reichenowi*, *P. gallinaceum*, and *P. falciparum*; rodent malaria parasites having 80% AT; and 60% AT in *P. knowlesi*, *P. vivax*, and *P. cynomolgi*. Introns and intergenic noncoding sections had a higher AT concentration than protein-coding exons, with a mean of 80.6% AT for the entire *P. falciparum* genome compared to 86.5% for non-coding sequences (Gardner et al., 2002). *P. falciparum*'s high AT content is due to a significant number of simple sequence repeats, low-complexity regions, and micro-satellites, as well as an irregular codon use bias (DePristo et al. , 2006, Su et al. , 1999, Su and Wellem, 1996). AT-rich repeat polymorphisms are frequent markers for drug resistance gene linkage mapping and analysing the evolution and organisation of parasite populations (Anderson and Roper, 2005, Ferdig et al. , 2004, Figan et al. , 2018, Roper et al. , 2003, Su et al. , 2007, Wootton et al. , 2002).

During its intra-erythrocytic lifetime, *Plasmodium falciparum* has a distinct chromatin architecture. Euchromatin, which is not organised into chromosome territories or otherwise structurally confined within the nucleus, maintains an extraordinarily high proportion of its genome (Lemieux et al. , 2013, Salcedo-Amaya et al. , 2009). There are, however, heterochromatin patches stretching from the telomeres into sub-telomeric domains, as well as heterochromatin regions distributed throughout the chromosomal bodies (Flueck et al. , 2009, Lopez-Rubio et al. , 2009).

Host	Parasite species or strain	No. of PIR genes <sup>a</sup>	Genome size (Mb)	GC content (%)	No. of scaffolds	No. of predicted genes <sup>b</sup>	No. of predicted proteins <sup>b</sup>
Humans	<i>P. falciparum</i> 3D7	189	23.2	19.3	14	5,712	5,460
	<i>P. vivax</i>	1,212	29.1	39.7	374	6,830	6,677
	<i>P. ovale</i>	>2,100	33.5	29.4	779	6,986	6,228
	<i>P. ovale</i> subsp. <i>wallikeri</i>	1,375	33.5	28.9	1,914	8,582	8,421
	<i>P. ovale</i> subsp. <i>curtisi</i>	1,949	33.5	28.4	4,025	7,280	7,162
	<i>P. malariae</i>	255	33.6	24.7	63	6,709	6,573
	<i>P. knowlesi</i>	71	24.4	38.7	28	5,483	5,323
	<i>P. inui</i> San Antonio		27.4	42.4	323	5,879	5,832
Chimpanzee	<i>P. reichenowi</i>	351	24.0	19.3	261	5,909	5,741
Old World monkeys	<i>P. cynomolgi</i> B	265	26.2	40.4	1,663	5,776	5,716
	<i>P. coatneyi</i> Hackeri	771	27.7	39.7	14	5,575	5,516
Rodents	<i>P. yoelii</i> 17X	980	22.8	21.1	154	6,257	6,091
	<i>P. berghei</i> ANKA	217	18.5	22.1	100	5,245	4,928
	<i>P. chabaudi</i> AS	201	18.9	23.6	39	5,364	5,217
	<i>P. vinckei</i>		18.2	23.4	49	5,009	4,954
Birds	<i>P. relictum</i> SGS1	4	22.6	18.4	498	5,306	5,138
	<i>P. gallinaceum</i> 8A	20	23.8	17.8	152	5,439	5,280

**Table 1:** Statistics on genomic sequences for major animal and human *Plasmodium* species. <sup>a</sup>PIR: *Plasmodium* Interspersed Repeat; <sup>b</sup>Obtained from PlasmoDB (Adapted from Su XZ et. al., 2019)

## **B. Nucleotide metabolism in the parasite**

Purines and pyrimidines must be synthesised from scratch, acquired by salvage, and interconverted before being assembled as nucleotides into the nucleic acids and their derivatives used in various metabolic pathways. A continual and ample supply of the constituent nucleotides is required for DNA replication and transcription to the different RNA species, which is quite a demanding requirement for rapidly dividing cells and diseases, such as malaria parasites or cancer cells.

The pyrimidine deoxyribonucleotide 5'-triphosphates dTTP and dCTP, as well as the purine deoxyribonucleotide 5'-triphosphates dGTP and dATP, are used in DNA synthesis; RNA production requires the ribose counterparts of G, A, and C, as well as uridine 5'-triphosphate, UTP. Furthermore, few of these molecules and their offshoots play critical roles in metabolic and gene regulation as valuable sources of chemical energy (e.g. GTP, ATP), precursors of more complex molecules (e.g. GTP to folates and pterins), nucleotide-based enzyme cofactors (e.g. FAD, NAD<sup>+</sup>, FMN), switch signals (e.g. GDP/GTP), and intracellular second messengers (e.g. cAMP) (Hyde, 2007). The said nucleotides and their nucleoside and nucleobase predecessors can be acquired through a variety of pathways, including *de novo* synthesis, salvage acquisition, or subsequent interconversions to produce the congruous stockpile of pyrimidine and purines derivatives found in the nucleic acids and other vital molecular species. For many years, drugs targeted at interrupting such chemical mechanisms have been successfully utilised against protozoan parasites of the phylum *Apicomplexa*, like *Toxoplasma* and *Plasmodium*, while the selection of resistant strains is a serious and growing concern, notably in the case of malaria parasites (White, 2004).

One of the most essential metabolic routes in human cells is nucleotide metabolism, which yields the building blocks for RNA and DNA synthesis. Nucleotides are also crucial for various cellular processes, including energy transfer, signalling, and synthesising several biomolecules in carbohydrate and lipid metabolisms (Welin and Nordlund, 2010). Purine and pyrimidine nucleotides can be obtained either by *de novo* biosynthesis or through salvage biosynthesis, in which nucleosides/deoxynucleosides and nucleobases are recovered from nutrients or destroyed RNA and DNA. The *de novo* and salvage mechanisms are active in humans for pyrimidine and purine nucleotide needs. In contrast, the salvage pathways have been reported

to be more operative than the *de novo* pathways (Pels Rijcken et al. , 1993, Weber, 1983).

The adult erythrocyte, which hosts *P. falciparum* during its intraerythrocytic phases, has a bounded ability to salvage purine and no potential for *de novo* purine synthesis. Similarly, the RBC (red blood cell) needs more capacity to synthesise pyrimidines from scratch, as evidenced by the non-existence or meagre amounts of enzymes involved in pyrimidine synthesis. Furthermore, even though both pyrimidine and purine nucleosides can be uptake by the host RBC, the salvage pathway for utilisation of pyrimidine bases and nucleosides like thymidine, uracil, and uridine has low activity (Krungskrai, 1993).

### • Purine metabolism

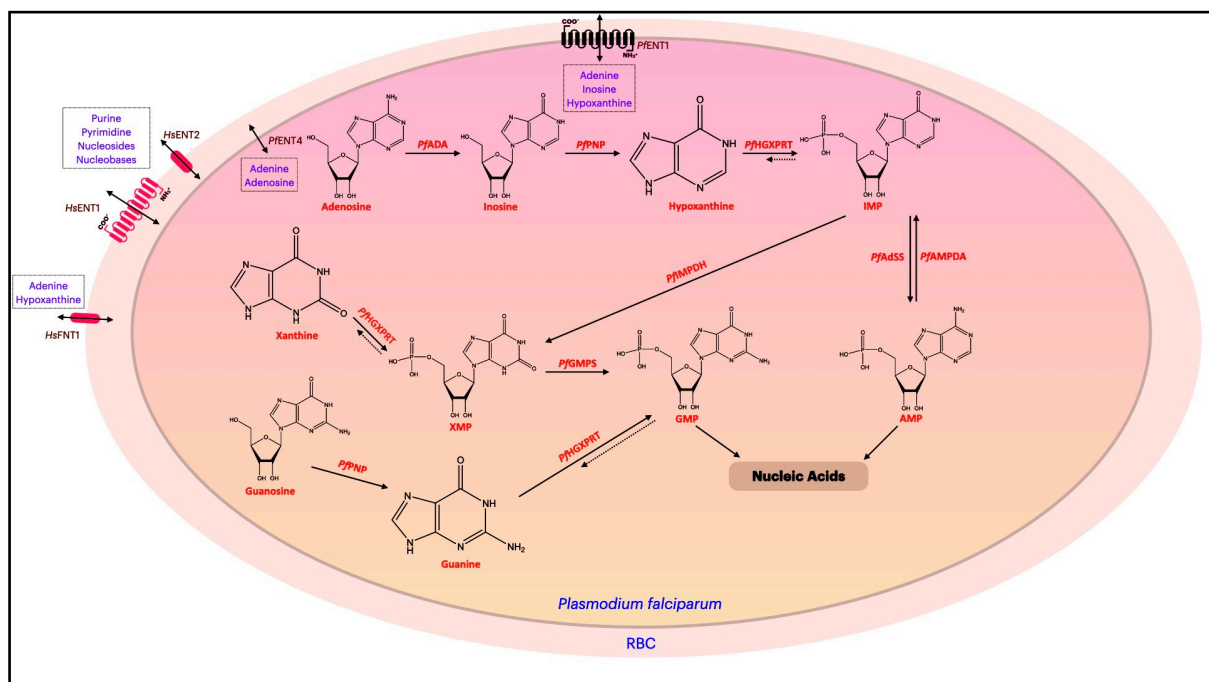


Figure 1: Purine metabolism (schematic) in malaria parasite.

*Plasmodium* parasites are purine auxotrophs that rely solely on purines taken from the RBCs to survive. Additionally, because the genome of *Plasmodium* has such an elevated adenine content (>80% AT-rich), the malaria parasite needs a large number of adenine nucleotides (ATP and dATP) to keep up the rapid duplication rate. The appropriate nucleosides and nucleobases are acquired from the plasma by the RBCs



and then followed by the parasites because erythrocytes are unable to do *de novo* purine synthesis (Quashie et al. , 2008, Quashie et al. , 2010).

At the plasma membrane, adult erythrocytes, like several human cells, have many transport systems (channels and transporters) that are in charge of the uptake of hexoses, amino acids, ions, and other nutrients. hENT1 and hENT2 (equilibrative nucleoside transporters) are in control of pyrimidine and purine uptake, with nucleosides being the most suited substrates, hCNTs (human nucleoside transporters) are concentrative ion-coupled nucleoside transporters, and hFNT1 (facilitated nucleobase transporter) transports adenine and hypoxanthine (Boswell-Casteel and Hays, 2017, Liu et al. , 2006). NPPs (new permeability pathways) are meant to assist in the uptake of low molecular weight metabolites such as polyamine, sugar-alcohols, sugar, nucleobases, nucleosides, amino acids, ions, and other metabolites essential for parasite growth (Gero et al. , 2003, Kirk and Lehane, 2014, Liu et al., 2006). Membrane transporters, such as ENTs, mediate purine import from the host cell, with *Pf*ENT1 being the most important of the four purine salvage transporters (*Pf*ENT1-4) identified thus far (Frame et al. , 2015). *Pf*ENT1 is a proton-dependent transporter that accepts hypoxanthine, inosine, adenosine, guanine, and guanosine as substrates, with adenosine and hypoxanthine having greater affinities ( $K_i$ : 300-700  $\mu$ M) (Hyde et al. , 2001, Riegelhaupt et al. , 2010). There is an 11 transmembrane helix segment protein with an internal N-terminus and an external C-terminus structurally the same as all mammalian and protozoan ENT1 (Sundaram et al. , 2001). *Pf*ENT1, like its human counterpart, may take pyrimidine nucleosides as a substrate (Jiang et al. , 2000). *Pf*ENT2 was found to be situated on the parasitic endoplasmic reticulum, suggesting it is not involved in purine uptake (Frame et al., 2015). *Pf*ENT3 has yet to be demonstrated as a purine or pyrimidine transporter (Downie et al. , 2010). *Pf*ENT4 does not transport AMP or hypoxanthine. Hence, its substrate profile is different from that of *Pf*ENT1 (Frame et al. , 2012).

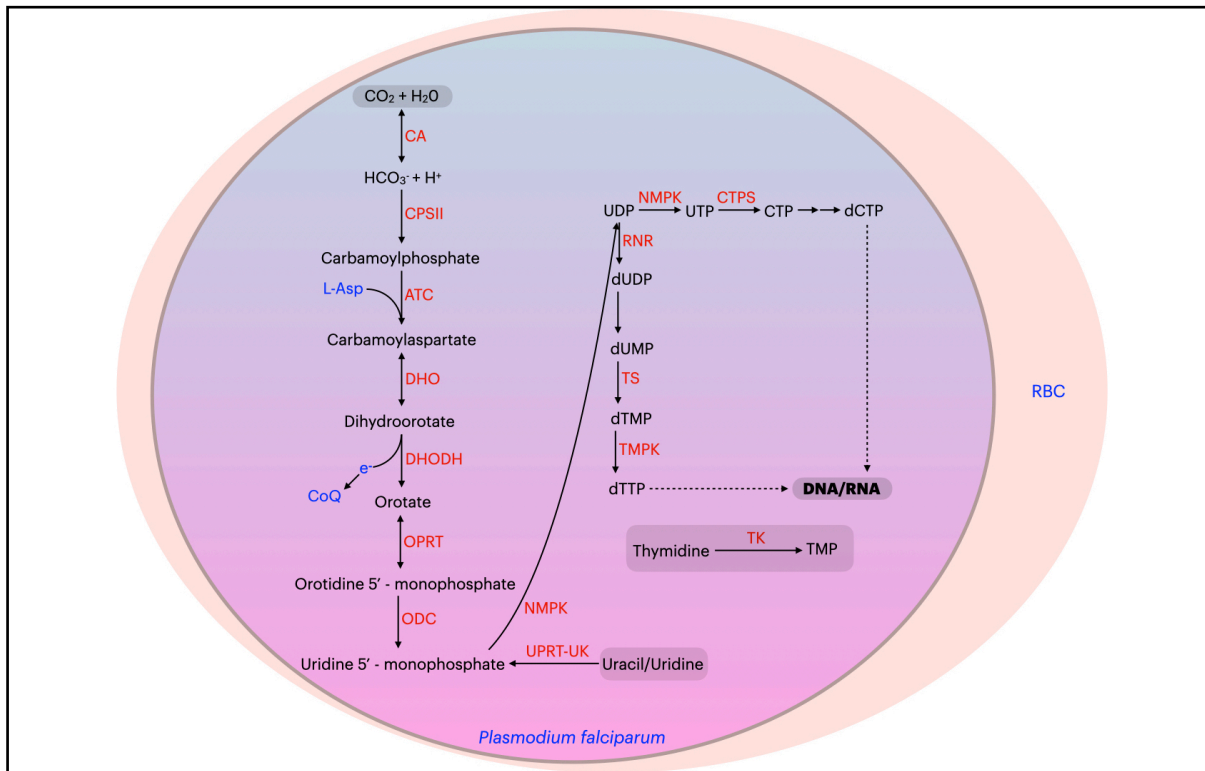
Purine phosphoribosyl transferases (PRT), purine nucleoside phosphorylases (PNP), and adenosine deaminases (ADA) are some of the enzymes involved in *Pf* purine metabolism. Phosphoribosyl transferases are found in many parasites as well as mammalian cells, and they cause the ribophosphorylation of purine bases in a single step. Hypoxanthine-guanine-xanthine-phosphoribosyl transferase (HGXPRT) in *Plasmodium* transforms guanine, hypoxanthine, and xanthine to guanosine-5'-monophosphate (GMP) inosine-5'-monophosphate (IMP), and xanthosine-5'-

monophosphate (XMP). Purine nucleoside phosphorylases break down nucleosides into their nucleobase and sugar equivalents. Purine nucleosides'/nucleotides' exocyclic amino groups are converted to their oxo-derivatives by adenosine deaminases. Furthermore, while the enzymes ADA, HGXPRT, and PNP are highly expressed and important in purine metabolism, other enzymes such as adenylosuccinate synthetase (AdSS), guanosine-5'-monophosphate synthase (GMPS), inosine-5'-monophosphate dehydrogenase (IMPDH), and adenosine-5'-monophosphate deaminase (AMPDA) are also required.

The malaria parasite draws adenosine from the RBCs, and the combined action of PNP and ADA produces hypoxanthine and inosine. Because the erythrocyte contains relatively low adenosine because of the activities of erythrocytic adenosine kinases, the malaria parasite must rely on hypoxanthine, which is also acquired from the RBCs. As a result, the main purine metabolism predecessor is hypoxanthine, and *Plasmodium* cultures are frequently supplemented with this nucleobase, thus serving as a nutrition to support *Plasmodium* multiplication. HGXPRT converts hypoxanthine to IMP. As a result, IMP remains the nucleotidic precursor of all other purine nucleotides essential for nucleic acid biosynthesis, including adenosine 5'-monophosphate (AMP). Because the malaria parasite lacks the genes encoding nucleoside kinases (which synthesise AMP directly from adenosine), there is no other way to get AMP, and IMP happens to be the only adenosine 5'-monophosphate metabolite available (Cassera et al. , 2008, Ward et al. , 2004). To a certain extent, it has been demonstrated that elevated amounts of adenosine in *Pf* cultures could stimulate erythrocytic AMP uptake into the parasite via AMP produced by RBC (Cassera et al., 2008). IMP is converted to XMP by IMPDH and subsequently to GMP by GMPS. GMP is also created via an alternate mechanism involving guanine and guanosine absorption, the latter of which are HGXPRT and PNP substrates. Likewise, XMP is formed due to HGXPRT activity after xanthine absorption (Cassera et al. , 2011).



## • Pyrimidine metabolism



**Figure 3:** Pyrimidine metabolism (schematic) in malaria parasite.

Protozoan parasites only generate pyrimidine derivatives via the *de novo* pathway, and they are not efficient at salvaging pyrimidines from the RBCs. In summary, *Plasmodium* pyrimidine biosynthesis contains six enzymatic processes, similar to the human host, that produce a crucial metabolite, uridine-5'-monophosphate (UMP), which is subsequently employed as a predecessor for all pyrimidine nucleotides required for DNA/RNA biosynthesis (dUMP, dCTP, dTTP, UTP, and CTP). The related enzymes can be split into mono-functional and multi-functional proteins. Carbamoyl phosphate synthetase II (CPS-II) and aspartate transcarbamoylase (ATC) have received little study, although *Pf* dihydroorotase (DHOase) has received a lot. The latter has been studied and discovered to have numerous similarities with the mammalian proteins (Krungkrai et al. , 2008). The three enzymes listed below, dihydroorotate hydrogenase (DHODH), orotate phosphoribosyltransferase (OPRT), and dihydroorotase (DHOase), are thought to be important in targeting the human parasite, with DHODH being the most extensively investigated (Phillips and Rathod, 2010, Singh et al. , 2017).





## C. Aberrations & the house-cleaning staff in malaria parasite

The constant fight to eliminate the plethora of hazardous substances in the environment is imperative for existence at the cellular level, particularly for unicellular organisms. The multi-drug resistance pumps, the outer membrane of the Gram-negative bacteria, and a range of exporters for specific substances, including hazardous metals, tellurite, arsenic compounds, and intracellular detoxification systems, all work together to protect against environmental toxins. The final group is especially significant for chemicals that easily enter the cell by simple diffusions, like H<sub>2</sub>O<sub>2</sub> or oxygen, or through commandeering cellular transport mechanisms, like arsenate. Hazardous or potentially toxic substances can be produced as byproducts of regular cellular metabolism, in addition to external risks. The most noticeable of these compounds are reactive oxygen species (ROS) produced by respiratory electron transport chains, for example, peroxide and superoxide. A sophisticated network of intracellular sensors monitors the amounts of peroxides and ROS inside the cell (Galperin, 2004), and these chemicals are scavenged by thioredoxin, superoxide dismutases, rubrerythrins, glutathione reductases, and many other systems (Ezraty et al. , 2005, Imlay, 2002, 2003). Non-canonical nucleoside (deoxy) triphosphates (d/NTPs), such as dITP, dUTP, 2-oxo-dATP or 8-oxo-dGTP, are another prominent class of potentially hazardous by-products that result from oxidation, deamination, or other changes of canonical nucleotides (Kamiya, 2003). When some of these aberrant NTPs are integrated into nascent DNA, they cause mispairing, dramatically increasing the mutation rate. The most critical responsibility of all the house-cleaning *in vivo* is safeguarding the genomic DNA integrity. Different DNA polymerase types integrate dATP, dGTP, dCTP, and dTTP into the nascent DNA. However, the capacity of DNA polymerases to discriminate against some mutagenic nucleotides is limited. As a result, several non-canonical nucleotides are highly likely to be integrated into the chromosomal DNA, thereby causing mispairing-like transitions and transversions (Hamid and Eckert, 2005, Hizi et al. , 1997). Intercepting and hydrolysing such non-canonical dNTPs prevents DNA damage and efficiently enhances the action of DNA repair mechanisms (Michaels and Miller, 1992).

The *Plasmodium* genome is haploid, and its fast DNA replication cycles may raise the likelihood of non-canonical nucleotide incorporation into the genomic DNA;



however, the proteins preventing such DNA aberrations in the *Plasmodium* parasite remain mainly understood. Intracellular nucleotide pools are required for DNA synthesis, operate as energy storage molecules, and function as regulators and cofactors in various signal transduction and metabolic pathways. Deoxyinosine triphosphate (dITP) is produced by oxidative deamination of the nitrogenous base from deoxyadenosine triphosphate (dATP), deoxyxanthosine triphosphate (dXTP) from deoxyguanosine triphosphate (dGTP), and deoxyuridine triphosphate (dUTP) from deoxycytosine triphosphate (dCTP). Because thymine lacks a free amino group, it cannot be oxidatively deaminated. Purine base oxidation, on the other hand, produces nucleotides such as 8-oxo-dATP, 2-oxo-dATP, and 8-oxo-dGTP (Kamiya, 2003). During DNA replication, such changed nucleotide analogues can be integrated. When the DNA repair machinery detects a break, single-strand breaks that must be repaired are introduced. As a result of the buildup of harmful mutations and double-strand breaks, cellular development may decrease, or the cell may perish (Rai, 2010). Cells have developed DNA house-cleaning enzymes that hydrolyse harmful nucleotides into their monophosphate forms (not toxic). These are harmful substrates for their respective nucleoside kinases and are not re-phosphorylated.

Sanitation enzymes are classified into four superfamilies based on structural characteristics:

Enzyme	Non-canonical NTP <sup>a</sup>				Hydrolysis of canonical NTPs <sup>b</sup>				References
	Name	Generated by	Pairs with	$K_m^{NTP}$ $\mu$ M	$K_m^{dATP}$ mM	$K_m^{dCTP}$ mM	$K_m^{dTTP}$ mM	$K_m^{dGTP}$ mM	
ITPase	dITP	IMP reduction, phosphorylation	A, C, T	150–250	7.3	2.1	5.5	4.4	Hwang <i>et al.</i> (1999); Chung <i>et al.</i> (2001)
Trimeric dUTPase	dXTP <sup>c</sup>	dGTP deamination	T, C	100	NA	NA	4	>20	Larsson <i>et al.</i> (1996a); Persson <i>et al.</i> (2001)
	dUTP	dCTP deamination	A, G	0.2–2.6	NA	NA	NA	NA	Harkiolaki <i>et al.</i> (2004); Moroz <i>et al.</i> (2004)
Dimeric dUTPase	dUTP	dCTP deamination	A, G	0.5–4.5	NA	NA	NA	NA	Maki and Sekiguchi (1992); Sarawat <i>et al.</i> (2002)
<i>Escherichia coli</i> MutT	8-oxo-dGTP	dGTP oxidation	A, C	0.48–0.52	NA	1.1	1.7	1.8	Fujikawa <i>et al.</i> (1999); Kamiya (2004)
Human MTH1	8-oxo-dGTP	dGTP oxidation	A, C	12–15	NA	0.26–0.87	NA	NA	
	8-oxo-dATP	dATP oxidation, $\gamma$ -irradiation	T, G, A	14					
	2-oxo-dATP	dATP oxidation	T, C, G, A	5.7–8.3					
	2-oxo-rATP	ATP oxidation	–	4.3					
UTPase	5-methyl-rUTP (rTTP)	RNA breakdown, phosphorylation	–	0.12–0.21	NA	NA	NA	NA	Xu <i>et al.</i> (2003)
MazG <sup>d</sup>	2-oxo-dATP <sup>d</sup>	dATP oxidation	T, G, C, A	nd	1.0	1.0	3.2	1.0	Zhang <i>et al.</i> (2003); Moroz <i>et al.</i> (2005)

a. Pairing data are from Kamiya (2003) and original references.

b. NA, no detectable activity.

c. Data with riboNTP substrate; no available data on dNTP hydrolysis.

d. Unconfirmed prediction for the *sulfolobus* enzyme.

**Figure 5:** Sanitation enzymes and their substrates. (Galperin *et al.*, 2006)

## 1. NuDiX superfamily (nucleotide diphosphate linked to some other moiety, X)

It is defined by the NuDiX box domain G-x(5)-E-x(5)-[UA]- x-R-E-x(2)-E-E-x-G-U, where U is a hydrophobic residue and x any residue. The NuDiX hydrolases are members of a superfamily of enzymes that are conserved across all species and were initially dubbed MutT family proteins after MutT, the first member (Bessman et al. , 1996, McLennan, 1999). MutT, an *E. coli* NuDiX enzyme, hydrolyses 8-oxo-dGTP and 8-oxo-GTP, cleaning the house at both the RNA and DNA levels. AT to GC transversions were found to be 100 to 10000 times more common in *mutT*-depleted *E. coli* (Mildvan et al. , 2005, Taddei et al. , 1997). MTH1, a human MutT homolog produced by the *NUDT1* gene, is anti-mutagenic because it inhibits oxidised dNTPs (e.g., 2-OH-dATP or 8-oxo-dGTP) from being incorporated into the DNA (Fujikawa et al. , 1999, Sakumi et al. , 1993). NuDiX hydrolases perform hydrolysis processes on various substrates, including canonical (d)NTPs, non-nucleoside polyphosphates, oxidised (d)NTPs, and capped mRNAs. The conserved 23-amino-acids NuDiX pattern (Nudix box), Gx5Ex5[UA]xREx2EEExGU, where U is an aliphatic, hydrophobic residue, is required for catalysis, albeit there are a few intriguing instances with different consensus residues. The Glu residues in the heart of the motif, REx<sub>2</sub>EE, take part in a critical function in binding vital divalent cations, and this sequence is found in a 'loop-helix-loop' structural motif. The distinctive NuDiX fold features an  $\alpha$ - $\beta$ - $\alpha$  sandwich architecture, and the consensus NuDiX structural motif is placed on a loop-helix (Mildvan et al., 2005, Ooga et al. , 2005).

Ap4A hydrolase, a member of the NuDiX hydrolase superfamily, maintains NpnN, Ap4A, Ap5A, and Gp4G levels in cells. NuDiX hydrolases are found in species ranging from 0 to 30 (*E. coli* has 12; humans have 24), with parasitic organisms having either extremely few or none (McLennan, 2006). The diadenosine tetraphosphate (Ap4A) hydrolase enzyme of the malaria parasite modulates the level of signalling molecules like Ap4A by hydrolysing them to ATP and AMP (Sharma et al. , 2016).

## 2. dUTPases

Misincorporation of dUTPs into DNA must be avoided if genetic information is to be preserved. Removing dUTP from the nucleotide pool is critical in most biological systems. The enzyme deoxyuridine 5'-triphosphate nucleotide-hydrolase (dUTPase; E.C. 3.6.1.23) uses  $Mg^{2+}$  as a cofactor to hydrolyse dUTP into dUMP and inorganic pyrophosphate (Bertani et al. , 1961, Shlomai and Kornberg, 1978). It limits dUTP buildup and guarantees the availability of dUMP, the thymidylate synthase substrate, in dTTP production. dUTPases are monomeric, dimeric, or trimeric based on their structure. Trimeric dUTPases are the most numerous and diverse among them. Human, bacterial, two retroviral dUTPases and *Plasmodium falciparum* (PfdUTPase) complexed with a trityl deoxyuridine derivative have all been resolved by X-ray crystallography. The active region of trimeric dUTPases has five highly conserved sequence motifs that provide residues that are required for activity (Barabas et al. , 2004, Chan et al. , 2004, Dauter et al. , 1999, Larsson et al. , 1996, Mol et al. , 1996, Persson et al. , 2001, Prasad et al. , 1996, Whittingham et al. , 2005).

Three of four conventional dNTPs can be made from their ribonucleoside diphosphate (NDP) equivalents (Nordlund and Reichard, 2006). On the other hand, the direct predecessor for dTTP is not found in the ribonucleoside pool and must be produced separately. The uracil base-containing precursors are used in the *de novo* synthesis of dTTP: dUMP is the direct input into the thymidylate synthase process. The deamination of a cytosine deoxyribonucleotide (dCMP or dCTP) is the primary source of dUMP in most organisms, with other alternative mechanisms, such as the dephosphorylation of dUDP, serving as modest supplements (Bianchi et al. , 1987, Mollgaard and Neuhaard, 1978, Neuhaard and Thomassen, 1971). On top of producing dUMP, the dUTPase activity also eliminates excess dUTP, preventing uracil from being incorporated into DNA instead of thymine (Lari et al. , 2006, Vertessy and Toth, 2009). Although uracil in DNA is not mutagenic when replaced with thymine, it is regarded as a mistake and triggers uracil-excision repair mechanisms (Visnes et al. , 2009). The dUTPase null mutants in *Plasmodium berghei* are not viable; hence, this protein is being exploited as a drug target (Kumar et al. , 2019). Given the parasite's elevated AT/GC ratio (about 80%) in its genetic code and the fact that *Plasmodium* has a dearth of dCMP/dCTP deaminase activities, dUTPase is likely to play a vital role in dUMP production (Vertessy and Toth, 2009).

### 3. All- $\alpha$ -helical NTPases

The NTP diphosphatases (apyrases, EC 3.6.1.5) hydrolyse NTPs to NMPs in two phosphate-releasing processes using NDPs as intermediates and are active against both NTPs and NDPs. The sequence relationship between the new dimeric dUTPase family and the NTP pyrophosphatase MazG, phage T4 dCTPase, phosphoribosyl-ATP pyrophosphatase HisE, and some uncharacterised protein families, including the human protein XTP3TPA (RS21-C6), which is over-expressed in cancer and embryonic cells, was discovered using structure-guided analysis. The amalgamation of these enzymes into one superfamily of all- $\alpha$  NTP pyrophosphatases was supported by comparison with the MazG-like protein's structure from *Sulfolobus solfataricus*, indicating that dimeric dUTPases originated from a tetrameric MazG-like progenitor by gene duplication (Moroz et al. , 2005).

### 4. ITPases (Inosine triphosphate pyrophosphatase): The crucial protein

**Backdrop:** Inosine triphosphate pyrophosphatase is a ubiquitous protective critical enzyme that controls non-canonical cell contamination. Liakopoulou and Alivisatos identified Inosine triphosphate pyrophosphatase (ITPase) in human erythrocytes for the first time in 1964. ITPase performed different functions than ATPase, was competitively inhibited by adenine derivatives, and was reliant on the presence of magnesium ( $Mg^{2+}$ ). Vanderheide demonstrated in 1970 that ITPase distributes  $PP_i$  from human erythrocytes using partly isolated ITPase (Bierau et al. , 2007). It was subsequently identified regarding enzyme kinetics for ITP, isolated 2-3000 fold from human RBCs, and examined to comprehend its function against GTP, ATP, UTP, and CTP over a decade later. Human ITPA has had two critical discoveries till the turn of the century. Firstly, researchers focused further on ITPA's sub-cellular localisation and tissue dispersion. Compared to ordinary erythrocytes, bone marrow fibroblasts were shown to have much greater activity. Second, Vanderheiden's findings show that ITPA was highly specific for ITP and dITP and that XTP was a substrate (Fraser et al. , 1975). Its sequence, however, was undiscovered for another 30 years. In the course of a structural genomics study in 1999, the 3D structure of the *Methanococcus jannaschii* protein MJ0226 was figured out, showing a unique nucleotide-binding enzyme that preferentially hydrolysed ITP and XTP (Hwang et al. , 1999). Several investigations were conducted in 2001 to better understand the expression of human

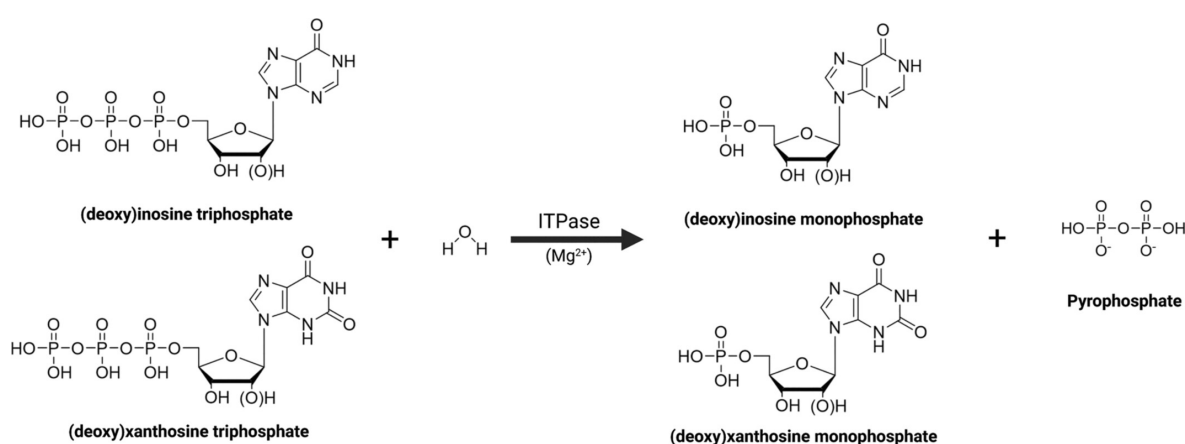
ITPA in *E. coli*. The human counterpart was identified and proven to be responsible for human ITPase activity (Lin et al. , 2001). It was extensively examined in 24 tissues using recombinant technology and northern blots, emphasising the pancreas, liver, heart, testis/ovary, thyroid, and adrenal glands. Several researchers' crystallisation of human ITPA and subsequent detailed visualisation of its structure was a remarkable breakthrough (Porta et al. , 2006, Stenmark et al. , 2007). The homologues from *E. coli* (Ec197/YggV/RdgB and *Archaeoglobus fulgidus* (AF2237), first described by its chromosomal fragmentation phenotype) were subsequently found to have this action (Bradshaw and Kuzminov, 2003, Chung et al. , 2001, Kouzminova and Kuzminov, 2004). The yeast (Ham1p) and *E.coli* homologues were also shown to secure cells against the harmful and mutagenesis effects of the base analogue 6-N-hydroxylaminopurine (HAP). By hydrolysing the deoxynucleoside triphosphate derivative dHAPTP, they are expected to hinder HAP inclusion in DNA (Burgis et al. , 2003, Noskov et al. , 1996). This yeast protein is similar to the Mj0226 protein, sharing roughly 30% of its sequence. Over-expression of Mj0226 protected the *E. coli* host against the toxic effects of HAP (Zhang and Kim, 2003), while the isolated enzyme had limited action against dHAPTP (Chung et al., 2001).

**Structural insight:** Many ITPase homologues have been identified due to structural genomics investigations. These include enzymes from *Pyrococcus horikoshii* PH1917 (1v7r, RIKEN Structural Genomics/Proteomics Initiative), *E. coli* YggV/RdgB (1k7k, Midwest Center for Structural Genomics), and *T. maritima* TM0159 (Protein Data Bank entries 1b78 and 2mjp, Berkeley Structural Genomics Center) (1vp2, Joint Center for Structural Genomics). The structures indicated the most conserved residues' potential active location but did not immediately reveal the enzyme's specificity or mechanism. The active site cavity size and shape vary among structures, including experimentally confirmed ITPases from *E. coli* and *M. jannaschii*. This suggests that the enzyme uses an induced-fit mechanism.

**Functional aspect:** ITP and XTP are hydrolysed efficiently by all characterised ITPases, but not the canonical NTPs, including structurally similar GTP; in other words, the canonical ones are hydrolysed much less efficiently when compared. The high selectivity of ITPase against GTP cannot be attributable to steric incompatibility. Still, it may be due to a highly adverse environment of the 2-amino group of guanine in the binding site, as shown by comparing the substrate structures. Indeed, at position 2 of the purine ring, where they vary from GTP, the structures of XTP and

ITP differ. The 2-keto group of xanthine, missing in hypoxanthine, is housed well at the binding site, where it most likely absorbs H-bonds from the protein donor groups, based on a modest preference for XTP over ITP. Though the 2-amino group of guanine can be sheltered at the same site without difficulty, the free energy cost of doing so can be pretty excessive, especially if the 2-amino group of guanine and the protein's H-bond donor groups are buried together with no access to solvent molecules or other H-bond acceptors (Galperin et al. , 2006).

ITPase catalyses the following reactions:



ITPase is responsible for sanitising nucleotide pools by eliminating non-canonical purines from (deoxy)nucleoside triphosphates ((d)NTPs) (Simone et al. , 2013). ITPase is a pyrophosphohydrolase that transforms non-canonical purine (d)NTPs such as (deoxy)inosine 5'-triphosphate ((d)ITP), to nucleoside monophosphate ((d)NMP), releasing pyrophosphate (PP<sub>i</sub>). It breaks the acidic anhydride link between the (d)NTP's alpha and beta phosphates (Holmes et al. , 1979). In cells, non-canonical purine (d)NTPs form naturally. Phosphorylation of inosine 5'-monophosphate (IMP), a predecessor to guanosine 5'-monophosphate (GMP) and adenosine 5'-monophosphate (AMP), can yield both ITP and dITP in the purine biosynthesis pathway (Galperin et al., 2006, Zalkin et al. , 1996). Additionally, inosine-containing nucleosides/nucleotides are formed by oxidative deamination of adenine-containing nucleosides/nucleotides or deamination of guanine-containing nucleosides/nucleotides (Friedberg et al. , 1995). Evidence suggests that ITPase and its orthologs inhibit the accumulation of non-canonical purine (d)NTPs and that they are conserved in all three domains of life, including viruses (Burgis and Cunningham, 2007, Hwang et al., 1999, Lin et al., 2001, Mbanzibwa et al. , 2009,



Porta et al., 2006). ITPase deficiency and polymorphism have been shown to cause sensitivity to non-canonical purines, higher mutation rates, DNA damage, impeded cell cycle progression, and chromosomal abnormalities such as double-strand breaks in bacterial, yeast, and murine systems (Abolhassani et al., 2010, Burgis et al., 2003, Noskov et al., 1996, Pang et al., 2012, Waisertreiger et al., 2010). ITPase only exhibits a significant affinity for NTPs containing non-canonical purines (dITP, ITP, and xanthosine 5'-triphosphate) (Burgis and Cunningham, 2007, Lin et al., 2001), which appears to be a critical step in the enzyme action. While interactions with NTPs containing canonical bases result in inappropriate alignment of the proposed catalytic residues and the scissile phosphoanhydride bond and a much lower rate of catalysis, tight binding of the non-canonical nucleobase in the nucleobase binding pocket of the enzyme allows proper alignment of distal catalytic residues to catalyse the hydrolysis of the phosphoanhydride bonds. It hydrolyses phosphoanhydride bonds in non-canonical NTPs and dNTPs with comparable activity, regardless of whether the carbohydrate moiety is ribose or deoxyribose (Porta et al., 2006, Stenmark et al., 2007).

***The human version of the enzyme:*** ITPase is a homodimeric protein in humans. A core elongated mixed sheet creates a platform to support two globular lobes in this protein. ITP attaches in a cleft in the dimer interface between the lobes. The specificity pocket is deep within each monomer's dimerisation lobe, whereas the catalytic site is at the dimer interface in the N-terminal lobe (Stenmark et al., 2007). In the human model,  $Mg^{2+}$  is required for catalysis (Vanderheiden, 1970), and it is expected to occur via acid-base chemistry (Stenmark et al., 2007). However, the exact mechanism is unknown. With an alkaline pH and a reducing agent like dithiothreitol (DTT), maximum activity has been seen the best (Simone et al., 2013). However, other working models might differ in enzymatic actions and requirements. Inosine 5'-diphosphate (IDP) inhibits human ITPase competitively, but not NMPs or any other nucleoside studied (Holmes et al., 1979). Substantial substrate inhibition was reported in many experiments utilising pure human ITPase in the presence of increased amounts of ITP or dITP (Burgis and Cunningham, 2007, Lin et al., 2001, Vanderheiden, 1970).  $Cd^{2+}$ ,  $Co^{2+}$ , and  $Ca^{2+}$  ions have also been demonstrated to inhibit the enzyme (Vanderheiden, 1979).

***Clinically significant polymorphisms & their effects:*** The pharmacogenetic importance of human ITPA variation has been shown throughout the previous

decade. At least 30 polymorphisms in the ITPA gene have been discovered in humans where seven of the variations have been demonstrated to be clinically significant thus far (D'Avolio et al. , 2013, Kevelam et al. , 2015, Nakauchi et al. , 2016, Sumi et al. , 2002, Tanaka et al. , 2011, Maeda et al. , 2005, Shipkova et al. , 2006). ITPA status has been linked to hepatitis C treatment (D'Avolio et al. , 2016, Pineda-Tenor et al. , 2015) and thiopurine therapy (Bierau et al., 2007, Marsh et al. , 2004) results in several studies. Furthermore, ITPA mutations have been associated with young-onset TB susceptibility, and variation has been connected to ITPA mutations causing early infantile encephalopathy (rare and recessive mutation in the *ITPA* gene). Next-generation sequencing (NGS) was used to discover single nucleotide polymorphisms in young TB patients from multi-case families, and two ITPA polymorphisms (g.19176G > A and c.94C > A (p.Pro32Thr)) were found to be related to young TB patients (Kevelam et al., 2015, Nakauchi et al., 2016). A robust molecular reason for lower enzyme activity is known for one clinically relevant variation, c.94C > A (p.Pro32Thr). In the year 2004, it was estimated that roughly 5% of the world's population had the c.94C > A (p.Pro32Thr) ITPA variant, with Asian populations having the highest penetrance, 14-19% (Marsh et al., 2004). Numerous additional polymorphisms have been discovered, with current findings claiming that roughly a third of the population may carry an ITPA polymorphism linked to lower ITPase activity (Jimmerson et al. , 2017, Rembeck et al. , 2014, Thompson et al. , 2010).

In detail, the clinical effects of the ITPA protein mutation or variation are quite a few to cite. ITPase is hypothesised to affect thiopurine drug metabolism directly (Bierau et al., 2007). Prodrugs like 6-mercaptopurine and azathioprine require enzymatic bioactivation to undergo phosphorylation and ribosylation before becoming active nucleotide forms. Thiopurines are antimetabolites that work by replacing guanosine-containing nucleotides in physiological processes in their active state. Thiopurines may wreak havoc on various biological mechanisms, including DNA and RNA metabolism (Sahasranaman et al. , 2008). 6-thio-inosine-5'-triphosphate (6-TITP), one of the intermediates in this process, has a structure almost comparable to ITP. 6-TITP is an ITPase substrate. This shows that the medication may enter a fruitless phosphorylation cycle to the triphosphate form by kinase enzymes and hydrolysis to the monophosphate form by ITPase. As a result, the ITPase enzyme reduces an intermediate in the route, hence the quantity of active drugs in human cells (Bierau et al., 2007). ITPA variation has been linked to higher thiopurine toxicity in several studies. Immunosuppressants known as thiopurines, such as azathioprine or 6-

mercaptopurine, are widely given to organ transplant recipients (Everitt et al. , 2012), as well as patients with ulcerative colitis (Bean, 1962), inflammatory bowel disease (Pasternak et al. , 2013), Crohn's disease (Brooke et al. , 1969), and several malignancies (Brem and Karran, 2012). Toxicity is thought to be caused by an increase in thiol-containing NTPs. As a result, researchers have proposed that patients be screened for ITPA polymorphism before a treatment to reduce the risk of medication toxicity.

Intracellular kinases activate the drug ribavirin to create a nucleoside triphosphate, which is then integrated into the viral genome as a substrate for the replicative RNA-dependent RNA polymerase, triggering chromosomal destruction. The role of ITPase directly in ribavirin metabolism has not been shown yet, although it is thought to influence overall nucleotide pools and ITPA status (Fellay et al. , 2010, Jimmerson et al., 2017). One of the possible adverse effects of the conventional therapy of pegylated interferon-alpha and ribavirin for the 170 million persons living with hepatitis C worldwide is haemolytic anaemia (Lavanchy, 2009). In a follow-up study, researchers discovered that those with the c.94C > A (p.Pro32Thr) or c.124 + 21A > C polymorphisms had a lower requirement for ribavirin dosage reduction, as well as a delayed onset of anaemia (Thompson et al., 2010). Recently, strategies have been devised for using ITPase activity to predict anaemia development after ribavirin therapy (Peltenburg et al. , 2015).

***Disease amplitude & ITPA gene's importance:*** In the 1960s, Vanderheiden observed individuals with an aberrant buildup of erythrocyte ITP and proposed that they were ITPase defective (Vanderheiden, 1965). In 2002, it was reported that RBCs from c.94C > A (p.Pro32Thr) homozygous individuals had zero per cent ITPase activity with no apparent biological consequences (Sumi et al., 2002). ITPase is now known to have a critical function in purine metabolism (Kevelam et al., 2015) and is highly conserved throughout all fields of biology (Lin et al., 2001) and expressed in all mammalian tissues studied (Hwang et al., 1999). The role of the enzyme in different tissues appears to be different, and activity in a single tissue type may not always mirror activity throughout the entire organism. As summarised above, more studies have found significant links between ITPA fluctuation and treatment regimen results over time. A couple of examples of lethality due to severe homozygous ITPA defects (ITPA knockout (KO) mouse data (Behmanesh et al. , 2009) where more than half of the *Itpa*<sup>-/-</sup> mice perished before birth, and those that survived died within two weeks;

and the infantile encephalopathy data (Kevelam et al., 2015), as well as an example of increased fitness due to potential ITPA over-expression (TB susceptibility data (Nakauchi et al., 2016), it appears more likely that there is a range of ITPA-related disease, as Kevelam *et. al.* (2015) indicated. As a result, most ITPA variations result in altered ITPA expression/activity.

Non-canonical (d)ITP and (d)XTP are presumably continually created in cells, causing genomic instability, abnormal protein production, and changes to GTP/ATP-dependent signalling pathways. ITPA removes these troublesome (d)NTPs. Conservation in all species and the severe biological consequences of ITPA depletion in model organisms highlight its relevance. Similarly, in *Plasmodium* model, sanitation enzymes are classified into four superfamilies based on structural characteristics: Ham1 (6-n-HydroxylAMinopurine sensitive) domain, which consists of a long central beta-sheet creating the active site's floor, defines ITPases; NuDiX box domain G-x(5)-E-x(5)-[UA]-x-R-E-x(2)-E-E-x-G-U, where 'x' is any residue and 'U' is a hydrophobic residue, defines the NuDiX superfamily; dUTPases, which have an eight-stranded jelly-roll beta-barrel and a trimeric fold; all-helical NTPases that are active against both dNTPs and dNDPs, resulting in the formation of dNMPs as a byproduct.

Here, in this broad, extensive study in **Experimental Chapters 1 & 2**, the *Plasmodium falciparum* 3D7 HAM1 gene was cloned, over-expressed, and purified by various protein filtration techniques to get a pure protein, and identity was confirmed using mass spectrometry. The protein was biophysically characterised in-depth to reveal its oligomeric status in its native state. The biochemical enzymatic characterisations demonstrated the non-canonical substrates best suited for maximal activity *in-vitro*. Antibodies were raised in rabbits against the protein of interest, and its specificity was confirmed. Inside the parasite, localisation studies were performed using antibodies and live-cell imaging techniques across the different erythrocytic stages of *Plasmodium falciparum*. mRNA levels of the gene across the three blood stages were also fished out. Binding kinetics with the various substrate(s) were found using calorimetric experiments. The effect of specific inhibitors on the enzyme activity was further assessed. Genetic manipulations in the parasite using a CRISPR/Cas9-DiCre system were used to check the gene's essentiality in parasite survival. The protein structure was elucidated in unbound and bound states to the substrate(s) with the help of X-ray crystallography and molecular dynamics simulations, respectively. In

brief, the PfHAM1 protein was structurally and functionally characterised holistically to understand the role of the protein in parasite biology and exploit it as a novel anti-malarial target. This is especially important given the emergence of resistance against artemisinin and other common anti-malarial drugs, which warrants further exploitation of new drug targets through structure-based drug design approaches.

## D. Conclusion

Recent investigations have discovered various house-cleaning enzymes that clear the cell of potentially harmful endogenous metabolites. While few are members of the NuDiX hydrolase family, many others have unique structures and specific substrate preferences. Some of these enzymes (ITPase, phage T4 dUTPase) have been known for decades, but their amino acid sequences have recently been discovered. Others (MazG) were recently found in genome sequences and given an enzymatic function. Many enzymes in the ITPase, NuDiX, and MazG superfamilies must be better characterised in many model organisms. Specificity is crucial for house-cleaning NTPases, which must identify sub-micromolar amounts of aberrant NTPs in the context of a  $10^3$  - fold excess of canonical NTPs. House-cleaning NTPases achieve high specificity by strategically placing substrate-binding residues that successfully distinguish between canonical and non-canonical NTPs. The significance of the house-cleaning function puts forward that there are likely to be plenty more such enzymes concealed among the unannotated 'conserved hypothetical' open reading frames (ORFs) found in microbial genomes, many of which have general nucleotidase, phosphatase, or esterase activity with low affinity for their substrates (Kim et al. , 2004, Kuznetsova et al. , 2005, Yakunin et al. , 2004). Current biochemical investigations have begun to understand the modus operandi of ITPase to distinguish between canonical and non-canonical purine-containing NTPs and the disease state's underlying mechanism. ITPase is a little-researched protein in general, and there is a knowledge gap in basic ITPase biochemistry science. In humans, there are now seven ITPA variants/mutants that have been identified as having an impact on clinical outcomes. Depending on the clinical situation, having an ITPA status might be advantageous or disadvantageous. Patients with the ITPA polymorphism experience drug toxicity while on thiopurine therapy, whereas those with the ITPA polymorphism develop anaemia much later in treating hepatitis C. ITPA variants anticipated to boost protein expression are thought to lessen TB susceptibility. These cases suggest the presence of a spectrum of ITPA-related sicknesses.

Malaria has been a primary worldwide health concern for people throughout history, and it is a primary cause of mortality and disease in many tropical and subtropical nations. Over the last fifteen years, improved control efforts have lowered malaria prevalence by more than half, boosting the likelihood of long-term elimination and maybe eradication. New tools like innovative antimalarial



medications, more effective vaccines, and a better knowledge of the illness and parasite biology must be developed to achieve this aim. Likewise, such a protein, *PfHAM1*, is crucial for the malaria parasite's survival in the RBCs, removing the rogue (non-canonical) nucleotides from the nucleotide pool to prevent chromosomal instabilities and safeguard the genome. Designing drugs against this novel malarial protein may benefit malaria mitigation globally.

## E. References

1. Abolhassani N, Iyama T, Tsuchimoto D, Sakumi K, Ohno M, Behmanesh M, et al. NUDT16 and ITPA play a dual protective role in maintaining chromosome stability and cell growth by eliminating dIDP/IDP and dITP/ITP from nucleotide pools in mammals. *Nucleic Acids Res.* 2010;38:2891-903.
2. Anderson TJ, Roper C. The origins and spread of antimalarial drug resistance: lessons for policy makers. *Acta Trop.* 2005;94:269-80.
3. Ansari HR, Templeton TJ, Subudhi AK, Ramaprasad A, Tang J, Lu F, et al. Genome-scale comparison of expanded gene families in *Plasmodium ovale wallikeri* and *Plasmodium ovale curtisi* with *Plasmodium malariae* and with other *Plasmodium* species. *Int J Parasitol.* 2016;46:685-96.
4. Barabas O, Pongracz V, Kovari J, Wilmanns M, Vertessy BG. Structural insights into the catalytic mechanism of phosphate ester hydrolysis by dUTPase. *J Biol Chem.* 2004;279:42907-15.
5. Bean RH. The treatment of chronic ulcerative colitis with 6-mercaptopurine. *Med J Aust.* 1962;49(2):592-3.
6. Behmanesh M, Sakumi K, Abolhassani N, Toyokuni S, Oka S, Ohnishi YN, et al. ITPase-deficient mice show growth retardation and die before weaning. *Cell Death Differ.* 2009;16:1315-22.
7. Bertani LE, Haggmark A, Reichard P. Synthesis of pyrimidine deoxyribonucleoside diphosphates with enzymes from *Escherichia coli*. *J Biol Chem.* 1961;236:PC67-PC8.
8. Bessman MJ, Frick DN, O'Handley SF. The MutT proteins or "Nudix" hydrolases, a family of versatile, widely distributed, "housecleaning" enzymes. *J Biol Chem.* 1996;271:25059-62.
9. Bianchi V, Pontis E, Reichard P. Regulation of pyrimidine deoxyribonucleotide metabolism by substrate cycles in dCMP deaminase-deficient V79 hamster cells. *Mol Cell Biol.* 1987;7:4218-24.
10. Bierau J, Lindhout M, Bakker JA. Pharmacogenetic significance of inosine triphosphatase. *Pharmacogenomics.* 2007;8:1221-8.
11. Bohme U, Otto TD, Cotton JA, Steinbiss S, Sanders M, Oyola SO, et al. Complete avian malaria parasite genomes reveal features associated with lineage-specific evolution in birds and mammals. *Genome Res.* 2018;28:547-60.

12. Bohme U, Otto TD, Sanders M, Newbold CI, Berriman M. Progression of the canonical reference malaria parasite genome from 2002-2019. *Wellcome Open Res.* 2019;4:58.
13. Boswell-Casteel RC, Hays FA. Equilibrative nucleoside transporters-A review. *Nucleosides Nucleotides Nucleic Acids.* 2017;36:7-30.
14. Bradshaw JS, Kuzminov A. RdgB acts to avoid chromosome fragmentation in *Escherichia coli*. *Mol Microbiol.* 2003;48:1711-25.
15. Brem R, Karran P. Oxidation-mediated DNA cross-linking contributes to the toxicity of 6-thioguanine in human cells. *Cancer Res.* 2012;72:4787-95.
16. Brooke BN, Hoffmann DC, Swarbrick ET. Azathioprine for Crohn's disease. *Lancet.* 1969;2:612-4.
17. Burgis NE, Brucker JJ, Cunningham RP. Repair system for noncanonical purines in *Escherichia coli*. *J Bacteriol.* 2003;185:3101-10.
18. Burgis NE, Cunningham RP. Substrate specificity of RdgB protein, a deoxyribonucleoside triphosphate pyrophosphohydrolase. *J Biol Chem.* 2007;282:3531-8.
19. Carlton J. The *Plasmodium vivax* genome sequencing project. *Trends Parasitol.* 2003;19:227-31.
20. Carlton JM, Angiuoli SV, Suh BB, Kooij TW, Pertea M, Silva JC, et al. Genome sequence and comparative analysis of the model rodent malaria parasite *Plasmodium yoelii yoelii*. *Nature.* 2002;419:512-9.
21. Cassera MB, Hazleton KZ, Riegelhaupt PM, Merino EF, Luo M, Akabas MH, et al. Erythrocytic adenosine monophosphate as an alternative purine source in *Plasmodium falciparum*. *J Biol Chem.* 2008;283:32889-99.
22. Cassera MB, Zhang Y, Hazleton KZ, Schramm VL. Purine and pyrimidine pathways as targets in *Plasmodium falciparum*. *Curr Top Med Chem.* 2011;11:2103-15.
23. Chan ER, Barnwell JW, Zimmerman PA, Serre D. Comparative analysis of field-isolate and monkey-adapted *Plasmodium vivax* genomes. *PLoS Negl Trop Dis.* 2015;9:e0003566.
24. Chan S, Segelke B, Lakin T, Krupka H, Cho US, Kim MY, et al. Crystal structure of the *Mycobacterium tuberculosis* dUTPase: insights into the catalytic mechanism. *J Mol Biol.* 2004;341:503-17.
25. Chung JH, Back JH, Park YI, Han YS. Biochemical characterization of a novel hypoxanthine/xanthine dNTP pyrophosphatase from *Methanococcus jannaschii*. *Nucleic Acids Res.* 2001;29:3099-107.

26. D'Avolio A, Cusato J, De Nicolo A, Allegra S, Di Perri G. Pharmacogenetics of ribavirin-induced anemia in HCV patients. *Pharmacogenomics*. 2016;17:925-41.
27. D'Avolio A, De Nicolo A, Cusato J, Ciancio A, Boglione L, Strona S, et al. Association of ITPA polymorphisms rs6051702/rs1127354 instead of rs7270101/rs1127354 as predictor of ribavirin-associated anemia in chronic hepatitis C treated patients. *Antiviral Res*. 2013;100:114-9.
28. Dauter Z, Persson R, Rosengren AM, Nyman PO, Wilson KS, Cedergren-Zeppezauer ES. Crystal structure of dUTPase from equine infectious anaemia virus; active site metal binding in a substrate analogue complex. *J Mol Biol*. 1999;285:655-73.
29. de Oliveira TC, Rodrigues PT, Menezes MJ, Goncalves-Lopes RM, Bastos MS, Lima NF, et al. Genome-wide diversity and differentiation in New World populations of the human malaria parasite *Plasmodium vivax*. *PLoS Negl Trop Dis*. 2017;11:e0005824.
30. DePristo MA, Zilversmit MM, Hartl DL. On the abundance, amino acid composition, and evolutionary dynamics of low-complexity regions in proteins. *Gene*. 2006;378:19-30.
31. Downie MJ, El Bissati K, Bobenchik AM, Nic Lochlainn L, Amerik A, Zufferey R, et al. PfNT2, a permease of the equilibrative nucleoside transporter family in the endoplasmic reticulum of *Plasmodium falciparum*. *J Biol Chem*. 2010;285:20827-33.
32. Everitt MD, Hammond ME, Snow GL, Stehlik J, Revelo MP, Miller DV, et al. Biopsy-diagnosed antibody-mediated rejection based on the proposed International Society for Heart and Lung Transplantation working formulation is associated with adverse cardiovascular outcomes after pediatric heart transplant. *J Heart Lung Transplant*. 2012;31:686-93.
33. Ezraty B, Aussel L, Barras F. Methionine sulfoxide reductases in prokaryotes. *Biochim Biophys Acta*. 2005;1703:221-9.
34. Fellay J, Thompson AJ, Ge D, Gumbs CE, Urban TJ, Shianna KV, et al. ITPA gene variants protect against anaemia in patients treated for chronic hepatitis C. *Nature*. 2010;464:405-8.
35. Ferdig MT, Cooper RA, Mu J, Deng B, Joy DA, Su XZ, et al. Dissecting the loci of low-level quinine resistance in malaria parasites. *Mol Microbiol*. 2004;52:985-97.

36. Figan CE, Sa JM, Mu J, Melendez-Muniz VA, Liu CH, Wellems TE. A set of microsatellite markers to differentiate *Plasmodium falciparum* progeny of four genetic crosses. *Malar J*. 2018;17:60.
37. Flueck C, Bartfai R, Volz J, Niederwieser I, Salcedo-Amaya AM, Alako BT, et al. *Plasmodium falciparum* heterochromatin protein 1 marks genomic loci linked to phenotypic variation of exported virulence factors. *PLoS Pathog*. 2009;5:e1000569.
38. Frame IJ, Deniskin R, Arora A, Akabas MH. Purine import into malaria parasites as a target for antimalarial drug development. *Ann N Y Acad Sci*. 2015;1342:19-28.
39. Frame IJ, Merino EF, Schramm VL, Cassera MB, Akabas MH. Malaria parasite type 4 equilibrative nucleoside transporters (ENT4) are purine transporters with distinct substrate specificity. *Biochem J*. 2012;446:179-90.
40. Fraser JH, Meyers H, Henderson JF, Brox LW, McCoy EE. Individual variation in inosine triphosphate accumulation in human erythrocytes. *Clin Biochem*. 1975;8:353-64.
41. Friedberg E, Walker G, Siede W. *DNA Repair and Mutagenesis* (Washington, DC: Am. Soc. Microbiol.). 1995.
42. Fujikawa K, Kamiya H, Yakushiji H, Fujii Y, Nakabeppu Y, Kasai H. The oxidized forms of dATP are substrates for the human MutT homologue, the hMTH1 protein. *J Biol Chem*. 1999;274:18201-5.
43. Galperin MY. Bacterial signal transduction network in a genomic perspective. *Environ Microbiol*. 2004;6:552-67.
44. Galperin MY, Moroz OV, Wilson KS, Murzin AG. House cleaning, a part of good housekeeping. *Mol Microbiol*. 2006;59:5-19.
45. Gardner MJ, Hall N, Fung E, White O, Berriman M, Hyman RW, et al. Genome sequence of the human malaria parasite *Plasmodium falciparum*. *Nature*. 2002;419:498-511.
46. Gero AM, Dunn CG, Brown DM, Pulenthiran K, Gorovits EL, Bakos T, et al. New malaria chemotherapy developed by utilization of a unique parasite transport system. *Curr Pharm Des*. 2003;9:867-77.
47. Hamid S, Eckert KA. Effect of DNA polymerase beta loop variants on discrimination of O6-methyldeoxyguanosine modification present in the nucleotide versus template substrate. *Biochemistry*. 2005;44:10378-87.

48. Hizi A, Kamath-Loeb AS, Rose KD, Loeb LA. Mutagenesis by human immunodeficiency virus reverse transcriptase: incorporation of O6-methyldeoxyguanosine triphosphate. *Mutat Res.* 1997;374:41-50.
49. Holmes SL, Turner BM, Hirschhorn K. Human inosine triphosphatase: catalytic properties and population studies. *Clin Chim Acta.* 1979;97:143-53.
50. Hupalo DN, Luo Z, Melnikov A, Sutton PL, Rogov P, Escalante A, et al. Population genomics studies identify signatures of global dispersal and drug resistance in *Plasmodium vivax*. *Nat Genet.* 2016;48:953-8.
51. Hwang KY, Chung JH, Kim SH, Han YS, Cho Y. Structure-based identification of a novel NTPase from *Methanococcus jannaschii*. *Nat Struct Biol.* 1999;6:691-6.
52. Hyde JE. Targeting purine and pyrimidine metabolism in human apicomplexan parasites. *Curr Drug Targets.* 2007;8:31-47.
53. Hyde RJ, Cass CE, Young JD, Baldwin SA. The ENT family of eukaryote nucleoside and nucleobase transporters: recent advances in the investigation of structure/function relationships and the identification of novel isoforms. *Mol Membr Biol.* 2001;18:53-63.
54. Imlay JA. How oxygen damages microbes: oxygen tolerance and obligate anaerobiosis. *Adv Microb Physiol.* 2002;46:111-53.
55. Imlay JA. Pathways of oxidative damage. *Annu Rev Microbiol.* 2003;57:395-418.
56. Jiang L, Lee PC, White J, Rathod PK. Potent and selective activity of a combination of thymidine and 1843U89, a folate-based thymidylate synthase inhibitor, against *Plasmodium falciparum*. *Antimicrob Agents Chemother.* 2000;44:1047-50.
57. Jimmerson LC, Urban TJ, Truesdale A, Baouchi-Mokrane F, Kottlilil S, Meissner EG, et al. Variant Inosine Triphosphatase Phenotypes Are Associated With Increased Ribavirin Triphosphate Levels. *J Clin Pharmacol.* 2017;57:118-24.
58. Kamiya H. Mutagenic potentials of damaged nucleic acids produced by reactive oxygen/nitrogen species: approaches using synthetic oligonucleotides and nucleotides: survey and summary. *Nucleic Acids Res.* 2003;31:517-31.
59. Kevelam SH, Bierau J, Salvarinova R, Agrawal S, Honzik T, Visser D, et al. Recessive ITPA mutations cause an early infantile encephalopathy. *Ann Neurol.* 2015;78:649-58.



60. Kim Y, Yakunin AF, Kuznetsova E, Xu X, Pennycooke M, Gu J, et al. Structure- and function-based characterization of a new phosphoglycolate phosphatase from *Thermoplasma acidophilum*. *J Biol Chem*. 2004;279:517-26.
61. Kirk K, Lehane AM. Membrane transport in the malaria parasite and its host erythrocyte. *Biochem J*. 2014;457:1-18.
62. Kouzminova EA, Kuzminov A. Chromosomal fragmentation in dUTPase-deficient mutants of *Escherichia coli* and its recombinational repair. *Mol Microbiol*. 2004;51:1279-95.
63. Krungkrai J. Dihydroorotase and dihydroorotate dehydrogenase as a target for antimalarial drugs. *Drugs Fut*. 1993;18.
64. Krungkrai SR, Wutipraditkul N, Krungkrai J. Dihydroorotase of human malarial parasite *Plasmodium falciparum* differs from host enzyme. *Biochem Biophys Res Commun*. 2008;366:821-6.
65. Kumar H, Kehrer J, Singer M, Reinig M, Santos JM, Mair GR, et al. Functional genetic evaluation of DNA house-cleaning enzymes in the malaria parasite: dUTPase and Ap4AH are essential in *Plasmodium berghei* but ITPase and NDH are dispensable. *Expert Opin Ther Targets*. 2019;23:251-61.
66. Kuznetsova E, Proudfoot M, Sanders SA, Reinking J, Savchenko A, Arrowsmith CH, et al. Enzyme genomics: Application of general enzymatic screens to discover new enzymes. *FEMS Microbiol Rev*. 2005;29:263-79.
67. Lari SU, Chen CY, Vertessy BG, Morre J, Bennett SE. Quantitative determination of uracil residues in *Escherichia coli* DNA: Contribution of ung, dug, and dut genes to uracil avoidance. *DNA Repair (Amst)*. 2006;5:1407-20.
68. Larsson G, Svensson LA, Nyman PO. Crystal structure of the *Escherichia coli* dUTPase in complex with a substrate analogue (dUDP). *Nat Struct Biol*. 1996;3:532-8.
69. Lavanchy D. The global burden of hepatitis C. *Liver Int*. 2009;29 Suppl 1:74-81.
70. Le Roch KG, Chung DW, Ponts N. Genomics and integrated systems biology in *Plasmodium falciparum*: a path to malaria control and eradication. *Parasite Immunol*. 2012;34:50-60.
71. Lemieux JE, Kyes SA, Otto TD, Feller AI, Eastman RT, Pinches RA, et al. Genome-wide profiling of chromosome interactions in *Plasmodium falciparum* characterizes nuclear architecture and reconfigurations associated with antigenic variation. *Mol Microbiol*. 2013;90:519-37.

72. Lin S, McLennan AG, Ying K, Wang Z, Gu S, Jin H, et al. Cloning, expression, and characterization of a human inosine triphosphate pyrophosphatase encoded by the itpa gene. *J Biol Chem*. 2001;276:18695-701.
73. Liu J, Istvan ES, Gluzman IY, Gross J, Goldberg DE. Plasmodium falciparum ensures its amino acid supply with multiple acquisition pathways and redundant proteolytic enzyme systems. *Proc Natl Acad Sci U S A*. 2006;103:8840-5.
74. Lopez-Rubio JJ, Mancio-Silva L, Scherf A. Genome-wide analysis of heterochromatin associates clonally variant gene regulation with perinuclear repressive centers in malaria parasites. *Cell Host Microbe*. 2009;5:179-90.
75. Maeda T, Sumi S, Ueta A, Ohkubo Y, Ito T, Marinaki AM, et al. Genetic basis of inosine triphosphate pyrophosphohydrolase deficiency in the Japanese population. *Mol Genet Metab*. 2005;85:271-9.
76. Manske M, Miotto O, Campino S, Auburn S, Almagro-Garcia J, Maslen G, et al. Analysis of Plasmodium falciparum diversity in natural infections by deep sequencing. *Nature*. 2012;487:375-9.
77. Marsh S, King CR, Ahluwalia R, McLeod HL. Distribution of ITPA P32T alleles in multiple world populations. *J Hum Genet*. 2004;49:579-81.
78. Mbanzibwa DR, Tian Y, Mukasa SB, Valkonen JP. Cassava brown streak virus (Potyviridae) encodes a putative Maf/HAM1 pyrophosphatase implicated in reduction of mutations and a P1 proteinase that suppresses RNA silencing but contains no HC-Pro. *J Virol*. 2009;83:6934-40.
79. McLennan AG. The MutT motif family of nucleotide phosphohydrolases in man and human pathogens (review). *Int J Mol Med*. 1999;4:79-89.
80. McLennan AG. The Nudix hydrolase superfamily. *Cell Mol Life Sci*. 2006;63:123-43.
81. Michaels ML, Miller JH. The GO system protects organisms from the mutagenic effect of the spontaneous lesion 8-hydroxyguanine (7,8-dihydro-8-oxoguanine). *J Bacteriol*. 1992;174:6321-5.
82. Mildvan AS, Xia Z, Azurmendi HF, Saraswat V, Legler PM, Massiah MA, et al. Structures and mechanisms of Nudix hydrolases. *Arch Biochem Biophys*. 2005;433:129-43.
83. Miles A, Iqbal Z, Vauterin P, Pearson R, Campino S, Theron M, et al. Indels, structural variation, and recombination drive genomic diversity in Plasmodium falciparum. *Genome Res*. 2016;26:1288-99.

84. Miotto O, Almagro-Garcia J, Manske M, Macinnis B, Campino S, Rockett KA, et al. Multiple populations of artemisinin-resistant *Plasmodium falciparum* in Cambodia. *Nat Genet.* 2013;45:648-55.
85. Mol CD, Harris JM, McIntosh EM, Tainer JA. Human dUTP pyrophosphatase: uracil recognition by a beta hairpin and active sites formed by three separate subunits. *Structure.* 1996;4:1077-92.
86. Mollgaard H, Neuhaard J. Deoxycytidylate deaminase from *Bacillus subtilis*. Purification, characterization, and physiological function. *J Biol Chem.* 1978;253:3536-42.
87. Moroz OV, Murzin AG, Makarova KS, Koonin EV, Wilson KS, Galperin MY. Dimeric dUTPases, HisE, and MazG belong to a new superfamily of all-alpha NTP pyrophosphohydrolases with potential "house-cleaning" functions. *J Mol Biol.* 2005;347:243-55.
88. Nair S, Nkhoma SC, Serre D, Zimmerman PA, Gorena K, Daniel BJ, et al. Single-cell genomics for dissection of complex malaria infections. *Genome Res.* 2014;24:1028-38.
89. Nakauchi A, Wong JH, Mahasirimongkol S, Yanai H, Yuliwulandari R, Mabuchi A, et al. Identification of ITPA on chromosome 20 as a susceptibility gene for young-onset tuberculosis. *Hum Genome Var.* 2016;3:15067.
90. Neuhaard J, Thomassen E. Deoxycytidine triphosphate deaminase: identification and function in *Salmonella typhimurium*. *J Bacteriol.* 1971;105:657-65.
91. Nordlund P, Reichard P. Ribonucleotide reductases. *Annu Rev Biochem.* 2006;75:681-706.
92. Noskov VN, Staak K, Shcherbakova PV, Kozmin SG, Negishi K, Ono BC, et al. HAM1, the gene controlling 6-N-hydroxylaminopurine sensitivity and mutagenesis in the yeast *Saccharomyces cerevisiae*. *Yeast.* 1996;12:17-29.
93. Ocholla H, Preston MD, Mipando M, Jensen AT, Campino S, MacInnis B, et al. Whole-genome scans provide evidence of adaptive evolution in Malawian *Plasmodium falciparum* isolates. *J Infect Dis.* 2014;210:1991-2000.
94. Ooga T, Yoshida S, Nakagawa N, Kuramitsu S, Masui R. Molecular mechanism of the *Thermus thermophilus* ADP-ribose pyrophosphatase from mutational and kinetic studies. *Biochemistry.* 2005;44:9320-9.
95. Otto TD, Bohme U, Jackson AP, Hunt M, Franke-Fayard B, Hoeijmakers WA, et al. A comprehensive evaluation of rodent malaria parasite genomes and gene expression. *BMC Biol.* 2014a;12:86.

96. Otto TD, Rayner JC, Bohme U, Pain A, Spottiswoode N, Sanders M, et al. Genome sequencing of chimpanzee malaria parasites reveals possible pathways of adaptation to human hosts. *Nat Commun.* 2014b;5:4754.
97. Pain A, Bohme U, Berry AE, Mungall K, Finn RD, Jackson AP, et al. The genome of the simian and human malaria parasite *Plasmodium knowlesi*. *Nature.* 2008;455:799-803.
98. Pang B, McFaline JL, Burgis NE, Dong M, Taghizadeh K, Sullivan MR, et al. Defects in purine nucleotide metabolism lead to substantial incorporation of xanthine and hypoxanthine into DNA and RNA. *Proc Natl Acad Sci U S A.* 2012;109:2319-24.
99. Pasini EM, Bohme U, Rutledge GG, Voorberg-Van der Wel A, Sanders M, Berriman M, et al. An improved *Plasmodium cynomolgi* genome assembly reveals an unexpected methyltransferase gene expansion. *Wellcome Open Res.* 2017;2:42.
100. Pasternak B, Svanstrom H, Schmiegelow K, Jess T, Hviid A. Use of azathioprine and the risk of cancer in inflammatory bowel disease. *Am J Epidemiol.* 2013;177:1296-305.
101. Pels Rijcken WR, Overdijk B, van den Eijnden DH, Ferwerda W. Pyrimidine nucleotide metabolism in rat hepatocytes: evidence for compartmentation of nucleotide pools. *Biochem J.* 1993;293 ( Pt 1):207-13.
102. Peltenburg NC, Bakker JA, Vroemen WH, de Knegt RJ, Leers MP, Bierau J, et al. Inosine triphosphate pyrophosphohydrolase activity: more accurate predictor for ribavirin-induced anemia in hepatitis C infected patients than ITPA genotype. *Clin Chem Lab Med.* 2015;53:2021-9.
103. Persson R, Cedergren-Zeppezauer ES, Wilson KS. Homotrimeric dUTPases; structural solutions for specific recognition and hydrolysis of dUTP. *Curr Protein Pept Sci.* 2001;2:287-300.
104. Phillips MA, Rathod PK. *Plasmodium* dihydroorotate dehydrogenase: a promising target for novel anti-malarial chemotherapy. *Infect Disord Drug Targets.* 2010;10:226-39.
105. Pineda-Tenor D, Garcia-Alvarez M, Jimenez-Sousa MA, Vazquez-Moron S, Resino S. Relationship between ITPA polymorphisms and hemolytic anemia in HCV-infected patients after ribavirin-based therapy: a meta-analysis. *J Transl Med.* 2015;13:320.

106. Poran A, Notzel C, Aly O, Mencia-Trinchant N, Harris CT, Guzman ML, et al. Single-cell RNA sequencing reveals a signature of sexual commitment in malaria parasites. *Nature*. 2017;551:95-9.
107. Porta J, Kolar C, Kozmin SG, Pavlov YI, Borgstahl GE. Structure of the orthorhombic form of human inosine triphosphate pyrophosphatase. *Acta Crystallogr Sect F Struct Biol Cryst Commun*. 2006;62:1076-81.
108. Prasad GS, Stura EA, McRee DE, Laco GS, Hasselkus-Light C, Elder JH, et al. Crystal structure of dUTP pyrophosphatase from feline immunodeficiency virus. *Protein Sci*. 1996;5:2429-37.
109. Quashie NB, Dorin-Semblat D, Bray PG, Biagini GA, Doerig C, Ranford-Cartwright LC, et al. A comprehensive model of purine uptake by the malaria parasite *Plasmodium falciparum*: identification of four purine transport activities in intraerythrocytic parasites. *Biochem J*. 2008;411:287-95.
110. Quashie NB, Ranford-Cartwright LC, de Koning HP. Uptake of purines in *Plasmodium falciparum*-infected human erythrocytes is mostly mediated by the human equilibrative nucleoside transporter and the human facilitative nucleobase transporter. *Malar J*. 2010;9:36.
111. Rai P. Oxidation in the nucleotide pool, the DNA damage response and cellular senescence: Defective bricks build a defective house. *Mutat Res*. 2010;703:71-81.
112. Rembeck K, Waldenstrom J, Hellstrand K, Nilsson S, Nystrom K, Martner A, et al. Variants of the inosine triphosphate pyrophosphatase gene are associated with reduced relapse risk following treatment for HCV genotype 2/3. *Hepatology*. 2014;59:2131-9.
113. Riegelhaupt PM, Cassera MB, Frohlich RF, Hazleton KZ, Hefter JJ, Schramm VL, et al. Transport of purines and purine salvage pathway inhibitors by the *Plasmodium falciparum* equilibrative nucleoside transporter PfENT1. *Mol Biochem Parasitol*. 2010;169:40-9.
114. Roper C, Pearce R, Bredenkamp B, Gumede J, Drakeley C, Mosha F, et al. Antifolate antimalarial resistance in southeast Africa: a population-based analysis. *Lancet*. 2003;361:1174-81.
115. Rutledge GG, Bohme U, Sanders M, Reid AJ, Cotton JA, Maiga-Ascofare O, et al. *Plasmodium malariae* and *P. ovale* genomes provide insights into malaria parasite evolution. *Nature*. 2017;542:101-4.
116. Sahasranaman S, Howard D, Roy S. Clinical pharmacology and pharmacogenetics of thiopurines. *Eur J Clin Pharmacol*. 2008;64:753-67.

117. Sakumi K, Furuichi M, Tsuzuki T, Kakuma T, Kawabata S, Maki H, et al. Cloning and expression of cDNA for a human enzyme that hydrolyzes 8-oxo-dGTP, a mutagenic substrate for DNA synthesis. *J Biol Chem.* 1993;268:23524-30.
118. Salcedo-Amaya AM, van Driel MA, Alako BT, Trelle MB, van den Elzen AM, Cohen AM, et al. Dynamic histone H3 epigenome marking during the intraerythrocytic cycle of *Plasmodium falciparum*. *Proc Natl Acad Sci U S A.* 2009;106:9655-60.
119. Sharma A, Yogavel M, Sharma A. Structural and functional attributes of malaria parasite diadenosine tetraphosphate hydrolase. *Sci Rep.* 2016;6:19981.
120. Shipkova M, Lorenz K, Oellerich M, Wieland E, von Ahsen N. Measurement of erythrocyte inosine triphosphate pyrophosphohydrolase (ITPA) activity by HPLC and correlation of ITPA genotype-phenotype in a Caucasian population. *Clin Chem.* 2006;52:240-7.
121. Shlomain J, Kornberg A. Deoxyuridine triphosphatase of *Escherichia coli*. Purification, properties, and use as a reagent to reduce uracil incorporation into DNA. *J Biol Chem.* 1978;253:3305-12.
122. Simone PD, Pavlov YI, Borgstahl GEO. ITPA (inosine triphosphate pyrophosphatase): from surveillance of nucleotide pools to human disease and pharmacogenetics. *Mutat Res.* 2013;753:131-46.
123. Singh A, Maqbool M, Mobashir M, Hoda N. Corrigendum to 'Dihydroorotate dehydrogenase: A drug target for the development of antimalarials' [*Eur. J. Med. Chem.* 125 (2017) 640-651]. *Eur J Med Chem.* 2017;128:346-7.
124. Stenmark P, Kursula P, Flodin S, Graslund S, Landry R, Nordlund P, et al. Crystal structure of human inosine triphosphatase. Substrate binding and implication of the inosine triphosphatase deficiency mutation P32T. *J Biol Chem.* 2007;282:3182-7.
125. Su X, Ferdig MT, Huang Y, Huynh CQ, Liu A, You J, et al. A genetic map and recombination parameters of the human malaria parasite *Plasmodium falciparum*. *Science.* 1999;286:1351-3.
126. Su X, Hayton K, Wellems TE. Genetic linkage and association analyses for trait mapping in *Plasmodium falciparum*. *Nat Rev Genet.* 2007;8:497-506.
127. Su X, Wellems TE. Toward a high-resolution *Plasmodium falciparum* linkage map: polymorphic markers from hundreds of simple sequence repeats. *Genomics.* 1996;33:430-44.



128. Sumi S, Marinaki AM, Arenas M, Fairbanks L, Shobowale-Bakre M, Rees DC, et al. Genetic basis of inosine triphosphate pyrophosphohydrolase deficiency. *Hum Genet.* 2002;111:360-7.
129. Sundaram M, Yao SY, Ingram JC, Berry ZA, Abidi F, Cass CE, et al. Topology of a human equilibrative, nitrobenzylthioinosine (NBMPR)-sensitive nucleoside transporter (hENT1) implicated in the cellular uptake of adenosine and anti-cancer drugs. *J Biol Chem.* 2001;276:45270-5.
130. Tachibana S, Sullivan SA, Kawai S, Nakamura S, Kim HR, Goto N, et al. *Plasmodium cynomolgi* genome sequences provide insight into *Plasmodium vivax* and the monkey malaria clade. *Nat Genet.* 2012;44:1051-5.
131. Taddei F, Hayakawa H, Bouton M, Cirinesi A, Matic I, Sekiguchi M, et al. Counteraction by MutT protein of transcriptional errors caused by oxidative damage. *Science.* 1997;278:128-30.
132. Talundzic E, Ravishankar S, Kelley J, Patel D, Plucinski M, Schmedes S, et al. Next-Generation Sequencing and Bioinformatics Protocol for Malaria Drug Resistance Marker Surveillance. *Antimicrob Agents Chemother.* 2018;62.
133. Tanaka Y, Kurosaki M, Nishida N, Sugiyama M, Matsuura K, Sakamoto N, et al. Genome-wide association study identified ITPA/DDRGK1 variants reflecting thrombocytopenia in pegylated interferon and ribavirin therapy for chronic hepatitis C. *Hum Mol Genet.* 2011;20:3507-16.
134. Thompson AJ, Fellay J, Patel K, Tillmann HL, Naggie S, Ge D, et al. Variants in the ITPA gene protect against ribavirin-induced hemolytic anemia and decrease the need for ribavirin dose reduction. *Gastroenterology.* 2010;139:1181-9.
135. Trevino SG, Nkhoma SC, Nair S, Daniel BJ, Moncada K, Khoswe S, et al. High-Resolution Single-Cell Sequencing of Malaria Parasites. *Genome Biol Evol.* 2017;9:3373-83.
136. Vanderheiden B. Inosine triphosphate in human erythrocytes: a genetic trait. *International Society of Blood Transfusion, 10th Congress 1964, Part 3: Karger Publishers; 1965. p. 540-8.*
137. Vanderheiden BS. Human erythrocyte "ITPase": an ITP pyrophosphohydrolase. *Biochim Biophys Acta.* 1970;215:555-8.
138. Vanderheiden BS. Purification and properties of human erythrocyte inosine triphosphate pyrophosphohydrolase. *J Cell Physiol.* 1979;98:41-7.
139. Vertessy BG, Toth J. Keeping uracil out of DNA: physiological role, structure and catalytic mechanism of dUTPases. *Acc Chem Res.* 2009;42:97-106.

140. Visnes T, Doseth B, Pettersen HS, Hagen L, Sousa MM, Akbari M, et al. Uracil in DNA and its processing by different DNA glycosylases. *Philos Trans R Soc Lond B Biol Sci.* 2009;364:563-8.
141. Waisertreiger IS, Menezes MR, Randazzo J, Pavlov YI. Elevated Levels of DNA Strand Breaks Induced by a Base Analog in the Human Cell Line with the P32T ITPA Variant. *J Nucleic Acids.* 2010;2010.
142. Ward P, Equinet L, Packer J, Doerig C. Protein kinases of the human malaria parasite *Plasmodium falciparum*: the kinome of a divergent eukaryote. *BMC Genomics.* 2004;5:79.
143. Weber G. Biochemical strategy of cancer cells and the design of chemotherapy: G. H. A. Clowes Memorial Lecture. *Cancer Res.* 1983;43:3466-92.
144. Welin M, Nordlund P. Understanding specificity in metabolic pathways--structural biology of human nucleotide metabolism. *Biochem Biophys Res Commun.* 2010;396:157-63.
145. White NJ. Antimalarial drug resistance. *J Clin Invest.* 2004;113:1084-92.
146. Whittingham JL, Leal I, Nguyen C, Kasinathan G, Bell E, Jones AF, et al. dUTPase as a platform for antimalarial drug design: structural basis for the selectivity of a class of nucleoside inhibitors. *Structure.* 2005;13:329-38.
147. Wootton JC, Feng X, Ferdig MT, Cooper RA, Mu J, Baruch DI, et al. Genetic diversity and chloroquine selective sweeps in *Plasmodium falciparum*. *Nature.* 2002;418:320-3.
148. Yakunin AF, Proudfoot M, Kuznetsova E, Savchenko A, Brown G, Arrowsmith CH, et al. The HD domain of the *Escherichia coli* tRNA nucleotidyltransferase has 2',3'-cyclic phosphodiesterase, 2'-nucleotidase, and phosphatase activities. *J Biol Chem.* 2004;279:36819-27.
149. Zalkin HJ, cellular S, biology m. Biosynthesis of purine nucleotides. 1996;2:561-79.
150. Zhang C, Kim SH. Overview of structural genomics: from structure to function. *Curr Opin Chem Biol.* 2003;7:28-32.

---

# Experimental Insights | Chapter 1

---

## Functional Characterisation of *Pf*HAM1

## A. Introduction

Malaria is a severe and often fatal illness that affects many people in tropical and subtropical countries. It has been a long-standing global public health concern, causing significant morbidity and mortality. According to the latest WHO reports for 2022, there were approximately 247 million malaria cases worldwide, resulting in 619,000 fatalities. In Africa, *P. falciparum* is responsible for 95% of the projected malaria cases in 2021. Shockingly, the mortality rate among children under five remains exceptionally high at 76%. Despite significant global efforts to control malaria, the lack of an effective vaccine (Rts et al. , 2012) and the emergence of drug-resistant strains of the disease, including artemisinin-resistant malaria in Southeast Asia and some regions of Africa (Ashley et al. , 2014), present significant challenges to disease control and eradication. These developments threaten the progress made in recent years towards reducing the global burden of malaria. In 2002, the genomic sequence of the *P. falciparum* 3D7 line was described, revealing the presence of approximately 5300 genes. However, only half of these genes have known functions because of poor sequence similarity to those from other genera (Gardner et al. , 2002). This presents an exciting opportunity to identify novel therapeutic intervention targets that could lead to developing new and more effective treatments for malaria.

The *Plasmodium* parasite is constantly exposed to exogenous and endogenous stress that causes high levels of genotoxic damage (Gupta et al. , 2016). The replication process, reactive oxygen species (ROS) produced by heme metabolism, and spontaneous deamination of nitrogenous bases are the primary causes of genetic damage in *Plasmodium* parasites (Chakarov et al. , 2014, Lee et al. , 2014). A significant cause of endogenous DNA damage in the *Plasmodium* parasite is the high concentration of non-canonical nucleotides in the nucleotide precursor pool (Galperin et al. , 2006, Mathews, 2006). Non-canonical nucleotides such as (d)ITP and XTP have the unusual trait of ambiguous base pairing during replication because they contain analogues of the typical nitrogenous bases (Friedberg et al. , 2004, Kamiya, 2003). This can lead to transition and transversion mutations when integrated into nascent DNA. Such non-canonical dNTPs are intercepted and metabolically hydrolysed to stop DNA damage (Hamid and Eckert, 2005, Hizi et al. , 1997). Both the free nucleotide pool and duplex DNA strands experience oxidative deamination, but the former is more susceptible to frequent chemical modifications

and is a significant site of deamination (He et al. , 2000, Hill-Perkins et al. , 1986, Lane and Fan, 2015, Nagy et al. , 2014, Rampazzo et al. , 2010, Rudd et al. , 2016). Deoxynucleoside and ribonucleoside triphosphates of inosine (dITP/ITP), xanthine (dXTP/XTP), 8-oxo-guanine (8-oxoG/8-oxodG), and others are among the contaminants of the precursor pool. These are produced as byproducts of cellular metabolism or by deamination or oxidation of bases in natural nucleotides (Menezes et al. , 2012). Therefore, the *Plasmodium* parasite is under constant attack from various sources of DNA damage, which can lead to mutations that may alter the parasite's protein-coding genes or regulatory regions. This increased understanding of the mechanisms of DNA damage in *Plasmodium* parasites is essential for developing new, more effective antimalarial therapies.

To safeguard against such atypical nucleotides and their effects, house-cleaning proteins are employed in the cells. In the case of *Plasmodium* parasites, these proteins can be classified into four groups based on their structural characteristics. This includes dUTPases (deoxy-uridine triphosphatase) (Greenberg and Somerville, 1962), NuDiX (nucleotide diphosphate linked to some other moiety, X) superfamily (Srouji et al. , 2017), all- $\alpha$ -helical NTPases (Moroz et al. , 2005), and ITPases (inosine triphosphate pyrophosphatase) (Porta et al. , 2006). The HAM1 domain characterises ITPases, which consist of a central beta-sheet forming the floor of the active site. These enzymes intercept and neutralise the non-standard nucleotides in the precursor pool to their respective diphosphate or monophosphate forms (Galperin et al., 2006). Research has shown that ITPase and its orthologs are conserved in all three domains of life and are even present in viruses (Burgis and Cunningham, 2007, Hwang et al. , 1999, Lin et al. , 2001, Mbanzibwa et al. , 2009, Noskov et al. , 1996, Straube et al. , 2023).

Different species display varying characteristics of mutants lacking these proteins. For instance, an *E. coli* *rdgB* mutant lacking the ITP pyrophosphatase is viable but shows synergistic lethality with *recA* or *recBC* mutations, an SOS-induced phenotype, and hyper-recombination (Bradshaw and Kuzminov, 2003, Burgis and Cunningham, 2007, Clyman and Cunningham, 1987). Studies have also shown that yeast lacking the *ham1* gene are hypersensitive and hypermutable to purine analogue 6-N-hydroxylaminopurine (HAP) when grown in a medium containing HAP (Noskov et al., 1996). In mammals, *itpa*<sup>-/-</sup> mice show these proteins are vital. These mice are born smaller and die within two weeks, with more than half dying

before birth due to structural and functional abnormalities of the heart (Behmanesh et al. , 2009). Furthermore, mouse embryonic fibroblasts (MEFs) acquire chromosomal aberrations and DNA single-strand breaks (Abolhassani et al. , 2010). Incorporating ITP into cellular RNA has been found to limit translation and cause mistranslation or even alter the RNA's secondary structure (Sakumi et al. , 2010). The genetic variation status of human ITPase was found to influence thiopurine therapy (Bierau et al. , 2007, Stocco et al. , 2009) and treatment against chronic hepatitis C (D'Avolio et al. , 2016, Pineda-Tenor et al. , 2015), as ITP conferred protection against ribavirin (RBV)-induced ATP depletion. Furthermore, variations in the *itpa* gene have been associated with young-onset TB susceptibility (Nakauchi et al. , 2016), early infantile encephalopathy (Kevelam et al. , 2015), and cardiomyopathy (Handley et al. , 2019). The over-expression of human ITPase in several tumour cell lines implies that it could be used as a diagnostic marker for certain cancers (Dai et al. , 2016), thereby proving the biomedical relevance of ITPase.

Despite extensive research on ITPases across various organisms, studies on the *P. falciparum* homolog of ITPase (*PfHAM1*) are limited. This enzyme's thorough exploration and characterisation is vital to determine its potential as a therapeutic target. To this end, an in-depth investigation of *PfHAM1*, which converts non-canonical (d)/ITP and XTP nucleotides into their respective monophosphate forms and pyrophosphate, was conducted. The comprehensive study involved examining the recombinant protein's structure, biophysics, and kinetics, identifying its intracellular localisation, and studying the phenotype of HAM1-deficient *P. falciparum*.



## **B. Experimental procedures**

### **1. Bioinformatics of PfHAM1**

The parasite genome database predicted the full-length open reading frame sequence of the gene encoding putative PfHAM1 with location on chromosome 7 (Annotation: PF3D7\_0720800, <http://www.PlasmoDB.org>). Using MAFFT software and the Jalview programme, multiple sequence alignment (MSA) of PfHAM1 and HAM1 from different organisms (*P. knowlesi*, *P. malariae*, *P. ovale*, *P. berghei*, *P. vivax*, *P. yoelli*, *T. gondii*, *L. donovani*, *S. cerevisiae*, *E. coli*, and *Homo sapiens*) was performed (Waterhouse et al. , 2009). PSI-PRED software was used to determine PfHAM1's secondary structure (Buchan et al. , 2013).

### **2. Culturing of parasites and transfections**

*In-vitro* cultures of *P. falciparum* 3D7 (Pf3D7) and Pf3D7-DiCre lines at a hematocrit of 3% were performed as previously described (Knuepfer et al. , 2017), using a complete RPMI 1640 (Gibco) medium with 0.5% w/v AlbuMAX II (Invitrogen). Incubators (Thermo Scientific) with 5% CO<sub>2</sub> were used to keep parasites in culture flasks (Nunc) at 37°C (Jensen and Trager, 1977). Fresh media was utilised to replace used media as necessary, and a 1000X bright-field microscope (Nikon) was used to evaluate the culture growth status using Giemsa staining (VWR). Parasites were synchronised by purifying the schizonts using a 70% Percoll gradient (Amersham), followed by a 5% D-sorbitol (Sigma) treatment, preceding a period of reinvasion of two hours. 0.05% saponin (Sigma) lysis was used to lyse the erythrocytes to isolate the parasite preferentially.

As previously mentioned (Moon et al. , 2013), the plasmids were electroporated into pure schizont-staged parasites using an Amaxa 4D-Nucleofector™ (Lonza). 30 µg of DNA was electroporated to generate mNeonGreen tagged parasite line using the selection-linked integration (SLI) technique. After 24 hours, 2.5 nM WR99210 (Jacobus Pharmaceuticals) was included in the culture for seven days of parasite selection. Drug G418 (Calbiochem) was added after the growth of transfected parasites at about 2-4% parasitemia for 7 days at a final concentration of 1000 µg/µl to select for integrants. 20 µg of CRISPR/Cas9 plasmids (containing sgRNAs) and 40

µg of rescue plasmids were electroporated for the generation of DiCre-based transgenic parasites, and drug WR99210 selection was applied for four days, beginning 24 hours after transfection. Fresh RBCs were added to the culture by the media changes. Ring-staged parasites were treated for 1 hour with 100 nM rapamycin (in DMSO) for DiCre-mediated DNA excision, followed by washing with complete media before being introduced back to the culture (Knuepfer et al., 2017).

### **3. Genomic DNA isolation, total RNA extraction and PCR amplification of the *pfham1* gene**

Using the QIAamp DNA Blood Mini Kit (Qiagen), the manufacturer's instructions extracted genomic DNA (gDNA) from 2 ml of parasitised RBCs. The gDNA that was so eluted was quantitated in a micro-volume spectrophotometer (Maestrogen), and the quality was examined in an agarose gel (Lonza) at a 0.8% concentration. For later usage, gDNA was aliquoted into several tubes and kept at -20°C.

Total RNA was promptly extracted using recently isolated iRBCs. Ambion PureLink RNA kit (Thermo Scientific) was used to extract total RNA from the parasites following the manufacturer's instructions. Verso cDNA synthesis kit (Thermo Scientific) was used to create cDNA from the total RNA that had been successfully extracted. The *pfham1* gene was amplified using primers P11 and P12 under the following optimal PCR reaction conditions: Initial denaturation: 95°C (3 minutes) for 1 cycle; Denaturation: 95°C (30 seconds); Primer annealing: 48°C (45 seconds); Extension: 72°C (60 seconds) with a reaction cycle of 35; Final extension: 72°C (7 minutes) for 1 cycle. A 1% agarose gel was used to evaluate the PCR result and compared to a 1 kb DNA ladder (Fermentas).

### **4. Cloning, over-expression, purification and MALDI-TOF/TOF MS/MS analysis**

Using the restriction enzymes *NcoI* (Fermentas) and *XhoI* (Fermentas), a PCR-amplified cDNA fragment (597 base pairs) corresponding to *pfham1* was cloned into pET28a (+) DNA vector (Novagen) to create the pET28a-*pfham1* construct in DH5α competent cells (Invitrogen), which was then verified through Sanger sequencing. The *Escherichia coli* Rosetta™ strain (Novagen) was transformed with the pET28a-

*pfham1* clone to produce the recombinant protein. When the culture's OD<sub>600</sub> reached 0.4 and 0.5 at 37°C, protein synthesis was stimulated with optimised 0.5 mM IPTG (Thermo Scientific). The culture was then grown for an additional night at 25°C and 200 rpm. Cold membrane filtered lysis buffer containing 50 mM Tris base (Merck), 300 mM NaCl (Fisher Scientific), 10 mM imidazole (Calbiochem), 10% glycerol (SRL), and pH 8.0 was used for resuspending the harvested cells. Sonication was used to lyse the cells, and the lysate was then centrifuged at 45,000 rpm for 45 minutes at 4°C to remove the clear supernatant. This clear supernatant was then placed onto a Ni<sup>++</sup>-NTA agarose column (Qiagen) that had already been set up and cooled to 4°C at a slow stirring. Cold membrane filtered wash solution with a pH of 8.0, 50 mM Tris base, 300 mM NaCl, 50 mM imidazole, and 10% glycerol was used to start the washing process for the column. The same buffer formulation was used for elution, followed by buffers containing 250 mM imidazole and 1M imidazole, both cold and at a pH of 7.5. In an FPLC instrument (Cytiva AKTA Pure) at 4°C, with a linear flow rate of 1 ml/minute, the fractions were concentrated before being put through to size exclusion chromatography using the filter sterilised and degassed buffer mix of 50 mM Tris base, 300 mM NaCl, pH 7.5. The purity of the resulting protein was examined using silver staining (Thermo Scientific) after fractions were run on a 12% SDS-PAGE. The molecular weight of *PfHAM1* was established using the MALDI-TOF-MS technique. According to the manufacturer's instructions, the purified protein was treated using ZipTip  $\mu$ -C18 tips (Millipore) to remove salts before being put through a MALDI analysis. Applied Biosystems 4700 Proteomics Analyzer170 was used to perform MALDI-TOF/TOF analysis on the protein solution that was thus obtained after elution. Utilising the In-Gel Tryptic Digestion Kit (Thermo Scientific), peptide mass fingerprinting was carried out to establish the identity of the protein. The MALDI-TOF/TOF MS/MS spectrum resulting from this process was then searched in the NCBI database by GPS Explorer utilising the MASCOT server.

## **5. Antibody generation from recombinant *PfHAM1* and western blotting**

The polyclonal antibody was produced against pure recombinant *PfHAM1* in two New Zealand white rabbits (around ten months old). Freund's Complete Adjuvant (Sigma) was used for the initial immunisation, and Freund's Incomplete Adjuvant (Sigma) was used for the subsequent three booster shots. On Day 0, pre-

immunisation sera was obtained. The central ear artery was used to collect blood after roughly 70 days. After centrifugation, the pale-yellow serum supernatant was collected, and IgG was purified using Protein-A Mag SepharoseXtra (Cytiva) affinity columns.

Western blotting was used to assess the efficacy of the antibody produced from the rabbit serum against recombinant protein-expressing *E. coli* lysate and saponin-lysed parasite lysate. SuperBlock blocking buffer (Thermo Scientific) was used for membrane blocking, and PBS-T with 0.1% (v/v) Tween-20 (Calbiochem) was used for washing. A 1:5000 dilution of the primary antibody in PBS (Takara) was used. The negative control used was pre-immune sera. After incubating with the anti-rabbit secondary antibody (Sigma), ECL substrate (Bio-Rad) was used to develop the blot in the ChemiDoc MP Imaging System (Bio-Rad). The anti-PfAldolase (Abcam) loading control was used, diluted to 1:5000.

## 6. Circular dichroism

Circular dichroism (CD) spectroscopy was used using 0.4 mg/ml pure protein in 10 mM PBS buffer to determine the secondary structure of PfHAM1. The spectrum was obtained using a spectro-polarimeter (Jasco J810) in a 0.1 cm CD cuvette between 250 nm and 200 nm wavelengths at 25°C in *mddeg*. Under the same settings, background noise was eliminated by performing scanning with just the buffer. The CD data were analysed using online BeStSel software (Micsonai et al. , 2015).

## 7. Dynamic light scattering studies

Using Nano-ZS (Malvern Instruments) equipment with a 5 mW power setting and a He-Ne laser source maintained at 632 nm at 25°C, a dynamic light scattering (DLS) experiment was conducted. The operation method followed the instructions provided by the DTS software. Each run was recorded for 30 seconds, and ten runs were averaged with an equilibration time of 3 minutes (Iqbal et al. , 2016). To check for oligomerisation, purified PfHAM1 (0.4 mg/ml) was added to a solution of 50 mM Tris-base and 100 mM NaCl (pH 7.5). The observed data were plotted against the number percentage and the calculated diameter (in nanometers, nm).

## 8. Chemical cross-linking studies

For cross-linking experiments, ethylene glycol bis(succinimidyl succinate) (EGS) (Thermo Scientific) was utilised (Iqbal et al., 2016). PBS containing 15 mg/ml PfHAM1 was combined with various EGS concentrations for 30 minutes at room temperature. The reaction was stopped by adding 1 M Tris base, pH 7.5. A 6% SDS-PAGE gel was used to analyse the samples.

## 9. Gel filtration chromatography for oligomeric status determination

PfHAM1 was passed through a gel filtration or size exclusion column at a flow rate of 1 ml/minute in a buffer solution made up of 50 mM Tris base, 300 mM NaCl, and pH 7.5, following the passage of the protein standard mixture through the same buffer recipe and conditions. The following standards from the Cytiva kit were used: Aprotinin (6.5 kDa), Ribonuclease A (13.7 kDa), Carbonic anhydrase (29 kDa), Ovalbumin (43 kDa), and Conalbumin (75 kDa). To estimate PfHAM1's estimated molecular weight and evaluate its oligomeric state, the elution profiles of both sets were monitored at 215 nm, and the associated values were plotted in MS Excel. A calibration curve was plotted by finding out ' $K_{av}$ ' (distribution coefficient), where  $K_{av} = (V_e - V_o)/(V_c - V_o)$ . Abbreviations stand for  $V_e$  is elution volume for standard;  $V_o$  is column void volume; and  $V_c$  is total column volume.

## 10. Size exclusion chromatography – multi-angle light scattering (SEC-MALS)

The SEC-MALS studies used Wyatt DAWN 8 MALS equipment linked to a Waters HPLC system. An Optilab differential refractometer was utilised to quantify concentration, while the DAWN system was employed to monitor light scattering (Dasgupta et al. , 2022). Briefly, Bovine Serum Albumin (Sigma), which has a molecular weight of 66 kDa, was used as a protein standard to normalise a Shim Pack Bio Diol 120 gel filtration column (Shimadzu) that had been pre-equilibrated with 50 mM Tris-HCl (pH 7.5) and 150 mM NaCl. PfHAM1 protein was injected at a flow rate of 0.5 ml/min at a concentration of 2.5 mg/ml of 100  $\mu$ l. The data were analysed using ASTRA (v7.3.2) software (Wyatt).

## 11. Enzymatic kinetics

The amount of  $P_i$  released in a coupled assay where the substrate(s) [ITP, dITP, XTP, IMP, IDP, XMP, XDP (Jena Bioscience); ATP, dATP, GTP, dCTP, dTTP, dUTP (Sigma)] were co-incubated with *PfHAM1* and inorganic pyrophosphatase (Sigma) as discussed previously with minor modifications (Lin et al., 2001, Siddiqui et al., 2020, Vidal et al., 2022) allowed for the determination of the kinetic parameters for substrate hydrolysis. An optimised 15-minute incubation of 1 mM substrate with 5 ng of *PfHAM1* and 1 unit of inorganic pyrophosphatase at 37°C in 50 mM Tris-HCl, pH 7.5, and 10 mM  $MgCl_2$  was used in the standard assay (50  $\mu$ l) for triphosphate nucleotide substrates. The impact of DTT or dithiothreitol on the enzymatic process was also examined. According to the instructions in the user handbook, the amount of released phosphate was determined using a malachite green assay using BIOMOL Green (Enzo) and compared to the standard curve for further calculations. The absorbance was measured using a multi-well plate reader at 620 nm.  $P_i$  released from triphosphate nucleotide substrates in control assays without *PfHAM1* was subtracted. Reaction mixtures mentioned above but without inorganic pyrophosphatase were also incubated at 37°C for 15 minutes in a volume of 50  $\mu$ l. All enzymatic reactions used Millipore water systems' milli-Q water. Each reaction was carried out three times with the relevant control sets. High-performance liquid chromatography (HPLC) was used to identify specific reaction products. A C8 column (Waters) was injected with aliquots (20  $\mu$ l) at a temperature of 25°C. The chromatographic parameters were, as previously mentioned (Decosterd et al., 1999). To determine which divalent ion corresponded to the highest relative enzymatic activity, the presence of divalent ions such as  $Ca^{++}$ ,  $Ni^{++}$ ,  $Cu^{++}$ ,  $Zn^{++}$ ,  $Co^{++}$ ,  $Mn^{++}$ , and  $Mg^{++}$  (Sigma salts) were screened. Then, while maintaining all other parameters at their original values, the effect of EDTA on the enzymatic activity via chelation of the divalent ion was carried out. The non-canonical substrates, dITP, XTP, and ITP, were analysed using non-linear regression in GraphPad Prism 9.0 to calculate their  $K_m$ ,  $V_{max}$ , and  $K_{cat}$  values with utmost confidence.

The search for nucleoside analogues in antiviral and antitumoral chemotherapy identified the active substances presently utilised as medications. As a result of testing some of these derivatives against the *Pf* purine salvage pathway, lead compounds that may be used as a starting point for synthesising new derivatives were identified. Hence, several available nucleos(t)ide analogues (Sigma) of the



purine metabolism pathway like ribavirin, 8-azaguanine, 6-mercaptopurine, 2-amino-6-chloropurine, acyclovir, and tubercidin were tested against *PfHAM1*, *in-vitro*, to check for its inhibition (Cheviet et al. , 2019).

## 12. Isothermal calorimetry (ITC)

Taking advantage of an Affinity-ITC (TA Instruments), ITC and titration tests were carried out to evaluate the binding characteristics of the *PfHAM1* with its best-reacting substrate. Before loading, all samples underwent a thorough vacuum degassing at a temperature of 25°C. Protein and substrate were kept in the same buffer, 50 mM NaCl and 25 mM Tris-HCl, at a pH of 7.5. The syringe was filled with 250  $\mu$ M dITP substrate, or 500  $\mu$ M ITP substrate, or 300  $\mu$ M XTP substrate solution(s), and the sample cell was loaded with a 41  $\mu$ M protein solution or 82  $\mu$ M protein solution (only for XTP substrate). With a stirring RPM of 75, the substrate solution was injected in volumes of 2.5  $\mu$ l up to 30 injections. In this experiment, the  $K_d$  values for each substrate-protein reaction were calculated using NanoAnalyze TA software, and the enthalpy (kJ/mol) plot with respect to the molar ratio was displayed.

## 13. Biolayer Interferometry (BLI)

BLI experiments were carried out in the ForteBio Octet RED 96 system. The data collected was processed and analysed using Octet Data Analysis software. Briefly, NTA sensors (Biozard) were dipped in 25 mM Tris-HCl (pH 7.5) and 50 mM NaCl buffer for 10 minutes and purified protein, 0.25 mg/ml *PfHAM1* was allowed to saturate the NTA sensor for 5 minutes. Later, the kinetics of reaction with different substrates, chiefly dITP, ITP and XTP, were set for analysing association/dissociation kinetics to get a comparative  $K_d$  value for all three binding reactions. Instrument RPM was set to 500 at 25°C, with 200  $\mu$ l of each substrate in the well in increasing concentrations, as depicted in the graph (nM).

## 14. Stage-specific expression of *pfham1* by qRT-PCR

The expression of *pfham1* at various stages of the parasite's blood stage lifecycle was examined using quantitative real-time PCR (qRT-PCR) (Goyal et al. , 2012).

Following the previously described cDNA preparation, different parasite stages were isolated via synchronisation, and total RNA was extracted. The *pfalas* gene was used as an internal control, and approximately 100 ng of cDNA served as the reaction's template. SYBR Premix Ex Taq (Tli RNase H Plus) (Takara) was used for the three-step PCR amplification for Light Cycler 96 (Roche). The thermal profile was as follows: Initial denaturation: 95 °C for 60 seconds for 1 cycle; Denaturation: 95 °C for 5 seconds; Annealing: 48 °C for 30 seconds; Extension: 72 °C for 60 seconds, following a cooling period. Reaction cycles were 40. Each reaction had a final volume of 10 µl and was done in triplicate for all stages. Software that is machine-integrated was used to carry out the quantitative analysis under the predetermined circumstances of threshold or quantification cycle (Cq) values. Primers P13 and P14 were utilised for *pfham1*, and P15 and P16 were used for *pfalas*. The experiment was set following the MIQE guidelines (Bustin et al. , 2009).

## 15. Generation of plasmids (Fusion & CRISPR-Cas9 constructs) and Cas9 guide RNA sequences

A mNeonGreen (mNG) construct of the *pfham1* gene was created utilising the restriction enzymes *Bgl*III (Fermentas) and *Pst*I (Fermentas) in the pTV016 vector using primer set P17 and P18 to investigate the gene's location in live parasites. The *pfham1*-mNeonGreen construct's optimised PCR settings were identical to those amplifying *pfham1* from cDNA. Sanger's sequencing was used to confirm the construct. DiCre-based constructs were developed for the *pfham1* locus to determine whether the gene is essential for the parasite's survival during the erythrocytic stages of its life cycle.

The rescue plasmid was synthesised from the Genscript (USA). In this, the 5'-utr of the gene was followed by exon 1 of the *pfham1* gene along with the *loxP* site, recodonised portion of the gene (724 bp); a *loxP* site and the 3'-utr of the gene. The prospective guide RNAs were located using the Protospacer programme (MacPherson and Scherf, 2015). Utilising the 19 nucleotides that were close to the chosen PAM sequence, the complementary oligonucleotides were synthesised, phosphorylated using T4 polynucleotide kinase (NEB), annealed, and ligated into the *Bbs*I (NEB) digested vector, pDC-cam-Cas9-hDHFRyFCUii. Four of these guide RNAs from various exon locations were chosen. The single guide RNA (sgRNA) plasmid and rescue plasmid mixture was ethanol precipitated, washed with 70%

ethanol, and resuspended in 10 µl of sterile TE buffer [10 mM Tris, 1 mM EDTA, pH 8.0] (NEB) before transfection. SLI sequence integration in the transfectant, as opposed to wild-type (WT) *Pf3D7* gDNA, was confirmed using integration PCR with primers P1 to P4. Primers P5 to P10 were utilised to verify integration in the DiCre-based transgenic parasites compared to the *Pf3D7*-DiCre line's gDNA. The DNA excision following rapamycin (RAPA) treatment in the *PfHAM1*cKO-guide04 parasite line (contains the modified *pgham1* locus) against the parental *Pf3D7*-DiCre parasite line was verified using primers P1 and P8. The additional data includes the diagnostic PCR primers, sgRNA sequences, and the recodonised DNA sequence (Tables 2-4).

## 16. Live cell imaging

After being treated with 1 µg/ml of Hoechst 33342 (Invitrogen) and 2 µg/ml anti-Wheat germ agglutinin (WGA)-Alexa 647 antibody (Thermo Scientific) for 30 minutes at 37°C, asynchronous cultured parasites expressing the *PfHAM1*-mNG fusion were washed with RPMI. Cells were diluted and added to the 6-channel µ-slides (Ibidi) for live cell imaging on the Nikon Eclipse Ti-E inverted microscope under a 100X oil objective lens with a Hamamatsu ORCA-Flash 4.0 Camera and Piezo stage driven by NIS elements software version 5.3. The following excitation wavelengths were used to acquire fluorescence images: 365 nm for Hoechst, 470 nm for Alexa 488 and mNeonGreen, and 635 nm for WGA. The Nikon NIS Elements AR software (Richardson-Lucy, 20 iterations) was used to deconvolve and process the images (Knuepfer et al., 2017).

## 17. Immunofluorescence studies

Immunofluorescence studies also determined *PfHAM1* localisation in *P. falciparum*. Briefly, 1 ml of parasite culture pellet was resuspended slowly in freshly prepared PBS. Cells were centrifuged and washed twice. The pellet was then fixed in 1 ml of freshly prepared 0.0075% glutaraldehyde (Agar Scientific) in 4% paraformaldehyde (Sigma) (in PBS) and incubated for 1 hour at room temperature. After incubation and PBS washings, cell permeabilisation with 0.1% Triton X-100 (USB) in PBS for 10 minutes was done under rotatory conditions. After multiple washes, the pellet was resuspended in 0.1 mg/ml sodium borohydride (SRL), incubated for 5 minutes, and then washed with PBS as before. SuperBlock blocking buffer was added to the cell

pellet and incubated for an hour at room temperature under rotating conditions. The cell pellet was incubated with primary antibody (anti-PfHAM1) in SuperBlock buffer at 1:2000 dilution, overnight at 4°C, on a slow-speed vertical rotor. The cell pellet was thrice washed and was finally resuspended in 1:2000 dilution of Alexa Fluor 647 conjugated goat anti-rabbit antibody (Thermo Scientific) in SuperBlock buffer for 2 hours at room temperature, following three washings in PBS and spread on a grease-free clean slide to form a thin smear which was air dried. 3 µl of ProLong® Diamond Antifade Mountant with DAPI (Invitrogen) was added to the smear, and a cover slip was carefully placed over it and allowed to dry. The slide was viewed under a 63X oil lens objective in a confocal microscope (Leica TCS SP8 STED). De-convolution of the images was performed using SVI Huygens' de-convolution software linked to LAS-X system software.

## **18. Growth assays**

The growth experiments that included rapamycin-treated and DMSO-treated (vehicle control) samples were used to evaluate parasitemia using a flow cytometry-based technique. Synchronous ring stage parasites were put in triplicate into six-well plates and adjusted to a parasitemia of 0.1% at 3% haematocrit. On days 0, 2, 4, and 6 for each well, 50 µl of the triplicate samples were collected and fixed in a PBS solution containing 8% paraformaldehyde and 0.2% glutaraldehyde (Agar Scientific). Attune NxT Flow Cytometer equipped with a Cytokick autosampler (Invitrogen) was used to examine fixed samples after being stained with the 1:5000 diluted SYBR Green I dye (Invitrogen) (Moon et al., 2013). The analysis was carried out using GraphPad Prism 9.0.

## **19. Statistical analysis**

All experiments were conducted in triplicate, and the images presented are a true representation of one of the independent replicates. The data were carefully analysed and reported as the mean ± standard error of the mean (SEM). A one-way analysis of variance (ANOVA) was adeptly performed to compare more than two groups, followed by Bonferroni's multiple-comparison test to determine the significance levels with high confidence.  $P$  value < 0.05 was considered statistically significant. \* $P$  < 0.05, \*\* $P$  < 0.01, \*\*\* $P$  < 0.001., \*\*\*\* $P$  < 0.0001. Also, n.s. = non-significant.

## **20. Ethics declarations**

All animals were obtained from the animal house of the CSIR-Indian Institute of Chemical Biology (IICB), Kolkata. The antibody generated in rabbits was by the institutional animal ethics committee of CSIR-IICB, registered with the Committee for the Purpose of Control and Supervision of Experiments on Animals (CPCSEA), India (Permit 147/1999/CPCSEA) and strictly adhering to the ARRIVE 2.0 guidelines (Percie du Sert et al. , 2020). Research red cells were obtained from the NHS Blood and Transplant Service, UK and Cambridge Bioscience, UK.

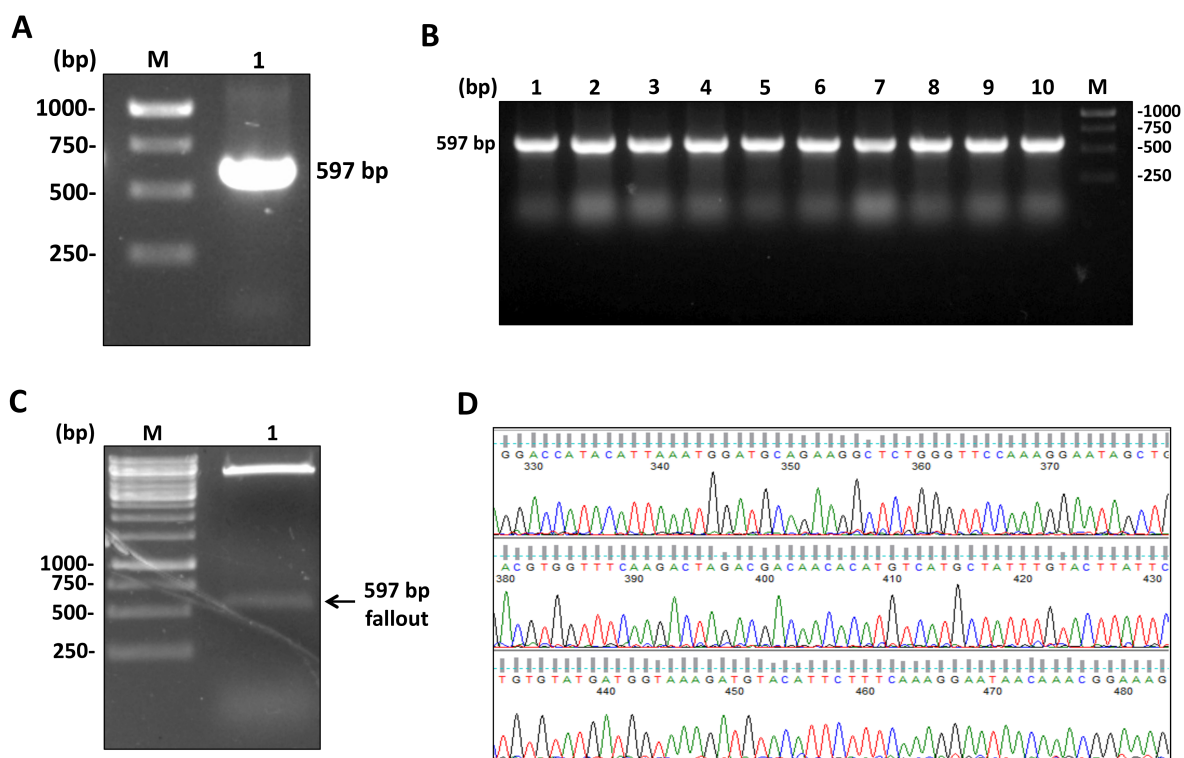




Page | 125

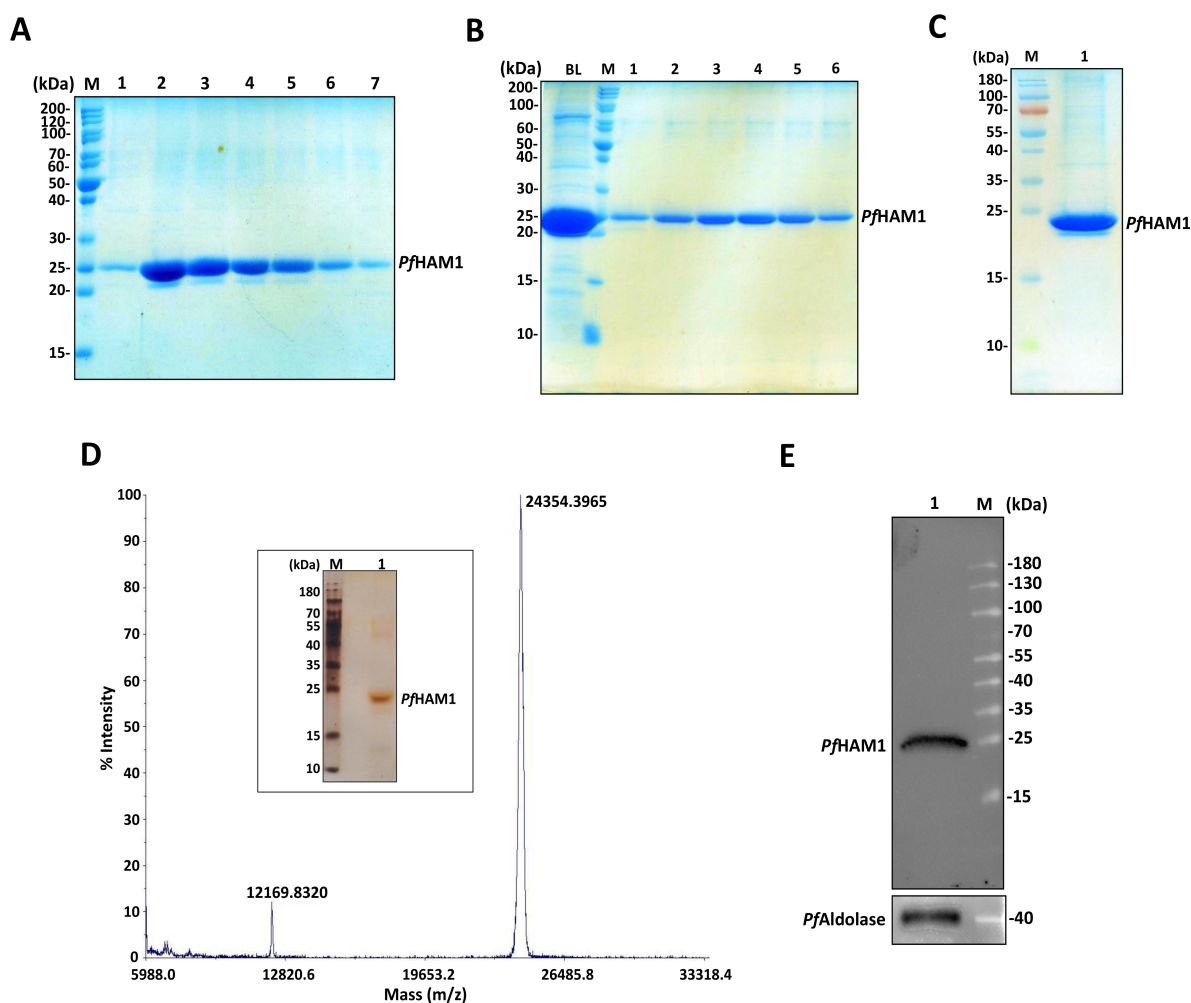
The genome of *P. falciparum* undoubtedly encodes a protein similar to PfHAM1, which has a calculated mass of approximately 23 kDa and 198 amino acids, according to the ExPASy ProtParam bioinformatics tool. The comparison of the PfHAM1 sequence with 11 other orthologues revealed conserved amino acid residues in specific sites, which are highlighted in colour in Figure 1A. Notably, P-BLAST analysis indicated only about 33% similarity between PfHAM1 and *Homo sapiens* ITPase, confirming the uniqueness of PfHAM1. Moreover, the PSI-PRED prediction revealed a high probability of the protein structure of PfHAM1 having  $\alpha$ -helices and  $\beta$ -sheets, with a propensity of about 37% and 23%, respectively, as demonstrated in Figure 1B.

## 2. Cloning, over-expression, purification and validation of *PfHAM1*



**Figure 2(I):** Cloning process of *pfham1*. (A) PCR amplification of *pfham1* (597 bp) from *Pf* cDNA in Lane 1. (B) Colony PCRs of *pfham1* in Lanes 1 to 10. (C) Fragment 'fallout' of 597 bp after restriction digestion with *NcoI* and *XhoI* on cloned pET28a (+) DNA vector in Lane 1. Lane 'M' contains a 1kb DNA ladder. (D) Raw sequencing data (chromatogram) of *pfham1* from plasmid sequencing.

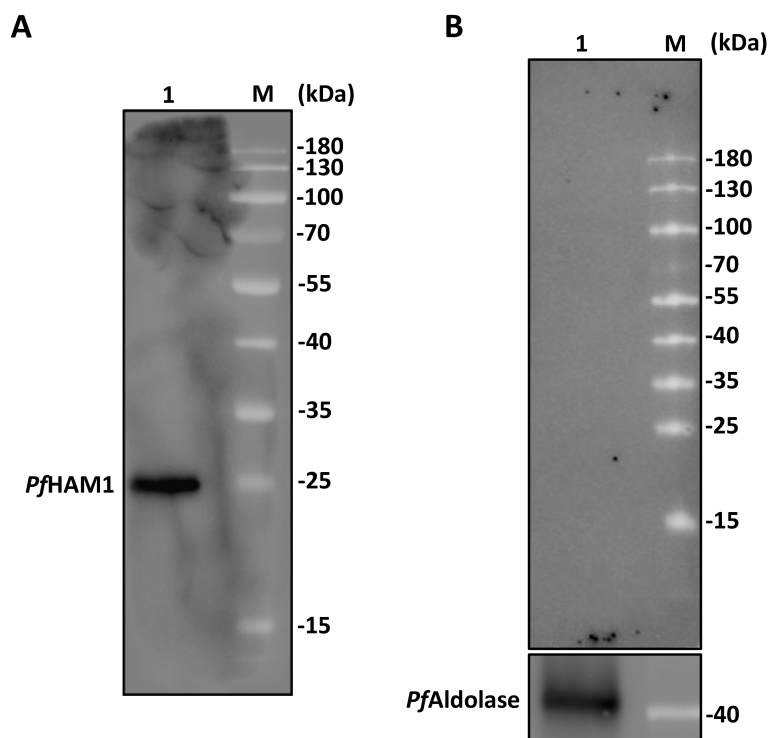
For *PfHAM1* to be functionally characterised, purified protein is necessary. To express the *PfHAM1* protein in a bacterial system, the *pfham1* gene was effectively PCR amplified from cDNA (Figure 2(I)A) and cloned into a pET28a (+) DNA vector with a C-terminal 6X His-tag. The bacterial transgenic colonies were screened for the uptake of the insert (Figure 2(I)B), and insert "fallout" was confirmed using restriction enzymes *NcoI* and *XhoI* (Figure 2(I)C). The sequencing outcome showed an exact match to the sequence in the PlasmidDB database (Gene ID: PF3D7\_0720800) (Figure 2(I)D).



**Figure 2(II):** Purification and validation of recombinant *PfHAM1*. (A) Protein fractions resolved by SDS-PAGE of recombinant *PfHAM1* after Ni<sup>++</sup>-NTA column purification from Lanes 1 to 7. (B) Eluted fractions of *PfHAM1* after size-exclusion chromatography from Lanes 1 to 6, resolved by SDS-PAGE. 'BL' stands for 'before load' fraction. (C) Purified recombinant *PfHAM1* (4 µg) resolved in a 12% SDS-PAGE. (D) A purity check of recombinant *PfHAM1* was done using silver-staining [Inset]. Mass analysis of recombinant *PfHAM1* using MALDI TOF/TOF. (E) Western blot of *PfHAM1* detection in parasite lysate. *PfAldolase* is shown as a loading control. Lane 'M' stands for protein molecular weight ladder.

The protein was purified using metal affinity chromatography (Figure 2(II)A), followed by size exclusion chromatography (Cytiva HiLoad 16/600 Superdex 75 pg column) (Figure 2(II)B), to provide a noticeable band at roughly 24 kDa in a 12% SDS-PAGE, as shown by Coomassie brilliant blue G-250 staining (Figure 2(II)C) and

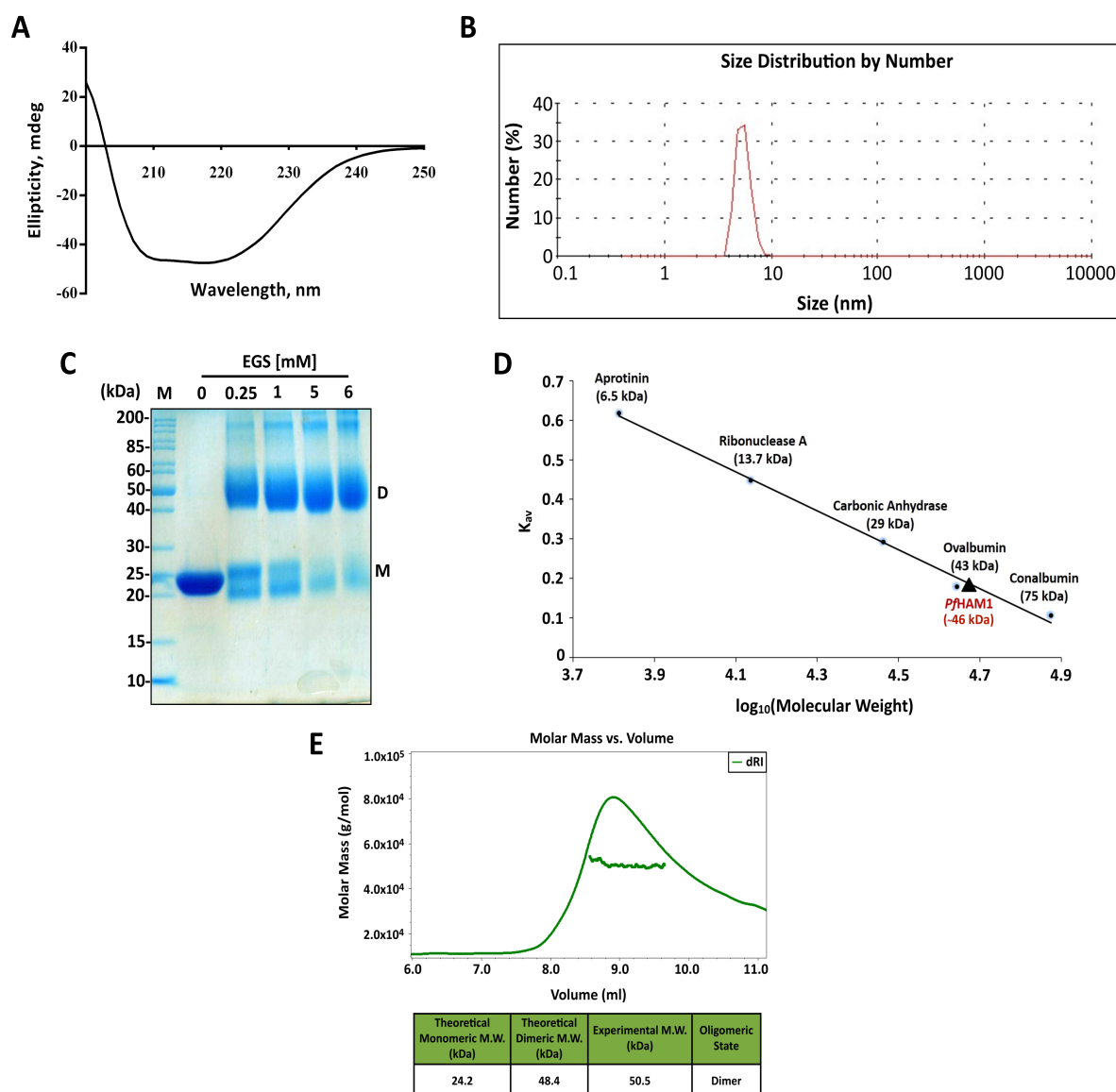
silver staining (Figure 2(II)D inset). Compared to online ExPASy PeptideCutter software, MALDI-TOF/TOF MS/MS revealed that the sample's total mass was approximately 24.4 kDa (Figure 2(II)D). PfHAM1 was found in *P. falciparum* lysate using the generated antibody against recombinant PfHAM1 (Figure 2(II)E). The produced antibody's titre was measured using the ELISA technique (data not shown), and the best antibody with the highest titre value was chosen for use in western blotting and other experiments.



**Figure 2(III):** (A) Western blot detection of recombinant PfHAM1 in *E. coli* lysate with the anti-PfHAM1 antibody. PfAldolase is shown as a loading control. Lane 'M' stands for protein molecular weight ladder. (B) Western blot detection of PfHAM1 in the *Pf3D7* lysate with the anti-pre-immune serum antibody.

Western blotting produced the desired band with the *E. coli* lysate that contained the over-expressed protein (Figure 2(III)A), and when it was done with *P. falciparum* lysate, a band at about 23 kDa was seen. In contrast, no band was visible in the control sera sample (Figure 2(III)B), proving the specificity of the generated antibody in the rabbit.

### 3. PfHAM1 is a homodimer

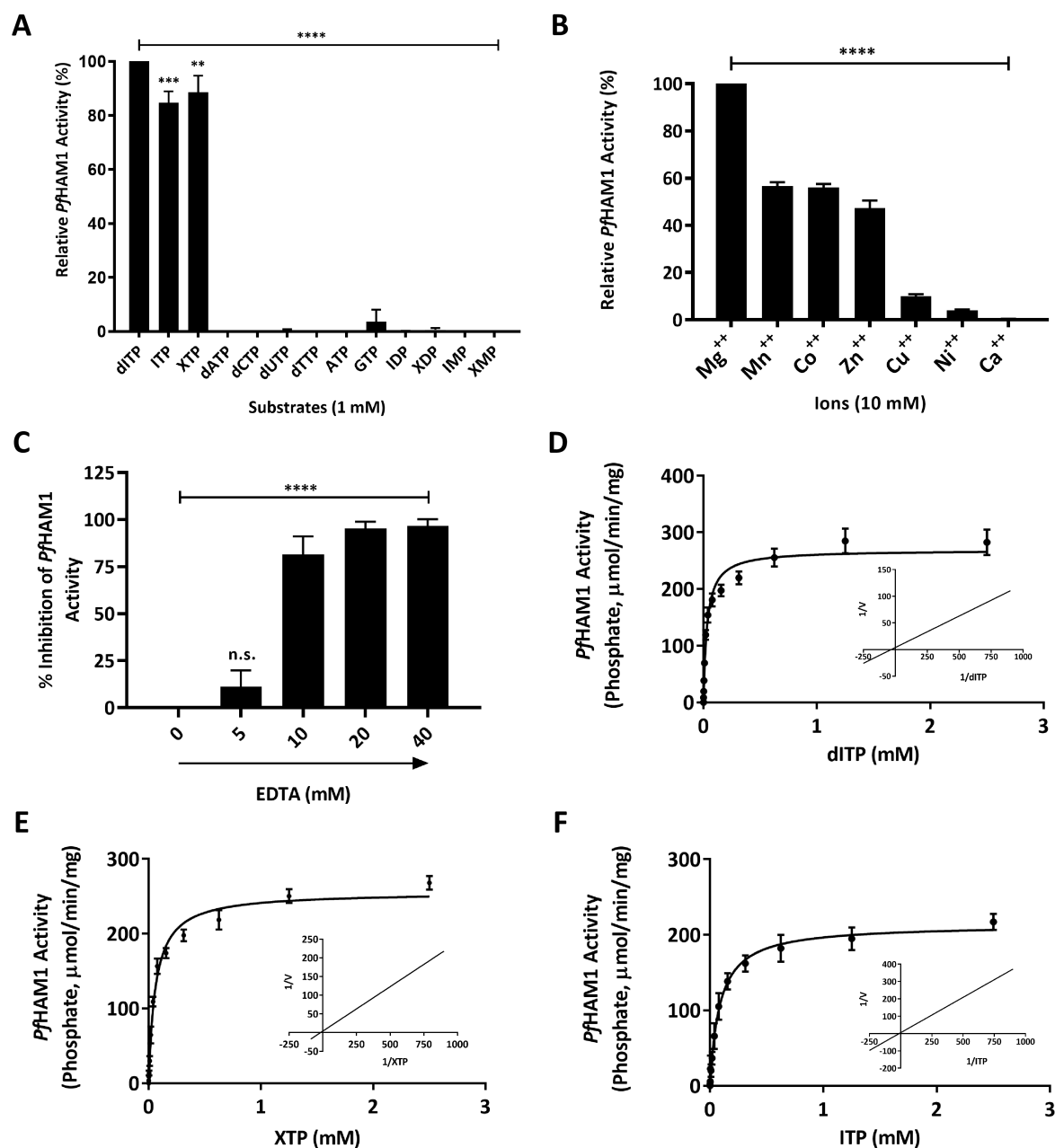


**Figure 3:** Oligomeric status of *PfHAM1*. (A) CD spectrum of *PfHAM1*. The spectrum is shown with ellipticity in *mdeg* against different wavelengths. (B) DLS plot of *PfHAM1*, where size distribution by number depicts a single form of the protein. (C) Chemical cross-linking by EGS in increasing concentrations, as shown, was resolved on an 8% SDS-PAGE, showing a prominent dimeric form of the protein. Lane 'M' stands for protein molecular weight markers. 'D' and 'M' are abbreviations for dimer and monomer, respectively. (D) Calibration curve from gel filtration chromatogram of marker proteins drawn with  $K_{av}$  (Distribution



coefficient) versus the logarithm of molecular mass for each protein proving the dimeric experimental molecular mass of *PfHAM1* (Monomeric mass: ~24.4 kDa). (E) SEC-MALS analysis of the *PfHAM1* protein. The solid green line denotes the refractive index trace for eluted protein, and the horizontal line under the peak corresponds to the average molar mass (Y-axis) distribution across the peak as determined by MALS. Table showing theoretical versus experimental molecular weight (M.W.) measurements.

CD spectroscopy was performed on *PfHAM1* to identify unique structural motifs that impact protein function. The protein was mainly composed of 29%  $\alpha$ -helices, 27.3%  $\beta$ -sheets, and remaining residues, likely as randomly coiled structures, according to the CD spectra, which displayed double minima at 208 and 222 nm (Figure 3A). This is consistent with the bioinformatics results. Using DLS and EGS-based cross-linking assays, the oligomeric state of the protein in the solution was ascertained. A single population of native *PfHAM1* was found, according to DLS studies, as shown by the size distribution graph in Figure 3B. When acting on *PfHAM1* in progressively higher concentrations, the non-cleavable chemical cross-linker EGS, with a spacer arm of 16.1 Å, revealed the presence of a 24 kDa band as well as a 48 kDa band in comparison to the control sample (Figure 3C). Due to the experiment's inability to achieve 100% cross-linking, a protein monomer was seen. A peak of *PfHAM1* was observed relative to protein standards, which suggested its dimeric form lay between 43 kDa and 75 kDa bands in gel filtration chromatography, further validating the recombinant protein's dimeric nature in solution. The calibration curve revealed that the experimental molecular weight was around 46 kDa (Figure 3D). According to experimental molecular weight calculations made by the Astra software using SEC-MALS data, the protein is dimeric with an approximate molecular weight of 50.5 kDa. (Figure 3E).

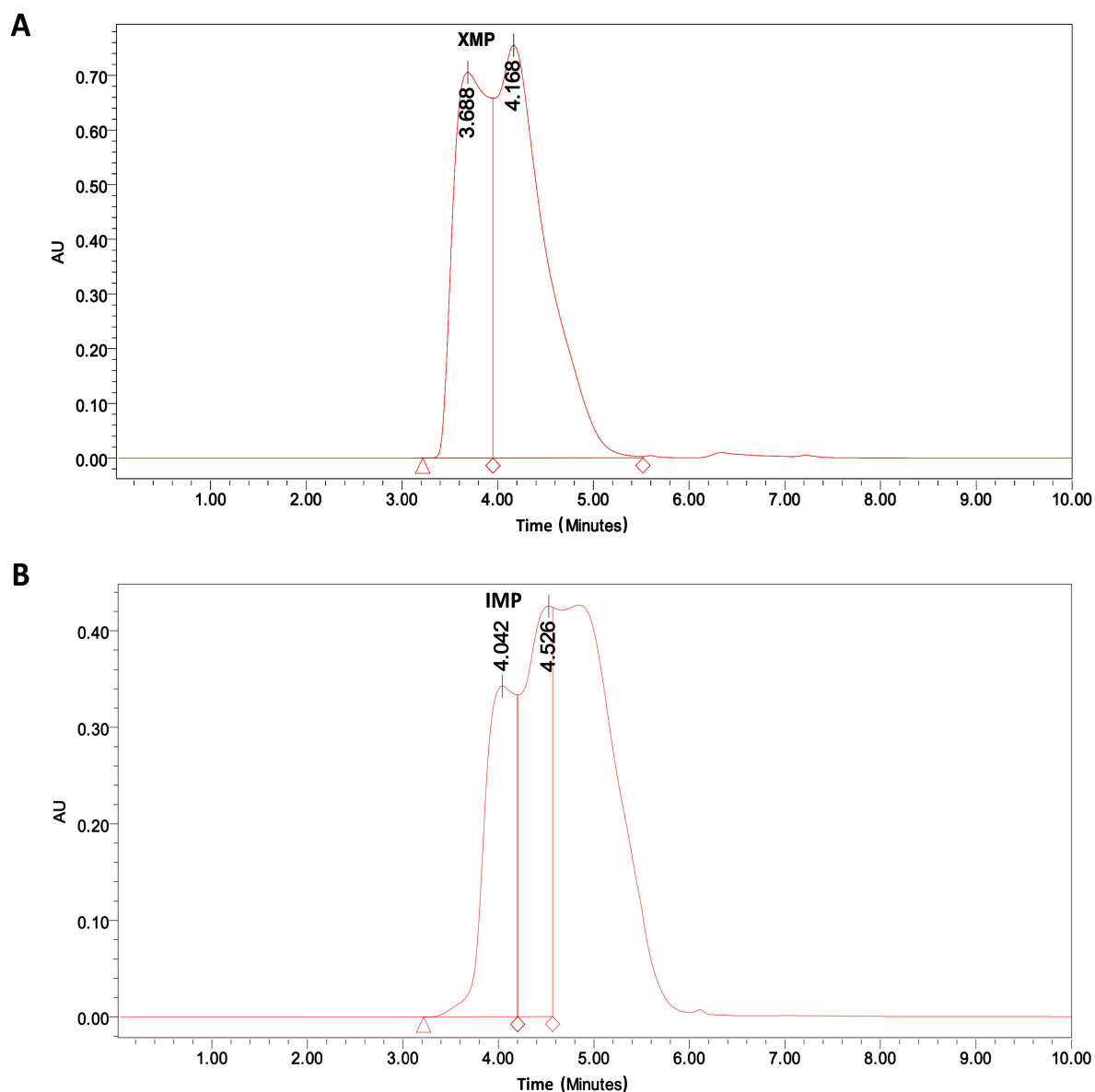
4. Pyrophosphohydrolase activity of *PfHAM1*

**Figure 4(I):** Enzyme kinetics of *PfHAM1*. (A) Effect of different substrates on *PfHAM1* activity. (B) Effect of various ions on *PfHAM1* activity. (C) Effect of EDTA on *PfHAM1* activity. (D-F) Michaelis Menten plots and Lineweaver-Burk plots (inset) for the hydrolysis of dITP (D), XTP (E), and ITP (F) by *PfHAM1*. Error bars are given as per the stated statistical analysis.

Substrate	$V_{\max}$ ( $\mu\text{mol}/\text{min}/\text{mg}$ )	$K_m$ ( $\mu\text{M}$ )	$K_{\text{cat}}$ ( $\text{sec}^{-1}$ )
dITP	$268.8 \pm 7.2$	$31.86 \pm 4.03$	108
XTP	$255.8 \pm 5.6$	$60.84 \pm 5.74$	103
ITP	$213.7 \pm 7.6$	$87.17 \pm 12.57$	84

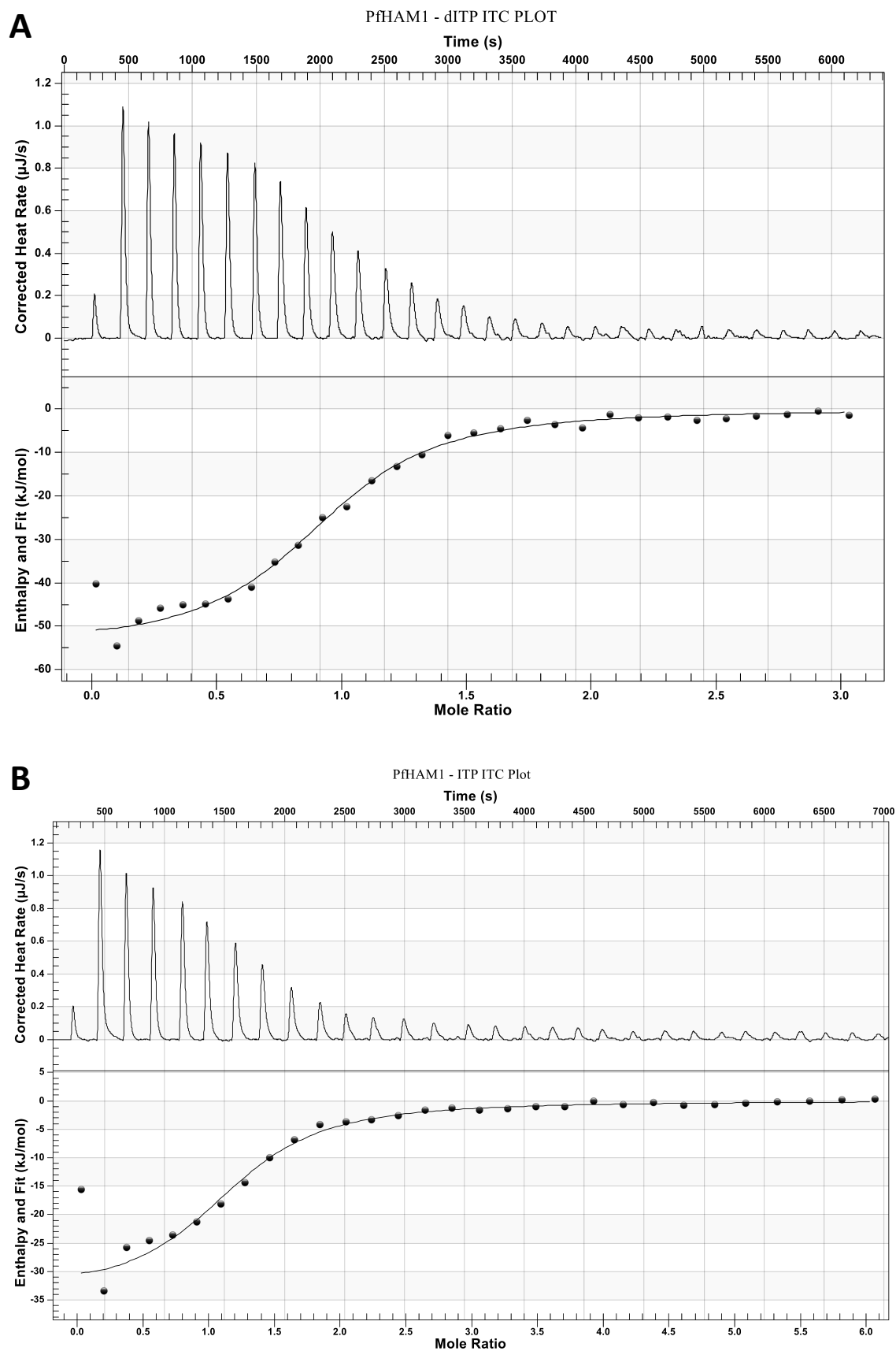
**Table 1:** Various kinetic parameters of *PfHAM1*.

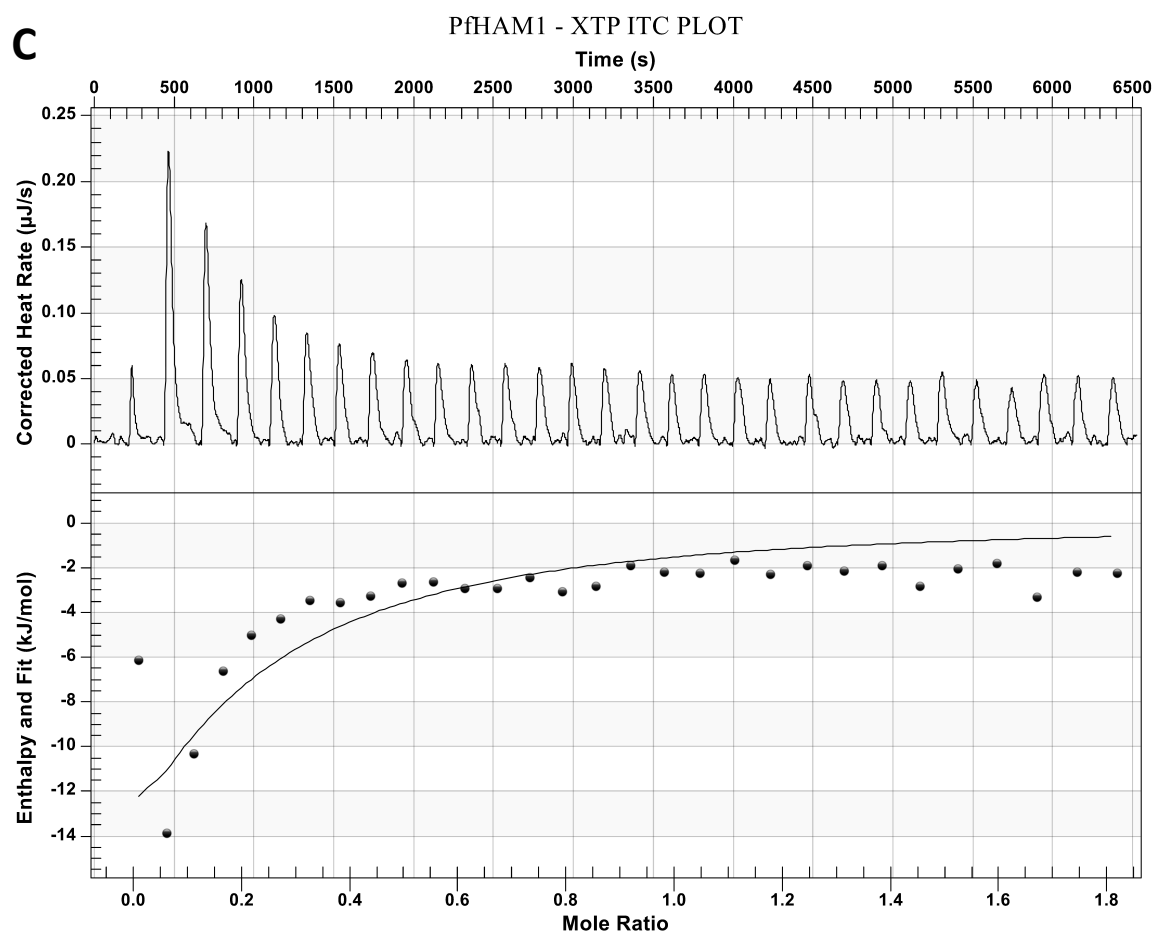
The *PfHAM1*'s activity towards six canonical deoxy-ribonucleoside and ribonucleoside triphosphates, as well as non-canonical nucleotides, including ITP, IDP, IMP, dITP, XTP, XDP, and XMP, were determined. The best substrates for the recombinant *PfHAM1* were dITP, XTP, and ITP, followed narrowly by GTP at a fixed concentration of about 1 mM. Comparatively, little to no activity was displayed by *PfHAM1* in response to other nucleoside triphosphates. *PfHAM1* is a nucleoside triphosphate pyrophosphohydrolase, as evidenced by the negligible hydrolysis of IDP/XDP and IMP/XMP (Figure 4(I)A). Compared to the standards, HPLC analysis demonstrated the formation of IMP and XMP as principal products but not IDP/XDP (Figure 4(II)). In the absence of inorganic pyrophosphatase, no  $P_i$  was produced; hence, there was no activity. Additionally, the  $\text{Mg}^{++}$  ion's presence is necessary for the enzyme's activity, but the presence of the reducing agent DTT had no impact on catalysis. Other divalent ions such as  $\text{Mn}^{++}$ ,  $\text{Co}^{++}$ , and  $\text{Zn}^{++}$  showed about half the activity in the reaction compared to  $\text{Mg}^{++}$  ion dependence (Figure 4(I)B). In the absence of metal ions, there was no enzymatic activity. Chelation with increasing amounts of EDTA was utilised to demonstrate about 75% activity inhibition at 10 mM EDTA and >90% inhibition at 20 mM EDTA (Figure 4(I)C), showing the necessity of  $\text{Mg}^{++}$  ion in the experiment. With dITP (Figure 4(I)D), XTP (Figure 4(I)E), and ITP (Figure 4(I)F) substrates, pure *PfHAM1* was found to have pyrophosphatase activity;  $K_m$  and  $V_{\max}$  parameters were determined for each. Further kinetic calculations revealed the  $K_{\text{cat}}$  for each substrate, which is displayed in Table 1.



**Figure 4(II):** Product analysis (Xanthine monophosphate [A] and Inosine monophosphate [B]) from enzymatic reaction(s) by HPLC. The Y-axis denotes ‘Absorbance Units’, and the X-axis denotes ‘Time’ in minutes.

## 5. ITC studies reveal strong binding of dITP as a substrate to PfHAM1



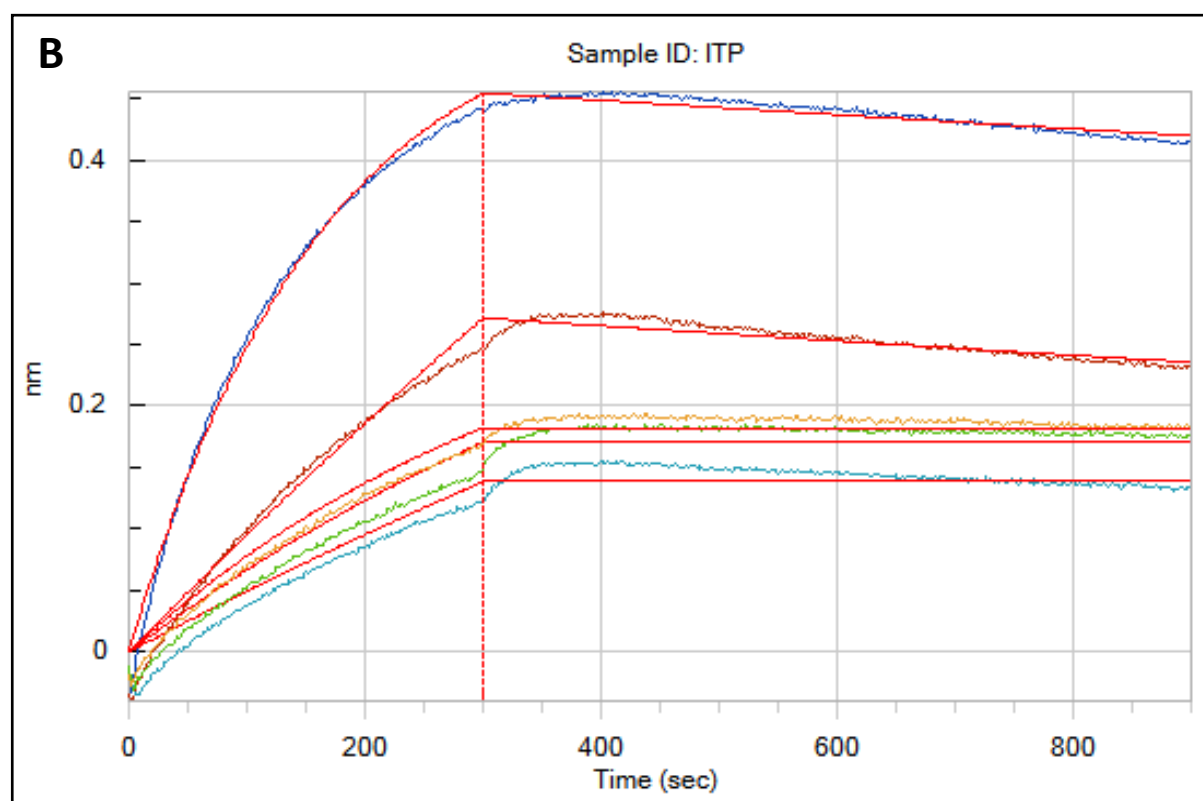
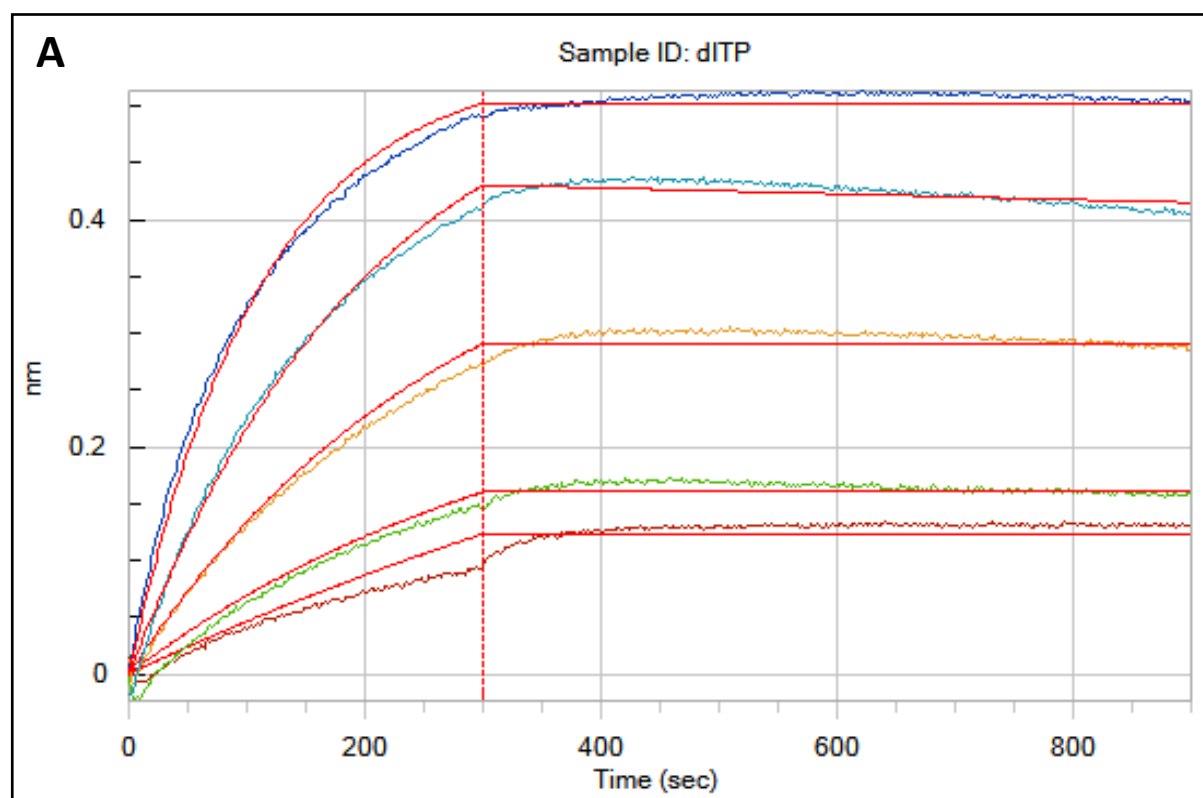


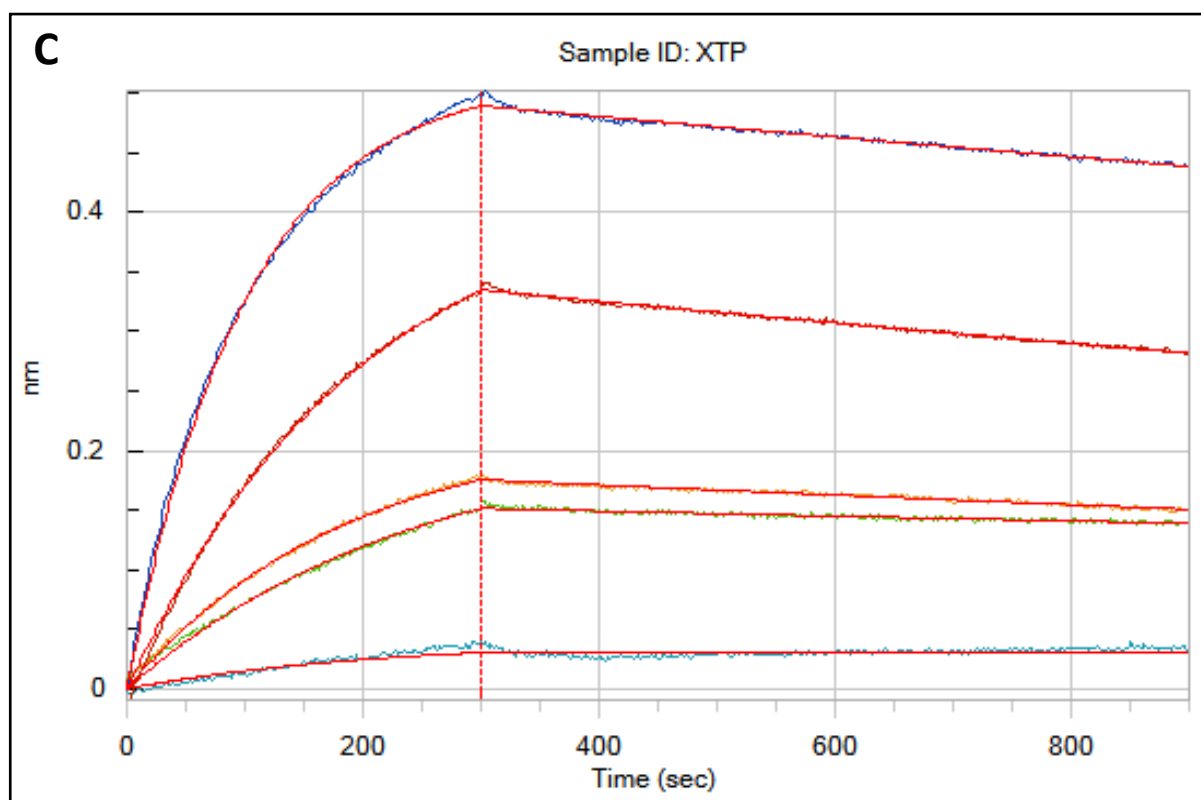
**Figure 5:** *PfHAM1*-substrate(s) Isothermal titration calorimetry (ITC) plot. (A) dITP, (B) ITP, and (C) XTP.

To obtain a comparative binding characteristic of the highest activity-yielding substrates, i.e., dITP/ITP/XTP to *PfHAM1*, ITC at pH 7.5 was performed. The ITC titration sigmoidal graph fitted into a single-site binding model for the substrates. The apparent equilibrium dissociation constant ( $K_d$ ) for dITP from the ITC titration sigmoidal graph was  $2.57 \times 10^{-6} \pm 5.71 \times 10^{-7}$  M with a significant negative enthalpy ( $\Delta H$ ) of  $-54.3 \pm 2.19$  kJ/mol. Substrates like ITP and XTP yielded a  $K_d$  of  $5.316 \times 10^{-6} \pm 1.862 \times 10^{-6}$  M with a  $\Delta H$  of  $-33.75 \pm 2.91$  kJ/mol and  $4.003 \times 10^{-5} \pm 2.312 \times 10^{-5}$  M with a  $\Delta H$  of  $-73.18 \pm 39.50$  kJ/mol, respectively (Figure 5).



## 6. BLI studies show a 1:1 stoichiometric binding pattern

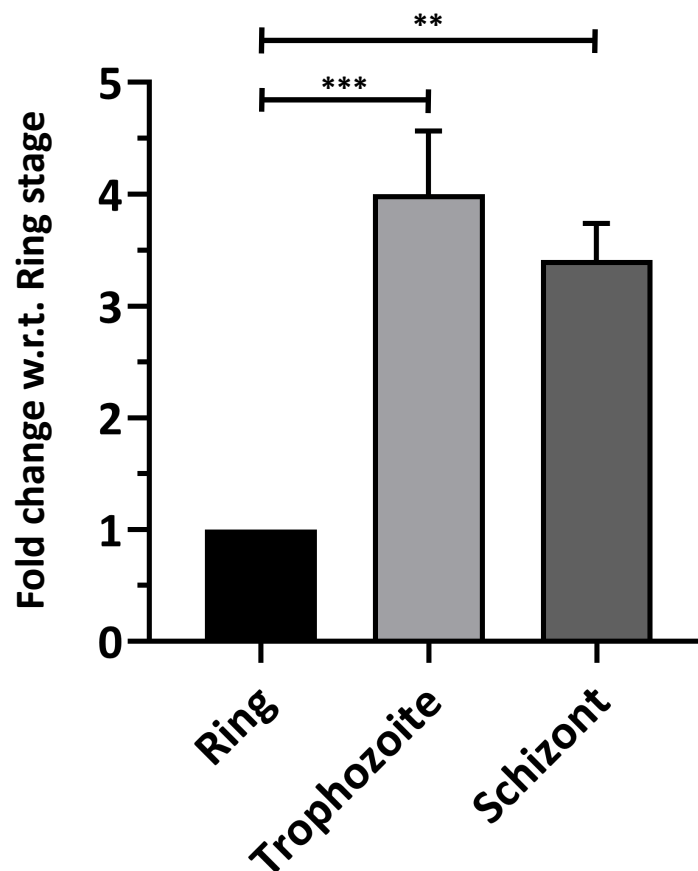




**Figure 6:** Sensorgram showing binding response between *PfHAM1* and its substrates, (A) dITP, (B) ITP, and (C) XTP.

The substrate concentrations used in the dITP-*PfHAM1* interactions were 0.9765, 1.95, 3.91, 31.3 and 250  $\mu\text{M}$ . For ITP-*PfHAM1* interactions, 1.95, 3.91, 7.81, 15.6 and 125  $\mu\text{M}$  and, finally, for XTP-*PfHAM1* interactions, 0.244, 1.95, 7.81, 15.6 and 125  $\mu\text{M}$  concentrations which were locally fitted using Octet system software and a fitting profile was thus generated. The  $K_d$  values obtained were  $7.83 \times 10^{-8} \pm 2.95 \times 10^{-8}$  M (for dITP),  $7.46 \times 10^{-7} \pm 6.88 \times 10^{-9}$  M (for XTP), and  $3.01 \times 10^{-6} \pm 7.12 \times 10^{-7}$  M (for ITP).

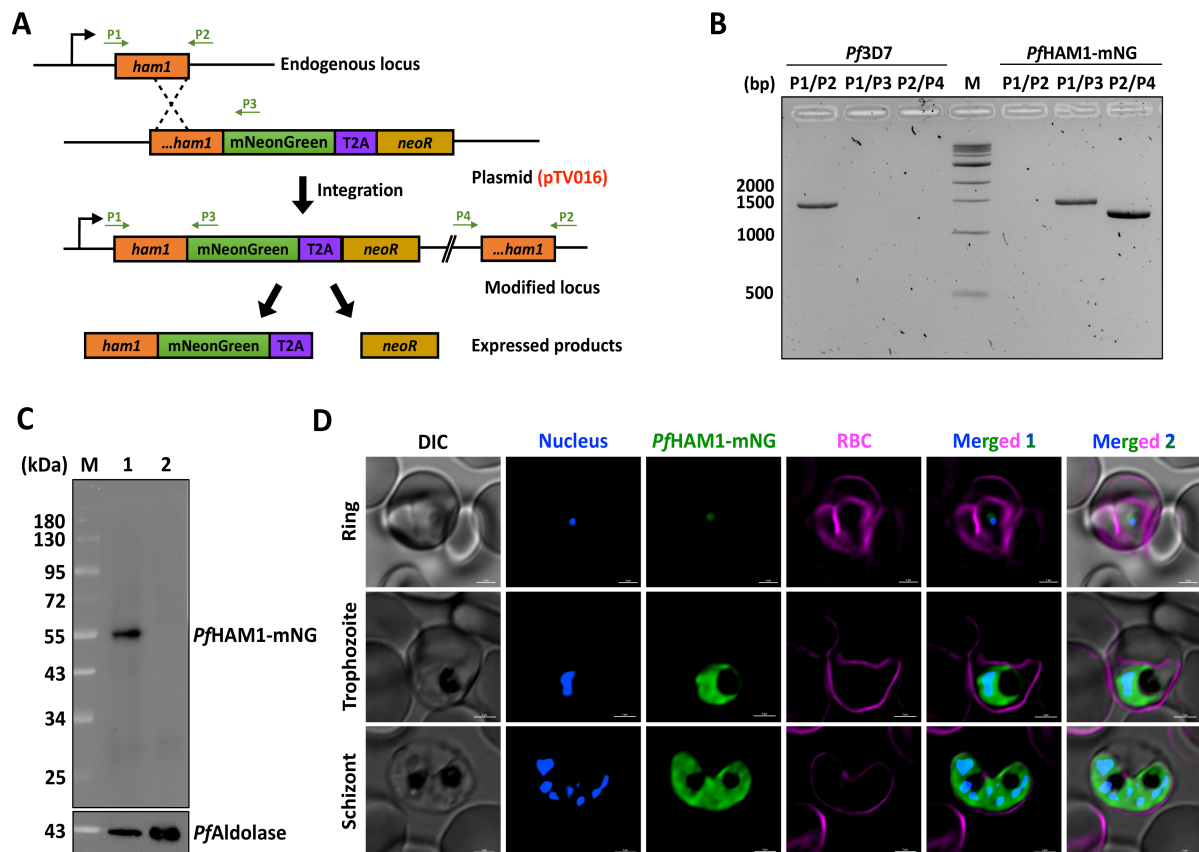
## 7. Transcriptional expression of *pfham1* is maximum in the trophozoite stage



**Figure 7:** Transcriptional pattern of *PfHAM1*. The stage-specific expression of *pfham1* is depicted in a column graph with a fold change in expression compared to the ring stage in the Y-axis. The X-axis represents the asexual blood stages of the parasite. Error bars are given as per mean  $\pm$  S.E.M.

Using *pfalas* (*Pf* gene for delta-aminolaevulinic synthase) to maintain a normalised level of gene expression throughout the experiment, qRT-PCR was used to monitor the transcriptional levels of the gene above during the asexual stages of the parasite's life cycle. The gene expression level was measured in all three of the parasite's blood stages. The trophozoite stage was found to have the highest level of *pfham1* expression, followed by the schizont and ring stages. Quantitatively, it was 4-fold higher in trophozoites than in schizonts, which had a 3.5-fold increase (Figure 7).

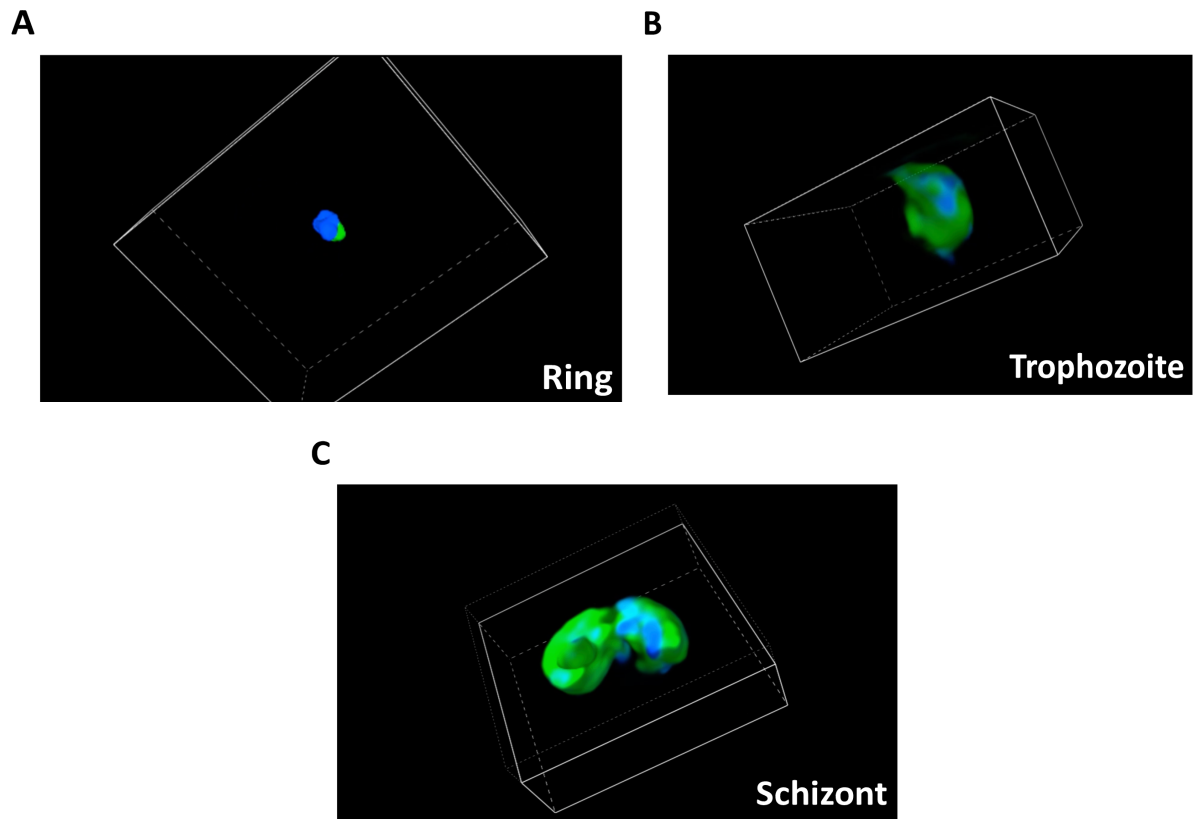
## 8. Live cell imaging of *PfHAM1* shows its predominant localisation in the cytoplasm



**Figure 8(I):** Localisation and transcriptional pattern of *PfHAM1* in *P. falciparum* 3D7. (A) Schematic representation for *PfHAM1*-mNeonGreen fusion parasite line generation using the SLI strategy. Primers “P” are shown in the cartoon for reference. “T2A” skip peptide, “*neoR*” Amino 3'-glycosyl phosphotransferase gene, the selectable marker conferring resistance to G418. (B) Diagnostic integration PCR analysis of gDNA from the *PfHAM1*-mNG parasite line confirms the successful modification of the *pfham1*. Primer pair sets 1&2 are specific to the endogenous *pfham1*, whereas 1&3 and 2&4 are transgene integration-specific primers. (C) Western blot shows the presence of the fusion protein in the *PfHAM1*-mNeonGreen parasite lysate (Lane 1) compared to the non-transfected *Pf3D7* parental line (Lane 2). *PfAldolase* is shown as a loading control. Lane 'M' stands for protein/DNA molecular weight ladder. (D) Imaging showing transfected *P.*

*falciparum* parasites incubated with Hoechst for nuclear staining (blue) and WGA-Alexa 647 for RBC membrane staining (pink). Green fluorescence is attributed to the mNeonGreen protein fused to PfHAM1. Each row represents a specific stage of the *Plasmodium* erythrocytic lifecycle. Scale bar: 2  $\mu$ m.

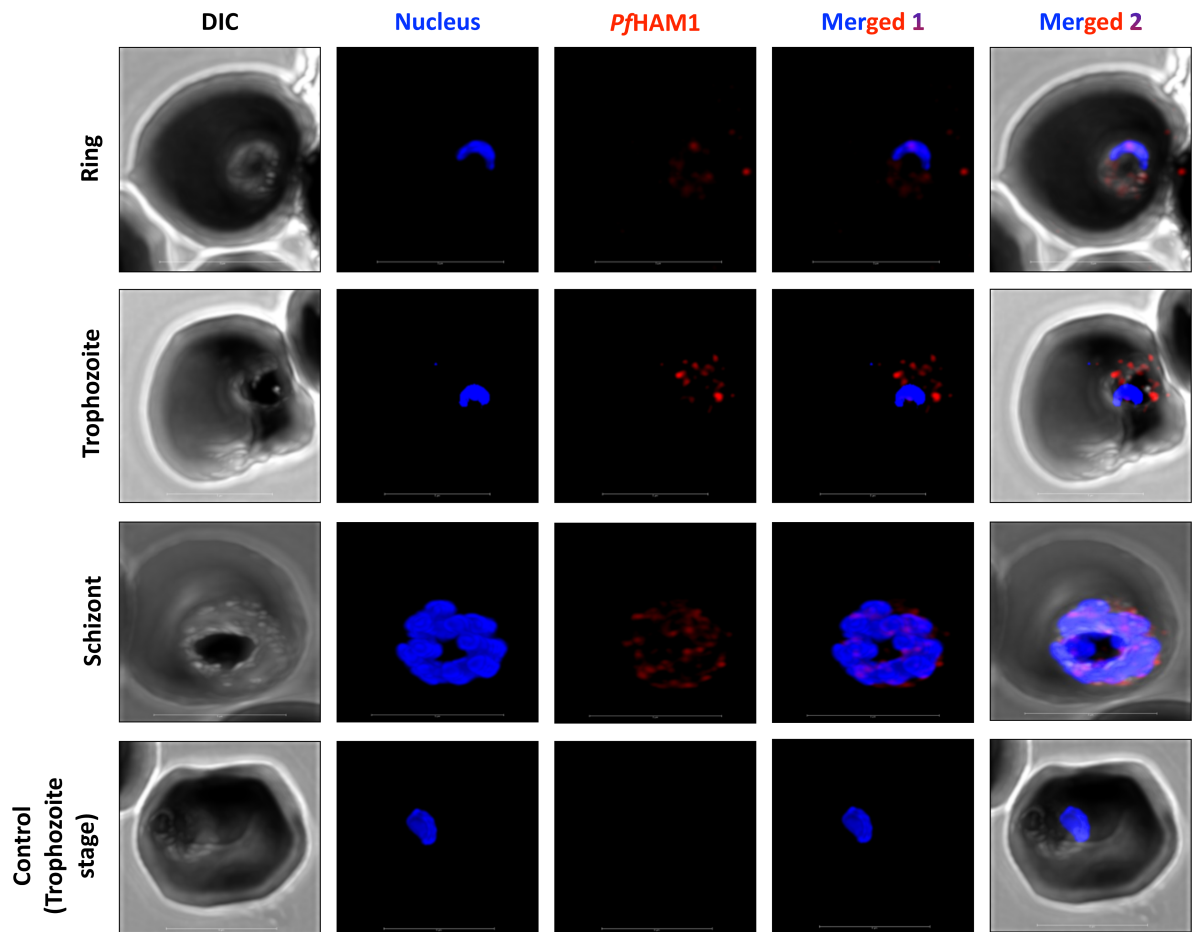
To locate PfHAM1 during the intraerythrocytic stages, the *pfham1* gene was fused with the gene encoding mNeonGreen using Selection-Linked Integration (SLI) (Birnbaum et al. , 2017). Figure 8(I)A presents a schematic representation of the C-terminus mNeonGreen fusion approach utilised in this investigation. This process aided in conducting high-resolution live-cell microscopy of *P. falciparum* parasites expressing the PfHAM1-mNG fusion in a time-dependent manner. The success of the plasmid integration into the *pfham1* locus was confirmed by diagnostic PCR using integration-specific PCR, which yielded desired bands at 1515 bp and 1312 bp Figure 8(I)B. A WT-specific PCR product of 1498 bp was produced using gDNA from the parental 3D7 parasite line. This indicates that the transfected parasite line had no remaining parasites in which the *pfham1* locus was not modified. Western blotting with rat anti-mNG antibody (CancerTools.org) of lysates from transgenic and wildtype parasites was conducted to confirm the production of the protein in the expected size (<55 kDa) that is not detected in lysates of the parental 3D7 parasite line Figure 8(I)C. PfAldolase was used as a loading control for the blots. The live-cell fluorescence microscopy results revealed that the mNG fusion protein was present in all intraerythrocytic stages, mainly in the parasite's cytoplasm, with less in the nucleus. The ring stage had no co-localisation, but the later blood stages showed partial co-localisation of the green fluorescent signal (PfHAM1-mNG) with the blue fluorescent signal (nucleus), as observed through 3D imaging (Figure 8(II)). When combined with a differential interference contrast (DIC) image, the green fluorescent channel corresponding to the mNeonGreen fusion of PfHAM1 and the blue channel relating to the Hoechst-stained nucleus verified the presence of the protein in the cytoplasm. Wheat germ agglutinin fused to Alexa-647 was used to label the RBC membrane for easy visualisation. It was observed that PfHAM1 expression was more intense in the trophozoites (16-32 h) and schizonts (32-48 h) compared to the rings, as shown in Figure 8(I)D.



**Figure 8(II):** 3D imaging. (A) Ring, (B) Trophozoite, and (C) Schizont stages. The green signal is from PfHAM1-mNG, and the blue signal is from Hoechst (nucleus).



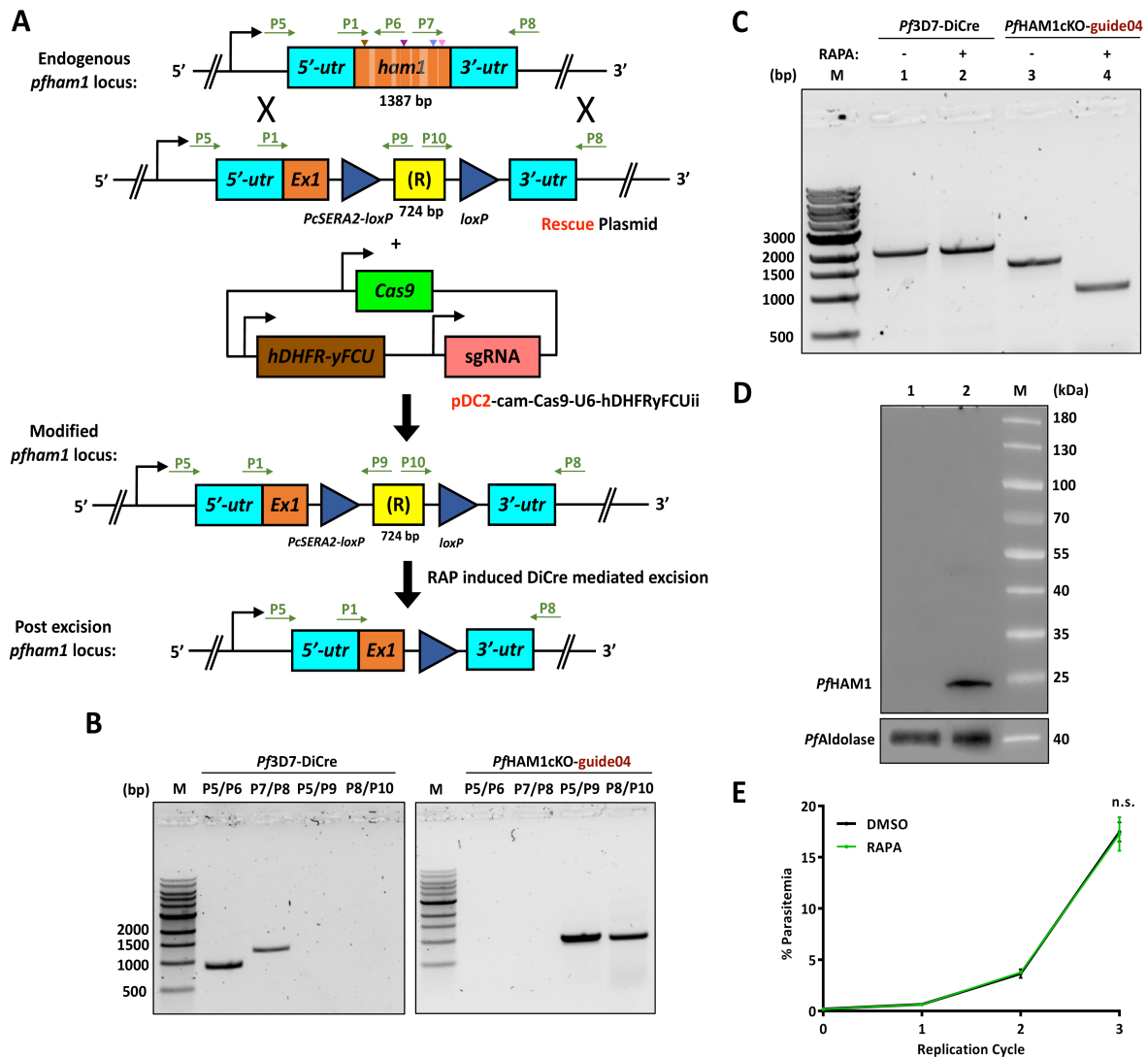
## 9. Immunofluorescence studies confirm cytoplasmic localisation



**Figure 9:** Localisation of *PfHAM1* in *P. falciparum*. iRBCs were processed and incubated with anti-*PfHAM1* antibody followed by anti-mouse antibody Alexa fluor 647 (red fluorescence) and DAPI for nuclear staining (blue fluorescence). Each row represents a specific stage of the *Plasmodium* erythrocytic lifecycle. Scale bar: 5  $\mu$ m.

Confocal microscopy was used to generate high-resolution deconvoluted optical images of the synchronised culture in a time-dependent manner to track the trajectory of *PfHAM1* in the parasite. All stages revealed its presence scattered in the cytoplasm of the parasite residing in RBCs. The fluorescent channel corresponding to anti-*PfHAM1* (red channel) and DAPI (blue channel), when merged with differential interference contrast (DIC) image, confirmed the presence of the protein in the cytoplasm (Figure 9). The image panel also shows a control set where pre-immune sera was used.

## 10. *PfHAM1* is dispensable in the blood stages of the lifecycle as shown using conditional knock-outs (cKO)



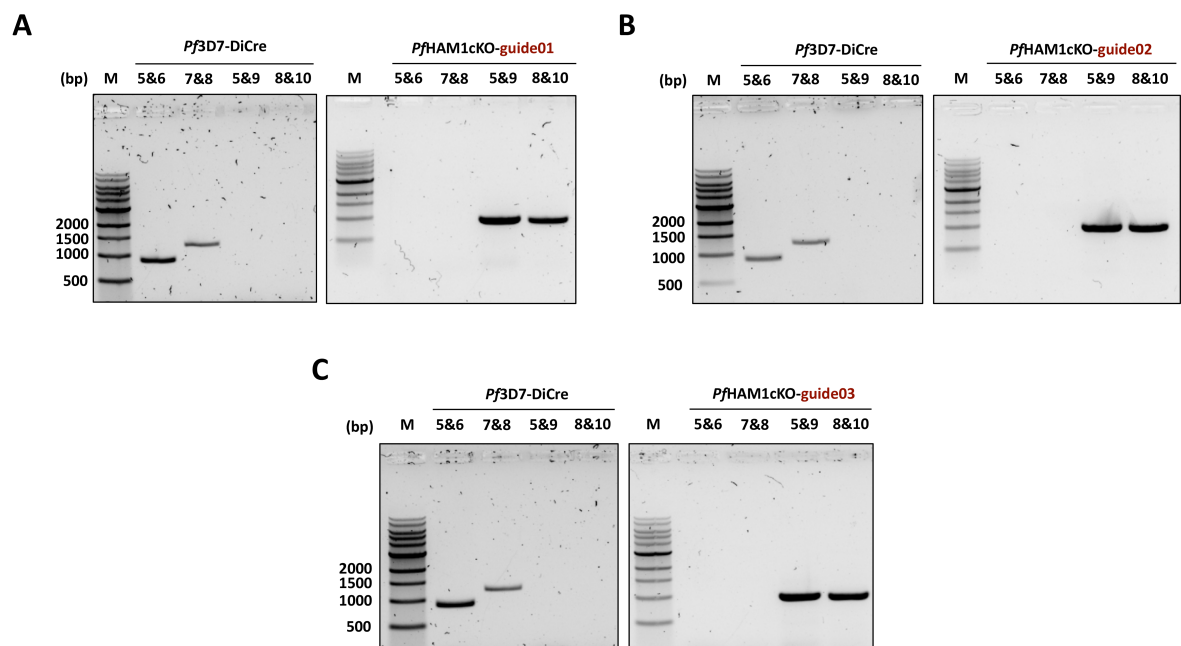
**Figure 10(I):** Generation of the *pfham1*-DiCre parasite line using the CRISPR-Cas9/DiCre-recombinase genetic tool. (A) Schematic representation of the constructs used to generate a *pfham1*-DiCre inducible KO parasite line and the resultant rapamycin-induced disruption of the modified locus. Primers “P” used for diagnostic PCR are shown. “(R)” stands for the 724 bp re-codonised DNA of the gene. The PcSERA2-*loxP* site on the left flanks the (R), and a *loxP* site on the right. “*loxP*” sequences are shown as right-tilted triangles. “*Ex1*” exon 1, “*utr*” untranslated regions at 5’ and 3’ ends, which were used for homologous

recombination (HR). The white rectangles in the “*ham1*” box show the six introns of the gene, whereas the four inverted coloured triangles point to the site for single guide RNA (sgRNA) action (L to R are Guides 01, 02, 03, and 04). (B) Diagnostic integration PCR analysis of gDNA from the transgenic *PfHAM1cKO*-guide04 parasite line (right) confirms a successfully modified *pfham1* target locus. Primer combination sets 5 & 6 and 7 & 8 are 3D7 WT-specific primers, whereas 5 & 9 and 8 & 10 are transgene integration-specific primer sets. Similar experiments were performed with the *Pf3D7*-DiCre parental parasite line (left) as a control. (C) Diagnostic excision PCR analysis with P1/P8 primer pair showing efficient excision of “floxed” sequences as observed in the rapamycin-treated sample (Lane 4) when compared to its vehicle control (DMSO) set (Lane 3) of the *PfHAM1cKO*-guide04 parasite line, whereas in the *Pf3D7*-DiCre control parental parasite line, no excision of the gene occurred in Lane 2 (RAPA-treated), and Lane 1 (DMSO-treated). (D) Western blot showing the lack of *PfHAM1* expression in the rapamycin-treated culture (Lane 1) compared to the DMSO control (Lane 2). *PfAldolase* is shown as a loading control. Lane 'M' stands for protein/DNA molecular weight ladder. (E) Growth curves showing % parasitemia as measured by flow cytometry of *PfHAM1cKO*-guide04 treated with DMSO (vehicle-only control) or rapamycin. The mean of results from three independent experiments is plotted with  $\pm$  S.E.M.

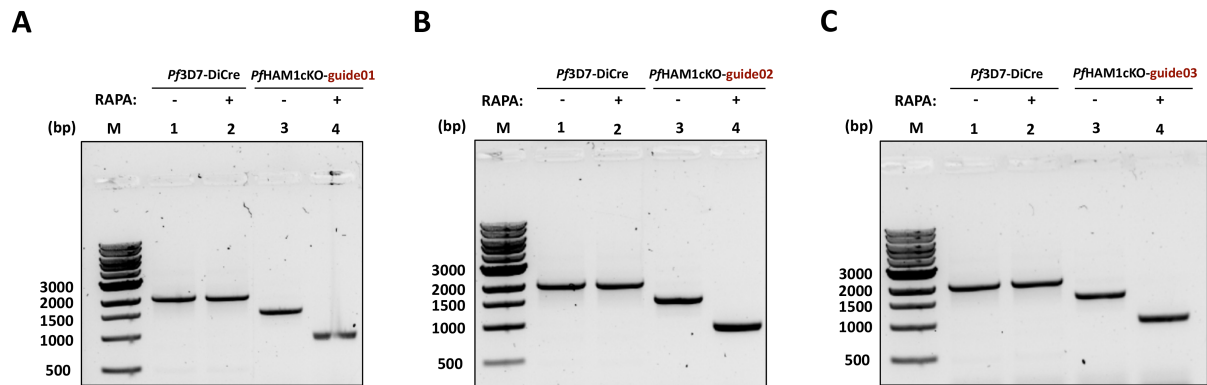
To gain a better understanding of the role of *PfHAM1* in the parasite's growth, inducible *pfham1* mutants were produced through Cas9-mediated gene replacement. The native *pfham1* gene was replaced with a recodonised version containing two *loxP* sites in a parasite line that expresses the rapamycin-inducible DiCre recombinase system (Figure 10(I)A). All four guide RNAs were transfected in the *Pf3D7*-DiCre line, and diagnostic PCRs were performed from all the transfected lines and compared with the control *Pf3D7*-DiCre gDNA (Figure 10(I)B). Primer sets P5/P6 and P7/P8 were used as WT-endogenous locus-specific primers, producing a band at 954 bp and 1308 bp, respectively. Primer sets P5/P9 and P8/P10 were used as integration-specific primers, which gave a band at 996 bp and 968 bp, respectively. Integration PCR confirmed the integration of the rescue plasmid, resulting in a modified *pfham1* locus in *PfHAM1cKO*-guide04. After treating highly synchronised

ring-stage cultures with rapamycin or DMSO (vehicle control), an excision PCR was performed with primer set P1/P8 to check for DiCre-mediated excision of the "floxed" region. The results were conclusive, with lanes 1 and 2 (non-transfected) in Figure 10(I)C giving bands at 2217 bp. In contrast, lanes 3 and 4 (transfected) showed bands at 1622 bp and 1018 bp, respectively, thus proving efficient and specific excision of the "floxed" region in the transfected line, *PfHAM1cKO-guide04*.

Moreover, in the western blot analysis, the protein removal in the rapamycin-treated sample, as compared to the DMSO-treated control sample, provided further evidence for the knockout of the gene (Figure 10(I)D). To determine the essentiality of *PfHAM1*, rapamycin was used to trigger the removal of the "floxed" *pfham1*, and the parasite's replication was assessed using flow cytometry. During the asexual stages of the parasite, rapamycin-treated *PfHAM1cKO-guide04* parasites did not exhibit any significant growth inhibition over three cycles, as compared to DMSO-treated control parasites (Figure 10(I)E). Three other guide RNAs were used in three independent experiments to confirm the results (Figure 10(II) and Figure 10(III)).



**Figure 10(II):** Integration PCR independently confirms a modified *pfham1* locus with three other guide RNAs (Guide 01, Guide 02, and Guide 03).



**Figure 10(III):** Excision PCR shows efficient excision of floxed sequences as observed in the rapamycin-treated sample (Lane 4) when compared to its vehicle control (DMSO) set (Lane 3). This experiment is independently performed with three other guide RNAs (Guide 01, Guide 02, and Guide 03).

## D. Discussion

To ensure that incorrect nucleotides do not hinder the parasite's development, it is crucial to have a comprehensive understanding of how proteins remove them from *P. falciparum*. In this context, we delve into the role of HAM1, a pyrophosphohydrolase enzyme that converts non-standard nucleotides into their respective monophosphate and pyrophosphate forms. The analysis provides an in-depth insight into how this enzyme helps maintain a consistent supply of correct nucleotides.

After thoroughly mining the PlasmoDB database and conducting a comprehensive BLAST search, a potential non-canonical NTPase ortholog in *P. falciparum* was identified. The putative ortholog, PfHAM1, was found to share about 33% of amino acid sequence identity with HsITPA and up to 60% similarity with other *Plasmodium* species such as *P. malariae*, *P. knowlesi*, *P. ovale*, *P. berghei*, *P. vivax*, and *P. yoelli*. This finding confidently reveals the ubiquitous existence of PfHAM1, which is essential in preventing the misincorporation of harmful non-canonical nucleotides into the chromosomal DNA. The *itpa* gene exhibits polymorphism in the human population, with various alleles contributing to atypical ITPase activities. However, the most clinically significant is the 94C→A mutation, which occurs in exon 2 and leads to a P32T missense mutation. This mutation has an allelic frequency ranging from 5 to 19%, with the highest incidence in the Asian population (Marsh et al. , 2004). ITPase enzyme activity is absent in individuals homozygous for the P32T mutation (Shipkova et al. , 2006). In heterozygotes, ITPase activity is only one-fourth of normal levels (Bierau et al., 2007). As a result, misfolded proteins are produced (Simone et al. , 2013), and the ITPase-mRNA undergoes alternate splicing (Arenas et al. , 2007), which leads to reduced amounts of ITPase in various tissues (Stepchenkova et al. , 2009). Interestingly, multiple sequence alignment shows that Asn25 replaces Pro32 in HsITPA in the PfHAM1 amino acid sequence. Although HAM1 in other *Plasmodium* species has Lys (*P. berghei*, *P. malariae*, *P. yoelli*, and *P. ovale*) or Glu (*P. knowlesi* and *P. vivax*) residues, suggesting the uniqueness of this residue in *P. falciparum*.

It was observed that the oligomeric status of PfHAM1 was similar to that of HsITPA and other species, such as *E. coli*, *P. horikoshii* OT3, and *T. maritima* (Lokanath et al. , 2008, Savchenko et al. , 2007). These species all exhibit a homodimeric nature. The SEC-MALS technique was used to determine the molecular mass of PfHAM1 in this



study. Basic physical equations connected the molar mass with scattered light intensity and protein concentration (Some et al. , 2019). The experimental molecular weight of *PfHAM1* was around 50.5 kDa, which is very close to the theoretical dimer molecular weight of approximately 48.4 kDa. Gel filtration chromatography is bound by assumptions that the protein conformation is similar to the standards and that there are no non-specific interactions between the column and the protein of interest. However, this is not the case in practical terms; hence, the elution time drifts, affecting the data (i.e., calculated kDa values). The MALS technique overcame this issue. Thus, it can be concluded that *PfHAM1* is homodimeric.

Kinetic analysis has shown that *PfHAM1* can efficiently hydrolyse dITP, XTP, and ITP to their monophosphate forms while almost inactive against the canonical nucleotides. This suggests that *PfHAM1* effectively prevents the accumulation of non-standard purine ribonucleoside triphosphates and deoxyribonucleoside triphosphates. It is worth noting that *PfHAM1* acts on both ribonucleotides and deoxyribonucleotides as its cognate substrates. This is consistent with a previous report on murine ITPase, which found that inosine misincorporation in the RNA of *itpa*-null mice cardiomyoblasts resulted in perturbed translation and cardiac dysfunction (Schroader et al. , 2022). *PfHAM1* showed the highest priority for dITP, followed by XTP and ITP, unlike ITPases of other organisms, where ITP, dITP, and XTP are differently hydrolysed in terms of kinetic affinity constants (Chung et al. , 2001, Lin et al., 2001). When comparing pyrophosphohydrolase activity using dITP as a substrate, *PfHAM1* had a  $K_m$  of  $31.86 \pm 4.03 \mu\text{M}$  and a turnover number of  $108 \text{ sec}^{-1}$ . In contrast, the *HsITPA* had a  $K_m$  of  $310 \pm 100 \mu\text{M}$  and a turnover number of  $360 \text{ sec}^{-1}$  (Lin et al., 2001). However, *S. cerevisiae* HAM1 had a  $K_m$  of  $3.06 \pm 0.6 \mu\text{M}$  and a  $K_{cat}$  of  $1.288 \text{ sec}^{-1}$  (Davies et al. , 2012), and *Arabidopsis thaliana* ITPase had a  $K_m$  of  $1.7 \pm 0.3 \mu\text{M}$  and a  $K_{cat}$  of  $1.5 \text{ sec}^{-1}$  (Straube et al., 2023). Further incubation of *PfHAM1* with various deaminated purines confirmed that *PfHAM1* is a bona fide inosine triphosphate pyrophosphatase (ITPase), and its predominant cytosolic localisation supports its house-cleaning function of eliminating the cytosolic non-canonical nucleoside triphosphate pools. Interestingly, dithiothreitol (DTT) did not affect the enzyme kinetics, implying that the two cysteines in the protein are non-bonded (Fariselli et al. , 1999). However, DTT increased the enzyme kinetics in the human homolog two-fold, suggesting a requirement for reducing environments (Lin et al., 2001). It was found that *PfHAM1* exhibited robust hydrolytic activity in the presence of  $\text{Mg}^{++}$ , suggesting a divalent metal ion-dependent alteration of enzyme

activity. However, ITPase orthologs in some organisms prefer  $Mg^{++}$  or  $Mn^{++}$  (Burgis and Cunningham, 2007, Hwang et al., 1999, Lin et al., 2001, Lokanath et al., 2008, Takayama et al. , 2007, Vidal et al., 2022). To determine the affinity parameter of the most robust interacting substrate, we investigated the kinetics of different substrates with *PfHAM1*. It was found that dITP is the most robust substrate for the protein. Calorimetric experiments and BLI confirmed a 1:1 stoichiometry.

The breakdown of haemoglobin (Liu et al. , 2006) and the hemolysis of infected red blood cells (Haldar and Mohandas, 2009) are two constant risk factors that lead to an overload of free heme within the cells. This heme is toxic to *Plasmodium* parasites but is converted to inert hemozoin (Hz) as a survival strategy (Egan, 2008). However, not all free heme gets converted into Hz crystals, which increases the chances of oxidative stress in the parasite (Becker et al. , 2004). Some anti-malarial drugs trigger oxidative stress as a primary mechanism to kill parasites (Vasquez et al. , 2021). This constant redox burden on the parasite genome can lead to the generation of non-canonical nucleotides like (d)ITP and XTP in the nucleotide pool due to oxidative deamination of purines (Ji et al. , 2017, Zheng et al. , 2005). Sanitation enzymes are then called into action to avoid misincorporating these aberrant nucleotides into the nucleic acids, specifically during the active multiplication stages of the parasite. The expression of *PfHAM1*-mNeonGreen fusion protein remains consistent across all intra-erythrocytic stages, exhibiting high levels during the trophozoite and schizont stages, primarily concentrated in the cytoplasm with limited presence in the nucleus. However, it is exclusively found within the cytoplasm during the ring stage, as evidenced by immunofluorescence studies and 3D imaging of the microscopic live cell images. This might be due to the progression from the ring to the later stages, which involves blood-stage schizogony, where three to four rounds of DNA synthesis, mitosis, and nuclear division occur to form a syncytial schizont (Arnot and Gull, 1998, Bannister et al. , 2000). Thus, there is a higher requirement of nucleotides during this phase, which increases the chances of misincorporation of aberrant nucleotides from the pool as the DNA and RNA polymerase may often fail to differentiate the non-canonical analogues (Hamid and Eckert, 2005, Kincaid et al. , 2005, Thomas et al. , 1998). The microscopic data supports the cytosolic localisation of *PfHAM1*. Similarly, an elevated expression of *PfHAM1* was also observed in the real-time PCR data, which is in corroboration with previously reported RNA-seq transcriptome profiling data from erythrocytic stages of *P. falciparum* (Otto et al. , 2010). The cytoplasmic localisation of the protein in other models, such as mice

(Behmanesh et al. , 2005), *T. brucei* (Vidal et al., 2022), and plants (Straube et al., 2023) has also been observed earlier. All these facts support the cytosolic non-canonical nucleotide pyrophosphohydrolase requirement to preserve genome integrity by explicitly cleaving the aberrant nucleotides.

It was necessary to investigate the impact of eliminating *PfHAM1* on the survival of *P. falciparum*. While the gene is crucial in mammalian cells (Abolhassani et al., 2010, Behmanesh et al., 2009, Handley et al., 2019), *pffham1*-null mutant parasites survived under standard growth conditions in culture, which is an intriguing observation. The transposon-mediated saturation mutagenesis experiment in *P. falciparum* (Zhang et al. , 2018) predicted it to be an essential gene. However, ITPase was annotated as non-essential in *P. berghei* in the PlasmoGEM database (Bushell et al. , 2017, Kumar et al. , 2019), suggesting that *Plasmodium* HAM1 may have a compensatory functioning role for nucleotide surveillance in *P. falciparum* that may not apply to other organisms where ITPase orthologs are vital for cell survival. This is supported by reports on *S. cerevisiae* HAM1 (Pang et al. , 2012) and *E. coli rdgB* single mutants (Clyman and Cunningham, 1987), where the ITPase activity was not critical for survival and mutants displayed viable phenotypes. Therefore, it can be concluded that *PfHAM1* plays an auxiliary role in eliminating the parasite's abnormal nucleotides from the cellular pool in the blood stages. Moreover, it is expected that the accumulation of deaminated purine will not reach the extent that causes lethality in standard culture conditions. Other hypothetical surveillance proteins in *P. falciparum* may also compensate for the role of *PfHAM1* under a single knockout condition.

## **E. Conclusion**

The detailed study demonstrates that *PfHAM1* is an active inosine triphosphate pyrophosphatase enzyme. It undoubtedly plays a crucial role in removing potentially harmful dITP, XTP, and ITP from the cytosolic nucleotide pool. Further research in male and female gametocytes will provide a definitive answer regarding the indispensability of *PfHAM1* activity for parasite survival in the vector, where the load of deaminated (d)NTPs can significantly impair normal cell function. The findings presented here establish a strong foundation for further research on the mechanisms employed by nucleotide quality surveillance enzymes to ensure precise nucleotide homeostasis in human malaria parasites. Identifying proteins with such importance will enhance our understanding of pool maintenance and cleanliness, which will be utilised to develop effective therapeutic interventions for human and animal parasites.

## F. Additional information

Primer	Strand	Description	Primer sequence (5' to 3')	Restriction site
P1	+	<i>pfham1</i> WT (F)	ATATCAGGATCCTAGATGGAGATATATT TAGTGACTGGAAATATGAATAAAAAG G	-
P2	-	<i>pfham1</i> WT (R)	CTTTTAAGATATTAACATACACAAA AAGGATGTGTAC	-
P3	-	mNG INT (R)	TTGGATTTCTGTTCTTGTCCAACC	-
P4	+	Vector-specific INT (F)	CAAAATGGTTAACAAAGAAGAAGC TCAGAG	-
P5	+	<i>pfham1</i> 5' KO (F)	CCGAGCTATTAGATGAAAATGATTG TCAAC	-
P6	-	<i>pfham1</i> 5' KO (R)	CACATATTAATATAGGTATATTTTAT TTGAATATCCATTATG	-
P7	+	<i>pfham1</i> 3' KO (F)	CCTAGAGGAAATAATAAATTCGGAT GGTAAACATG	-
P8	-	<i>pfham1</i> 3' KO (R)	GCGCTACCTTTTTTTGTTTTATCATA TCCTC	-
P9	+	<i>pfham1</i> Recod (R)	GATCTCAACAATGTCTTGCGCC	-
P10	-	<i>pfham1</i> Recod (F)	CTTTAAGGCATTCGTCCAGCTTAAG G	-
P11	+	<i>pfham1</i> Cloning (F)	GGGTGCCATGGAGATATATTTAGTG ACTGGAATATG	<i>NcoI</i>
P12	-	<i>pfham1</i> Cloning (R)	GCGGGCTCGAGAAATTCATTATTGTA TTTTTATGCTCATTG	<i>XhoI</i>
P13	+	<i>pfham1</i> RT (F)	TCCCAGGACCATACATTAAATGG	-
P14	-	<i>pfham1</i> RT (R)	CCTCTAGGTTCAACTATCTTTCCG	-
P15	+	<i>pfalas</i> RT (F)	ATTCGGCAGAAAAGTGTAACAG	-
P16	-	<i>pfalas</i> RT (R)	GAAATGGTGATGGTGTATGCG	-
P17	+	<i>pfham1-mNG</i> Cloning (F)	TATAAGATCTTGGAAGAAATCCAGG CTCAAGACATAG	<i>BglIII</i>
P18	-	<i>pfham1-mNG</i> Cloning (R)	TTTTCTGCAGCAAATTCATTATTGTAT TTTTTATGCTCATTCAATAAAATTC	<i>PstI</i>

**Table 2:** Primers (P) used in the study.

Guide RNA	Strand	Sequence (5' to 3')
Guide 01	+	attgTTTGGAAAGACTTTCTGGT
	-	aaacACCAGAAAGTCTTTCCAAA
Guide 02	+	attgGAAAGATAGTTGAACCTAG
	-	aaacCTAGGTTCAACTATCTTTC
Guide 03	+	attgACGAAGGCCTTAAATCGTG
	-	aaacCACGATTTAAGGCCTTCGT
Guide 04	+	attgTTCTACTATGTCTTGAGCC
	-	aaacGGCTCAAGACATAGTAGAA

**Table 3:** Guide RNA sequences used for the cKO study of *PfHAM1*.

Recodonised (R) DNA sequence of <i>pfham1</i> gene
ATGGAGATATATTTAGTGACTGGAAATATGAATAAAAAGGAAGAATTTTAAAAATGATGGA TGAAGAATTAAACGTTGAATTTGTAAATATAAATTGTAAGTCTATCCTTCTTAAGACAATAAC TTCGTATAGCATACATTATACGAAGTTATTAATTTTTAACAAAAAATCTTATGAATAACTAAA AATGTAACCATTTTAACTTTCTTCATTTTTTATAGTGGAAGAGATTCAGGCGCAAGACATTGT TGAGATCAACGAGCATAAAGTCAAAACCGCTTATAATATTTGAAAAAGCAAGATAACAAC AAAAATAAAAAGCGTTATGTGATTACGGATGACACGGGTCTGTTCATTTCCAAGTTGAATAA TTTTCTGGACCATACATTAAATGGATGCAGAAGGCACTGGGTAGCAAAGGAATCGCCGAT GTCGTCTCCCGCCTTGATGATAATACTTGTCATGCAATCTGCACATACTCCGTGTACGACGGC AAAGATGTCCATAGCTTTAAGGGGATTACGAAGGGCAAGATTGTGCAACCTCGTGGTAATA ACAAATTCGGTTGGGATAACATTTTTCAGCCAGAAAGTCTGTCAAAGACGTTTGGGGAAAT GACGTTTCGATGAAAAACAAAATTTATCGCCTCGCTTTAAGGCATTCGTCCAGCTTAAGGAAT TTTTAATGAACGAGCACAAGAAGTACAACAACGAGTTCTGA

**Table 4:** The recodonised 724 base pairs in *pfham1* (Exon 2 to Exon 7).



## G. References

1. Abolhassani N, Iyama T, Tsuchimoto D, Sakumi K, Ohno M, Behmanesh M, et al. NUDT16 and ITPA play a dual protective role in maintaining chromosome stability and cell growth by eliminating dIDP/IDP and dITP/ITP from nucleotide pools in mammals. *Nucleic Acids Res.* 2010;38:2891-903.
2. Arenas M, Duley J, Sumi S, Sanderson J, Marinaki A. The ITPA c.94C>A and g.IVS2+21A>C sequence variants contribute to missplicing of the ITPA gene. *Biochim Biophys Acta.* 2007;1772:96-102.
3. Arnot DE, Gull K. The Plasmodium cell-cycle: facts and questions. *Ann Trop Med Parasitol.* 1998;92:361-5.
4. Ashley EA, Dhorda M, Fairhurst RM, Amaratunga C, Lim P, Suon S, et al. Spread of artemisinin resistance in Plasmodium falciparum malaria. *N Engl J Med.* 2014;371:411-23.
5. Bannister LH, Hopkins JM, Fowler RE, Krishna S, Mitchell GH. A brief illustrated guide to the ultrastructure of Plasmodium falciparum asexual blood stages. *Parasitol Today.* 2000;16:427-33.
6. Becker K, Tilley L, Vennerstrom JL, Roberts D, Rogerson S, Ginsburg H. Oxidative stress in malaria parasite-infected erythrocytes: host-parasite interactions. *Int J Parasitol.* 2004;34:163-89.
7. Behmanesh M, Sakumi K, Abolhassani N, Toyokuni S, Oka S, Ohnishi YN, et al. ITPase-deficient mice show growth retardation and die before weaning. *Cell Death Differ.* 2009;16:1315-22.
8. Behmanesh M, Sakumi K, Tsuchimoto D, Torisu K, Ohnishi-Honda Y, Rancourt DE, et al. Characterization of the structure and expression of mouse Itpa gene and its related sequences in the mouse genome. *DNA Res.* 2005;12:39-51.
9. Bierau J, Lindhout M, Bakker JA. Pharmacogenetic significance of inosine triphosphatase. *Pharmacogenomics.* 2007;8:1221-8.
10. Birnbaum J, Flemming S, Reichard N, Soares AB, Mesen-Ramirez P, Jonscher E, et al. A genetic system to study Plasmodium falciparum protein function. *Nat Methods.* 2017;14:450-6.
11. Bradshaw JS, Kuzminov A. RdgB acts to avoid chromosome fragmentation in Escherichia coli. *Mol Microbiol.* 2003;48:1711-25.
12. Buchan DW, Minneci F, Nugent TC, Bryson K, Jones DT. Scalable web services for the PSIPRED Protein Analysis Workbench. *Nucleic Acids Res.* 2013;41:W349-57.

13. Burgis NE, Cunningham RP. Substrate specificity of RdgB protein, a deoxyribonucleoside triphosphate pyrophosphohydrolase. *J Biol Chem.* 2007;282:3531-8.
14. Bushell E, Gomes AR, Sanderson T, Anar B, Girling G, Herd C, et al. Functional Profiling of a Plasmodium Genome Reveals an Abundance of Essential Genes. *Cell.* 2017;170:260-72 e8.
15. Bustin SA, Benes V, Garson JA, Hellemans J, Huggett J, Kubista M, et al. The MIQE guidelines: minimum information for publication of quantitative real-time PCR experiments. *Clin Chem.* 2009;55:611-22.
16. Chakarov S, Petkova R, Russev GC, Zhelev N. DNA damage and mutation. Types of DNA damage. 2014;11.
17. Cheviet T, Lefebvre-Tournier I, Wein S, Peyrottes S. Plasmodium Purine Metabolism and Its Inhibition by Nucleoside and Nucleotide Analogues. *J Med Chem.* 2019;62:8365-91.
18. Chung JH, Back JH, Park YI, Han YS. Biochemical characterization of a novel hypoxanthine/xanthine dNTP pyrophosphatase from *Methanococcus jannaschii*. *Nucleic Acids Res.* 2001;29:3099-107.
19. Clyman J, Cunningham RP. *Escherichia coli* K-12 mutants in which viability is dependent on recA function. *J Bacteriol.* 1987;169:4203-10.
20. D'Avolio A, Cusato J, De Nicolo A, Allegra S, Di Perri G. Pharmacogenetics of ribavirin-induced anemia in HCV patients. *Pharmacogenomics.* 2016;17:925-41.
21. Dai J, Lu Y, Wang J, Yang L, Han Y, Wang Y, et al. A four-gene signature predicts survival in clear-cell renal-cell carcinoma. *Oncotarget.* 2016;7:82712-26.
22. Dasgupta A, Mondal P, Dalui S, Das C, Roy S. Molecular characterization of substrate-induced ubiquitin transfer by UBR7-PHD finger, a newly identified histone H2BK120 ubiquitin ligase. *FEBS J.* 2022;289:1842-57.
23. Davies O, Mendes P, Smallbone K, Malys N. Characterisation of multiple substrate-specific (d)ITP/(d)XTPase and modelling of deaminated purine nucleotide metabolism. *BMB Rep.* 2012;45:259-64.
24. Decosterd LA, Cottin E, Chen X, Lejeune F, Mirimanoff RO, Biollaz J, et al. Simultaneous determination of deoxyribonucleoside in the presence of ribonucleoside triphosphates in human carcinoma cells by high-performance liquid chromatography. *Anal Biochem.* 1999;270:59-68.
25. Egan TJ. Recent advances in understanding the mechanism of hemozoin (malaria pigment) formation. *J Inorg Biochem.* 2008;102:1288-99.

26. Fariselli P, Riccobelli P, Casadio R. Role of evolutionary information in predicting the disulfide-bonding state of cysteine in proteins. *Proteins*. 1999;36:340-6.
27. Friedberg EC, McDaniel LD, Schultz RA. The role of endogenous and exogenous DNA damage and mutagenesis. *Curr Opin Genet Dev*. 2004;14:5-10.
28. Galperin MY, Moroz OV, Wilson KS, Murzin AG. House cleaning, a part of good housekeeping. *Mol Microbiol*. 2006;59:5-19.
29. Gardner MJ, Hall N, Fung E, White O, Berriman M, Hyman RW, et al. Genome sequence of the human malaria parasite *Plasmodium falciparum*. *Nature*. 2002;419:498-511.
30. Goyal M, Alam A, Iqbal MS, Dey S, Bindu S, Pal C, et al. Identification and molecular characterization of an Alba-family protein from human malaria parasite *Plasmodium falciparum*. *Nucleic Acids Res*. 2012;40:1174-90.
31. Greenberg GR, Somerville RL. Deoxyuridylate kinase activity and deoxyuridinetriphosphatase in *Escherichia coli*. *Proc Natl Acad Sci U S A*. 1962;48:247-57.
32. Gupta DK, Patra AT, Zhu L, Gupta AP, Bozdech Z. DNA damage regulation and its role in drug-related phenotypes in the malaria parasites. *Sci Rep*. 2016;6:23603.
33. Haldar K, Mohandas N. Malaria, erythrocytic infection, and anemia. *Hematology Am Soc Hematol Educ Program*. 2009:87-93.
34. Hamid S, Eckert KA. Effect of DNA polymerase beta loop variants on discrimination of O6-methyldeoxyguanosine modification present in the nucleotide versus template substrate. *Biochemistry*. 2005;44:10378-87.
35. Handley MT, Reddy K, Wills J, Rosser E, Kamath A, Halachev M, et al. ITPase deficiency causes a Martsolf-like syndrome with a lethal infantile dilated cardiomyopathy. *PLoS Genet*. 2019;15:e1007605.
36. He B, Qing H, Kow YW. Deoxyxanthosine in DNA is repaired by *Escherichia coli* endonuclease V. *Mutat Res*. 2000;459:109-14.
37. Hill-Perkins M, Jones MD, Karran P. Site-specific mutagenesis in vivo by single methylated or deaminated purine bases. *Mutat Res*. 1986;162:153-63.
38. Hizi A, Kamath-Loeb AS, Rose KD, Loeb LA. Mutagenesis by human immunodeficiency virus reverse transcriptase: incorporation of O6-methyldeoxyguanosine triphosphate. *Mutat Res*. 1997;374:41-50.
39. Hwang KY, Chung JH, Kim SH, Han YS, Cho Y. Structure-based identification of a novel NTPase from *Methanococcus jannaschii*. *Nat Struct Biol*. 1999;6:691-6.

40. Iqbal MS, Siddiqui AA, Alam A, Goyal M, Banerjee C, Sarkar S, et al. Expression, purification and characterization of Plasmodium falciparum vacuolar protein sorting 29. *Protein Expr Purif.* 2016;120:7-15.
41. Jensen JB, Trager W. Plasmodium falciparum in culture: use of outdated erythrocytes and description of the candle jar method. *J Parasitol.* 1977;63:883-6.
42. Ji D, Stepchenkova EI, Cui J, Menezes MR, Pavlov YI, Kool ET. Measuring deaminated nucleotide surveillance enzyme ITPA activity with an ATP-releasing nucleotide chimera. *Nucleic Acids Res.* 2017;45:11515-24.
43. Kamiya H. Mutagenic potentials of damaged nucleic acids produced by reactive oxygen/nitrogen species: approaches using synthetic oligonucleotides and nucleotides: survey and summary. *Nucleic Acids Res.* 2003;31:517-31.
44. Kevelam SH, Bierau J, Salvarinova R, Agrawal S, Honzik T, Visser D, et al. Recessive ITPA mutations cause an early infantile encephalopathy. *Ann Neurol.* 2015;78:649-58.
45. Kincaid K, Beckman J, Zivkovic A, Halcomb RL, Engels JW, Kuchta RD. Exploration of factors driving incorporation of unnatural dNTPS into DNA by Klenow fragment (DNA polymerase I) and DNA polymerase alpha. *Nucleic Acids Res.* 2005;33:2620-8.
46. Knuepfer E, Napiorkowska M, van Ooij C, Holder AA. Generating conditional gene knockouts in Plasmodium - a toolkit to produce stable DiCre recombinase-expressing parasite lines using CRISPR/Cas9. *Sci Rep.* 2017;7:3881.
47. Kumar H, Kehrer J, Singer M, Reinig M, Santos JM, Mair GR, et al. Functional genetic evaluation of DNA house-cleaning enzymes in the malaria parasite: dUTPase and Ap4AH are essential in Plasmodium berghei but ITPase and NDH are dispensable. *Expert Opin Ther Targets.* 2019;23:251-61.
48. Lane AN, Fan TW. Regulation of mammalian nucleotide metabolism and biosynthesis. *Nucleic Acids Res.* 2015;43:2466-85.
49. Lee AH, Symington LS, Fidock DA. DNA repair mechanisms and their biological roles in the malaria parasite Plasmodium falciparum. *Microbiol Mol Biol Rev.* 2014;78:469-86.
50. Lin S, McLennan AG, Ying K, Wang Z, Gu S, Jin H, et al. Cloning, expression, and characterization of a human inosine triphosphate pyrophosphatase encoded by the itpa gene. *J Biol Chem.* 2001;276:18695-701.
51. Liu J, Istvan ES, Gluzman IY, Gross J, Goldberg DE. Plasmodium falciparum ensures its amino acid supply with multiple acquisition pathways and

- redundant proteolytic enzyme systems. *Proc Natl Acad Sci U S A*. 2006;103:8840-5.
52. Lokanath NK, Pampa KJ, Takio K, Kunishima N. Structures of dimeric nonstandard nucleotide triphosphate pyrophosphatase from *Pyrococcus horikoshii* OT3: functional significance of interprotomer conformational changes. *J Mol Biol*. 2008;375:1013-25.
53. MacPherson CR, Scherf A. Flexible guide-RNA design for CRISPR applications using Protospacer Workbench. *Nat Biotechnol*. 2015;33:805-6.
54. Marsh S, King CR, Ahluwalia R, McLeod HL. Distribution of ITPA P32T alleles in multiple world populations. *J Hum Genet*. 2004;49:579-81.
55. Mathews CK. DNA precursor metabolism and genomic stability. *FASEB J*. 2006;20:1300-14.
56. Mbanzibwa DR, Tian Y, Mukasa SB, Valkonen JP. Cassava brown streak virus (Potyviridae) encodes a putative Maf/HAM1 pyrophosphatase implicated in reduction of mutations and a P1 proteinase that suppresses RNA silencing but contains no HC-Pro. *J Virol*. 2009;83:6934-40.
57. Menezes MR, Waisertreiger IS, Lopez-Bertoni H, Luo X, Pavlov YI. Pivotal role of inosine triphosphate pyrophosphatase in maintaining genome stability and the prevention of apoptosis in human cells. *PLoS One*. 2012;7:e32313.
58. Micsonai A, Wien F, Kernya L, Lee YH, Goto Y, Refregiers M, et al. Accurate secondary structure prediction and fold recognition for circular dichroism spectroscopy. *Proc Natl Acad Sci U S A*. 2015;112:E3095-103.
59. Moon RW, Hall J, Rangkuti F, Ho YS, Almond N, Mitchell GH, et al. Adaptation of the genetically tractable malaria pathogen *Plasmodium knowlesi* to continuous culture in human erythrocytes. *Proc Natl Acad Sci U S A*. 2013;110:531-6.
60. Moroz OV, Murzin AG, Makarova KS, Koonin EV, Wilson KS, Galperin MY. Dimeric dUTPases, HisE, and MazG belong to a new superfamily of all-alpha NTP pyrophosphohydrolases with potential "house-cleaning" functions. *J Mol Biol*. 2005;347:243-55.
61. Nagy GN, Leveles I, Vertessy BG. Preventive DNA repair by sanitizing the cellular (deoxy)nucleoside triphosphate pool. *FEBS J*. 2014;281:4207-23.
62. Nakauchi A, Wong JH, Mahasirimongkol S, Yanai H, Yuliwulandari R, Mabuchi A, et al. Identification of ITPA on chromosome 20 as a susceptibility gene for young-onset tuberculosis. *Hum Genome Var*. 2016;3:15067.

63. Noskov VN, Staak K, Shcherbakova PV, Kozmin SG, Negishi K, Ono BC, et al. HAM1, the gene controlling 6-N-hydroxylaminopurine sensitivity and mutagenesis in the yeast *Saccharomyces cerevisiae*. *Yeast*. 1996;12:17-29.
64. Otto TD, Wilinski D, Assefa S, Keane TM, Sarry LR, Bohme U, et al. New insights into the blood-stage transcriptome of *Plasmodium falciparum* using RNA-Seq. *Mol Microbiol*. 2010;76:12-24.
65. Pang B, McFaline JL, Burgis NE, Dong M, Taghizadeh K, Sullivan MR, et al. Defects in purine nucleotide metabolism lead to substantial incorporation of xanthine and hypoxanthine into DNA and RNA. *Proc Natl Acad Sci U S A*. 2012;109:2319-24.
66. Percie du Sert N, Ahluwalia A, Alam S, Avey MT, Baker M, Browne WJ, et al. Reporting animal research: Explanation and elaboration for the ARRIVE guidelines 2.0. *PLoS Biol*. 2020;18:e3000411.
67. Pineda-Tenor D, Garcia-Alvarez M, Jimenez-Sousa MA, Vazquez-Moron S, Resino S. Relationship between ITPA polymorphisms and hemolytic anemia in HCV-infected patients after ribavirin-based therapy: a meta-analysis. *J Transl Med*. 2015;13:320.
68. Porta J, Kolar C, Kozmin SG, Pavlov YI, Borgstahl GE. Structure of the orthorhombic form of human inosine triphosphate pyrophosphatase. *Acta Crystallogr Sect F Struct Biol Cryst Commun*. 2006;62:1076-81.
69. Rampazzo C, Miazzi C, Franzolin E, Pontarin G, Ferraro P, Frangini M, et al. Regulation by degradation, a cellular defense against deoxyribonucleotide pool imbalances. *Mutat Res*. 2010;703:2-10.
70. Rts SCTP, Agnandji ST, Lell B, Fernandes JF, Abossolo BP, Methogo BG, et al. A phase 3 trial of RTS,S/AS01 malaria vaccine in African infants. *N Engl J Med*. 2012;367:2284-95.
71. Rudd SG, Valerie NCK, Helleday T. Pathways controlling dNTP pools to maintain genome stability. *DNA Repair (Amst)*. 2016;44:193-204.
72. Sakumi K, Abolhassani N, Behmanesh M, Iyama T, Tsuchimoto D, Nakabeppu Y. ITPA protein, an enzyme that eliminates deaminated purine nucleoside triphosphates in cells. *Mutat Res*. 2010;703:43-50.
73. Savchenko A, Proudfoot M, Skarina T, Singer A, Litvinova O, Sanishvili R, et al. Molecular basis of the antimutagenic activity of the house-cleaning inosine triphosphate pyrophosphatase RdgB from *Escherichia coli*. *J Mol Biol*. 2007;374:1091-103.



74. Schroader JH, Jones LA, Meng R, Shorrock HK, Richardson JI, Shaughnessy SM, et al. Disease-associated inosine misincorporation into RNA hinders translation. *Nucleic Acids Res.* 2022;50:9306-18.
75. Shipkova M, Lorenz K, Oellerich M, Wieland E, von Ahsen N. Measurement of erythrocyte inosine triphosphate pyrophosphohydrolase (ITPA) activity by HPLC and correlation of ITPA genotype-phenotype in a Caucasian population. *Clin Chem.* 2006;52:240-7.
76. Siddiqui AA, Saha D, Iqbal MS, Saha SJ, Sarkar S, Banerjee C, et al. Rab7 of *Plasmodium falciparum* is involved in its retromer complex assembly near the digestive vacuole. *Biochim Biophys Acta Gen Subj.* 2020;1864:129656.
77. Simone PD, Struble LR, Kellezi A, Brown CA, Grabow CE, Khutsishvili I, et al. The human ITPA polymorphic variant P32T is destabilized by the unpacking of the hydrophobic core. *J Struct Biol.* 2013;182:197-208.
78. Some D, Amartely H, Tsadok A, Lebendiker M. Characterization of Proteins by Size-Exclusion Chromatography Coupled to Multi-Angle Light Scattering (SEC-MALS). *J Vis Exp.* 2019.
79. Srouji JR, Xu A, Park A, Kirsch JF, Brenner SE. The evolution of function within the Nudix homology clan. *Proteins.* 2017;85:775-811.
80. Stepchenkova EI, Tarakhovskaya ER, Spitler K, Frahm C, Menezes MR, Simone PD, et al. Functional study of the P32T ITPA variant associated with drug sensitivity in humans. *J Mol Biol.* 2009;392:602-13.
81. Stocco G, Cheok MH, Crews KR, Dervieux T, French D, Pei D, et al. Genetic polymorphism of inosine triphosphate pyrophosphatase is a determinant of mercaptopurine metabolism and toxicity during treatment for acute lymphoblastic leukemia. *Clin Pharmacol Ther.* 2009;85:164-72.
82. Straube H, Straube J, Rinne J, Fischer L, Niehaus M, Witte CP, et al. An inosine triphosphate pyrophosphatase safeguards plant nucleic acids from aberrant purine nucleotides. *New Phytol.* 2023;237:1759-75.
83. Takayama S, Fujii M, Kurosawa A, Adachi N, Ayusawa D. Overexpression of HAM1 gene detoxifies 5-bromodeoxyuridine in the yeast *Saccharomyces cerevisiae*. *Curr Genet.* 2007;52:203-11.
84. Thomas MJ, Platas AA, Hawley DK. Transcriptional fidelity and proofreading by RNA polymerase II. *Cell.* 1998;93:627-37.
85. Vasquez M, Zuniga M, Rodriguez A. Oxidative Stress and Pathogenesis in Malaria. *Front Cell Infect Microbiol.* 2021;11:768182.

86. Vidal AE, Yague-Capilla M, Martinez-Arribas B, Garcia-Caballero D, Ruiz-Perez LM, Gonzalez-Pacanowska D. Inosine triphosphate pyrophosphatase from *Trypanosoma brucei* cleanses cytosolic pools from deaminated nucleotides. *Sci Rep*. 2022;12:6408.
87. Waterhouse AM, Procter JB, Martin DM, Clamp M, Barton GJ. Jalview Version 2--a multiple sequence alignment editor and analysis workbench. *Bioinformatics*. 2009;25:1189-91.
88. Zhang M, Wang C, Otto TD, Oberstaller J, Liao X, Adapa SR, et al. Uncovering the essential genes of the human malaria parasite *Plasmodium falciparum* by saturation mutagenesis. *Science*. 2018;360.
89. Zheng J, Singh VK, Jia Z. Identification of an ITPase/XTPase in *Escherichia coli* by structural and biochemical analysis. *Structure*. 2005;13:1511-20.

---

## Experimental Insights | Chapter 2

---

### Structural Characterisation of *Pf*HAM1

## A. Introduction

In structural biology, "seeing is believing" is the guiding principle. For determining the three-dimensional (3D) structures of biological macromolecules, single-particle cryogenic electron microscopy (cryo-EM) and X-ray crystallography (XRC) have both become indispensable techniques. With almost 200,000 entries in the protein data bank (PDB), X-ray crystallography is the most established and fruitful area of structural biology. In this field, crystals of the target protein are exposed to X-ray photons. The crystal divides the X-ray beam into distinct diffraction spots, also known as reflections. The amplitudes are monitored during the experiment, and the missing phases are obtained using *ab initio* (Rodriguez et al. , 2009), multiple isomorphous replacement (MIR) (Ke, 1997), single- or multiple-wavelength anomalous dispersion (SAD or MAD) (Hendrickson and Ogata, 1997, Rose and Wang, 2016), or molecular replacement (MR) (McCoy, 2007, Read, 2001).

Due to the recent surge in drug-resistant malaria parasites, there is an urgent need to find new targets for creating antimalarial medications with novel mechanisms of action (Conrad and Rosenthal, 2019, Thu et al. , 2017, Uwimana et al. , 2020). The parasite disease known as malaria, which is spread by the *Anopheles* mosquito and causes acute, life-threatening illness, is dangerous to global health. In addition to the 125 million travellers and the two billion people who live in 90 countries where malaria is endemic, 1.5 to 2.7 million people die from malaria each year (Buck and Finnigan, 2023). Many of the molecular mechanisms underlying the biology and pathology of parasites are still unknown. Structure determination is crucial in addressing these unknowns because it frequently reveals previously unknown interactions and pathways, giving vital new information about possible therapeutic targets' roles and molecular mechanisms. Unfortunately, several obstacles to correctly folding and assembling malarial protein complexes in heterologous systems have prevented many critical *P. falciparum* protein complexes from being structurally and biochemically studied using standard methods. With an average AT content of 80.6% and a strongly skewed codon use bias, the *P. falciparum* genome is unusually AT-rich and challenging to clone into heterologous expression systems (Carlton et al. , 2008). A significant barrier to the heterologous expression of many *P. falciparum* proteins is the proteome's high propensity for aggregation, low complexity regions, and extensive charged-residue repeats, even though the use of codon optimisation algorithms has now solved this problem (Aravind et al. , 2003,

Burgess-Brown et al. , 2008). These barriers have prevented structural studies of the *P. falciparum* proteome using conventional techniques like X-ray crystallography (XRC) and nuclear magnetic resonance (NMR), which heavily rely on the production of large amounts of highly purified protein via recombinant over-expression (Derewenda, 2004). This is demonstrated by the severe lack of high-resolution *P. falciparum* structures in the Protein Data Bank (PDB) relative to other organisms. These issues have hampered the development of a deeper understanding of novel malaria parasite biology.

Intracellular nucleotide pools function as energy storage molecules, cofactors, and regulators in various metabolic and signal transduction pathways, in addition to being crucial components of DNA. Due to cellular redox processes, reactive oxygen species can oxidise the DNA precursor pool and create non-canonical deoxynucleoside triphosphates (dNTPs). Oxidative deamination of the nitrogenous base produces deoxyinosine triphosphate (dITP) from deoxyadenosine triphosphate (dATP), deoxyuridine triphosphate (dUTP) from deoxycytosine triphosphate (dCTP) and deoxyxanthosine triphosphate (dXTP) from deoxyguanosine triphosphate (dGTP). Thymine is not oxidatively deaminated because it lacks a free amino group (Kamiya, 2003). During DNA replication, these altered nucleotide analogues can be integrated. Single-strand breaks are introduced and must be repaired when the DNA repair system detects them. As a result of the buildup of harmful mutations and double-strand breaks, cell growth may slow down or even stop altogether (Rai, 2010). Cells have developed "house-cleaning" or "DNA sanitation" enzymes to hydrolyse harmful nucleotides into their non-toxic monophosphate forms, which are poor substrates for their respective nucleoside kinases and are not phosphorylated to their toxic nucleotide forms. This prevents DNA damage.

Sanitation enzymes can be divided into four superfamilies based on structural characteristics:

**Ham1** (6-n-HydroxylAMinopurine sensitive) domain, which consists of a long central beta-sheet creating the active site's floor, defines ITPases (Porta et al. , 2006); NuDiX box domain G-x(5)-E-x(5)-[UA]-x-R-E-x(2)-E-E-x-G-U, where 'x' is any residue and 'U' is a hydrophobic residue, defines the **NuDiX** superfamily (McLennan, 2006); **dUTPases**, which have an eight-stranded jelly-roll beta-barrel and a trimeric fold (Greenberg and Somerville, 1962); **all-helical NTPases** that are

active against both dNTPs and dNDPs, resulting in the formation of dNMPs as a byproduct (Moroz et al. , 2005).

Here, in this extensive study of the human malignant malaria parasite protein, *PfHAM1*, after biochemically, biophysically and genetically characterising the protein, crystallising the protein using X-ray crystallographic methods, both in its apoenzyme form and ligand-bound (dITP) form, was performed. Still, success was achieved only in the former. A detailed description of the findings is presented below.



## B. Experimental procedures

### 1. Protein purification

The pET28a-PfHAM1 vector was transformed into the *Escherichia coli* Rosetta™ strain (Novagen) to obtain the desired PfHAM1 protein in bulk. Briefly, after a primary seed culture, the secondary culture's OD<sub>600</sub> was monitored to 0.5 at 37°C when protein synthesis was stimulated with 0.5 mM IPTG (Thermo Scientific) after cooling the culture's temperature. The culture was kept at 25°C at 200 rpm overnight. Bacterial cells were harvested at 6000 rpm for 10 minutes at 4°C and dissolved in cold membrane-filtered re-suspension buffer (25 mM Tris (Sigma), 150 mM NaCl (Sigma), 5 mM imidazole (SRL), and pH 8.0) with 1 mM PMSF (Calbiochem) before sonication. The lysed cells were ultra-centrifuged at 45,000 rpm for an hour at 4°C to obtain a clear supernatant, which was then loaded onto a pre-equilibrated Ni<sup>++</sup>-NTA agarose column (Qiagen) and kept for some time under slow stirring at 4°C. One column volume of cold membrane-filtered wash buffer 1 (25 mM Tris, 150 mM NaCl, 35 mM imidazole, and pH 8.0) followed by three column volumes of wash buffer 2 (25 mM Tris, 150 mM NaCl, 50 mM imidazole, and pH 8.0) were added to get rid of the impurities. The protein was eluted with the cold membrane-filtered elution buffer (25 mM Tris, 150 mM NaCl, 250 mM imidazole, and pH 8.0). The collected fractions were concentrated and loaded onto the Cytiva HiLoad 16/600 Superdex 75 pg prep grade column, pre-equilibrated with gel filtration buffer (25 mM Tris, 150 mM NaCl, and pH 8.0). The eluted pure protein fractions were concentrated to ~10 mg/ml. The purity of the protein was checked by SDS-PAGE analysis.

### 2. Protein crystallisation, data collection and refinement

The sitting drop vapour diffusion technique crystallised purified PfHAM1 at a final concentration of 10 mg/ml. Initial crystal hits were discovered in the JBS Basic screen using 20% (w/v) PEG 4000, 20% (v/v) 2-propanol, and 100 mM Tris-sodium citrate buffer (pH 5.6). These crystals displayed a thin, plate-like shape and were stacked. At 20°C, the entire setup was incubated. In 16% (w/v) PEG 4000, 20% (v/v) 2-propanol, and 100 mM Tris-sodium citrate buffer (pH 5.5), single and big crystals were produced in a week. The Cu K<sub>α</sub> source ( $\lambda = 1.54 \text{ \AA}$ ) and Photon III CCD

detector were utilised in the in-house Bruker D8 Venture XRD diffractometer to capture the data, which was then used to collect the frames. The data was collected at a temperature of 100 Kelvin, with 15% glycerol used as a cryoprotectant. With unit cell characteristics of  $a = 63.313 \text{ \AA}$ ,  $b = 73.685 \text{ \AA}$ ,  $c = 112.029 \text{ \AA}$ , and  $\alpha=\beta=\gamma=90^\circ$ , it was determined that the data belonged to space group  $P2_12_12_1$ , as scaled from the PROTEUM 3 software. Human inosine triphosphatase (PDB ID: 2CAR) was used as a model (Liebschner et al. , 2019) in PHENIX's molecular replacement approach to create the original structure. To obtain the final structure, Coot and PHENIX (v1.14-3260) underwent manual rebuilding and several cycles of refining, respectively (Emsley and Cowtan, 2004). PYMOL (v2.5.4) was used to create all structural representations. The interface area was calculated using the PISA server (Krissinel and Henrick, 2007). The secondary structure topology was represented using the online tool PDBsum. In the Protein Data Bank, under the **PDB ID: 8JI1**, are the atomic coordinates for HAM1 from *Plasmodium falciparum*.

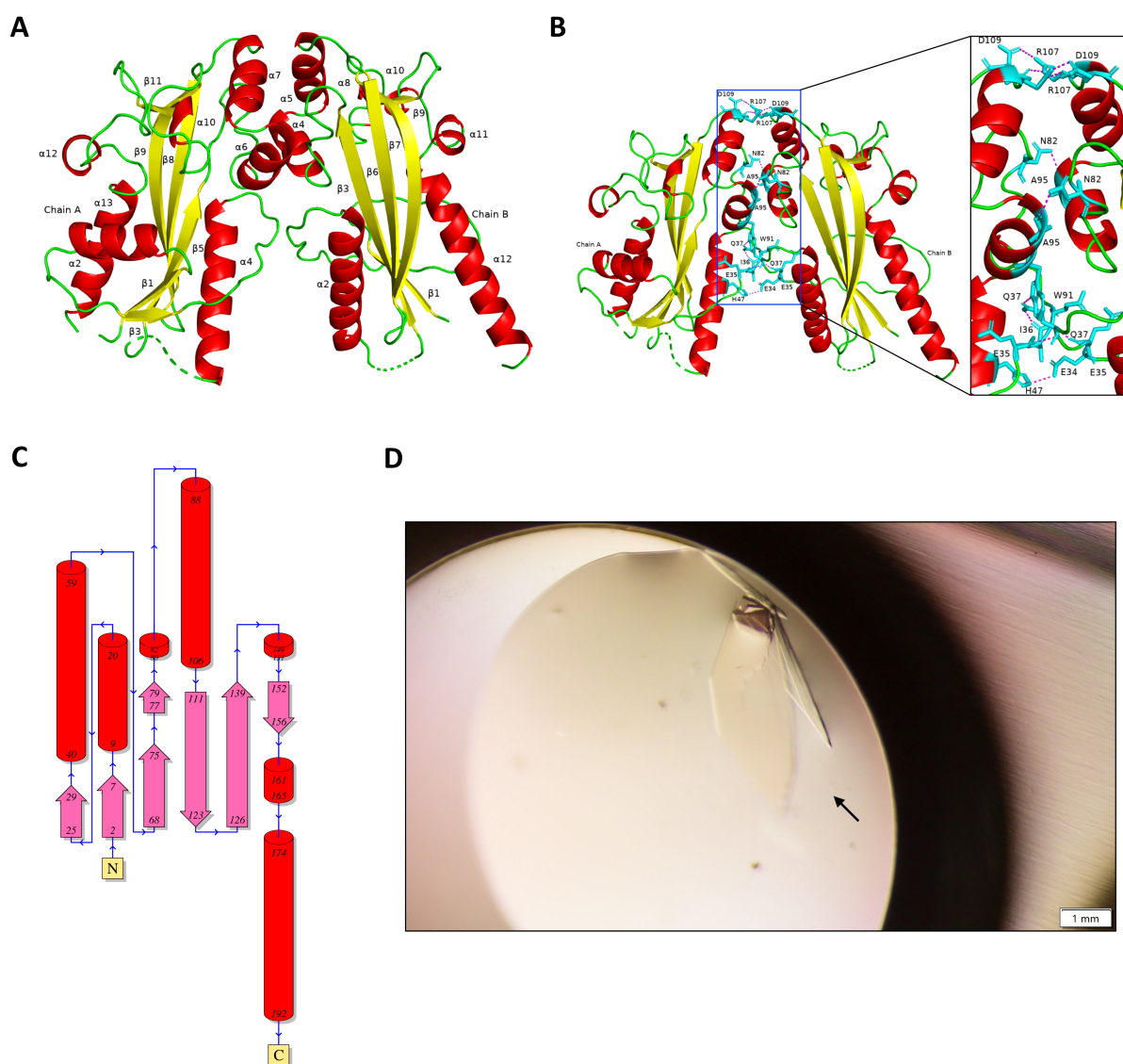
### 3. Molecular docking and dynamic simulations

The chemical structures of three substrates, dITP (ChemSpider ID: 129052), ITP (ChemSpider ID: 8265), and XTP (ChemSpider ID: 388429), were obtained from the Royal Society of Chemistry's ChemSpider database. The crystal structure of *Pf*HAM1 was retrieved from the PDB ID: 8JI1. To perform molecular docking simulations, the protein crystal structures were first preprocessed: any bound crystallographic water molecules were removed, missing side chains were filled using PDB\_Hydro (Azuara et al. , 2006), alternate atom positions were removed, and polar hydrogen atoms were added using AutoDockTools (Morris et al. , 2009). AutoDock4 atom types were assigned, and all the rotatable bonds in the ligands were set free. The ligand structures were similarly prepared. The molecular docking simulation was done using AutoDock Vina (v1.2.3) following a standard protocol (Trott and Olson, 2010). Molecular dynamics (MD) simulations were conducted on free and ligand-bound *Pf*HAM1. The MD simulation selected the lowest energy conformations. The simulation was performed under an OPLS (optimised potentials for liquid simulations) force field in a SPC (simple point-charge) water environment, following a previous protocol (Pal et al. , 2016). To mimic the experimental conditions, 10 mM  $\text{MgCl}_2$  and neutralised counter ions were added to the system. Schrodinger Maestro (Academic Release 2020-4) was used to obtain structural changes in terms of root mean square deviations (RMSD), residue-wise fluctuations in terms of root mean

square fluctuations (RMSF), secondary structural properties, time-correlated interactions, and interaction energies from the simulation trajectories. This information has been provided in Figures 3-6.

## C. Results

### 1. PfHAM1 is a homodimer with monomers arrayed in a parallel pattern



**Figure 1:** Crystal structure of *Plasmodium falciparum* HAM1. (A) Dimeric unit of PfHAM1, where  $\alpha$ -helices and  $\beta$ -sheets are labelled sequentially.  $\alpha$ -helices are in red, and  $\beta$ -sheets are in yellow. (B) Interacting residues involved at the dimeric interfaces of PfHAM1. Only polar residues are labelled here. Inset: Polar contacts are shown in magenta and sticks are represented in cyan. (C) Secondary structure representation of PfHAM1 as obtained by PDBsum. (D) Plate-shaped crystals (arrow-marked) of PfHAM1 as observed under a Nikon stereo microscope.

Parameters	Dataset
<b>Data Statistics</b>	
Wavelength (Å)	1.54
Space group	$P2_12_12_1$
Unit cell dimensions	a = 63.313, b = 73.685 and c = 112.029
Total reflections <sup>a</sup>	197333 (12424)
Unique reflections <sup>a</sup>	12064 (1151)
Redundancy	16.4
Completeness (%) <sup>a</sup>	99.7 (97.4)
Overall I/ $\sigma$ <sup>a</sup>	35 (8.2)
R <sub>merge</sub> (%) <sup>a</sup>	0.076 (0.276)
CC <sup>1/2</sup> <sup>a</sup>	0.999 (0.977)
<b>Refinement statistics</b>	
Resolution range (Å)	28 - 2.9
Number of used reflections	11911
R <sub>work</sub> (%)	19.94 (25.21)
R <sub>free</sub> (%)	25.79 (33.14)
Total number of atoms	3108
Number of water molecules	24
Average B-factors (Å <sup>2</sup> )	34
Average B-factors (Å <sup>2</sup> ) of water molecules	19.87
<b>Root mean square deviations</b>	
Bonds (Å)	0.009
Angles (°)	1.056
<b>Ramachandran plot</b>	
Most favoured region (%)	94.84
Ramachandran outliers (%)	0.54

<sup>a</sup> Values in parentheses refer to the highest-resolution shell.

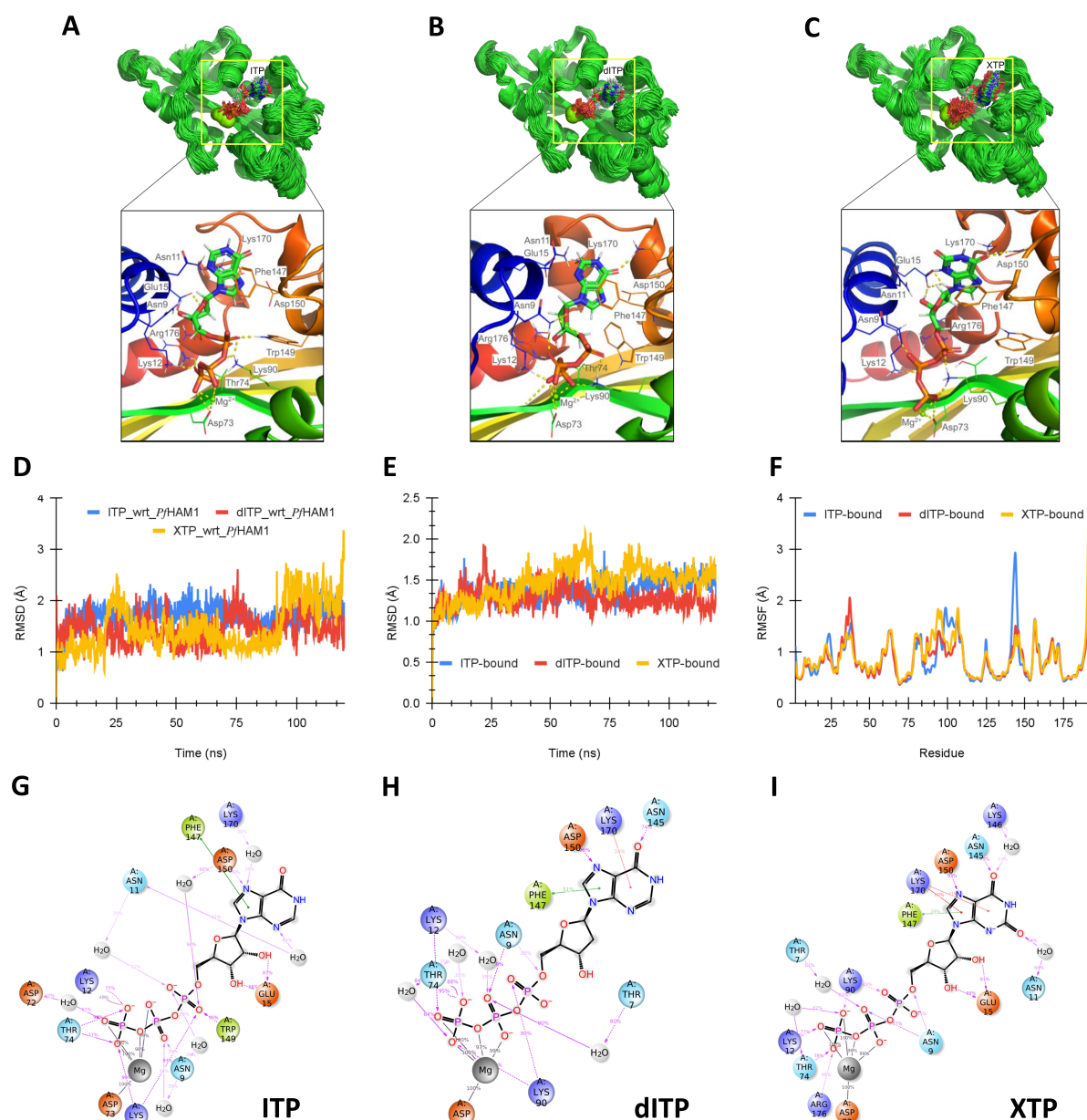
**Table 1:** Data collection and refinement statistics.

This experimental chapter describes the crystal structure of HAM1, a (d)ITP/XTP pyrophosphatase from *Plasmodium falciparum*. The molecular replacement approach was used to solve the structure at 2.9 Å, confirming the presence of two molecules in the crystallographic asymmetric unit. Therefore, as shown by numerous other biophysical investigations in the previous experimental chapter, the overall structure comprises two monomers that combine to create a dimer that acts as a stable unit, as observed post-symmetry mates generation and PISA analysis (Figure 1A). Table 1 contains statistics on structural refinements. The overall PfHAM1's structure shares multiple similarities to the non-canonical NTPases (PDB ID: 1B78, 1V7R, 3TQU) and human ITPase (PDB ID: 2CAR) (Hwang et al. , 1999, Lokanath et al. , 2008, Stenmark et al. , 2007). Each monomer has a core  $\beta$ -sheet surrounded by two lobes with an  $\alpha/\beta$  mixed fold. In a dimeric unit of dimension 75.7 × 54.8 × 36.1 Å, each monomer is connected to the other by a two-fold axis. Each monomer has a comparable overall shape, but their arrangements of the  $\alpha/\beta$  mix differ noticeably (the R.M.S.D. between chains A and B over  $C_\alpha$  atoms is ~0.457). The core region comprises three central strands, each between 7 and 12 residues long, with the half being connected by two lengthy  $\alpha$ -helices. In contrast to chain B, which lacks  $\alpha 2$ - $\beta 3$ , chain A's N-terminus end begins with a  $\beta 1$  strand, followed by  $\alpha 2$ - $\beta 3$  and a lengthy  $\alpha 4$  helix (Ile41 - Lys58). The C-terminus of chain A was made up of a short  $\alpha 12$  helix (Phe167 - Lys170), followed by a long  $\alpha 13$  helix (Lys178 - His191), while the C-terminus of chain B was made up of a long  $\alpha$ -helical area (Glu169 - Asn196). The electron density was absent from Asp60 - Asn64 in chain A and Asn62 - Asn64 in chain B. This lengthy  $\alpha$ -helical region was bent by Ser174 to create two  $\alpha 11$  (Glu169 - Leu173) and  $\alpha 12$  (Pro175 - Asn196) helices. Pro175 - Phe180 of  $\alpha 12$  has a small inclination in the direction of the kink. The total surface area buried in the dimeric interface is ~1137 Å<sup>2</sup>, and each monomer contributes a portion. The carbonyl oxygen of Glu35 in chain A formed a hydrogen bond with Gln37 in chain B. Conversely, the side chain carbonyl oxygen and amide nitrogen of Gln37 in chain B formed two hydrogen bonds with the -NH group of Trp91 and the peptide oxygen of Ile36 in chain A. The peptide nitrogen of Gln37 in chain A made a polar contact with the peptide oxygen of Glu35 in the opposite chain B. The peptide oxygen of Ala95 in chain A was involved in a hydrogen bond interaction with the side chain carbonyl amide of Asn82 in chain B, and vice versa. In contrast, Arg107 of chain A established two hydrogen bonds with Arg107 of chain B. Additionally, the carbonyl oxygen of the side chain of Asp109 in chain A had a polar interaction with the -NH<sub>2</sub> group of Arg107 in chain B and vice versa (Figure 1B). The crystal structure of PfHAM1 was



represented as a secondary structure using the PDBsum tool, as shown in Figure 1C. The pocket of the (d)NTP binding site is comparable to that of other non-canonical NTPases. This *PfHAM1* dimeric assembly has both monomers arrayed in a parallel pattern. In summary, the XRC structure, as obtained from processing the plate-shaped crystals of *PfHAM1* (Figure 1D), provides valuable insights into its mechanism of action. Although several attempts were made to crystallise the protein with its substrates, they were unsuccessful.

## 2. Molecular dynamics identified critical residues involved in substrate binding

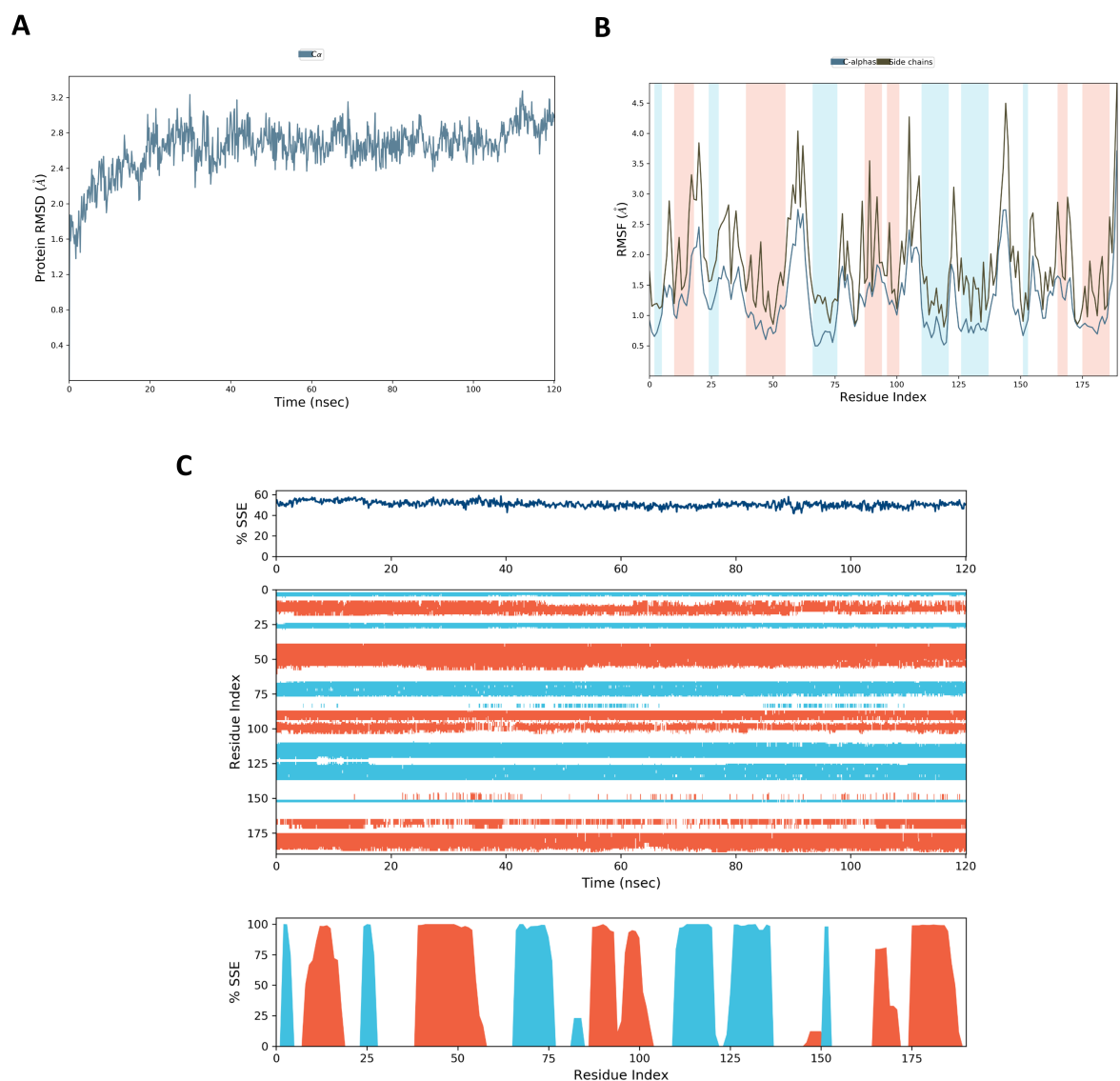


**Figure 2:** Ensembles of substrate-bound PfHAM1 complexes obtained from 120 ns molecular dynamics simulation. (A) PfHAM1-ITP complex in SPC water under OPLS-AA force field for 120 ns. 10 snapshots at 12 ns intervals are superimposed. Protein is shown in cartoon representation, and the ITP binding region is outlined. Detailed interactions, as shown in the last frame of the MD simulation, are shown in the zoomed-in section, and interacting residues are labelled. (B) dITP bound

states of PfHAM1. Detailed interactions are shown in the zoomed-in section. (C) PfHAM1-XTP complex. Detailed interactions are shown in the zoomed-in section. (D) Protein backbone C $\alpha$  RMSD for apoenzyme and all the substrate-bound complexes of apoenzyme with respect to the initial conformations. (E) RMSD of the substrates in all the three bound complexes with respect to the initial conformation of the complexes. (F) Residue-wise fluctuations (RMSF) in protein backbone under substrate-bound conditions. (G-I) Time average interaction of ITP (G), dITP (H), and XTP (I) with PfHAM1 as obtained from molecular dynamics simulations, respectively. Polar, positively charged, negatively charged and hydrophobic residues are shown in cyan, blue, red and green, respectively. Phe147 forms a pi-stacking (green line) interaction with inosine, whereas Lys170 forms a pi-cation (red line) interaction; Asn145 and Asp150 form two hydrogen bonds (pink arrows) with the inosine moiety. Glu15 forms hydrogen bonds with the ribose sugar; the terminal phosphate group interacts with the Asp73 through the metal cofactor Mg<sup>++</sup>; Lys12, Lys90, Asn9, Asn11, Thr74, Trp149, Arg176 forms hydrogen bonds/water bridges (pink dashed arrows) with the phosphate groups.

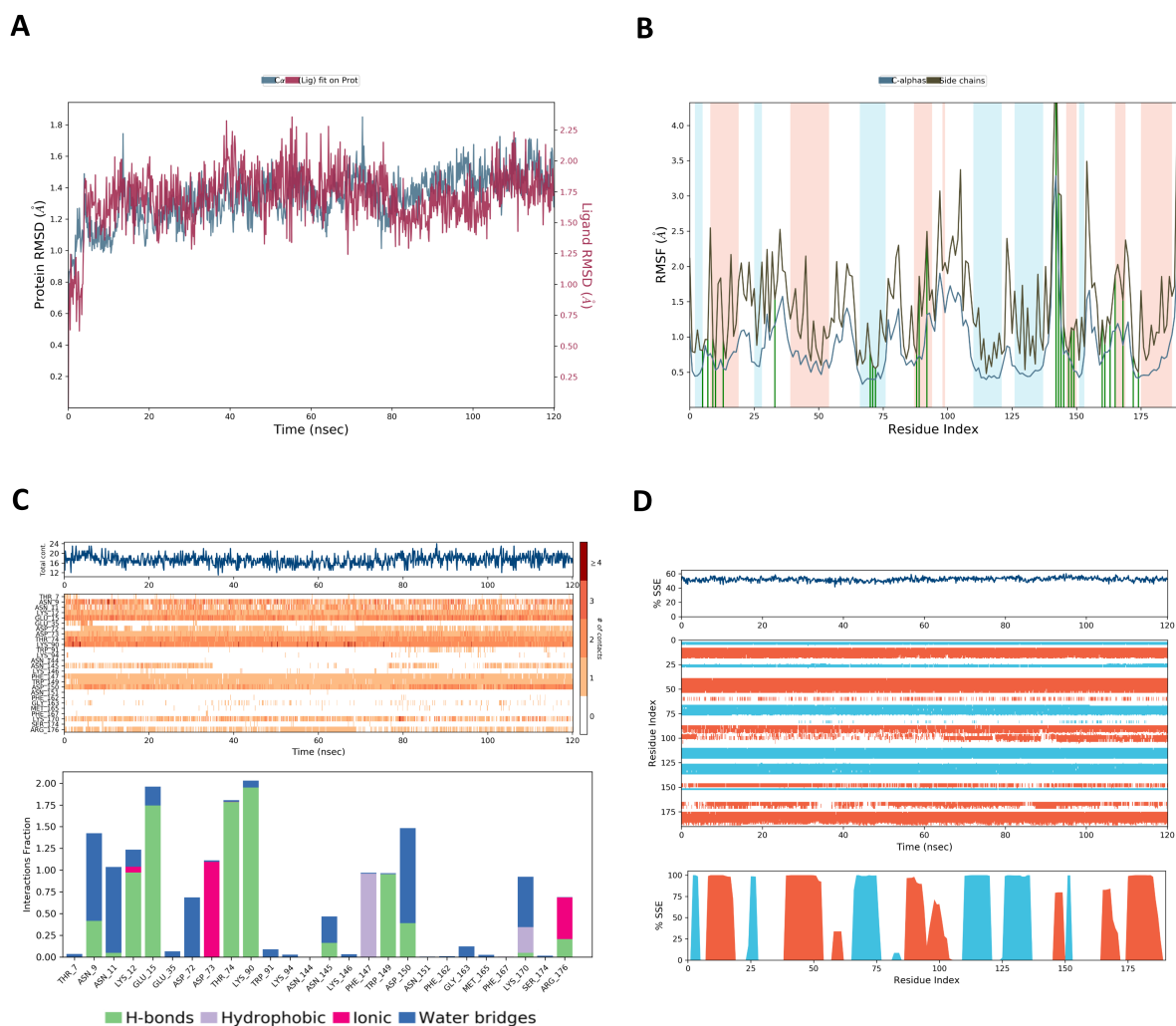
During the simulation, the substrate-bound complexes and the free PfHAM1 enzyme maintained a stable substrate-bound conformation and reached equilibrium. The binding free energies calculated for ITP, dITP and XTP were  $-275.03 \pm 80.44$ ,  $-232.85 \pm 86.12$  and  $-299.17 \pm 168.94$  kcal/mol, respectively, implying a thermodynamically stable interaction. The interaction between the negatively charged phosphate groups and the positively charged amino acid residues in the binding site contributed significantly to the binding energies. Water bridges and metal coordination also played a crucial role in the interaction, as indicated in Table 2. The stability of the interaction within the active site of PfHAM1 was qualitatively assessed using ensemble snapshots taken at specific intervals during the simulation, as shown in Figures 2A-C. Figures 2D-E show the time-correlated standard deviations (RMSD) of proteins and the substrates. The fluctuations of the apo and substrate-bound enzymes on a residue-wise level are shown in Figure 2F and Figures (3-6)B. The amino acid residues in PfHAM1 involved in substrate recognition are depicted in Figures 2G-I. Several positively charged (Lys12, Lys90, Lys170 and Lys176) and negatively charged (Glu15, Glu35, Glu72, Glu73, Asp150) residues form hydrogen bonding interactions and water bridges with the substrates

in the substrate binding site. Furthermore, some polar residues, such as Thr7, Asn9, Asn11, Thr74, and Asn145, also form hydrogen bonds with the substrates. Hydrophobic residues such as Phe147, Trp149, Phe167 and Met10 also participate in the interactions. Kindly refer to Figures (3-6)C for a better understanding of the interactions.

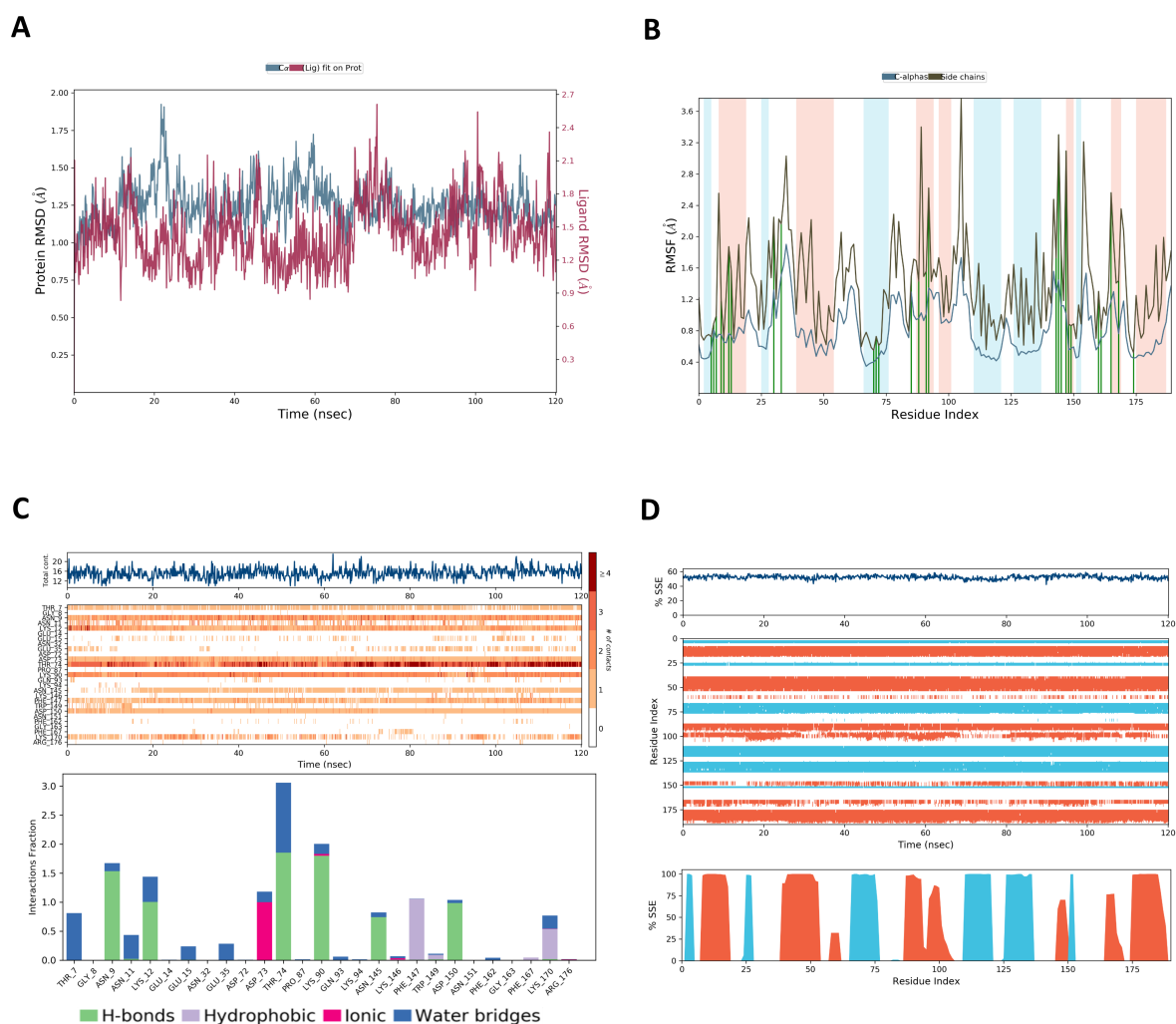


**Figure 3:** (A) RMSD of *PfHAM1*. The protein reaches an equilibrium state within 20 ns of simulation. (B) RMSF of *PfHAM1*. The blue line indicates the backbone fluctuations, whereas the brown line shows side-chain fluctuations. Alpha helical and beta-sheet regions are shown with background shades of red and blue, respectively. White regions indicate the more fluctuating random coil regions. (C) Secondary structural element (SSE) of *PfHAM1* over time (top); residue-wise SSE

over time (middle); average residue-wise SSE (below). Colour key: **red**, alpha-helix; **cyan**, beta-sheet.

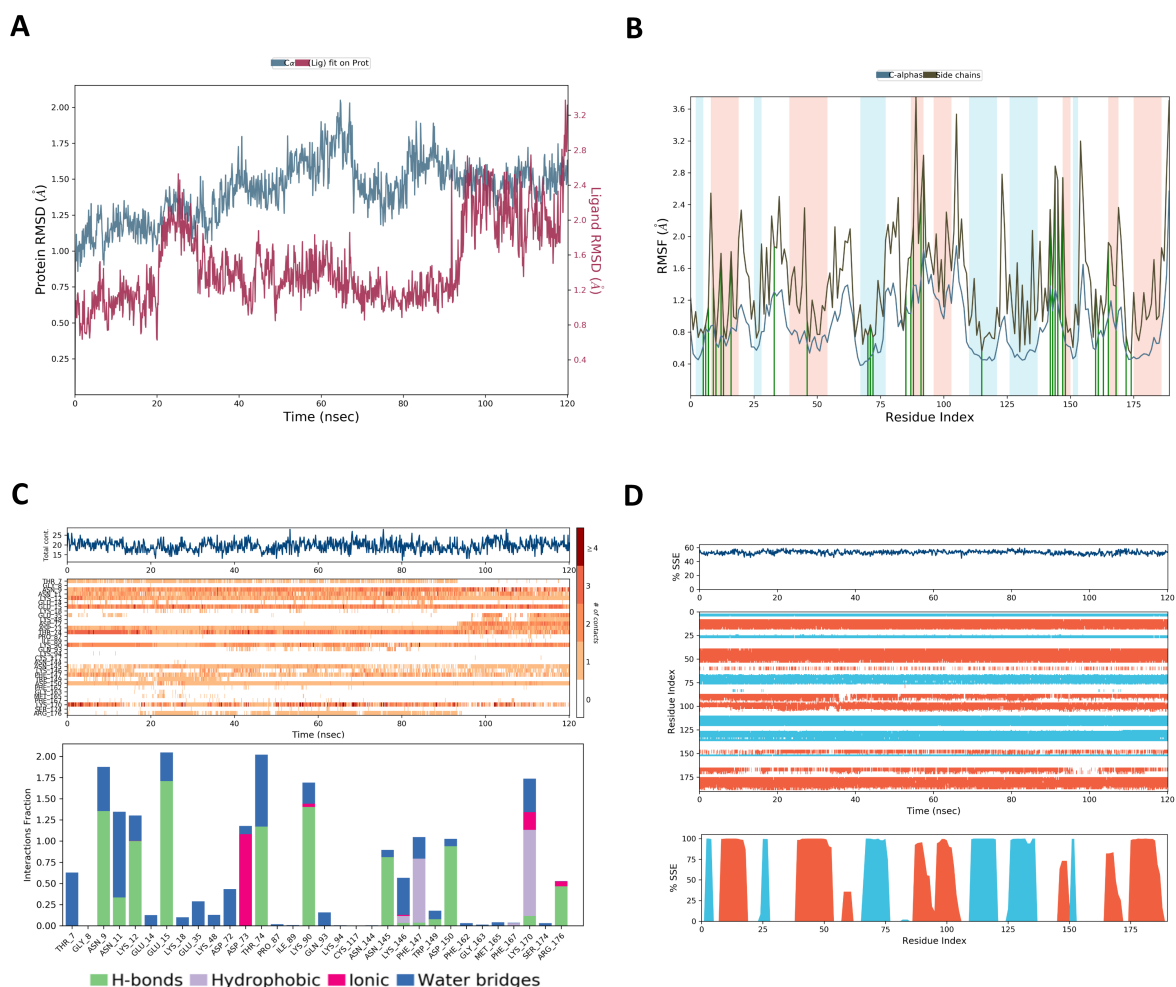


**Figure 4:** (A) RMSD profile of PfHAM1-ITP complex. **Blue**, RMSD of protein backbone; **red**, ligand RMSD with respect to protein. (B) RMSF profile of PfHAM1 in PfHAM1-ITP complex. **Blue** line, backbone; black line, side chain. **Green** lines show ligand contacts. Shaded regions indicate alpha-helical (**red**), beta-sheet (**blue**) or random (white) structure. (C) Ligand contacts with PfHAM1 in PfHAM1-ITP complex over time (top) and residue-wise interaction statistics (bottom). (D) Secondary structural element (SSE) of PfHAM1 in PfHAM1-ITP complex over time (top); residue-wise SSE over time (middle); average residue-wise SSE (below). Colour key: **red**, alpha-helix; **cyan**, beta-sheet.



**Figure 5:** (A) RMSD profile of *Pf*HAM1-dITP complex. Blue, RMSD of protein backbone; red, ligand RMSD with respect to protein. (B) RMSF profile of *Pf*HAM1 in *Pf*HAM1-dITP complex. Blue line, backbone; black line, side chain. Green lines show ligand contacts. Shaded regions indicate alpha-helical (red), beta-sheet (blue) or random (white) structure. (C) Ligand contacts with *Pf*HAM1 in *Pf*HAM1-dITP complex over time (top) and residue-wise interaction statistics (bottom). (D) Secondary structural element (SSE) of *Pf*HAM1 in *Pf*HAM1-dITP complex over time (top); residue-wise SSE over time (middle); average residue-wise SSE (below). Colour key: red, alpha-helix; cyan, beta-sheet.





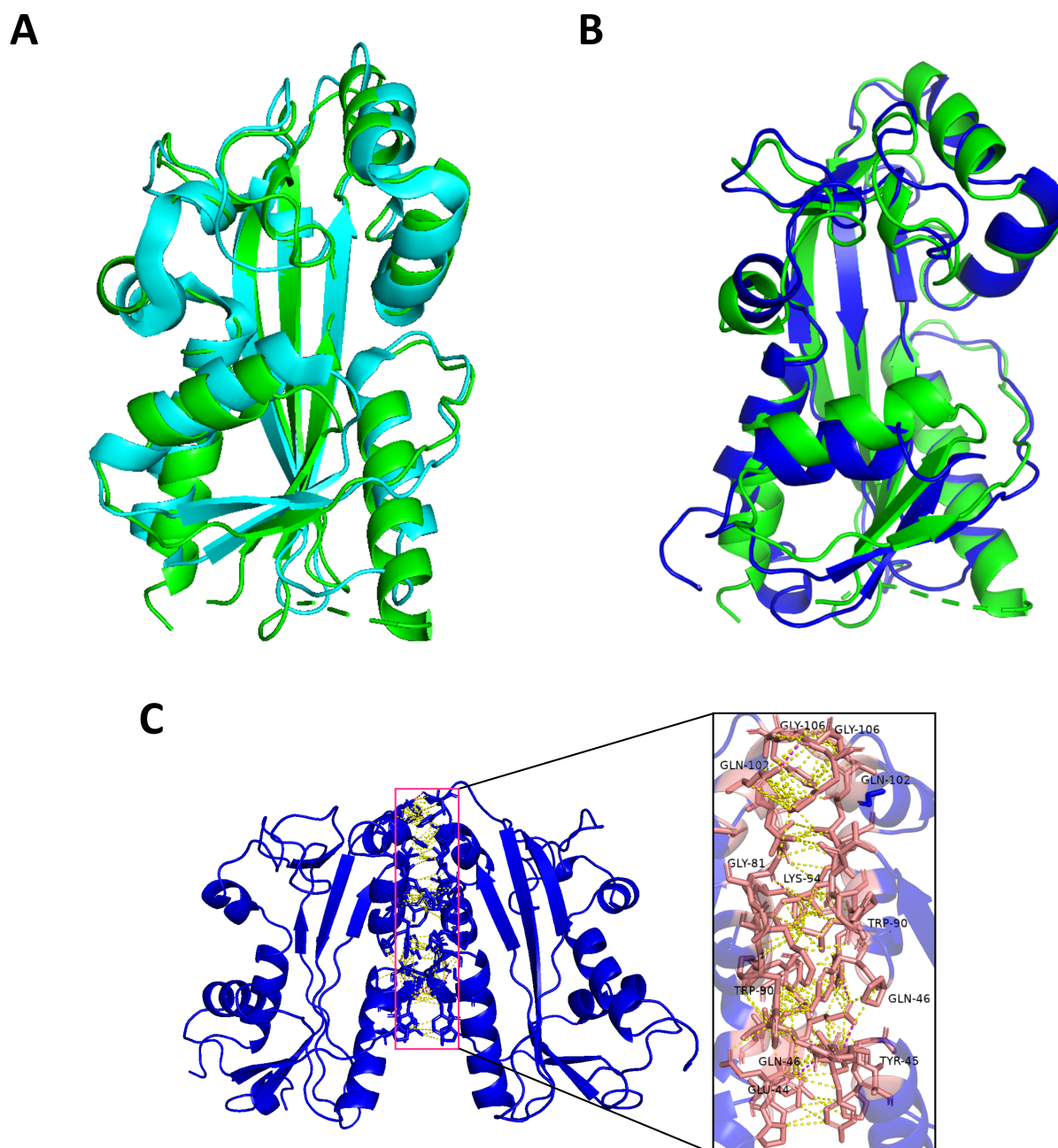
**Figure 6:** (A) RMSD profile of *PfHAM1*-XTP complex. Blue, RMSD of protein backbone; red, ligand RMSD with respect to protein. (B) RMSF profile of *PfHAM1* in *PfHAM1*-XTP complex. Blue line, backbone; black line, side chain. Green lines show ligand contacts. Shaded regions indicate alpha-helical (red), beta-sheet (blue) or random (white) structure. (C) Ligand contacts with *PfHAM1* in *PfHAM1*-XTP complex over time (top) and residue-wise interaction statistics (bottom). (D) Secondary structural element (SSE) of *PfHAM1* in *PfHAM1*-XTP complex over time (top); residue-wise SSE over time (middle); average residue-wise SSE (below). Colour key: red, alpha-helix; cyan, beta-sheet.

With (Type)	ITP	dITP	XTP
Protein (Coulomb)	-1426.08 ± 48.64	-1410.18 ± 51.08	-1519.93 ± 103.24
Protein (vdW)	-4.69 ± 6.31	-8.71 ± 6.27	-0.24 ± 7.2
<b>Protein (Total) [1]</b>	<b>-1430.76 ± 49.05</b>	<b>-1418.88 ± 51.46</b>	<b>-1520.16 ± 103.49</b>
Water (Coulomb)	-197.05 ± 62.4	-175.93 ± 66.21	-331.3 ± 123.29
Water (vdW)	9.74 ± 5.99	8.8 ± 5.55	13.22 ± 6.41
<b>Water (Total) [2]</b>	<b>-187.31 ± 62.69</b>	<b>-167.13 ± 66.44</b>	<b>-318.09 ± 123.45</b>
Ions (Coulomb)	-20.82 ± 35.74	-19.5 ± 39.5	-44.68 ± 62.03
Ions (vdW)	-0.05 ± 0.16	-0.06 ± 0.3	-0.03 ± 0.15
<b>Ions (Total) [3]</b>	<b>-20.87 ± 35.74</b>	<b>-19.56 ± 39.5</b>	<b>-44.71 ± 62.03</b>
Self (Coulomb)	-367.93 ± 6.29	-440.07 ± 7.93	-460.02 ± 9.05
Self (vdW)	18.43 ± 2.94	18.31 ± 3.32	20.33 ± 3.08
Self (Bond)	22.04 ± 4.57	21.35 ± 4.26	21.16 ± 4.28
Self (Angle)	50.16 ± 5.36	49.06 ± 5.25	52.8 ± 5.31
Self (Torsion)	3.07 ± 2.12	6.69 ± 2.32	-1.78 ± 2.98
<b>Self (Total) [4]</b>	<b>-274.24 ± 10.11</b>	<b>-344.69 ± 11.17</b>	<b>-367.54 ± 12.11</b>
<b>Solvation [5]</b>	<b>-1638.14 ± 35.26</b>	<b>-1717.4 ± 36.48</b>	<b>-1951.32 ± 37.45</b>
<b>Free energy [1+2+3+4-5]</b>	<b>-275.03 ± 80.44</b>	<b>-232.85 ± 86.12</b>	<b>-299.17 ± 168.94</b>

**Table 2:** Energetics of the substrate interactions with PfHAM1 obtained from MD simulation. Contributions from different components to the free energy are shown. Values are in kcal/mol.

## D. Discussion

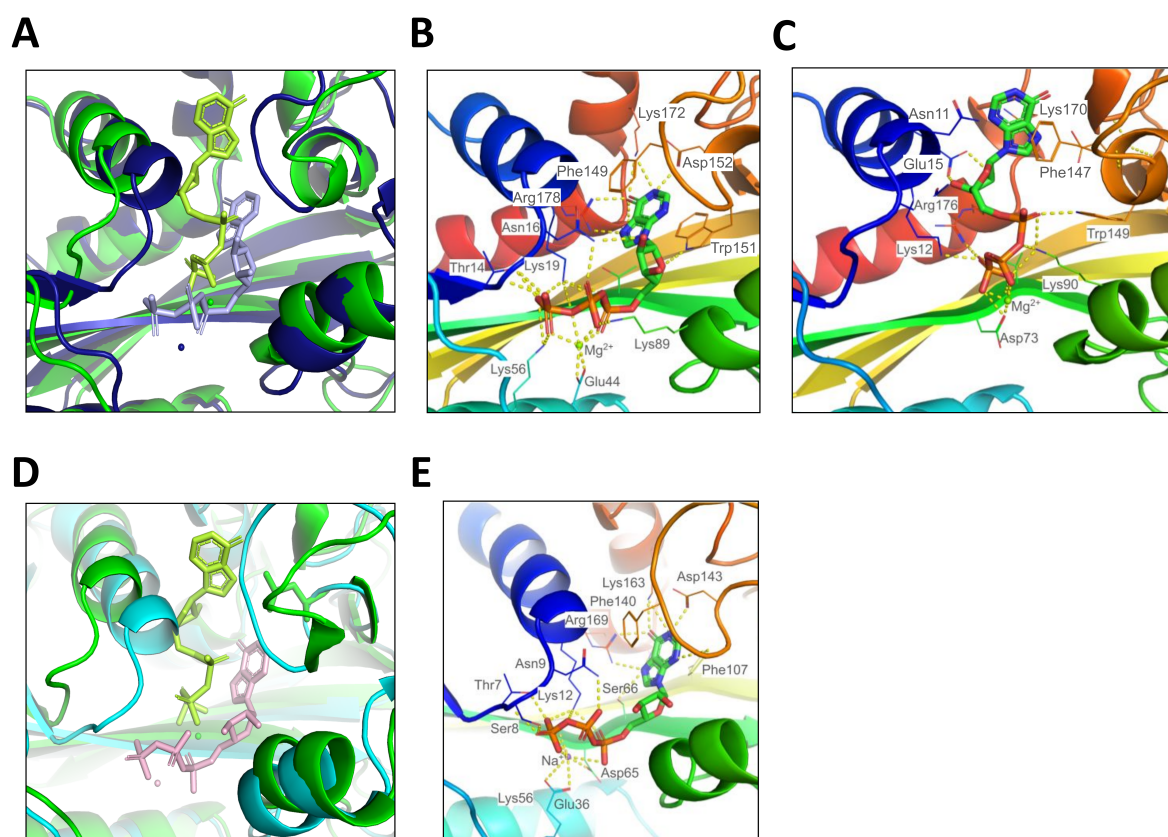
The oligomeric status of PfHAM1, a protein involved in the metabolism of purine nucleotides, was determined to be homodimeric, meaning it is composed of two identical subunits. This characteristic is shared by other similar proteins such as HsITPA (Simone et al. , 2013), *E. coli*, *P. horikoshii* OT3, and *T. maritima* (PDB ID: 1VP2) (Lokanath et al., 2008, Savchenko et al. , 2007). The X-ray crystallography of PfHAM1's monomeric unit, which is the basic building block of the homodimer, revealed that it shares multiple structural similarities with other non-canonical NTPases (the R.M.S.D. value over C $_{\alpha}$  atoms between monomeric PfHAM1 and non-canonical NTPases ranging from bacteria to humans is between 1.5 - 5.0 Å). To better understand PfHAM1's structure, it was compared to the non-standard NTPase from *P. horikoshii*, PhNTPase (PDB ID: 2DVP). It was discovered that both structures have a long centrally located  $\beta$ -strand. However, the  $\alpha 6$ - $\alpha 7$  helix in PfHAM1 is replaced by an elongated stretch of the  $\alpha 7$  helix in PhNTPase, the non-standard NTPase found in *P. horikoshii* (see Figure 7A for a visual comparison). In contrast, PfHAM1 and HsITPA differ significantly in their  $\beta$ -sheet main frame., and the R.M.S.D. value over C $_{\alpha}$  was found to be ~1.57 Å. The core region of PfHAM1 consists of three stranded parallel  $\beta$ -sheets ranging from seven to twelve residues, while the central region of chain A in HsITPA consists of three short parallel  $\beta$ -strands ranging from three to six residues (Stenmark et al. , 2007). Chain B's central region in HsITPA is similar to PfHAM1. The interface area of HsITPA is also approximately 1100 Å<sup>2</sup>, similar to PfHAM1. In the HsITPA protein, there were H-bonding interactions between the side chain of Gln46 of chain A and Tyr45 and Trp90 of its counter chain B. Similarly, the peptide oxygen of Glu44 of chain A made an H-bond with the peptide nitrogen of Gln46 of chain B and vice versa. Additionally, chain A's Gly81, Gln102, and Gly106 made H-bonding interactions with chain B's Lys94, Gly106, and Gln102, correspondingly (Figures 7B-C). We have also shown the polar residues involved in overall dimeric stability in both PfHAM1 and HsITPA (Figures 1B and 7C).



**Figure 7:** Structural comparison between *HsITPA*, *PhNTPase* and *PfHAM1*. (A) Structural superposition of *PfHAM1* in green and *PhNTPase*, non-standard NTPase of *P. horikoshii* (archaea) in cyan. (B) Structural superposition of *PfHAM1* in green and *HsITPA* in blue. (C) Residues involved in the dimeric interaction of *HsITPA* are shown. The structure of *HsITPA* and interface residues were shown in blue and salmon colour, respectively. **Inset:** Only polar residues are labelled here, and all polar and non-polar contacts are shown in magenta and yellow, respectively.

The molecular dynamics simulation of the substrate-bound complexes of *PfHAM1* revealed the active site residues responsible for substrate recognition. The substrate specificity of *PfHAM1* is provided by a set of residues that interact with different substrate regions. For example, Phe147 stabilises the nucleobase by forming a stacking interaction. Lys170 creates a pi-cation interaction with the purine ring, while Asn145 and Asp150 form hydrogen bonds with carbonyl (at 6<sup>th</sup>) and nitrogen (at 7<sup>th</sup>) groups of the purine ring, respectively. Asn11 forms a water bridge with the nitrogen at the 3<sup>rd</sup> position of purine or the carbonyl at the 2<sup>nd</sup> position in the case of xanthosine, thereby providing definitive substrate specificity to *PfHAM1*. Glu15 recognises hydroxyl groups of the sugar moieties. Asp73 is the metal cofactor binding site, and they interact with the terminal phosphate group through the cofactor  $Mg^{++}$ . Several positively charged residues such as Lys12, Lys90, and Arg176 stabilise the triphosphate moiety through hydrogen bonding and Coulombic attractions, reflected in the sizeable Coulombic contribution in the binding free energies. Finally, Thr7/Thr74/Asn9 appear to be the proton donor in the hydrolysis of the phosphate group. *PfHAM1* shares about 33% of its identity with *HsITPA*, and most active site residues are conserved, suggesting similar substrate-binding interactions (Figures 8A-B). However, due to a difference in one of the critical residues (Glu44 in *HsITPA* to Gln37 in *PfHAM1*), the  $Mg^{++}$  cofactor binding position shifted in *PfHAM1* (Figures 8C and 9), leading to the rearrangement of the roles of several substrate binding residues and the recruitment of new residues (Table 3). For example, Asn9 (Asn16 in *HsITPA*) interacts with the  $\alpha$ -phosphate instead of the ribose, and the  $Mg^{++}$  binding position shifted to Asp73. Several similarities were observed between non-standard *PhNTPase* and *PfHAM1* (Figures 8D-E). In particular, the metal binding to Asp65 of non-standard *PhNTPase* is equivalent to the Asp73 of *PfHAM1*. It is worth noting that the substrate binding site is located away from the dimer interface (Figure 10). Therefore, dimerisation may not affect substrate binding.



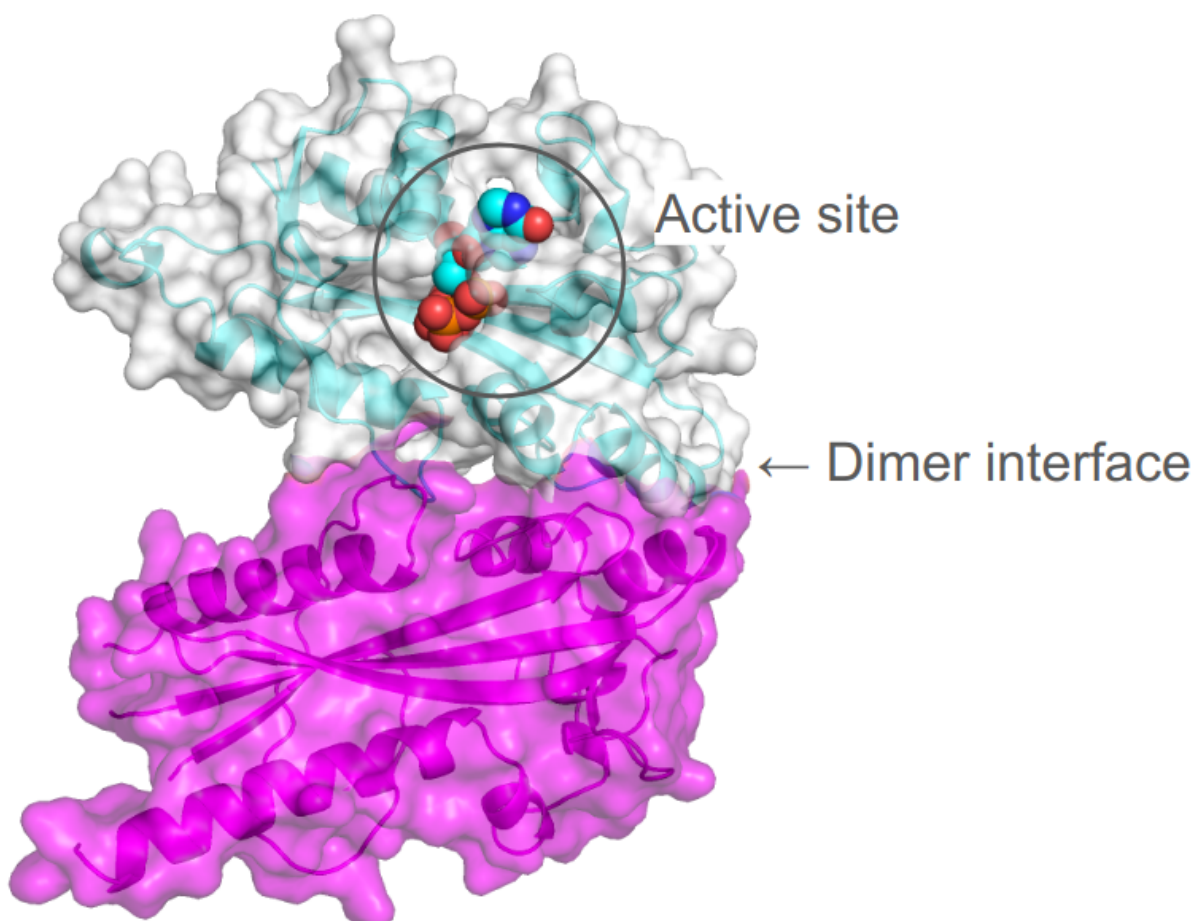


**Figure 8:** Active site comparison of ITP binding between *HsITPA*, *PhNTPase* and *PfHAM1*. (A) Superposition of ITP-bound *HsITPA* (PDB ID: 2J4E) with ITP-bound *PfHAM1* (as obtained from MD simulation). *HsITPA* is shown in blue, and *PfHAM1* is in green. ITP is shown in the stick model, and protein is shown in the cartoon model. (B) Detailed interaction of ITP with *HsITPA*.  $Mg^{++}$  and other interacting residues are labelled. The N to C terminal of the protein is coloured in the rainbow, and the standard colour is used for atoms other than carbon. (C) Detailed interaction of ITP with *PfHAM1* as obtained from MD simulation.  $Mg^{++}$  and other interacting residues are labelled. (D) Superposition of ITP-bound *P. horikoshii* non-standard NTPase (PDB ID: 2DVO) with ITP-bound *PfHAM1*. *P. horikoshii* non-standard NTPase is shown in cyan. (E) Detailed interaction of ITP with *P. horikoshii* non-standard NTPase.  $Na^{+}$  and other interacting residues are labelled.



sp Q8IBP3 ITPA_PLAF7	-----MEIYLVITGNMNNKEEFKMMDEELNVEFVNINLEETQAQDIVEINEHKVKYTAY	53
sp Q9BY32 ITPA_HUMAN	MAASLVGKKIVFVTGNNAKKLEEVVQILGDKFPCTLVAKIDLPETQ-----GEPDEI	52
	:*	
	<div style="display: inline-block; width: 10px; height: 10px; border: 1px solid black; margin: 0 5px;"></div> Mg <sup>2+</sup> <div style="display: inline-block; width: 10px; height: 10px; border: 1px solid black; margin: 0 5px;"></div> Mg <sup>2+</sup>	
sp Q8IBP3 ITPA_PLAF7	NILKKQDNNKNKKRYVITDDTGLFISKLNFPGPYIKWMQKALGSKGIADVSRLLDNTC	113
sp Q9BY32 ITPA_HUMAN	SIQKQAEAVRQVQGPVLVEDTCLCFNALGGLPGPYIKWFLEKLKPEGLHQLLAGFEDKSA	112
	.*:*	
sp Q8IBP3 ITPA_PLAF7	HAICTYSVYDGK---DVHSFKGITNGKIVEPRGNNKFGWDNIFQPESLSKTFGEMTFDEK	170
sp Q9BY32 ITPA_HUMAN	YALCTFALSTGDPSPVRLFRGRTSGRIVAPRGCDPFGWDPCFQPDGYEQTYAEMPKAEK	172
	:*	
sp Q8IBP3 ITPA_PLAF7	QNLSPRFKAFVQLKEFLMNEHKKYNNF	198
sp Q9BY32 ITPA_HUMAN	NAVSHRFRALLELQEYFGSLAA-----	194
	:*:	

**Figure 9:** Comparison of *PfHAM1* (ITPA\_PLAF7) amino acid sequence with *HsITPA* (ITPA\_HUMAN). \*, identical; :, strongly similar; ., weakly similar residues. Active site residues are encompassed with rectangles. Mg(II) binding sites in *PfHAM1* and *HsITPA* are labelled.



**Figure 10:** Position of the active site concerning the dimer interface in *PfHAM1*. ITP-bound *PfHAM1* complex, obtained from MD simulation, is coloured cyan. The

other monomeric unit of the crystal is coloured **magenta**, and the interface between the two monomeric units is shown with an arrow. The active site position concerning the dimer interface is marked.

Role	Residue ( <i>PfHAM1</i> )	Residue ( <i>HsITPA</i> )	Residue ( <i>PhNTPase</i> )
Inosine ring stacking	<b>Phe147</b>	<b>Phe149</b> , Trp151	<b>Phe140</b> , Phe107
Inosine specificity	Asn11, <b>Asp150</b> , Asn145, Lys146, <b>Lys170</b> ,	<b>Asp152</b> , <b>Lys172</b> , His177, Arg178	Ser66, <b>Asp143</b> , Arg169, His168, <b>Lys163</b>
Ribose specificity	Glu15	Asn16	-
$\alpha$ -phosphate binding	Asn9, Asn11, Lys90, Trp149, Asp150	Lys19, Glu44/Mg <sup>++</sup> , Asp 72	Lys12, Asp65/Mg <sup>++</sup>
$\beta$ -phosphate binding	Thr7, <b>Asn9</b> , <b>Lys12</b> , Asp73/Mg <sup>++</sup>	<b>Asn16</b> , <b>Lys19</b> , Glu44/ Mg <sup>++</sup> , Lys89	<b>Asn9</b> , <b>Lys12</b>
$\gamma$ -phosphate binding	Lys12, Asp72, Asp73/ Mg <sup>++</sup> , Thr74, Lys90, Arg176	Thr14, Gly15, Glu44/ Mg <sup>++</sup> , Lys56	Thr7, Ser8, Asp65/ Mg <sup>2+</sup> , Glu36/Mg <sup>2+</sup>

**Table 3:** Comparison of substrate binding residues between *PfHAM1*, *HsITPA*, and *PhNTPase*. Equivalent residues are shown in **bold**.

## E. Conclusion

This report marks a significant milestone as the first crystal structure report of a non-canonical sanitation protein from the human malaria parasite, *Plasmodium falciparum*. The structure of PfHAM1's apoenzyme is described in detail in this article. Despite several attempts to co-crystallise the protein with one of its substrates, dITP, no proper diffraction image was obtained. However, this challenge was overcome by resorting to molecular dynamics simulation of the three most preferred substrates, dITP, ITP, and XTP, to the protein PfHAM1. The simulation was designed to simulate the experimental conditions accurately. As a result, critical amino acid residues involved in substrate binding and catalysis were identified. Despite the low similarity (about 33%) between *Plasmodium falciparum* HAM1 and its human counterpart HsITPA, the subtle differences in substrate binding modes can be leveraged to develop competitive inhibitors specific to PfHAM1. This approach can minimise off-target inhibition of the host HsITPA, thereby reducing side effects. By characterising proteins with such relevance, we can better understand sanitation and pool maintenance and develop drugs against parasites that affect humans and livestock.

## F. References

1. Aravind L, Iyer LM, Wellems TE, Miller LH. Plasmodium biology: genomic gleanings. *Cell*. 2003;115:771-85.
2. Azuara C, Lindahl E, Koehl P, Orland H, Delarue M. PDB\_Hydro: incorporating dipolar solvents with variable density in the Poisson-Boltzmann treatment of macromolecule electrostatics. *Nucleic Acids Res*. 2006;34:W38-42.
3. Buck E, Finnigan NA. Malaria. StatPearls. Treasure Island (FL) ineligible companies. Disclosure: Nancy Finnigan declares no relevant financial relationships with ineligible companies.2023.
4. Burgess-Brown NA, Sharma S, Sobott F, Loenarz C, Oppermann U, Gileadi O. Codon optimization can improve expression of human genes in *Escherichia coli*: A multi-gene study. *Protein Expr Purif*. 2008;59:94-102.
5. Carlton JM, Adams JH, Silva JC, Bidwell SL, Lorenzi H, Caler E, et al. Comparative genomics of the neglected human malaria parasite *Plasmodium vivax*. *Nature*. 2008;455:757-63.
6. Conrad MD, Rosenthal PJ. Antimalarial drug resistance in Africa: the calm before the storm? *Lancet Infect Dis*. 2019;19:e338-e51.
7. Derewenda ZS. The use of recombinant methods and molecular engineering in protein crystallization. *Methods*. 2004;34:354-63.
8. Emsley P, Cowtan K. Coot: model-building tools for molecular graphics. *Acta Crystallogr D Biol Crystallogr*. 2004;60:2126-32.
9. Greenberg GR, Somerville RL. Deoxyuridylate kinase activity and deoxyuridinetriphosphatase in *Escherichia coli*. *Proc Natl Acad Sci U S A*. 1962;48:247-57.
10. Hendrickson WA, Ogata CM. [28] Phase determination from multiwavelength anomalous diffraction measurements. *Methods Enzymol*. 1997;276:494-523.
11. Hwang KY, Chung JH, Kim SH, Han YS, Cho Y. Structure-based identification of a novel NTPase from *Methanococcus jannaschii*. *Nat Struct Biol*. 1999;6:691-6.
12. Kamiya H. Mutagenic potentials of damaged nucleic acids produced by reactive oxygen/nitrogen species: approaches using synthetic oligonucleotides and nucleotides: survey and summary. *Nucleic Acids Res*. 2003;31:517-31.
13. Ke H. [25] Overview of isomorphous replacement phasing. *Methods Enzymol*. 1997;276:448-61.
14. Krissinel, E., & Henrick, K. (2007). Inference of macromolecular assemblies from crystalline state. *Journal of molecular biology*. 2007;372(3),774–797.

15. Liebschner D, Afonine PV, Baker ML, Bunkoczi G, Chen VB, Croll TI, et al. Macromolecular structure determination using X-rays, neutrons and electrons: recent developments in Phenix. *Acta Crystallogr D Struct Biol.* 2019;75:861-77.
16. Lokanath NK, Pampa KJ, Takio K, Kunishima N. Structures of dimeric nonstandard nucleotide triphosphate pyrophosphatase from *Pyrococcus horikoshii* OT3: functional significance of interprotomer conformational changes. *J Mol Biol.* 2008;375:1013-25.
17. McCoy AJ. Solving structures of protein complexes by molecular replacement with Phaser. *Acta Crystallogr D Biol Crystallogr.* 2007;63:32-41.
18. McLennan AG. The Nudix hydrolase superfamily. *Cell Mol Life Sci.* 2006;63:123-43.
19. Moroz OV, Murzin AG, Makarova KS, Koonin EV, Wilson KS, Galperin MY. Dimeric dUTPases, HisE, and MazG belong to a new superfamily of all-alpha NTP pyrophosphohydrolases with potential "house-cleaning" functions. *J Mol Biol.* 2005;347:243-55.
20. Morris GM, Huey R, Lindstrom W, Sanner MF, Belew RK, Goodsell DS, et al. AutoDock4 and AutoDockTools4: Automated docking with selective receptor flexibility. *J Comput Chem.* 2009;30:2785-91.
21. Pal U, Pramanik SK, Bhattacharya B, Banerji B, N CM. Binding interaction of a gamma-aminobutyric acid derivative with serum albumin: an insight by fluorescence and molecular modeling analysis. *Springerplus.* 2016;5:1121.
22. Porta J, Kolar C, Kozmin SG, Pavlov YI, Borgstahl GE. Structure of the orthorhombic form of human inosine triphosphate pyrophosphatase. *Acta Crystallogr Sect F Struct Biol Cryst Commun.* 2006;62:1076-81.
23. Rai P. Oxidation in the nucleotide pool, the DNA damage response and cellular senescence: Defective bricks build a defective house. *Mutat Res.* 2010;703:71-81.
24. Read RJ. Pushing the boundaries of molecular replacement with maximum likelihood. *Acta Crystallogr D Biol Crystallogr.* 2001;57:1373-82.
25. Rodriguez DD, Grosse C, Himmel S, Gonzalez C, de Ilarduya IM, Becker S, et al. Crystallographic ab initio protein structure solution below atomic resolution. *Nat Methods.* 2009;6:651-3.
26. Rose JP, Wang BC. SAD phasing: History, current impact and future opportunities. *Arch Biochem Biophys.* 2016;602:80-94.
27. Savchenko A, Proudfoot M, Skarina T, Singer A, Litvinova O, Sanishvili R, et al. Molecular basis of the antimutagenic activity of the house-cleaning inosine

- triphosphate pyrophosphatase RdgB from *Escherichia coli*. *J Mol Biol.* 2007;374:1091-103.
28. Simone PD, Struble LR, Kellezi A, Brown CA, Grabow CE, Khutsishvili I, et al. The human ITPA polymorphic variant P32T is destabilized by the unpacking of the hydrophobic core. *J Struct Biol.* 2013;182:197-208.
29. Stenmark P, Kursula P, Flodin S, Graslund S, Landry R, Nordlund P, et al. Crystal structure of human inosine triphosphatase. Substrate binding and implication of the inosine triphosphatase deficiency mutation P32T. *J Biol Chem.* 2007;282:3182-7.
30. Thu AM, Phyo AP, Landier J, Parker DM, Nosten FH. Combating multidrug-resistant *Plasmodium falciparum* malaria. *FEBS J.* 2017;284:2569-78.
31. Trott O, Olson AJ. AutoDock Vina: improving the speed and accuracy of docking with a new scoring function, efficient optimization, and multithreading. *J Comput Chem.* 2010;31:455-61.
32. Uwimana A, Legrand E, Stokes BH, Ndikumana JM, Warsame M, Umulisa N, et al. Emergence and clonal expansion of in vitro artemisinin-resistant *Plasmodium falciparum* kelch13 R561H mutant parasites in Rwanda. *Nat Med.* 2020;26:1602-8.



## Synopsis

Around 247 million cases and 619,000 deaths occurred worldwide in the year 2022 owing to malaria, which lurks around to be recognised as a global public health menace. The intertropical belt provides the finest climatic and geographical features for the spread of the female *Anopheles* mosquito, the vector of the disease. The prevalence of *P. vivax* and *P. falciparum* is astounding, with the malignant nature of *P. falciparum*. The growth of antimalarial resistance, mainly in Southeast Asia, as a result of antimalarial overuse and inadequate malaria medicine therapy, highlights the urgent need for the creation of more substantial and more effective antimalarial medications. Despite significant improvements in malaria prevention, there are still more deaths worldwide as a result of the lack of a malaria vaccine that is genuinely effective. The WHO prequalified an innovative malaria vaccine in 2022 to reduce *P. falciparum* infections. The WHO advised the immunisation of children as young as five months old who resided in areas of moderate to high *P. falciparum* transmission in Africa with this vaccine, known as RTS, S/AS01 (Mosquirix), which was created in collaboration with the commercial pharmaceutical company GSK. However, this vaccine's efficiency is insufficient to stop the global escalation of severe malaria cases. Approximately 5300 genes are present in the genomic sequence of the *P. falciparum* 3D7 line, reported in 2002. However, only half of these genes are known to have functions because of their weak sequence similarity to those from other genera. This provides an excellent structure for comprehending the intricate details of the human malaria parasite, *Plasmodium falciparum*'s molecular biology and identifying new therapeutic intervention targets.

The DNA of the parasite is constantly under stress by internal and external factors. Throughout its intricate life cycle, *Plasmodium falciparum*'s DNA sustains unusually high levels of genotoxic damage in both the human host and the vector. The presence of non-canonical nucleotides in the nucleotide precursor pool is a typical cause of endogenous DNA damage that lowers DNA replication fidelity. Some non-canonical nucleotides display the unusual trait of confusing base pairing during replication because they contain analogues of the standard nitrogenous bases. These aberrant nucleotides have the potential to cause mispairing, which substantially raises the mutation rate and results in transition and transversion mutations if they are incorporated into the growing DNA. Such non-canonical dNTPs may be

recognised and hydrolysed to stop DNA deterioration and aid DNA repair mechanisms. Although both the free nucleotide pool and duplex DNA strands experience oxidative deamination of DNA bases, the former is more susceptible to frequent chemical modifications. 8-oxo-guanine (8-O-dGTP/8-O-GTP), deoxy and ribonucleoside triphosphates of xanthine (dXTP/XTP), inosine (dITP/ITP), and other contaminants that are either waste products of cellular metabolism or that are produced by the deamination and oxidation of bases in natural nucleotides can be found in the precursor pool. The four superfamilies of household cleaning enzymes based on their structural characteristics: the NuDiX box domain [G-x(5)-E-x(5)-[UA]-x-R-E-x(2)-E-E-x-G-U] superfamily, all- $\alpha$ -helical NTPases, dUTPases (deoxy-uridine triphosphatases), and protein Ham1 (6-n-hydroxylAMinopurine sensitive). The nucleotidic precursor pool's non-canonical nucleotides are identified and changed into di- or monophosphate forms.

This thesis thoroughly describes the *P. falciparum* ortholog of ITPase (*PfHAM1*). This enzyme transforms non-canonical (d)/ITP and XTP nucleotides into the appropriate monophosphate forms and pyrophosphate. Since preserving genomic integrity is crucial for a parasite's functional operation and the successful transfer of genetic information during cell division, the current investigation's objective was to elucidate this protein's structural and functional characteristics. This research will significantly enhance our understanding of the protein's critical role in non-canonical nucleotide surveillance and its overall function in parasite biology.

---

# Research Publications

---

## Publications

1. **Structure-function analysis of nucleotide housekeeping protein HAM1 from human malignant malaria parasite *Plasmodium falciparum*.** Debanjan Saha, Atanu Pramanik, Aline Freville, Asim Azhar Siddiqui, Uttam Pal, Chinmoy Banerjee, Shiladitya Nag, Subhashis Debsharma, Saikat Pramanik, Somnath Mazumder, Nakul C. Maiti, Soumen Datta, Christiaan van Ooij, Uday Bandyopadhyay. [Under Review]
2. **Rab7 of *Plasmodium falciparum* is involved in its retromer complex assembly near the digestive vacuole.** Asim Azhar Siddiqui, Debanjan Saha, Mohd Shameel Iqbal, Shubhra Jyoti Saha, Souvik Sarkar, Chinmoy Banerjee, Shiladitya Nag, Somnath Mazumder, Rudranil De, Saikat Pramanik, Subhashis Debsharma, Uday Bandyopadhyay. *Biochim Biophys Acta Gen Subj*, PMID: 32512169, 2020.
3. **Nuclease activity of *Plasmodium falciparum* Alba family protein PfAlba3.** Chinmoy Banerjee, Shiladitya Nag, Manish Goyal, Debanjan Saha, Asim Azhar Siddiqui, Somnath Mazumder, Subhashis Debsharma, Saikat Pramanik, Uday Bandyopadhyay. *Cell Reports*, PMID: 36947546, 2023.
4. **Hydrazonophenol, a Food Vacuole-Targeted and Ferriprotoporphyrin IX-Interacting Chemotype Prevents Drug-Resistant Malaria.** Shubhra Jyoti Saha, Asim Azhar Siddiqui, Saikat Pramanik, Debanjan Saha, Rudranil De, Somnath Mazumder, Subhashis Debsharma, Shiladitya Nag, Chinmoy Banerjee, and Uday Bandyopadhyay. *ACS Infect Dis*, PMID: 30472841, 2019.
5. ***Plasmodium falciparum* Alba6 exhibits DNase activity and participates in stress response.** Shiladitya Nag, Chinmoy Banerjee, Manish Goyal, Asim Azhar Siddiqui, Debanjan Saha, Somnath Mazumder, Subhashis Debsharma, Shubhra Jyoti Saha, Saikat Pramanik, Rudranil De, Uday Bandyopadhyay. [Under Revision]
6. **Honokiol, an inducer of Sirtuin 3, protects against NSAID-induced gastric mucosal mitochondrial pathology, apoptosis and inflammatory tissue injury.** Subhashis Debsharma, Saikat Pramanik, Samik Bindu, Somnath Mazumder,

- Troyee Das, Debanjan Saha, Rudranil De, Shiladitya Nag, Chinmoy Banerjee, Asim Azhar Siddiqui, Zhumur Ghosh, Uday Bandyopadhyay. **British Journal of Pharmacology**, PMID: 36914615, 2023.
7. **SIRT3, a target of non-steroidal anti-inflammatory drug to trigger mitochondrial dysfunction and gastric cancer cell death.** Subhashis Debsharma; Saikat Pramanik; Samik Bindu; Somnath Mazumder; Troyee Das; Uttam Pal; Debanjan Saha; Rudranil De; Shiladitya Nag; Chinmoy Banerjee; Nakul Chandra Maiti; Zhumur Ghosh; Uday Bandyopadhyay. **iScience (Just Accepted)**, 2024.
  8. **Indomethacin impairs mitochondrial dynamics by activating the PKC $\zeta$ -p38-DRP1 pathway and inducing apoptosis in gastric cancer and normal mucosal cells.** Somnath Mazumder, Rudranil De, Subhashis Debsharma, Samik Bindu, Pallab Maity, Souvik Sarkar, Shubhra Jyoti Saha, Asim Azhar Siddiqui, Chinmoy Banerjee, Shiladitya Nag, Debanjan Saha, Saikat Pramanik, Kalyan Mitra, Uday Bandyopadhyay. **J Biol Chem**, PMID: 30940726, 2019.
  9. **Macrophage migration inhibitory factor regulates mitochondrial dynamics and cell growth of human cancer cell lines through CD74-NF- $\kappa$ B signaling.** Rudranil De, Souvik Sarkar, Somnath Mazumder, Subhashis Debsharma, Asim Azhar Siddiqui, Shubhra Jyoti Saha, Chinmoy Banerjee, Shiladitya Nag, Debanjan Saha, Saikat Pramanik, Uday Bandyopadhyay. **J Biol Chem**, PMID: 30366984, 2018.
  10. **Acute mental stress induces mitochondrial bioenergetic crisis and hyperfission along with aberrant mitophagy in the gut mucosa in rodent model of stress-related mucosal disease.** Rudranil De, Somnath Mazumder, Souvik Sarkar, Subhashis Debsharma, Asim Azhar Siddiqui, Shubhra Jyoti Saha, Chinmoy Banerjee, Shiladitya Nag, Debanjan Saha, Uday Bandyopadhyay. **Free Radical Biology & Medicine**, PMID: 28993273, 2017.

---

## Conferences & Fellowships

---



## Conferences & Fellowships

1. **Newton-Bhabha PhD 2019-2020 Fellow<sup>†</sup>** at the London School of Hygiene & Tropical Medicine (LSHTM), UK, and working with Dr Christiaan van Ooij's group.
2. **Poster presentation<sup>†</sup>** at the 'Molecular Parasitology Meeting 2023' at Marine Biology Laboratory (University of Chicago), Wood's Hole, MA, USA.  
**Title:** House-cleaning services offered by *Plasmodium falciparum* HAM1.
3. **Oral presentation<sup>†</sup>** at the 'Mechanistic and Therapeutic Approaches in Human and Animal Health Meet - 2021' at the Department of Zoology (Cooch Behar Panchanan Barma University), WB, India.  
**Title:** Attachments! Retromer & Rab7.
4. **Participation<sup>†</sup>** at the Indian International Science Festival 2020 (IISF 2020); One-day seminar on "Research Methodology in Science - 2023" at Raja Peary Mohan College, Hooghly; One-day International webinar on "Current Perspectives on Disease Biology Research - 2021" organised by Raja Peary Mohan College, Hooghly; and "Jigyasa 2017" at CSIR-IICB.

<sup>†</sup>Certificates are attached at the end of the thesis.

---

## Miscellaneous Attachments

---

Order Number: 1206457

Order Date: 01 Apr 2022

## Payment Information

Debanjan Saha  
djan@csiriicb.res.in

Payment method: Invoice

Billing Address:  
Mr. Debanjan Saha  
4 Raja S C Mullick Road  
Kolkata  
India+91 24995735  
djan@csiriicb.res.inCustomer Location:  
Mr. Debanjan Saha  
4 Raja S C Mullick Road  
Kolkata  
India

## Order Details

## 1. Clinical microbiology reviews

Article: Plasmodium Genomics and Genetics: New Insights into Malaria Pathogenesis, Drug Resistance, Epidemiology, and Evolution.

Billing Status  
Open

Order License ID	1206457-1	Type of use	Republish in a thesis/dissertation
Order detail status	Completed	Publisher	AMERICAN SOCIETY FOR MICROBIOLOGY,
ISSN	0893-8512	Portion	Chart/graph/table/figure
			0.00 US Republication Permissi

## LICENSED CONTENT

Publication Title	Clinical microbiology reviews	Rightsholder	American Society for Microbiology - Journals
Article Title	Plasmodium Genomics and Genetics: New Insights into Malaria Pathogenesis, Drug Resistance, Epidemiology, and Evolution.	Publication Type	Journal
Author/Editor	AMERICAN SOCIETY FOR MICROBIOLOGY.	Issue	4
Date	01/01/1988	Volume	32
Language	English	URL	https://journals.asm.org/journal/cmr
Country	United States of America		

## REQUEST DETAILS

Portion Type	Chart/graph/table/figure	Distribution	Worldwide
Number of charts / graphs / tables / figures requested	1	Translation	Original language of publication
Format (select all that apply)	Print,Electronic	Copies for the disabled?	No
Who will republish the content?	Academic institution	Minor editing privileges?	No
Duration of Use	Current edition and up to 10 years	Incidental promotional use?	No
Lifetime Unit Quantity	Up to 499	Currency	USD
Rights Requested	Main product		

## NEW WORK DETAILS

Title	Plasmodium genome architecture	Institution name	IICB
Instructor name	Uday Bandyopadhyay	Expected presentation date	2023-01-02

## ADDITIONAL DETAILS

The requesting person / organization to appear on the license	IICB
---	------

## REUSE CONTENT DETAILS

Title, description or numeric reference of the portion(s)	Plasmodium genomes	Title of the article/chapter the portion is from	Plasmodium Genomics and Genetics: New Insights into Malaria Pathogenesis: Drug Resistance, Epidemiology, and Evolution.
Editor of portion(s)	Su, Xin-zhuan; Lane, Kristin D.; Xia, Lu; Sá, Juliana M.; Wellems, Thomas E.	Author of portion(s)	Su, Xin-zhuan; Lane, Kristin D.; Xia, Lu; Sá, Juliana M.; Wellems, Thomas E.
Volume of serial or monograph	32	Issue, if republishing an article from a serial	4
Page or page range of portion	Table 1	Publication date of portion	2019-09-18

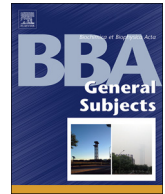
### American Society for Microbiology - Journals Terms and Conditions

We ask that you review the copyright information associated with the article that you are interested in, as some articles in the ASM Journals are covered by creative commons licenses that would permit free reuse with attribution. Please note that ASM cannot grant permission to reuse figures or images that are credited to publications other than ASM journals. For images credited to non-ASM journal publications, you will need to obtain permission from the journal referenced in the figure or table legend or credit line before making any use of the image(s) or table(s). ASM is unable to grant permission to reuse supplemental material as copyright for the supplemental material remains with the author.

This journal title may publish some Open Access articles, which provide specific user rights for reuse. Please refer to the article copyright line to determine whether the content you wish to use is Open Access. For Open Access content, permission to reuse is granted subject to the terms of the License under which the work was published. Please check the License conditions for the work which you wish to reuse. Full and appropriate attribution must be given. This permission does not cover any third party copyrighted material which may appear in the work requested. Please contact the publisher with any questions.

---

**Total Items: 1****Subtotal: 0.00 US****Order Total: 0.00 US**



# Rab7 of *Plasmodium falciparum* is involved in its retromer complex assembly near the digestive vacuole

Asim Azhar Siddiqui, Debanjan Saha, Mohd Shameel Iqbal, Shubhra Jyoti Saha, Souvik Sarkar, Chinmoy Banerjee, Shiladitya Nag, Somnath Mazumder, Rudranil De, Saikat Pramanik, Subhashis Debsharma, Uday Bandyopadhyay\*

Division of Infectious Diseases and Immunology, CSIR-Indian Institute of Chemical Biology, 4, Raja S. C. Mullick Road, Jadavpur, Kolkata 700032, West Bengal, India

## ARTICLE INFO

### Keywords:

*Plasmodium falciparum*  
Rab7  
GTPase  
Digestive vacuole  
Retromer complex

## ABSTRACT

### Background:

Intracellular protein trafficking is crucial for survival of cell and proper functioning of the organelles; however, these pathways are not well studied in the malaria parasite. Its unique cellular architecture and organellar composition raise an interesting question to investigate.

### Methods:

The interaction of *Plasmodium falciparum* Rab7 (PfRab7) with vacuolar protein sorting-associated protein 26 (PvPS26) of retromer complex was shown by coimmunoprecipitation (co-IP). Confocal microscopy was used to show the localization of the complex in the parasite with respect to different organelles. Further chemical tools were employed to explore the role of digestive vacuole (DV) in retromer trafficking in parasite and GTPase activity of PfRab7 was examined.

### Results:

PfRab7 was found to be interacting with retromer complex that assembled mostly near DV and the Golgi in trophozoites. Chemical disruption of DV by chloroquine (CQ) led to its disassembly that was further validated by using compound 5f, a heme polymerization inhibitor in the DV. PfRab7 exhibited  $Mg^{2+}$  dependent weak GTPase activity that was inhibited by a specific Rab7 GTPase inhibitor, CID 1067700, which prevented the assembly of retromer complex in *P. falciparum* and inhibited its growth suggesting the role of GTPase activity of PfRab7 in retromer assembly.

### Conclusion:

Retromer complex was found to be interacting with PfRab7 and the functional integrity of the DV was found to be important for retromer assembly in *P. falciparum*.

### General significance:

This study explores the retromer trafficking in *P. falciparum* and describes a mechanism to validate DV targeting antiparasmodial molecules.

## 1. Introduction

*Plasmodium falciparum* is an intracellular parasite that infects the erythrocytes of its host. The intraerythrocytic stages of the parasite are responsible for its pathogenesis when it digests host hemoglobin in its DV that is a temporary organelle formed only during intraerythrocytic stages of the parasite [1]. DV is often regarded as the metabolic head-quarter of the parasite and a known target for several antiparasmodial compounds [2]. The parasite thrives in the host erythrocyte and depends on its hemoglobin for nutrition and growth. It has a specialized

machinery of various proteases to digest host hemoglobin inside DV [3]. Hemoglobin digestion in DV results in the release of free heme that is highly toxic to the cell. The DV of the parasite utilizes a unique mechanism where it converts free heme into an insoluble and non-toxic crystalline pigment called hemozoin [4]. Because of these factors, DV is one of the most potential targets of antiparasmodial molecules. Organellar architecture of *Plasmodium* is highly dissimilar from other eukaryotes. It has a very unusual single mitochondrion per cell [5], its endoplasmic reticulum is not well defined [6], Golgi bodies in *Plasmodium* are primitive [7]. This peculiar organization of organelles

\* Corresponding author.

E-mail address: [udayb@iicb.res.in](mailto:udayb@iicb.res.in) (U. Bandyopadhyay).

<https://doi.org/10.1016/j.bbagen.2020.129656>

Received 24 January 2020; Received in revised form 22 April 2020; Accepted 2 June 2020

Available online 05 June 2020

0304-4165/ © 2020 Elsevier B.V. All rights reserved.

## Article

# Nuclease activity of *Plasmodium falciparum* Alba family protein PfAlba3

Chinmoy Banerjee,<sup>1</sup> Shiladitya Nag,<sup>1</sup> Manish Goyal,<sup>1</sup> Debanjan Saha,<sup>1</sup> Asim Azhar Siddiqui,<sup>1</sup> Somnath Mazumder,<sup>1</sup> Subhashis Debsharma,<sup>1</sup> Saikat Pramanik,<sup>1</sup> and Uday Bandyopadhyay<sup>1,2,3,\*</sup>

<sup>1</sup>Division of Infectious Diseases and Immunology, CSIR-Indian Institute of Chemical Biology, 4, Raja S. C. Mullick Road, Jadavpur, Kolkata, West Bengal 700032, India

<sup>2</sup>Division of Molecular Medicine, Bose Institute, EN 80, Sector V, Bidhan Nagar Kolkata, 700091, West Bengal, India

<sup>3</sup>Lead contact

\*Correspondence: [ubandy\\_1964@yahoo.com](mailto:ubandy_1964@yahoo.com)

<https://doi.org/10.1016/j.celrep.2023.112292>

## SUMMARY

*Plasmodium falciparum* Alba domain-containing protein Alba3 (PfAlba3) is ubiquitously expressed in intra-erythrocytic stages of *Plasmodium falciparum*, but the function of this protein is not yet established. Here, we report an apurinic/apyrimidinic site-driven intrinsic nuclease activity of PfAlba3 assisted by divalent metal ions. Surface plasmon resonance and atomic force microscopy confirm sequence non-specific DNA binding by PfAlba3. Upon binding, PfAlba3 cleaves double-stranded DNA (dsDNA) hydrolytically. Mutational studies coupled with mass spectrometric analysis indicate that K23 is the essential residue in modulating the binding to DNA through acetylation-deacetylation. We further demonstrate that PfSir2a interacts and deacetylates K23-acetylated PfAlba3 in favoring DNA binding. Hence, K23 serves as a putative molecular switch regulating the nuclease activity of PfAlba3. Thus, the nuclease activity of PfAlba3, along with its apurinic/apyrimidinic (AP) endonuclease feature identified in this study, indicates a role of PfAlba3 in DNA-damage response that may have a far-reaching consequence in *Plasmodium* pathogenicity.

## INTRODUCTION

Nucleases play a fundamental role in a growing number of biological pathways ranging from cellular defense, nutrient regeneration, and apoptosis to nucleic acid metabolism.<sup>1</sup> *Plasmodium falciparum*, the etiological agent of human malignant malaria, has mastered the art of survival by capitalizing on its complex life cycle and intriguingly specialized metabolism to counter host-defense strategies. The oxidative environment under which its intra-erythrocytic stage perpetuates poses a lethal threat to its vulnerable AT-biased genome.<sup>2</sup> Oxidative stress, an inevitable consequence of the parasites' metabolism along with the host immune system as a countermeasure, inflicts DNA damage as a consequence of its interaction with reactive oxygen species (ROS), specifically the hydroxyl radical. Among the several DNA lesions associated, apurinic/apyrimidinic (AP) sites formed due to spontaneous hydrolysis or specific excision of inappropriate or damaged bases by DNA N-glycosylases are one of the most frequent to be observed.<sup>3,4</sup> It is estimated that in mammalian cells, around 10,000 bases are lost per day.<sup>5,6</sup> The subsequent loss of an encoding base in the DNA template may end up blocking the DNA and RNA polymerases, thereby stalling DNA replication and transcription. Moreover, translesional DNA synthesis may further culminate into single-nucleotide replacements or deletions/insertions leading to mutations. AP sites are crucial, owing to their high chemical reactivity, and may enhance the

production of DNA breaks as well as render DNA-protein and DNA-DNA crosslink. These AP sites, if left untreated, can have deleterious consequences, as they are highly mutagenic and cytotoxic.<sup>7,8</sup> Hence, for maintaining genome integrity, the repair of AP sites is a major mechanism wherein AP endonucleases serve as key enzymes to initiate the repair process. Out of the four nucleobases, adenine and guanine exhibit maximum propensity for impromptu base loss. Considering the fact that the *Plasmodium falciparum* genome exhibits unusually high adenine (A) and thymine (T) content (~80%) and spontaneous de-adenination of DNA occurs naturally, it is quite apparent that an active AP repair process is prevalent. Ten DNA endonucleases encoded by the genome of *Plasmodium falciparum* 3D7 clone have been identified, of which seven are predicted to harbor an endonuclease/exonuclease/phosphatase (IPR005135) domain that plays a crucial role in DNA catalysis.<sup>9</sup> The repair of nuclear DNA in *Plasmodium falciparum* has been proposed to involve homologous recombination, mismatch repair (MMR) pathways, and alternative end joining.<sup>10,11</sup> Putative proteins involved in nucleotide excision repair have also been reported.<sup>12</sup> Base excision repair (BER) in *Plasmodium falciparum* is mediated via long patch repair mechanism by class II AP endonucleases present in the parasite lysate. Recent studies have identified two mitochondrial AP endonucleases in *Plasmodium falciparum*.<sup>13,14</sup> Apart from these two mitochondrial AP endonucleases, three more enzymes (uracil DNA glycosylase, flap endonuclease 1,



# Hydrazonophenol, a Food Vacuole-Targeted and Ferriprotoporphyrin IX-Interacting Chemotype Prevents Drug-Resistant Malaria

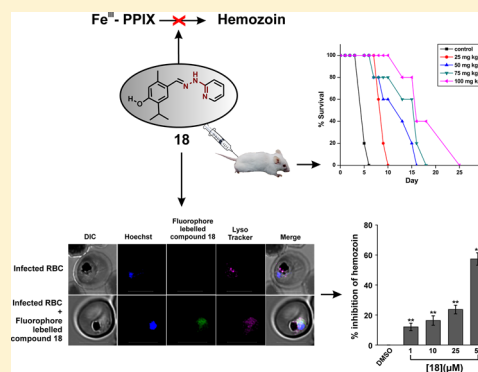
Shubhra Jyoti Saha,<sup>ID</sup> Asim Azhar Siddiqui,<sup>ID</sup> Saikat Pramanik, Debanjan Saha,<sup>ID</sup> Rudranil De, Somnath Mazumder, Subhashis Debsharma, Shiladitya Nag, Chinmoy Banerjee, and Uday Bandyopadhyay<sup>\*ID</sup>

Division of Infectious Diseases and Immunology, CSIR - Indian Institute of Chemical Biology, 4 Raja S. C. Mullick Road, Jadavpur, Kolkata 700032, West Bengal, India

## Supporting Information

**ABSTRACT:** The rapid emergence of resistance against frontline antimalarial drugs essentially warrants the identification of new-generation antimalarials. Here, we describe the synthesis of (*E*)-2-isopropyl-5-methyl-4-((2-(pyridin-4-yl)hydrazono)methyl)phenol (**18**), which binds ferriprotoporphyrin-IX ( $\text{Fe}^{\text{III}}$ -PPIX) ( $K_d = 33 \text{ nM}$ ) and offers antimalarial activity against chloroquine-resistant and sensitive strains of *Plasmodium falciparum* in vitro. Structure–function analysis reveals that compound **18** binds  $\text{Fe}^{\text{III}}$ -PPIX through the  $-\text{C}=\text{N}-\text{NH}-$  moiety and 2-pyridyl substitution at the hydrazine counterpart plays a critical role in antimalarial efficacy. Live cell confocal imaging using a fluorophore-tagged compound confirms its accumulation inside the acidic food vacuole (FV) of *P. falciparum*. Furthermore, this compound concentration-dependently elevates the pH in FV, implicating a plausible interference with  $\text{Fe}^{\text{III}}$ -PPIX crystallization (hemozoin formation) by a dual function: increasing the pH and binding free  $\text{Fe}^{\text{III}}$ -PPIX. Different off-target bioassays reduce the possibility of the promiscuous nature of compound **18**. Compound **18** also exhibits potent in vivo antimalarial activity against chloroquine-resistant *P. yoelii* and *P. berghei* ANKA (causing cerebral malaria) in mice with negligible toxicity.

**KEYWORDS:** *Plasmodium*, malaria, hemozoin, food vacuole, parasite metabolism



The adverse effect of malaria across the globe demands serious attention due to the increasing number of reports of multi-drug-resistant (MDR) strains posing a severe threat to human life and productivity.<sup>1,2</sup> Reports of 216 million cases with 445 000 deaths in 2016 repeatedly accentuate the desideratum of new antimalarial chemotherapeutics against MDR strains.<sup>3</sup> Moreover, the emergence of drug resistance against artemisinin partner drugs such as piperazine and mefloquine has resulted in a significant failure of artemisinin combination therapy (ACT) on the Thai–Cambodian border, where chloroquine (CQ) resistance was developed almost 50 years ago.<sup>4</sup> The spread of resistance therefore needs to be dealt with in the identification of new antimalarial chemotypes that are efficacious against MDR malaria in the most unfortified regions.<sup>1,5</sup>

Intraerythrocytic stages of *P. falciparum* are responsible for its clinical symptoms, and during these stages, the parasite digests hemoglobin in the acidic food vacuole (FV) and thereby releases heme ( $\text{Fe}^{\text{III}}$ -PPIX), a nonprotein constituent of hemoglobin as a byproduct.<sup>6,7</sup> This free  $\text{Fe}^{\text{III}}$ -PPIX, a well-known pro-oxidant, may cause severe oxidative damage to the lipid bilayers of the parasitic cell membrane, leading to

membrane lesion.<sup>8–10</sup> In order to evade the detrimental consequences of free  $\text{Fe}^{\text{III}}$ -PPIX accumulation, *Plasmodium* crystallizes it into nontoxic inert hemozoin (Hz).<sup>11,12</sup> It was found that the development of CQ resistance in parasites was mainly due to multiple mutations in the *P. falciparum* CQ resistance transporter (*PfCRT*) that results in structure-specific efflux of the drug from FV.<sup>13</sup> Despite this resistance, the Hz crystallization pathway within the parasite is still essential, and thus it may be used as a sustainable drug target.<sup>14</sup> Thus, scaffolds which bind to free  $\text{Fe}^{\text{III}}$ -PPIX and inhibit Hz crystallization can be detrimental to parasites due to free  $\text{Fe}^{\text{III}}$ -PPIX accumulation within the FV and have merit as potent antimalarials.

In the search for new antimalarial chemotypes, we focused our study on  $\text{Fe}^{\text{III}}$ -PPIX binding moieties that are capable of interacting with high affinity. A novel class of chiral gallium(III) complexes of amine-phenol ligand and schiff-base phenol ligand were reported to possess decent efficacy against CQ-sensitive and -resistant strains.<sup>15</sup> These cationic


Received: July 23, 2018

Published: November 25, 2018



## RESEARCH ARTICLE

# Honokiol, an inducer of sirtuin-3, protects against non-steroidal anti-inflammatory drug-induced gastric mucosal mitochondrial pathology, apoptosis and inflammatory tissue injury

Subhashis Debsharma<sup>1</sup> | Saikat Pramanik<sup>1</sup> | Samik Bindu<sup>2</sup> |  
 Somnath Mazumder<sup>3</sup> | Troyee Das<sup>4</sup> | Debanjan Saha<sup>1</sup> | Rudranil De<sup>5</sup> |  
 Shiladitya Nag<sup>1</sup> | Chinmoy Banerjee<sup>1</sup> | Asim Azhar Siddiqui<sup>1</sup> | Zhumur Ghosh<sup>4</sup> |  
 Uday Bandyopadhyay<sup>1,6</sup> 

<sup>1</sup>Division of Infectious Diseases and Immunology, CSIR-Indian Institute of Chemical Biology, Kolkata, West Bengal, India

<sup>2</sup>Department of Zoology, Cooch Behar Panchanan Barma University, Cooch Behar, West Bengal, India

<sup>3</sup>Department of Zoology, Raja Peary Mohan College, Uttarpara, West Bengal, India

<sup>4</sup>Division of Bioinformatics, Bose Institute, Kolkata, West Bengal, India

<sup>5</sup>Amity Institute of Biotechnology, Amity University, Kolkata, Kolkata, West Bengal, India

<sup>6</sup>Division of Molecular Medicine, Bose Institute, Kolkata, West Bengal, India

## Correspondence

Dr Uday Bandyopadhyay, Division of Molecular Medicine, Bose Institute, EN 80, Sector V, Bidhan Nagar, Kolkata, West Bengal 700091, India.

Email: [ubandyoy\\_1964@yahoo.com](mailto:ubandyoy_1964@yahoo.com); [udayb@jcbse.ac.in](mailto:udayb@jcbse.ac.in)

## Funding information

Department of Biotechnology, Ministry of Science and Technology, India; Science and Engineering Research Board, Grant/Award Number: SB/S2/JCB-54/2014

**Background and Purpose:** Mitochondrial oxidative stress, inflammation and apoptosis primarily underlie gastric mucosal injury caused by the widely used non-steroidal anti-inflammatory drugs (NSAIDs). Alternative gastroprotective strategies are therefore needed. Sirtuin-3 pivotally maintains mitochondrial structural integrity and metabolism while preventing oxidative stress; however, its relevance to gastric injury was never explored. Here, we have investigated whether and how sirtuin-3 stimulation by the phytochemical, honokiol, could rescue NSAID-induced gastric injury.

**Experimental Approach:** Gastric injury in rats induced by indomethacin was used to assess the effects of honokiol. Next-generation sequencing-based transcriptomics followed by functional validation identified the gastroprotective function of sirtuin-3. Flow cytometry, immunoblotting, qRT-PCR and immunohistochemistry were used to measure effects on oxidative stress, mitochondrial dynamics, electron transport chain function, and markers of inflammation and apoptosis. Sirtuin-3 deacetylase activity was also estimated and gastric luminal pH was measured.


**Key Results:** Indomethacin down-regulated sirtuin-3 to induce oxidative stress, mitochondrial hyperacetylation, 8-oxoguanine DNA glycosylase 1 depletion, mitochondrial DNA damage, respiratory chain defect and mitochondrial fragmentation leading to severe mucosal injury. Indomethacin dose-dependently inhibited sirtuin-3 deacetylase activity. Honokiol prevented mitochondrial oxidative damage and inflammatory tissue injury by attenuating indomethacin-induced depletion of both sirtuin-3 and its transcriptional regulators PGC1 $\alpha$  and ERR $\alpha$ . Honokiol also accelerated gastric wound healing but did not alter gastric acid secretion, unlike lansoprazole.

**Conclusions and Implications:** Sirtuin-3 stimulation by honokiol prevented and reversed NSAID-induced gastric injury through maintaining mitochondrial integrity.

**Abbreviations:** 8-oxo-dG, 8-oxo-7,8-dihydro-2'-deoxyguanosine; DEG, differentially expressed gene; ERR $\alpha$ , oestrogen-related receptor  $\alpha$ ; ETC, electron transport chain; i.g., intragastric; IL, injury index; MFN, mitofusin; MOS, mitochondrial oxidative stress; NRF2, nuclear factor erythroid 2-related factor 2; NSAIDs, non-steroidal anti-inflammatory drugs; OGG1, 8-oxoguanine DNA glycosylase 1; OPA1, optic atrophy 1; PGC1 $\alpha$ , peroxisome proliferator-activated receptor-gamma coactivator 1- $\alpha$ ; PPI, proton pump inhibitor; RIN, RNA integrity number; Sirt3, sirtuin-3; SOD2, superoxide dismutase; TBS, Tris-buffered saline;  $\Delta\Psi_m$ , mitochondrial transmembrane potential.

# Indomethacin impairs mitochondrial dynamics by activating the PKC $\zeta$ –p38–DRP1 pathway and inducing apoptosis in gastric cancer and normal mucosal cells

Received for publication, June 12, 2018, and in revised form, March 27, 2019. Published, Papers in Press, April 2, 2019, DOI 10.1074/jbc.RA118.004415

Somnath Mazumder<sup>†1</sup>, Rudranil De<sup>†1</sup>, Subhashis Debsharma<sup>‡</sup>, Samik Bindu<sup>§</sup>, Pallab Maity<sup>‡</sup>, Souvik Sarkar<sup>‡</sup>, Shubhra Jyoti Saha<sup>‡</sup>, Asim Azhar Siddiqui<sup>‡</sup>, Chinmoy Banerjee<sup>‡</sup>, Shiladitya Nag<sup>‡</sup>, Debanjan Saha<sup>‡</sup>, Saikat Pramanik<sup>‡</sup>, Kalyan Mitra<sup>¶</sup>, and  Uday Bandyopadhyay<sup>‡2</sup>

From the <sup>†</sup>Division of Infectious Diseases and Immunology, CSIR-Indian Institute of Chemical Biology, Kolkata, West Bengal 700032, the <sup>§</sup>Department of Zoology, Cooch Behar Panchanan Barma University, Cooch Behar, West Bengal 736101, and the <sup>¶</sup>Sophisticated Analytical Instrument Facility, CSIR-Central Drug Research Institute, Sector 10, Jankipuram Extension, Sitapur Road, Lucknow 226031, Uttar Pradesh, India

Edited by Luke O'Neill

The subcellular mechanism by which nonsteroidal anti-inflammatory drugs (NSAIDs) induce apoptosis in gastric cancer and normal mucosal cells is elusive because of the diverse cyclooxygenase-independent effects of these drugs. Using human gastric carcinoma cells (AGSs) and a rat gastric injury model, here we report that the NSAID indomethacin activates the protein kinase C $\zeta$  (PKC $\zeta$ )–p38 MAPK (p38)–dynamin-related protein 1 (DRP1) pathway and thereby disrupts the physiological balance of mitochondrial dynamics by promoting mitochondrial hyper-fission and dysfunction leading to apoptosis. Notably, DRP1 knockdown or SB203580-induced p38 inhibition reduced indomethacin-induced damage to AGSs. Indomethacin impaired mitochondrial dynamics by promoting fissionogenic activation and mitochondrial recruitment of DRP1 and down-regulating fusogenic optic atrophy 1 (OPA1) and mitofusins in rat gastric mucosa. Consistent with OPA1 maintaining cristae architecture, its down-regulation resulted in EM-detectable cristae deformity. Deregulated mitochondrial dynamics resulting in defective mitochondria were evident from enhanced Parkin expression and mitochondrial proteome ubiquitination. Indomethacin ultimately induced mitochondrial metabolic and bioenergetic crises in the rat stomach, indicated by compromised fatty acid oxidation, reduced complex I-associated electron transport chain activity, and ATP depletion. Interestingly, Mdivi-1, a fission-preventing mito-protective drug, reversed indomethacin-induced DRP1 phosphorylation on Ser-616, mitochondrial proteome ubiquitination, and mitochondrial metabolic crisis. Mdivi-1 also prevented indomethacin-induced mitochondrial macromolecular damage, caspase activation, mucosal inflammation, and gastric mucosal injury. Our results identify

mitochondrial hyper-fission as a critical and common subcellular event triggered by indomethacin that promotes apoptosis in both gastric cancer and normal mucosal cells, thereby contributing to mucosal injury.

Nonsteroidal anti-inflammatory drugs (NSAIDs)<sup>3</sup> are the most effective medicines for treating pain and inflammation (1, 2). In addition to their anti-nociceptive action, NSAIDs are also gaining significant importance because of their anti-neoplastic effects against a wide spectrum of cancers. In fact, prolonged NSAID users are at lower risk of developing cancers (3, 4), and these noncanonical anti-cancer drugs are now included in a combination–chemotherapy regimen as they potentiate chemotherapy and radiotherapy (5). Although prostaglandin depletion due to cyclooxygenase (COX) inhibition is primarily responsible for both anti-inflammatory as well as cytotoxic anti-cancer action of NSAIDs (6), COX-independent targets, including cGMP phosphodiesterase, peroxisome proliferator-activated receptors, retinoid X receptor, IKK $\beta$ , AMP kinase, and other targets of these drugs as well as their metabolites (7), help to trigger cell death by apoptosis while blocking proliferation. Hence, NSAIDs are gaining immense importance and have been under exploration in various diseases, including cancer (7–10). Despite their multidimensional health benefits, the toxic actions of NSAIDs are observed against various normal cells of the body that compromise metabolic homeostasis and tissue integrity (6, 11, 12). Of the several organs affected by long-term NSAID usage (13–16), the gastrointestinal system

This work was supported by a Council of Scientific and Industrial Research, New Delhi, India, fellowship (to S. M. and R. D.), Research Grants BEnD, BSC 0206, and DST (J. C. Bose Fellowship) Grant SB/S2/JCB-54/2014. The authors declare that they have no conflicts of interest with the contents of this article.


<sup>1</sup> Both authors contributed equally to this work.

<sup>2</sup> To whom correspondence should be addressed: Division of Infectious Diseases and Immunology, CSIR-Indian Institute of Chemical Biology, 4 Raja S.C. Mullick Rd., Kolkata 700032, West Bengal, India. Tel.: 91-33-2499-5735 or 91-33-2473-5197; Fax: 91-33-2473-0492 or 91-33-2472-3967; E-mail: ubandyu\_1964@yahoo.com.

<sup>3</sup> The abbreviations used are: NSAID, nonsteroidal anti-inflammatory drug; MFF, mitochondrial fission factor; MTT, 3-(4,5-dimethylthiazol-2-yl)-2,5-diphenyltetrazolium bromide; STED, stimulated emission depletion microscopy; ETC, electron transport chain; ROS, reactive oxygen species; OCR, oxygen consumption ratio; ANOVA, analysis of variance; TEM, transmission EM; COX, cyclooxygenase; IMM, inner mitochondrial membrane; MOS, mitochondrial oxidative stress; RCR, respiratory control ratio; qPCR, quantitative PCR; NAO, nonyl acridine orange; AGS, human gastric epithelial cell; PSI, pseudo-substrate inhibitor; FCCP, carbonyl cyanide *p*-trifluoromethoxyphenylhydrazone; II, injury index; ROI, region of interest; MAPK, mitogen-activated protein kinase; ERK, extracellular signal-regulated kinase; JNK, c-Jun N-terminal kinase; PG, prostaglandin; FtMt, mitochondrial ferritin; DAPI, 4',6-diamidino-2-phenylindole; DAB, 3,3'-diaminobenzidine.

# Macrophage migration inhibitory factor regulates mitochondrial dynamics and cell growth of human cancer cell lines through CD74–NF- $\kappa$ B signaling

Received for publication, May 11, 2018, and in revised form, September 25, 2018. Published, Papers in Press, October 26, 2018, DOI 10.1074/jbc.RA118.003935

Rudranil De<sup>1</sup>, Souvik Sarkar<sup>1</sup>, Somnath Mazumder, Subhashis Debsharma, Asim Azhar Siddiqui, Shubhra Jyoti Saha, Chinmoy Banerjee, Shiladitya Nag, Debanjan Saha, Saikat Pramanik, and  Uday Bandyopadhyay<sup>2</sup>

From the Division of Infectious Diseases and Immunology, CSIR-Indian Institute of Chemical Biology, Jadavpur, Kolkata 700032, West Bengal, India

Edited by Luke O'Neill

The indispensable role of macrophage migration inhibitory factor (MIF) in cancer cell proliferation is unambiguous, although which specific roles the cytokine plays to block apoptosis by preserving cell growth is still obscure. Using different cancer cell lines (AGS, HepG2, HCT116, and HeLa), here we report that the silencing of MIF severely deregulated mitochondrial structural dynamics by shifting the balance toward excess fission, besides inducing apoptosis with increasing sub-G<sub>0</sub> cells. Furthermore, enhanced mitochondrial Bax translocation along with cytochrome *c* release, down-regulation of Bcl-xL, and Bcl-2 as well as up-regulation of Bad, Bax, and p53 indicated the activation of a mitochondrial pathway of apoptosis upon MIF silencing. The data also indicate a concerted down-regulation of Opa1 and Mfn1 along with a significant elevation of Drp1, cumulatively causing mitochondrial fragmentation upon MIF silencing. Up-regulation of Drp1 was found to be further coupled with fissionogenic serine 616 phosphorylation and serine 637 dephosphorylation, thus ensuring enhanced mitochondrial translocation. Interestingly, MIF silencing was found to be associated with decreased NF- $\kappa$ B activation. In fact, NF- $\kappa$ B knockdown in turn increased mitochondrial fission and cell death. In addition, the silencing of CD74, the cognate receptor of MIF, remarkably increased mitochondrial fragmentation in addition to preventing cell proliferation, inducing mitochondrial depolarization, and increasing apoptotic cell death. This indicates the active operation of a MIF-regulated CD74–NF- $\kappa$ B signaling axis for maintaining mitochondrial stability and cell growth. Thus, we propose that MIF, through CD74, constitutively activates NF- $\kappa$ B to control mitochondrial dynamics and stability for promoting carcinogenesis via averting apoptosis.

Macrophage migration inhibitory factor (MIF)<sup>3</sup> is a pluripotent inflammatory marker, which is widely known for its proinflammatory role in generating immune response by activating macrophages and T cells (1). MIF has been shown to promote tumorigenesis in many models of colorectal adenomas, intestinal tumors, ovarian cancer, and hepatocellular carcinoma (2, 3). MIF is high in both serum and epithelial cells of gastric cancer patients (4, 5). The intricate association of up-regulated MIF expression in gastrointestinal tract malignancies makes MIF a biomarker for gastric cancer as well as a potential target in anti-cancer therapies. Despite its significance in cancer, the precise role of MIF in carcinogenesis is still elusive, although some critical MIF-mediated pathways including p115 (6), inactivation of p53 (7), and stimulation of angiogenesis (2) have been investigated. The literature also suggests that CD74, the cognate receptor of MIF, upon stimulation activates NF- $\kappa$ B, a key molecular player in cancer and inflammation, which triggers the entry of stimulated cells into the S-phase, elevates DNA synthesis and cell division and augments BCL-X<sub>L</sub> expression (8). CD74-MIF signaling is suspected to play a vital prognostic role in many malignancies (9). Notably, clinical immunotherapies are also being conducted targeting CD74 by milatuzumab, the monoclonal anti-CD74 antibody, in malignancies like B-cell lymphomas (10) and multiple myeloma (11).

Mitochondria are organelles that provide the majority of the energy in most cells by synthesizing ATP (12). As mitochondria are dynamic organelles that continuously undergo fission and fusion (12), mitochondrial structural integrity plays a critical role in metabolic functions (13). Severe defects in either mitochondrial fusion or fission lead to mitochondrial dysfunction (14). The Warburg effect proposes redundancy of mitochondrial oxidative phosphorylation as a major source of cellular bioenergy production; however the heterogeneity of cancer

This work was supported by a fellowship (to R. D.) and Research Grants BEnD and BSC 0206 from the Council of Scientific and Industrial Research, New Delhi. This work also was supported by J. C. Bose Fellowship SB/S2/JCB-54/2014 from the Department of Science and Technology, Ministry of Science and Technology (DST). The authors declare that they have no conflicts of interest with the contents of this article.

<sup>1</sup> Both authors contributed equally to this work.

<sup>2</sup> To whom correspondence should be addressed: Division of Infectious Diseases and Immunology, CSIR-Indian Institute of Chemical Biology, 4 Raja S. C. Mullick Rd., Jadavpur, Kolkata 700032, West Bengal, India. Tel.: 91-33-24995735; Fax: 91-33-4730284; E-mail: [ubandyo\\_1964@yahoo.com](mailto:ubandyo_1964@yahoo.com) or [udayb@iicb.res.in](mailto:udayb@iicb.res.in).

<sup>3</sup> The abbreviations used are: MIF, macrophage migration inhibitory factor; MTT, 3-(4,5-dimethylthiazol-2-yl)-2,5-diphenyl tetrazolium bromide; PI, propidium iodide; AGS, human gastric adenocarcinoma (cells); DMEM, Dulbecco's modified Eagle's medium; JC-1, 5,5',6,6'-tetrachloro-1,1',3,3'-tetraethylbenzimidazolylcarbocyanine iodide; RLU, relative light unit; STED, stimulated emission depletion (microscopy); qPCR, real-time quantitative PCR; ANOVA, analysis of variance; ROI, region of interest; KD, knock down; L-DOPA, L-Dopachrome methyl ester.



## Original article

# Acute mental stress induces mitochondrial bioenergetic crisis and hyper-fission along with aberrant mitophagy in the gut mucosa in rodent model of stress-related mucosal disease



Rudranil De, Somnath Mazumder, Souvik Sarkar, Subhashis Debsharma, Asim Azhar Siddiqui, Shubhra Jyoti Saha, Chinmoy Banerjee, Shiladitya Nag, Debanjan Saha, Uday Bandyopadhyay\*

Division of Infectious Diseases and Immunology, CSIR-Indian Institute of Chemical Biology, 4, Raja S. C. Mullick Road, Jadavpur, Kolkata 700032, West Bengal, India

## ARTICLE INFO

## Keywords:

Stress  
Mitochondria  
Mitophagy  
Superoxide ion  
Oxidative stress

## ABSTRACT

Psychological stress, depression and anxiety lead to multiple organ dysfunctions wherein stress-related mucosal disease (SRMD) is common to people experiencing stress and also occur as a side effect in patients admitted to intensive care units; however the underlying molecular aetiology is still obscure. We report that in rat-SRMD model, cold restraint-stress severely damaged gut mitochondrial functions to generate superoxide anion ( $O_2^{\cdot-}$ ), depleted ATP and shifted mitochondrial fission-fusion dynamics towards enhanced fission to induce mucosal injury. Activation of mitophagy to clear damaged and fragmented mitochondria was evident from mitochondrial translocation of Parkin and PINK1 along with enhanced mitochondrial proteome ubiquitination, depletion of mitochondrial DNA copy number and TOM 20. However, excess and sustained accumulation of  $O_2^{\cdot-}$ -generating defective mitochondria overpowered the mitophagic machinery, ultimately triggering Bax-dependent apoptosis and NF- $\kappa$ B-intervened pro-inflammatory mucosal injury. We further observed that stress-induced enhanced serum corticosterone stimulated mitochondrial recruitment of glucocorticoid receptor (GR), which contributed to gut mitochondrial dysfunctions as documented from reduced ETC complex 1 activity, mitochondrial  $O_2^{\cdot-}$  accumulation, depolarization and hyper-fission. GR-antagonism by RU486 or specific scavenging of mitochondrial  $O_2^{\cdot-}$  by a mitochondrially targeted antioxidant mitoTEMPO ameliorated stress-induced mucosal damage. Gut mitopathology and mucosal injury were also averted when the perception of mental stress was blocked by pre-treatment with a sedative or antipsychotic. Altogether, we suggest the role of mitochondrial GR- $O_2^{\cdot-}$ -fission cohort in brain-mitochondria cross-talk during acute mental stress and advocate the utilization of this pathway as a potential target to prevent mitochondrial unrest and gastropathy bypassing central nervous system.

## 1. Introduction

Sustained mental ailments like anxiety and depression significantly affect our health by altering physiological homeostasis [1–3]. Stress-related mucosal disease (SRMD) is one such manifestation documented worldwide in patients experiencing stress [4]. Moderate to acute mucosal bleeding in critically ill patients of Intensive Care Unit (ICU) is one of the critical stress-associated phenomena and the mortality rate is significantly high (40–50%) [5,6]. Stomach houses a semi-autonomous nervous system (enteric nervous system, ENS) consisting of five hundred million nerves in the lining of the human gut. It is also the source and/or the depository of many neurotransmitters. ENS is sometimes called the “second brain,” and it arises from the same tissue as the central nervous system (CNS) during development. CNS and ENS continue to influence each other lifelong and interestingly the stress

response is manifested through ENS more promptly than any other organ leading to functional gastrointestinal disorders, mucosal bleeding, inflammation, pain, and other bowel symptoms. On the other hand poor gut health has been implicated in various psychophysical disorders [7].

Being the cellular powerhouse, mitochondrial health, biogenesis and protein quality control are matters of critical concern; imbalance of mitochondrial metabolism is associated with oxidative stress and various cytopathologies [8,9]. Mitochondrial structural dynamics [10] is delicately tuned with outer environment. While mild stress induces organellar hyperfusion, moderate to acute stress evokes fragmentation followed by mitophagy in eukaryotes [11,12]. Several quality control proteases like PINK1, PARL and Parkin constantly monitor mitochondrial integrity and ensure timely clearance of damaged organelles [13,14]. Apart from its roles in mitophagy, PINK1 also participates in

\* Corresponding author.

E-mail addresses: [ubandyo\\_1964@yahoo.com](mailto:ubandyo_1964@yahoo.com), [udayb@iicb.res.in](mailto:udayb@iicb.res.in) (U. Bandyopadhyay).



Student first name: **DEBANJAN**

Student last name: **SAHA**

Start Date: **06.06.2022**

Finish Date: **31.10.2022**

Country: **INDIA**

Did the PhD student complete the placement as planned?

Yes ☒ No ☐ Comments (if any) \_\_\_\_\_

Did the PhD student achieve the planned outputs?

Yes ☒ No ☐ Comments (if any) \_\_\_\_\_

**Any comments (Including, for example, highlights and challenges):**

**It was an absolute pleasure to host Debanjan in the lab. He added a lot to the lab, and it was good to see that he could achieve his aims.**

**Supervisor's signature:**

**Date:** November 7, 2022



# You have been chosen for a POSTER - 34th Molecular Parasitology Meeting (MPM), September 2023

---

From: Llinas, Manuel (manuel@psu.edu)

Date: Tuesday, 15 August 2023 at 08:46 PM IST

---

Dear Colleague,

We are writing to inform you that your abstract has been chosen for a **POSTER** at the 34th Molecular Parasitology Meeting. You should be prepared to present on either the Monday, Tuesday, or Wednesday session. If you will attend virtually you will present via Zoom. Poster number assignments will be available in the abstract book, which will be posted online prior to the meeting and also provided to all attendees upon arrival in Woods Hole.

In-person poster presenters will present live in a physical poster session. In-person presenters are encouraged to also upload a PDF of your poster for viewing, but this is not required. You are also welcome to present during a virtual poster session. In-person posters should NOT EXCEED 42 inches (106.5 cm) width x 60 inches (152 cm) height (We recommend: 3 ft. (91 cm) wide x 4 ft. (122 cm) high).

Virtual presenters will also upload PDFs of their posters to an online folder that all MPM attendees can view at any time. This will help attendees from time zones that can't join the live zoom poster session, and it will help live zoom attendees who need to zoom in on your poster. All MPM attendees will be invited to attend the virtual poster sessions.

Additional information regarding poster instructions can be found here: [Poster instructions](#)

**Please inform us if you are unable to present your work by Friday, August 25 – [mpmmeeting@gmail.com](mailto:mpmmeeting@gmail.com)**

This year we received more than 400 abstracts encompassing a wide variety of approaches and parasites. Unfortunately, not all of the many excellent abstracts submitted could be presented in the oral sessions. Although this means that the meeting promises to be as stimulating as in the past, the selection process for the program was extremely difficult. We have strived to put together a balanced program that reflects the breadth of exciting research being pursued by our colleagues.

The meeting this year will begin with dinner on Sunday, September 17, 2023 followed by a plenary session at 7:00 PM US Eastern standard time. The meeting will end with an oral session on Thursday morning September 21, 2023 at 12:30 PM. For in-person attendees, registration will begin in the early afternoon on September 17 at the MBL Swope Center, North Street, Woods Hole, and the last session on September 21 will be followed by lunch.

This year's plenary lecture will be given by Alan Cowman on Wednesday evening prior to the lobster dinner.

We will contact you soon with the final program and Zoom links. We look forward to seeing you in Woods Hole in September in person or via Zoom.

Your MPM XXXIV Co-organizers,

Maryse Lebrun, Bibo Li, Manuel Llinás

Technical and logistical assistance: Omar Harb

Education and Inclusion lead: Deepali Ravel

Additional MPMXXXIV information can be found here: <https://www.parasitesrule.com/mpm-xxxiv>



smime.p7s  
1.6kB



Conference Office  
MBL  
7 MBL Street  
Woods Hole, MA 02543  
USA

T 508.289.7668  
conferences@mbl.edu

### Molecular Parasitology Meeting 2023

---

**Sunday, September 17, 2023 – Thursday, September 21, 2023**

Marine Biological Laboratory in Woods Hole, MA (USA).

September 26, 2023

(Certificate of Attendance)

Dear **DEBANJAN SAHA**,

This Certificate of Attendance confirms your attendance at the Molecular Parasitology Meeting held from Sunday, September 17, 2023 to Thursday, September 21, 2023.

We thank you for your scientific contribution to MPM 2023.

Kerri A Mills  
Assistant Director of Housing, Dining, and Conferences  
Marine Biological Laboratory  
conferences@mbl.edu

On behalf of:

Bibo Li, Manuel Llinas, Maryse Lebrun, Omar S. Harb, and Deepali Ravel  
2023 MPM Meeting Organizers



International Conference  
on  
**MECHANISTIC AND THERAPEUTIC APPROACHES  
IN HUMAN AND ANIMAL HEALTH**

*Organised by*  
Department of Zoology  
Cooch Behar Panchanan Barma University  
West Bengal, India

*Certificate of Appreciation*

This is to certify that Prof. / Dr. / Mr. / Mrs. / Ms. .... participated  
of *CSIR-Indian Institute of Chemical Biology* ..... participated  
and presented a paper in the International Conference on Mechanistic and Therapeutic Approaches in Human and Animal  
Health, organised by the Department of Zoology, Cooch Behar Panchanan Barma University from 6<sup>th</sup> -8<sup>th</sup> December, 2021.

Title of the Paper presented:

*Rab7 of Plasmodium falciparum is involved in its retromer complex assembly*  
near the digestive vacuole

*Hadida Yasmin Samikshita*

*Organising Secretary*

*Prodyot Kumar Das*

*Chairperson*



# Certificate of Participation

This is to certify that

MR DEBANJAN SAHA

from \_\_\_\_\_ has successfully participated in  
Young Scientists Conference (YSC) conducted from 22-12-2020 to 25-12-2020, as part of

## INDIA INTERNATIONAL SCIENCE FESTIVAL 2020 (IISF 2020)

organised by Ministry of Science and Technology; Ministry of Earth Sciences,  
and Ministry of Health and Family Welfare, Govt. of India  
in collaboration with Vijnana Bharati (VIBHA)  
by Council of Scientific & Industrial Research (CSIR).

Dr. Shekhar C. Mande  
Director General, CSIR

Dr. Vijay P. Bhatkar  
President, Vijnana Bharati



# One Day Seminar Research Methodology in Science

organised by Research Sub-committee in association with Internal Quality Assurance Cell

**Raja Peary Mohan College, Hooghly**



## *Certificate of Participation*

This is to certify that *Debanjan Saha* of *CSIR-Indian Institute of Chemical Biology* has participated in the seminar entitled "Research Methodology in Science" organised by the Research Sub-committee in association with Internal Quality Assurance Cell on 19th May, 2023.

PRINCIPAL  
**Principal**  
Raja Peary Mohan College  
Jugurra, Hooghly  
Raja Peary Mohan College



## One Day International Webinar

# Current Perspectives on Disease Biology Research

organised by Department of Zoology and IQAC, with support from SERB, DST, Govt. of India

**Raja Peary Mohan College, Hooghly**



## *Certificate of Participation*

This is to certify that **Debanjan Saha** of **CSIR - Indian Institute of Chemical Biology** has participated in the webinar entitled “**Current Perspectives on Disease Biology Research**” organised by the Dept. of Zoology on 18<sup>th</sup> September, 2021.

**Co-ordinator**  
IQAC

**Convenor**

**Principal**  
Raja Peary Mohan College



# Certificate of Appreciation / प्रशंसा प्रमाण पत्र

जिज्ञासा' 2017: केन्द्रीय विद्यालय छात्रों के लिये  
ग्रीष्मकालीन अनुसंधान शिविर



JIGYASA' 2017: A Summer Research Program for

"Kendriya Vidyalaya Students"

यह प्रमाणपत्र ..... श्री. देवानंजन साहा ..... को

सी.एस.आई.आर- भारतीय रासायनिक जीवविज्ञान संस्थान, कोलकाता द्वारा आयोजित  
जिज्ञासा 2017: केन्द्रीय विद्यालय छात्रों के लिये ग्रीष्मकालीन अनुसंधान शिविर (3-7 जुलाई 2017) में  
विद्यार्थियों को अपने ज्ञान और मुल्यवान विचारों को साझा करने के लिए प्रदान किया जाता है।

This certificate is awarded to ..... Mr. Debanjan Saha.....

for Sharing his/her knowledge and valuable thoughts to students in

JIGYASA 2017: a summer research program for "Kendriya Vidyalaya Students"  
organized by

CSIR-Indian Institute of Chemical Biology, Kolkata, from to July 3 - 7, 2017.

Coordinator / समन्वयक

Director / निदेशक



CSIR-Indian Institute of Chemical Biology / सी.एस.आई.आर- भारतीय रासायनिक जीवविज्ञान संस्थान





Enrolment No. : PhD CW / ..... 2017/08

# CSIR-Indian Institute of Chemical Biology

(An autonomous body, under the Ministry of Science & Technology, Government of India)

## Certificate

(Courses offered as per UGC guidelines, July 2009)

This is to certify that Mr. / Ms. Debanjan Saha .....

has successfully completed the Ph.D Course Work conducted by CSIR-IICB for the session  
2017 .....

Uday Bandyopadhyay

Uday Bandyopadhyay  
Chairperson, Academic Affairs Committee

Samit Chattopadhyay

Samit Chattopadhyay  
Director



যাদবপুর বিশ্ববিদ্যালয়  
কলকাতা-৭০০০৩২, ভারত



\*JADAVPUR UNIVERSITY  
KOLKATA-700 032, INDIA

Ref.No.: D-7/sc/751/18

Dated: 31.08.2018.

To,  
Sri Debanjan Saha  
C/O – Dr. Uday Bandyopadhyay  
Sr. Principal Scientist  
CSIR- Indian Institute of Chemical Biology  
4, Raja S.C. Mullick Road  
Kolkata - 700 032.

INDEX NO:- 175/18/Life Sc./26

Dear Sir,

With reference to your application for the registration for Ph.D.(Science) degree of Jadavpur University, I am to inform you that you are permitted to register your name on payment of requisite fees for Ph.D. programme of Rs.22,000/- (Rupees Twenty-Two Thousand Only), payable in three installments (Rs.8000/- + Rs.8000/- + Rs.6000/-). It may be noted that this offer is provisional until all the documents mentioned below are submitted.

The registration will be valid from the date on which the fees are paid and shall remain valid for six years from that date. Subsequently the period of registration may be extended as per Regulation 2017 if the grounds for extension satisfy the Research Advisory Committee, Ph.D. Research Committee and the Doctorate Committee accordingly. An application requesting extension and citing the grounds for the same must be submitted in due time, duly forwarded and recommended by the supervisor(s), before the date on which the validity of the registration expires.

The scheme of the work and title of the thesis, if not submitted along with the application, shall have to be submitted within two years from the date of registration or within one year from the date of successful completion of the course work result of the candidate. Otherwise, the registration is liable to cancellation as per Regulations 2017 of the University.

If the registration fee is not paid within one month from the date of issue of this letter, your application stated above will be treated as cancelled. A report on the progress of the research work shall have to submit once in every six months from the date of registration as per Regulation 2017. The registration is liable to cancellation if the progress of work is not satisfactory. It may be noted that you will have to fulfill the condition as per Regulation 2017 and have to complete the course work within two years from the date of registration.

Mode of payment as follows:

- 1<sup>st</sup> instalment – within 30 days.  
2<sup>nd</sup> instalment – within 180 days  
3<sup>rd</sup> instalment – within 365 days.

List of required documents:

- i) Migration Certificate in original. → Submitted on 18.09.18.

Yours faithfully,

(Dr. Atiskumar Chattopadhyay)  
Principal Secretary  
Faculty Council of Science.

18/09/18





# JADAVPUR UNIVERSITY

KOLKATA-700 032

MARK SHEET

NO.: CW/16052/ 000801

(For Ph.D/M. Phil. Course Work)

Results of the PH.D. COURSE WORK EXAMINATION, 2020  
In LIFE SCIENCE & BIO-TECHNOLOGY held in DECEMBER, 2019 - JANUARY, 2020  
Name DEBANJAN SAHA Class Roll No. 201920502012  
Examination Roll No. PHDLSBT2012 Registration No. of

Subject Code / Name	Credit Hr.(ci)	Marks
COMPULSORY UNITS:: EX/LSBT/PHD/1.1 REVIEW OF LITERATURE & RESEARCH METHODOLOGY	4	76
ELECTIVE UNITS :: EX/LSBT/PHD/1.2A :: TISSUE CULTURE TECHNIQUES EX/LSBT/PHD/1.2B :: MICROBIOLOGY EX/LSBT/PHD/1.2C :: PRINCIPLE OF MOLECULAR BIOLOGY TECHNIQUES EX/LSBT/PHD/1.2D :: INTRODUCTION TO MOLECULAR BIOLOGY TECHNIQUES	4	69

Total Marks : 145 (out of 200 )

Remarks: P

Prepared by :

Checked by :

Date of issue : 16 - 09 - 2020

Controller of Examinations



No.Sc. 0236

# Jadavpur University



## Registration Certificate

Shri/Sri Debanjan Saha

has been registered as a student of Ph.D. programme of this  
university

His/her Registration Number is SLSBT/117518

Kolkata 18th September 2018

[Signature]  
Registrar

Resilience.  
Patience.  
Fulfilment.  
Gratitude.